# The Relationship between RAF-1 protein level, radiosensitivity, and post-irradiation $G_2$+M cell cycle accumulation in the context of P53 mutational status

**Thesis submitted in accordance with the requirements of The University of Liverpool for the degree of Doctor of Philosophy**

**by Mark Jones**

**September 2009**

***Acknowledgements***

*I would not have dreamt about attempting to undertake this Ph. D. without the support and guidance of the many members of the oncology research unit with whom I have had the privilege of working along side.*

*I would like specifically to acknowledge Chris Thompson for helping me understand some of the techniques that I now use routinely, rather than simply following recipes. Chris was solely responsible for rekindling my scientific interest.*

*Finally, I would like to thank my partner, Penny, for her patience, understanding and support during these last few hectic years. Penny has taken on more than her fair share in care for our two young daughters so that I may get time to finish this thesis.*

**Abbreviations**

| | |
|---|---|
| Arg | Arginine |
| ASK-1 | Apoptosis signal-regulating kinase 1 |
| Asp | Aspartic acid |
| AT | Ataxia Telangiectasia |
| ATM | Ataxia Telangiectasia mutated |
| BAD | Bal-2 associated death promoter |
| Brca1 | Breast cancer 1 |
| BrdU | Bromodeoxyuridine |
| BSA | Bovine serum albumin |
| CAK | CDK activated kinase |
| CDK | Cyclin dependent kinase |
| CDKI | Cyclin dependent kinase inhibitor |
| CHO | Chinese hamster ovary |
| CIP1/KIP1/WAF1 | p21 |
| CV | Coefficient of variance |
| DSB | Double stranded breaks |
| ERK | Extracellular signal-regulated kinase |
| GADD45 | Growth arrest and DNA damage 45 |
| Grb10 | Growth factor receptor-bound 10 |
| HAT | Histone acetyltransferase |
| HCl | Hydrochloric acid |
| INK4 | p27 |
| KSR | Kinase suppressor of Ras |
| MAPK | Mitogen-activated protein kinase |
| MDM2 | Murine double minute 2 |
| MEK | Mitogen-activated protein kinase kinase |
| MEKK | Mitogen-activated protein kinase kinase kinase |
| MPF | Maturation promoting factor |
| NEAA | Non-essential amino acids |
| O.D. | Optical density |
| p53 | p53 protein |
| PCNA | Proliferating cell nuclear antigen |
| PDGF | Platelet derived growth factor |

| | |
|---|---|
| PI | Propidium iodide |
| RO | Reverse osmosis |
| RBD | Ras binding site |
| Rb | Retinoblastoma protein |
| S.E.M. | Standard error of the mean |
| Ser | Serine |
| $SF_n$ | Survival fraction at dose nGy |
| SDS | Sodium dodecyl sulphate |
| SDS-PAGE | Sodium dodecyl sulphate polyacrylamide gel electrophoresis |
| TBS | Tris-buffered saline |
| Thr | Threonine |
| TTBS | Tris-buffered saline with Tween-20 |
| wt-p53 | wild-type-p53 |

**Abstract**

More than 1 in 4 deaths reported in 2006 resulted directly from cancer. Radiotherapy remains the most efficacious non-surgical medium for the treatment and cure of malignancies and overcoming radioresistance is a major obstacle in the positive outcome for the majority of cancer therapies. Though radiation has been employed in a curative capacity for over 100 years, there are still no predictive markers as to indicate whether a tumour will be radioresponsive.

Radiation has been shown to be capable of inducing a variety of reversible delays throughout the mitotic cell cycle. Thus it is likely that proteins involved in the regulation of cell cycle progression may play a role in influencing radiosensitivity. Progress continues to be made in elucidating the molecular mechanisms, the clock and dominoes, which regulate the cell cycle. Identified as central in regulation of the cell cycle was the tumour suppressor gene p53. The protein of this gene, p53, has been ascribed to have many functions and activities, and along with the positive signal transduction factors such as RAS, RAF-1 and MYC may not only play an important role in cell cycle progression but might also be predictive of malignancy and radiotherapeutic outcome. I therefore elected to undertake a study into the possible relationship between the level of proteins involved in cell cycle regulation and their relationship to radiosensitivity following the clinically relevant dose of 2Gy per fraction.

I have demonstrated here that the intrinsic level of the proto-oncogene RAF-1 is predictive of radiosensitivity in a variety of human cancer cell lines. These cell lines, which reflect the range of common human cancers, demonstrated a post-radiation induced accumulation in the $G_2$+M cell cycle phase This $G_2$+ M accumulation was found to be reversible. Indeed, the rate at which the cells exited $G_2$+M accumulation,

deemed $T_{50}$, following exposure to ionising radiation correlated with the level of RAF-1 and also radiosensitivity as measured by clonogenic survival (surviving fraction) following 2Gy ($SF_2$), but only in cells possessing wild-type p53. This relationship between the intrinsic level of RAF-1, $T_{50}$, and survival fraction was not present at higher doses of radiation of 4 and 8Gy.

Disruption of p53 function with the small molecule inhibitor Pifithrin-α negated the relationship between RAF-1 protein level and $T_{50}$, and $SF_2$ and $T_{50}$ in p53-wild-type cells. These data support the observation that RAF-1 and wild-type p53 co-operate in modulating $G_2$+M transit and radiosensitivity at clinically relevant doses of γ-radiation.

# Chapter 1

# Introduction

## 1.1 Overview

Although disruptions to somatic cell division following exposure of cells to ionising radiation were first described over 50 years ago by Howard and Pelc [1], it is still not fully understood how the arrest of cells at discrete cell cycle checkpoints is related to radiation-induced cell death. Whilst early work concentrated on DNA damage and its repair, it has become apparent since the early 1980's that cellular radiosensitivity may also be related to proteins that promote or suppress cell cycle progress. Discoveries of cyclins and their kinase partners, the cyclin dependent kinases (CDK), along with the kinase antagonists, the cyclin dependent kinase inhibitors (CDKI) and tumour suppressors such as p53 and the Retinoblastoma protein (Rb), have provided molecular mechanisms to explain the original observations of Howard and Pelc [1].

Described in this thesis is an exploration of the relationship(s) between ionising radiation dose, clonogenic human cancer cell post-irradiation survival and post-irradiation cell cycle delay, in the context of our increased understanding of the molecular control of the cell cycle and protein expression of the tumour suppressor protein p53 and the mitotically significant RAF-1 protein. This introduction thus reviews;

1- A description of the cell cycle.

2- The molecular control of cell cycle progression and the cell cycle checkpoints.

3- The effect of radiation on cancer cell survival.

4- A review of relevant aspects of p53 and RAF-1 with relation to the above points.

## 1.2 Somatic cell proliferation

### 1.2.1 Introduction

The discovery that cells reproduce by dividing into two identical daughter cells gave an insight into the very origin, and nature of cells and became a cornerstone of cell theory. Walther Flemming first used the term 'Mitosis', in 1882 to describe the process by which cells proliferate following the observation of the formation of thread-like structures, the mitotic chromosomes [7].

### 1.2.2 Arrest at discrete points in the progression of cell division

Mitotic cell devision was initially described as a series of visually accessible physical events and divided into two stages, the intermitotic and mitotic stages. The four-phase convention that is now routinely used to describe the asexual proliferative process in somatic cells was first described over five decades ago and is depicted in Figure 1 below [1]. This four-phased cell cycle followed observations by Howard and Pelc on post-irradiation DNA synthesis and chromosome breakage in the root meristem of the bean species *Vicia faba*, where the terms $G_1$, S, $G_2$ and D were first used to describe the key stages of molecular as well as structural activity in dividing cells.

Using radio-labelled $^{32}P$, determination of the duration of DNA synthesis (S-phase) was achieved and tissue section staining was undertaken to determine the mitotic index. From these parameters the length of division (D - time taken for mitosis) was ascertained. Two periods of apparent inactivity were also noted ($G_1$ and $G_2$). D is

now widely termed M-phase, for mitosis, where chromosome separation and cytokinesis results in the production of two identical daughter cells. These experiments, carried out prior to the discovery of the structure of DNA, were the first to show that the inhibitory effect of ionising on cell division was restricted to clearly definable checkpoints in what became known as the cell cycle.

The two apparent gap phases, $G_1$ and $G_2$, have now been established as periods of intense metabolic activity. Further to the conventional four-stage cell cycle is the less well understood quiescent state. This resting state, often refered to as $G_0$ [11], lies between cycles of somatic/mitotic cellular proliferation is being seen as an increasingly important cell cycle component that may well contribute to differentiation fate [12, 13]. An overview of the mitotic cell cycle compartments of $G_0$, $G_1$, S, $G_2$ and M is given below;

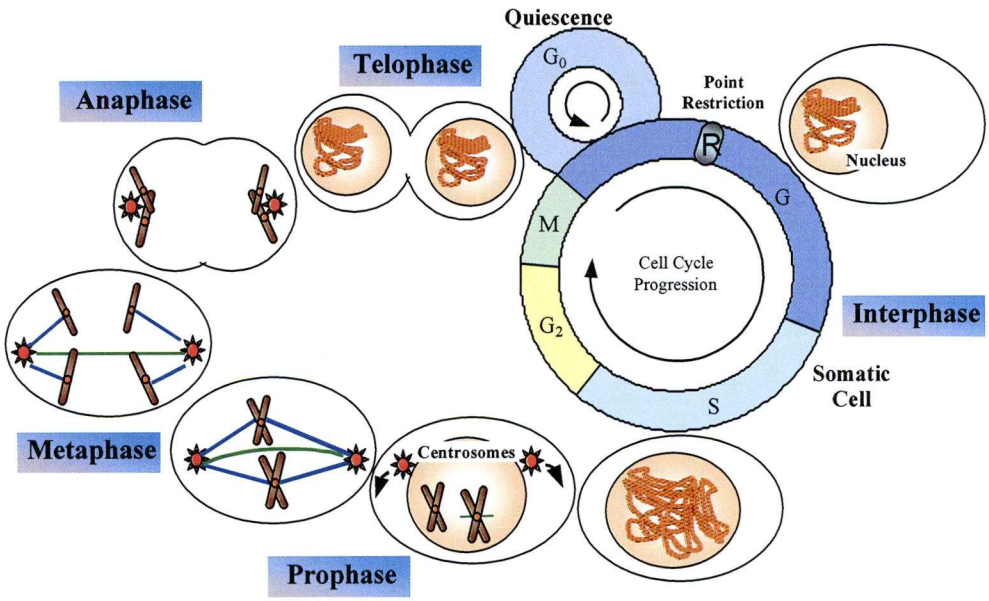


**Figure 1. The mitotic cell cycle**

The four stages of the mitotic cell cycle and the visible characteristics of this cycle are depicted in the above pictogram. Adapted from Mitchison and Salmon [7].

### 1.2.3 Quiescence ($G_0$)

Yeasts, bacteria and other unicellular organisms will proliferate continuously, taking advantage of the availability of nutrients in their immediate environment as circumstances dictate. In a multicellular organism however, cells must maintain a balance of proliferation and differentiation and cell death via senescence and programmed cell death, apoptosis [16], in accordance with the growth criteria of the organism as a whole, rather than merely that of the individual cell. Following observations of non-dividing cells in many tissues, Lajtha proposed, in 1968, the existence of another cell cycle phase, that of $G_0$ [18].

Quiescence, a pseudo-$G_1$ state, so determined because it precedes DNA synthesis, is that of a cell that, although not presently undertaking cell division, has the ability to do so, given an appropriate stimulus. In contrast to certain cells which have lost the ability to divide, such as neurons that are described as terminally differentiated, these diploid quiescent cells, though not actively reproducing, are still very much metabolically active. For example, liver cells that are continually metabolically active, may be quiescent for long periods of time before entering into division [20], whereas some gut epithelia can have a far shorter $G_0$, typically dividing daily [21]. In damaged liver, hepatocytes in the uninjured portion of the liver will undergo successive rounds of proliferation until the liver is restored to near normal mass [22]. Cells undergoing somatic cell proliferation, be it from continual division, or induction into division from quiescence, proceed via a series of regulated sequential temporally and biochemically separated stages, termed the cell cycle. Individual cells of the same type that do enter mitotic cell division have been shown to quickly become asynchronous with respect to their entry into the cell cycle following exit from a quiescent state [23]. The stochastic nature of $G_0$ confers an advantage on the

organism, since simultaneous mitoses of large numbers of cells and the associated structural and functional changes therein, could well be harmful to the integrity of individual tissues.

### 1.2.4 The first growth/gap phase ($G_1$)

$G_1$ and $G_0$, occupy the period traditionally described as interphase. Initially perceived as a state of proliferative inactivity, $G_1$ is the stage in the cell cycle in which the cell prepares itself for the coming S-phase. During $G_1$ phase the cell commits to a round of mitotic cell division when it elects to pass the 'Restriction Point' (R). Prior to the R point, cells must continually receive external mitotic signals to ensure entry into mitosis, whilst once passed, the cell becomes independent of these signals [24]. During $G_1$ rRNA and tRNA synthesis is initiated and protein synthesis occurs [25-27].

### 1.2.5 S-phase

S-phase is also a feature of interphase. S-phase is typified by the induction of genomic DNA replication. This is probably the most critical stage of the cell cycle, as it is here that the faithful and complete duplication of the cellular genome is undertaken. Errors during this stage could result in the loss, incomplete, or erroneous replication of important genetic elements, resulting in the loss of long term cellular viability. Indeed, cells that have been prevented from completing S-phase by pharmacological agents, such as hydroxyurea, often develop gross chromosomal abnormalities or die [28, 29]. It is now that centriole replication (budding) occurs [30] and the chromosomes can be observed to separate [31] and mRNA synthesis occurs [32].

### 1.2.6 The second growth/gap phase ($G_2$) and mitosis

Following the completion of genomic replication the cells undergo a second phase of growth, during which the cell must undergo cellular organelle synthesis as the cell grows dramatically in density along with the synthesis of mitochondrial DNA [33] and mRNA [34]. It is during this phase of the cell cycle that the cell undergoes the 'visibly accessible' stages of the cell proliferative process; prophase, metaphase, anaphase and telophase normally result in the production of two 'identical' daughter cells.

The purpose of M-phase of the cell cycle is to achieve equal segregation of chromosomes to the daughter cells. This physical process is readily observed under the microscope as in prophase; the duplicated centrosomes condense into two chromatids and migrate around the nucleus. This is then followed by the breakdown of the nuclear envelope and golgi apparatus [35] during prometaphase along with equatorial alignment of the chromatids. Then during metaphase, the sister chromatids align, followed by the migration of the two chromatids to 'opposite' poles of the cell in anaphase. Finally, the cells enter Telophase, where they undergo cell-cell scission, nuclear envelope reassembly and abscission, resulting in the completion of mitosis with the production of two separated daughter cells.

## 1.3 Molecular events controlling the cell cycle

### 1.3.1 Introduction

A proliferating cell must coordinate DNA-replication and chromosomal separation to ensure that the genome is passed faithfully through successive generations. The molecular events that control the somatic, mitotic cell cycle have evolved to guarantee that this principal goal is achieved and the step-wise progression of these events has been known for almost two decades, with Murray and Kirchner [36, 37] describing the cell cycle as 'being akin to dominoes and clocks'. Work with yeasts suggested a direct triggering of responses as in a biochemical pathway and Murray and Kirschner used the analogy of a chain of tumbling dominoes to describe the committal to each successive phase of the cell cycle being dependent upon the completion of an earlier stage. Secondly, oscillations of proteins at different stages of the cell cycle in *Xenopus* extracts presents a picture of strict time-dependent controls in a clockwork-like mechanism[38].

Co-ordination of the temporal and sequential events of the cell cycle are governed by a family of conserved and constitutively expressed serine/threonine protein kinases, the CDK, that are positively activated by the 'Cyclin Dependent Kinase Activating Kinase' CAK [39] and their transient partners the cyclin family [40]. In addition to molecular events that drive the cell cycle onward, a complex array of 'brakes' has evolved to

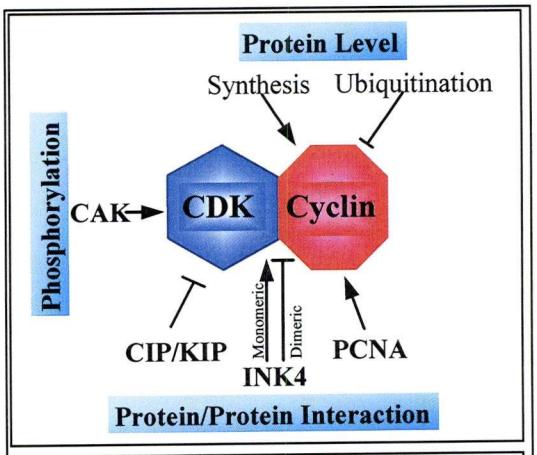


**Figure 2. Cyclin/CDK regulation.** Depiction of the basic molecular control of the dimeric cyclin/CDK complex in eukaryotes. Arrows indicate promotion of function, whilst blunt ends indicate inhibition.

negatively regulate cell cycle progression. A diverse family of proteins that are the CDKI undertakes this negative control of the cell cycle [41].

### 1.3.2 Cyclin dependent kinases

The transfer of a γ-phosphate from ATP to the hydroxyl group of a Serine/Threonine residue of a regulatory protein is the primary controlling mechanism that underpins the entire complex progression of the eukaryotic cell cycle. The proteins central to this process, dictate when cell cycle progression can begin and proceed, belong to a family of kinases, the CDK [42]. Central to cell proliferation, the CDK's are highly regulated, both in response to intra- and extra-cellular signals [41, 43-45].

CDK nomenclature is chronological with respect to their discovery; CDC2 (cell division cycle protein 2) [46], first discovered in yeasts is now designated CDK1. Meyerson *et al.* [47] cloned a series of CDK's identified through shared sequence motifs. This led to the realisation of the possibilities of combinatorial regulation of the CDK's through discrete interactions with the cyclins.

The physical association with a cyclin positively regulates CDK activity. This association results in a conformational change in the CDK [48]. Further activation of the CDK is achieved through phosphorylation of the T-loop threonine by the CDK-activating Kinase (CAK), a serine/threonine kinase that is also involved in transcription and DNA repair [49].

Though the CDK's activity is dependent upon binding to their cyclin partner, this 'marriage' of molecules is far from monogamous, for either the cyclin or the CDK. In addition to the association of cyclin B1 with CDK1, cyclin A can also binds CDK1 although the function of cyclin A in the regulation of DNA synthesis depends upon binding to CDK2 [50, 51]. The cyclin A/CDK2 complex can then bind to and

phosphorylate the Rb protein and has a role in maintaining the integrity of DNA synthesis [52].

### 1.3.3 The cyclins and cell cycle progression

#### 1.3.3.1 Introduction

The catalytic subunits of the CDK's are only active when the CDK molecule is complexed with the transient and unstable regulatory subunits whose fluctuations in abundance during the cell cycle led to their being termed 'cyclin', derived from observations of proliferating cell nuclear antigen (PCNA) at the induction of the cell cycle [53].

Cyclin degradation occurs via phosphorylation dependent [54] and independent ubiquitination [55].

| Cyclin | Function |
|---|---|
| A | S Phase transit and $G_2$/M entry and transition. Anchorage-dependent growth |
| B1, B2 | $G_2$ exit, and mitosis |
| C | Transcriptional regulation, $G_0$ to S-phase transition |
| D1, D2, D3 | $G_0$ to $G_1$ progression and $G_1$ to S-phase transition |
| E | $G_1$ and $G_1$ to S-phase transition |
| F | $G_2$ to Mitosis progression |
| G1, G2 | DNA damage response |
| H | CDK activation, transcriptional regulation, DNA repair |
| I | Anti-apoptotic |
| J | Nuclear Division |
| K | Transcriptional regulation, CDK activation |
| L1, L2 | mRNA splicing |
| O | Apoptosis in Lymphocytes |
| S | Memory |
| T1, T2 | Transcriptional regulation |
| X | Transcriptional activation of c-MYC |

**Table1. The eukaryotic cyclins** Summary of the cyclins and their function in eukaryotic cells. Adapted from a review by Johnson and Walker [2] Cyclins and cell cycle checkpoints.

A summary of the mammalian cyclins and their function throughout the cell cycle is given in the adjacent Table 1, with a fuller description of their activity and interactions with other proteins that facilitate their activity below.

### 1.3.3.2 $G_1$ cyclins

The first cyclins to be induced during the mammalian mitotic cell cycle, the D-type cyclins facilitate progress of cells as they traverse from $G_0$ to $G_1$, stimulating entry into the cell cycle [56] and then progression through $G_1$. Three D-type cyclin homologous isoforms are differentially and combinatorially expressed in various *in vitro* cell types and *in vivo* in an organ and tissue specific manner [57, 58]. Most cells express D3 and D1 or D2. The levels of cyclin D protein levels do not spontaneously oscillate during the cell cycle; their presence depends on persistent growth factor stimulation [59], suggesting that the D-type cyclins provide a link between mitogen signalling and the cell cycle machinery.

D-type cyclins are found in the nucleus [60] and cyclin D1 has been implicated in control of cell cycle progression at the late $G_1$ restriction point, which determines whether the cell will proceed into DNA synthesis [61]. Microinjection of antibodies or antisense molecules to cyclin D1 into normal fibroblasts is effective in halting cell cycle progression up to the $G_1$/S boundary [60, 62].

Depending on cell type, D-type cyclins associate with CDK4, CDK2, CDK5 or CDK6 [63, 64]. On binding to cyclin D, CDK4 becomes activated as a kinase by phosphorylation on Thr172 [65], an event mediated, as in $p34^{cdc2}$, by CAK [66-68]. Cyclin D/CDK holoenzyme complexes can fully phosphorylate their substrates *in vitro*, but the formation of quaternary complexes may be critical to their cellular function, as when isolated from proliferating mammalian cells they have also found to be associated with the CDKI $p21^{WAF1/CIP1}$ and PCNA [69].

Cyclin D exerts its influence on the regulation of $G_1$/S by its association with the protein product of the Rb tumour suppressor gene, which is phophorylated from the $G_1$ restriction point through to mitosis [70, 71]. Since cyclin D can bind to Rb protein

[72, 73] and its CDK-bound holo-enzyme kinase activity has been demonstrated to phosphorylate Rb protein *in vitro* [63, 64, 74] it is assumed that Rb protein is a cyclin D/CDK4 substrate *in vivo*. Hypophosphorylated retinoblastoma protein functions as a "pocket protein" binding and thus sequestering the E2F transcription factors. In this way hypophosphorylated Rb protein negatively regulates $G_1$/S transit induction [75]. Upon further phosphorylation by cyclin D/CDK4, Rb protein can no longer bind E2F and the transition from $G_1$ to S-phase is initiated. E2F-binding by cyclin A/CDK2 has been suggested as an inactivation step for DNA synthesis [76, 77].

In Rb-negative tumour cells, whether Rb loss results from genetic silencing [78] or where DNA tumour virus oncoproteins - including SV40 T-antigen [79] and adenovirus protein, E1A [80], inactivate the growth-suppressive function of Rb, cyclin D levels are reduced and CDK4 and CDK6 bind to form inactive complexes with p16 [81].

Through the activation of E2F, cyclin E appears next in the cell cycle progression through $G_1$ [82, 83]. Exhibiting periodical expression, peaking at the $G_1$/S boundary [84, 85], cyclin E associates with CDK2 [85]with consequent kinase activity peaking in late $G_1$. Microinjection of antibodies to either cyclin E or CDK2 proteins results in cell cycle arrest in $G_1$, implicating both components of the cyclin E-CDK2 holoenzyme complex as being required for the initiation of DNA synthesis [86, 87].

Cyclin E transcription is activated when the retinoblastoma protein is hyper-phosphorylated and it then participates in maintaining retinoblastoma protein in the hyper-phosphorylated state [71, 88]. Cyclin E is thus involved in a positive feedback loop resulting in the accumulation of active E2F. The subsequent accumulation of cyclin E may also depend upon the activity of cytosolic chaperones, which mediate

the ATP-dependent folding of newly translated cyclin E into a mature form that can associate with CDK2 [89].

### 1.3.3.3 S-phase cyclins

Cyclin A, which is also regulated in part by E2F [90], accumulates at the $G_1$/S-phase transition boundary and persists throughout S-phase, being required for S-phase entry, transition and entry into mitosis [91-93]. Following cyclin E degradation, cyclin A is found to associate initially with CDK2. Cyclin A/CDK2 complex then participate in DNA synthesis via binding to a transcription factor [94].

### 1.3.3.4 $G_2$+M cyclins

The first cell cycle regulatory proteins to be assigned a role were those governing the pre-mitotic checkpoint. The *cdc2* gene product, CDK1, was isolated from a temperature sensitive mutant of *S. pombe* and demonstrated to be homologous to *cdc28* in *S. cerevisiae* [95], a gene first identified by Hartwell in 1974 [96]. The product of *cdc2* gene, CDK1, initially referred to as $p34^{cdc2}$, was shown to be a protein kinase [97] and its human homologue was subsequently identified due to its ability to complement a mutant of *cdc2* gene in *S. pombe* [98].

Gautier [99] revealed that purified maturaton promoting factor (MPF) contained a component that was the *Xenopus* homologue of CDK1 and Draetta [100] subsequently identified cyclins as the essential binding partners for active MPF. The resulting holoenzyme is regulated by CDK1 and entry into mitosis has been shown to be blocked by the abrogation of CDK1 activity upon microinjection of rat fibroblasts with antibodies directed against it [101]. Activation of CDK1 requires binding to a

cyclin of which there are many types. First described in sea urchins [102], they have since been identified on the basis of sequence homology in fission yeast, as the product of the *cdc13* gene [36, 103-105] and *Xenopus* [106]. Two types of mitotic cyclin have been described, A and B, both of which have been shown to bind to CDK1 but which form distinct complexes [100, 107].

B-type cyclins follow the typical cyclical pattern of accumulation and several types have been identified. Two classes, B1 and B2, were isolated in *Xenopus* [106] and a human cyclin [108], which has homology with *Xenopus* B1. A third B-type cyclin, B3, initially described in chickens [109] and *C. elegans* [110] and more recently in humans and mouse [111].

There are several B-type cyclins in yeasts. These B-type cyclins fulfil a varity of functions. In *S. cerevisiae* cyclins B1 and B2 function in mitosis whereas cyclin B3-6 undertake roles prior to mitosis; cyclin B3 and cyclin B4 are still active in M-phase, including involvement in spindle assembly [112-114]. In *S. pombe*, in addition to CDC13, two other B-type cyclin proteins function in the cell cycle; cig1 is a $G_1$ cyclin [115] whereas CIG2 has a role in both G1 and at mitosis [116, 117].

### 1.3.4 Cyclin-dependent kinase inhibitors (CDKI)

Besides facilitation of cell cycle progress, negative checks and balances are essential, such that the cell can respond to adverse cellular events that could otherwise compromise the cell's

| CDKI Family | Protein Member |
|---|---|
| Monomeric Inhibitors<br>INK4 | INK4A (p16) |
| | INK4B (p15) |
| | INK4C (p18) |
| | INK4D (p19) |
| Dimeric Inhibitors | p21 |
| | p27 |
| | p57 |

**Table 2. The members of the cyclin-dependent kinase inhibitors**
Summary of the CDKI's in eukaryotic cells.

genomic integrity. Thus, it is critically important that the activity of the CDK family can be negatively regulated. This process is undertaken by the CDKI, the induction of which can be multifaceted [118, 119] and provides critical links to other signal transduction pathways during proliferation, differentiation and senescence [41].

In mammalian cells there are at least two classes of CDKI's, the INK4 proteins [81, 120, 121], which, containing four members, bind competitively to the monomeric forms of CDK4 and CDK6, the partners of the D-type cyclins and as such can inhibit $G_1$ progression [122, 123]. The second class of inhibitors, the CIP/KIP family demonstrate significant conserved homology and are permissive in cyclin/CDK binding. The three members of this CIP/KIP family form heterotrimeric complexes with the $G_1$/S cyclin/CDK complexes. This second group of CKDI's only bind after the cyclin/CDK complex has formed and the binding of two CDKI's is required for the inhibition of the cyclin/CDK complex. It should be noted that the CIP/KIP CDKI's also function as adaptors to promote cyclin/CDK complex assembly [124].

p21 (alternatively known as WAF1, CIP1, OR SDI1) is a universal CDK inhibitor [125] that is directly regulated by p53 [126]. The induction of p21 by p53 causes both cell cycle arrest in $G_1$ and $G_2$+M phases and inhibition of DNA synthesis in response to genotoxic assault and the subsequent inhibition of transition from the S to M phases of the cell cycle. In the absence of p21, cells with damaged DNA arrest in $G_2$ and then undertake repeated cycles of DNA replication without undergoing mitosis. The loss of p21, or of its regulator p53, resulting in the uncoupling of the S to M phase transition control may contribute to the acquisition of chromosomal abnormalities manifested in many tumour cells when apoptosis pathways have been circumvented.

The CDKI, p21 has several distinctive features. The carboxyl terminus of p21 contains a PCNA binding sequence and inhibits PCNA-dependent DNA replication [127]. This carboxyl sequence is overlapped by a cyclin-binding motif and has been shown to inhibit CDK activity both *in vitro* and *in vivo* [128]. This would indicate that p21 modulation of the cell cycle is complex and multifaceted. The carboxyl nuclear localization signal in p21 can facilitate the sequestration of cyclin/CDK complexes to the nucleus [124].

In the structural context, p21 forms a quaternary complex with a cyclin/CDK and PCNA, which functions in DNA replication and repair as a subunit of DNA polymerase δ [125]. p27(Kip1) is a p21-related CDKI [129] that may act to regulate both cyclin E/CDK2 and cyclin D/CDK4 activity by virtue of its stoichiometic binding with the cyclin D/CDK complex. p27 has also been shown to bind CDK6, which again affects the activity of the D-type cyclins. Cyclins A and B can also be inhibited by this p27 [130]. p27 is negatively regulated by mitogens, such as platelet derived growth factor (PDGF), facilitating the progression of cells from quiescence, to mitotic division [131]; blocking p27 function with anti-sense cDNA results in unrestrained cell proliferation [132].

## 1.4 Cellular effect of ionising radiation and radiosensitivity

### 1.4.1 Introduction

On 8th November 1895 Wilhelm Conrad Roentgen discovered the existence of ionising radiation (X-rays) by its ability to blacken unexposed photographic film and used this phenomenon to produce the first X-ray of the hand of his colleague Herr Kölliger [133]. Antoine Henri Becquerel then discovered spontaneous radioactivity the following year (1896), for which he shared the 1903 Nobel Prize in Physics with Pierre and Marie Curie [133] and in 1897 Professor Leopold Freund demonstrated, before the Vienna Medical School, that X-rays were capable of destroying a hairy mole [134]. Since these early observations ionising radiation has become increasingly utilised as an effective physical agent at the centre of cancer therapy.

Cellular susceptibility to ionising radiation is varied. As a result of aberrant cell division and loss of genomic surveillance, one of the key alterations in cancer cells is that chromosomal and genetic organisation may be de-stabilised such that variant cells arise with higher frequencies [135, 136]. These events may influence both the growth and malignant characteristics of the tumour and the tumours responsiveness to radiotherapy.

The radiotherapeutic responsive and particularly the intrinsic radiosensitivity of tumours, both across tumour types [137] and within a tumour [138], differs largely, reflecting the varying radio-sensitivities of individual cancer cells [139, 140]. This spectrum of therapeutic responsiveness can be seen *in vivo*, in patients following radiotherapy and is reflected by the *in vitro* radiosensitivity of cancer cell lines at the clinically relevant radiation dose of 2Gy [4, 141-146].

### 1.4.2 Cell cycle delays and cellular radiosensitivity

One of the most obvious and profound responses of cells to ionising radiation is a delay in progress through the mitotic cell cycle. Such observations have prompted many studies seeking a putative relationship between the degree of post-irradiation cell cycle delay and the intrinsic radiosensitivity of that particular cell line.

The identification of a relationship to post-irradiation cell cycle delay could potentially lead to a more detailed understanding of the mechanisms of post-irradiation cell survival. A longer $G_1$ delay (see section 1, The mitotic cell cycle) might allow damaged DNA to be assessed and possibly repaired prior to replication. A pause in $G_2$ may be necessary to repair damage following DNA synthesis and increase the chances of a viable mitosis. The loss of $G_1$ or $G_2$ checkpoint could relate to increased radiosensitivity. The studies prompted by such a hypothesis have elicited some interesting but often conflicting information.

### 1.4.3 Does loss of $G_1$ delay relate to radiosensitivity?

$G_1$ delay is not a ubiquitous response of all cells to ionising radiation and there is scant compelling evidence for a link between the degree of $G_1$ delay and the intrinsic radiosensitivity of the cell. Some studies have shown both positive and negative relationships.

A positive relationship came from a study in 1983 by Nagasawa and Little [147]. They investigated a mechanism for a link between chromosomal aberrations and cell killing in fibroblasts after X-irradiation. The above study compares Retinoblastoma cells of differing sensitivity with Ataxia Telangiectasia (AT) derived cells, a human autosomal recessive disorder conferring hypersensitivity to ionising radiation. The

AT cells had a much higher incidence of chromosomal aberrations than the Retinoblastoma cells. Investigation of cell cycle kinetics using [$^3$H] thymidine labelling revealed $G_1$ delay at 2Gy and 4Gy in Retinoblastoma cell but no $G_1$ delay in AT cells at either dose. Interpretation of these data however is not straightforward. The different shapes of the Retinoblastoma and AT survival curves, however, made it impossible to provide a meaningful interpretation of this data in terms of any clear relationship between loss of the $G_1$ checkpoint delay and radiosensitivity. Thus these experiments did not necessarily support the concept of inherent radiosensitivity being attributed to $G_1$ delay.

Painter and Young had earlier proposed that a lack of $G_1$ arrest in AT cells increased their radiosensitivity [148]. Subsequent work sought to demonstrate that the loss of the p53 mediated $G_1$ arrest increased the radiosensitivity of the human cancer cells [149]. A mutant-p53 gene was transfected into a wild type p53 (wt-p53) cell line. Though decreasing the $G_1$ delay, there was however no effect on radiosensitivity.

Other studies have indicated increased radioresistance did accompany a lack of $G_1$ arrest. p53 mutations in murine bone marrow cells were shown to related to increased resistance to ionising radiation [150]. Moreover, a significant correlation at 2Gy between $G_1$ arrest and increasing radiosensitivity was observed. In a study in thirteen human tumour lines with $SF_2$ (surviving fraction of cells at 2Gy) with values ranging from 0.11 to 0.8; that is 11-80% of cells survive after 2Gy, the radiosensitive cells, i.e those with a low $SF_2$ value undergoing a $G_1$ delay. Radioresistant cells with a high $SF_2$ having had little or no $G_1$ delay. Wt-p53 was shown to be necessary to mediate this response and loss of this function could lead to induced radioresistance [151]. No correlation between $G_2$ arrest and p53 mutational status was described.

However, in this study samples were taken at 6, 12, 24 and 48 hours (H) and a relatively short $G_2$ delay may not have been noticed.

### 1.4.4 Studies supporting the concept that $G_2$ delay is related to radiosensitivity

In 1975, Tobey had postulated that a surveillance mechanism might operate in $G_2$ to repair or remove the cells not deemed capable of completing mitosis [152]. A wide range of studies have linked a prolonged $G_2$ delay with increased radio-resistance. Rat embryo fibroblasts transfected with the oncogenes *H-ras* and v-*myc*. demonstrated a more radio-resistant phenotype, which correlated with an increase in $G_2$ delay, not attributable to differences in induction or repair of DNA double stranded breaks (DSB) [153]. The effects of *H-ras* and *v-myc* have been shown to confer the greatest resistance is S and $G_2$ phases [154]. A similar relationship was reported for activated *ras* and/or SV40 T-antigen transfected human diploid cells irradiated at 2 to 8 Gy [155] and human testicular cancer cells rendered resistant by transfection with SV40 virus sequences [156]. Conversely, the radio-sensitising drug caffeine both reduces radiation-induced $G_2$ delay and concomitantly increases cell killing [157].

AT cells demonstrate a less pronounced post-irradiation decrease in mitotic index that was associated with a radiosensitive phenotype. Additionally, cells irradiated whilst in $G_2$ were significantly more radiosensitive than cells in other cell cycle phases [158, 159]. In AT lymphoblastoid lines exposed to BrdU labelling and 3 Gy $\gamma$-rays, AT cells irradiated in S phase had an increase in $G_2$/M arrest whilst those irradiated in $G_2$ showed a reduction [160-162]. Overall however, they described a decrease in arrest for the first 2h post-irradiation, but a greatly increased delay thereafter.

Many of the control mechanisms underlying the cell cycle have been elucidated from work in yeast. In *Saccharomyces cerevisiae* wild-type haploid cells demonstrate a $G_2$ delay induced following irradiation. Cells irradiated in $G_2$ left this arrest at a time proportional to the dose given and continued to divide successful. Cells with mutant *Rad9* however, failed to arrest and died within a few generations. They highlighted the importance of the delay by blocking the mutant cells post-irradiation using the protein synthesis inhibitor cycloheximide. 4h was sufficient to produce a dramatic increase in survival rate [163].

In the fission yeast *Schizosaccharomyces pombe* further evidence for a correlation between radiosensitivity and lack of $G_2$ arrest exists. *Rad1* cells, having a mutated version of the *rad1* gene were more radiosensitive than the wild type *rad1* cells and did not arrest in response to γ-rays. After 6h of density inhibition of division they showed a greatly inceased resistance, thus *rad1* were still repair proficient and had a radiosensitive phenotype directly as a result of failure to arrest [164]. Mutations of *rad1*, *3* and *17*, result in reduced $G_2$ arrest after UV irradiation [165]. Later, again in response to UV radiation, a gene termed *chk1* (for checkpoint kinase) was shown to be responsible for a lack of arrest when in a disrupted form. When over-expressed in *chk1* wild-type cells, a delay in mitosis was observed. Overexpression of *chk1* in *rad1* mutant cells resulted in mitotic arrest. Another group of genes, *hus1-hus5*, originally noted as hydroxyurea sensitive, were demonstrated to possess a UV sensitive checkpoint role [166].

A greater $G_2$ delay along with an increasing radiosensitivity was shown by van Oostrum *et al.* In five human tumour xenografts in nude mice which where exposure to ionising radiation no effect on the timing of maximal accumulation in $G_2$ was observed, however the duration of this $G_2$ delays appeared to relate to cell cycle time [167]. In three

radiosensitive mutants of V79 cells (*irs1-3*), a range of $G_2$ delays after 4 and 6 Gy were observed. The relationship with sensitivity was not explainable by DNA damage as measured by differences in the induction of DSB [168].

One of the earliest studies by Terasima and Tolmach implicated $G_2$ as the major component of cell cycle delay following irradiation with relatively low doses of radiation (2-6 Gy). A $G_2$ arrest of 10-20h was seen before cells moved semi-synchronously into mitosis [169]. Cells irradiated in M-phase did not arrest immediately, but did so in $G_2$ after another round of division. The robust nature of this $G_2$ block was observed following high doses (20-50 Gy) in mouse cells [170]. Whilst the sensitivity of the $G_2$ perturbance was observed to contribute to overall depression of division in HeLa cells, murine lymphoma and CHO (Chinese Hamster Ovary) cells [171]. An observation repeated in CHO cells by Leeper and co-workers [172].

These observations are controversal. Smeets *et al.* irradiated two human squamous carcinoma lines, SCC61 (sensitive) and SQ20B (resistant) and found the same degree of $G_2$ delay and induction and repair of DSB at 5 or 10 Gy [173] A larger study of six sensitive and seven resistant human tumour lines at 2 Gy also revealed no link between radiosensitivity and survival [151].

## 1.5 The tumour suppressor gene p53

### 1.5.1 Introduction

The p53 protein was originally thought to be a tumour antigen because it co-precipitated with SV40 T-antigen; subsequently, following a convoluted process, it was identified as a tumour suppressor, the function of which is central to the control of checkpoint pathways, coordination of DNA repair with cell cycle progression, survival or apoptosis. This vast array of functions has lead to p53 being declared the 'Guardian of the Genome' [174] and the 'Cellular Gatekeeper' [175].

The gene of the p53 tumour suppressor is frequently a target for recessive mutations in a wide range of sporadic human malignancies (summarised in Table 3), where it is found to be mutated in more than 50% of tumours [176] and in the autosomal dominant Li-Fraumeni syndrome, the inheritance of a mutant p53 allele and one wt-p53 allele, results in the predisposition of individuals to develop cancer. This predisposition results in diverse tumours at multiple sites in the body, such as sarcomas [177], lymphomas

| Tumour site | Frequency (%) |
|---|---|
| Lung | 50 |
| Colorectum | 50 |
| Oesophagus | 45 |
| Ovary | 44 |
| Pancreas | 44 |
| Skin | 44 |
| Stomach | 41 |
| Head and Neck | 37 |
| Bladder | 34 |
| Prostate | 30 |
| Hepatocellular | 29 |
| Brain | 25 |
| Adrenal | 23 |
| Breast | 22 |
| Endometrium | 22 |
| Kidney | 19 |
| Thyroid | 13 |
| Haemopoietic system | 12 |
| Carcinoid | 11 |
| Melanoma | 9 |
| Parathyroid | 8 |
| Cervix | 7 |

**Table 3. Frequency of p53 mutations in different human tumour types**
Adapted from a review on: The p53 tumour suppressor gene, Steele *et al* 1998.

[178], breast [179] and brain [180]. The loss of wt-p53 protein in tumour cells appears to provide the cell with a selective growth advantage, both *in vitro* and *in vivo*.

p53 is clearly influential in tumourogenesis. In p53 null-mice models, a very marked increase in the incidence of malignancies is indicative of a role of p53 in tumour suppression. However the mere existence of mice that are p53 null indicates that p53 expression is not in itself essential for survival [181].

Two models have been proposed to explain the role of p53 as a tumour suppressor; briefly these could be described as cell survival, or cell death. In the cell survival model, p53 participates in the cellular response to DNA damage by delaying cell cycle progression. Cells have evolved elaborate mechanisms (checkpoints), the nature of which are conserved throughout evolution to ensure genomic integrity through faithful and accurate transmission of genetic information from generation to generation of the cell and eliminating lesions and mutations that might otherwise be perpetuated in progeny cells.

In support of the cell death model, p53 protein has been shown to initiate apoptosis in response to agents that cause DNA strand breakage. Failure to eliminate cells that have undergone genetic alterations following DNA damage could lead to the appearance of transformed clones with increased growth capacity. Genetic and biochemical studies indicate that the two properties of p53 protein, namely site-specific binding to double stranded DNA and transcriptional activation of genes bearing p53-responsive elements, are closely associated with its ability to act as a tumour suppressor. p53 protein exhibits double stranded DNA binding activity that is both sequence-specific and sequence-independent [182-184].

A key function of the wt-p53 protein is that it is a transcription factor; wt-p53 transactivates genes containing p53 response elements and represses a number of genes independently of these elements [185, 186]. These p53 induced elements act as significant effector proteins of p53 function [187].

With such diverse and critical activities, p53 can be thought of as a critical node in the cellular circuitry [188]. A more detailed review of the p53 gene, the structure of the protein and covalent modifications of the protein and how this profoundly influences the function of p53 and its interactions with other proteins is given below.

### 1.5.2 Location and structure of the p53 gene

First identified as a co-immunoprecipited protein of 53 KDa with large T antigen from monkey virus SV40 [189], it was concluded that p53 was a cellular-encoded protein present in relatively abundant levels in transformed tumourigenic cells. Though initially thought of as a tumour antigen [190] and then later an oncogene [191-193], it was subsequently concluded that p53 was a tumour suppressor gene following demonstration that wt-p53 was unable to transform cells [194, 195] and that, the wt-p53 gene or cDNA could inhibit or block the transformation of cells by other oncogenes [196] and that wt-p53 alleles suppressed the tumourigenic potential of p53 null cells [197].

The whole human p53 gene (introns and exons) encompasses 20kb of DNA and is located in the short arm of chromosome 17 at position 17p13.1 [198]. A p53 homologue has been found to be present in a variety of vertebrates and is evolutionary conserved, a further indication of its central importance to a variety of cellular processes. The p53 mRNA is a 2.8-3.0 kb molecule that is ubiquitously expressed.

### 1.5.3 Structure of the p53 protein

Analysis of the amino acid sequence of p53 protein from human, monkey, mouse, rat, chicken, frog and rainbow trout, reveals five clusters of highly conserved amino

acids (domains I to V) [199-204]. A contiguous stretch of 18 amino acids within domain IV and a 12 amino acid stretch in domain V are conserved in all of the above species (representing amino acids 237-254 and 270-282 respectively in human p53). p53 self-associates to form homo-oligomers; the predominant form *in vivo* and in solution has been found to be the tetramer [205, 206]. The oligomerisation of p53 was further supported by the observation that p53 containing mutations within its DNA binding domain interfere with the ability of wt-p53 protein to bind DNA following hetero-oligomerisation [194]. The mediation of this oligomerisation is thought to be a function of the carboxyl terminus [207, 208] and occur independently of DNA interactions [209]. Proteolysis experiments have subsequently identified amino acids 326-355 as being responsible for the tetramerisation domain and amino acids 363 to 393 comprising a regulatory region [210]. The tetramerisation domain is also present in the other members of the p53 family, p63 and p73 [211], although the sequence of this domain is less well preserved when compared to other regions of the protein [212]. This tetrameric protein structure is highly symmetrical and comprises a dimer of dimers. Each monomeric unit contains a turn, a β strand (amino acids 326

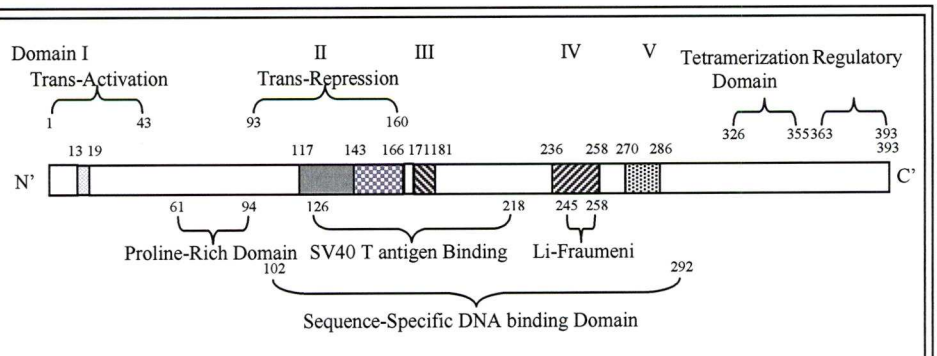


**Figure 3. The linearised structure of p53**
The above diagram depicts the lineararised p53 protein. Indicated are the five conserved domains along with the regions which have been ascribed specific and important sites of interaction.

to 333), a second turn and a relatively stable α helix (amino acids 335 to 355). Each

unit interacts with another unit such that the helices and β strand are anti-parallel. Two such dimers interact, forming a four-helix bundle [213-215]. The mainly hydrophobic interactions between the helices are stabilised by several salt bridges, possibly between Arg337 from one monomer and Asp352 from the other monomer [213, 216].

This carboxyl terminus does not appear to be required for interactions with DNA, nor does the tetrameric association of p53 appear to be required. The nuclear localisation sequence overlaps with the tetramer-structural association sequence, amino acids 316-325 suggesting that a partial DNA binding sequence is sufficient for p53 to bind DNA [217]. Truncated p53 protein fragment corresponding to amino acids 94-312, which exists as a monomer in solution is capable of binding DNA in a sequence specific manner [218] indicating that the amino acids 316-325 are not required for DNA binding. However, etramisation of p53 increases binding as the monomers exhibit a 10 to 100 times lower affinity for DNA than the tetromeric form [219].

The core domain structure consists of two anti-parallel β sheets that act as a scaffold for three distinct structures. These structural elements include a loop-sheet-helix motif that binds the chromatin major groove making contact with the DNA bases and two large loops arround a core of a zinc atom. One of these loops binds the chromatin minor groove. These three structural elements form the DNA binding surface of p53 and contain the majority of the p53 mutations occurring in tumours. The location of the majority of mutations within the p53 DNA binding regions support the importance of DNA binding and sequence-specific transactivation for the biological activity of p53 [220].

### 1.5.4 Control of p53 activity

The p53 tumour suppressor protein is involved in many cellular processes. These include cell cycle regulation, senescence, apoptosis, differentiation, angiogenesis and DNA repair (by DNA annealing and a 3'→5' exonuclease activity). Regulation of p53 appears to be complex and manifested at many levels. These regulations and activities of p53 are mediated by localisation, transcriptional activation, transrepression, stabilisation, translation, conformational changes and various covalent and non-covalent modifications [221, 222].

The diverse actions of p53 functions involve many target genes and interactions a variety of proteins [175, 223-228]. The anti-proliferative function of p53 is one such process involving protein-protein interactions and covalent modifications. This is seen through the activity of the cyclin A/CDK2 complex. This proliferative complex potentiates the phosphorylation of murine double minute 2 (MDM2), reducing the phosphorylation of p53 by MDM2 and hence partially inhibiting MDM2-mediated degradation of p53 by ubiquitination and providing a feed-back mechanism to proliferation [229], a process that could be especially essential during normal growth and development. A more complete over-view of the multitude of the events that regulate the function of p53 is given below.

#### 1.5.4.1 p53-protein interactions

Several proteins can interact with p53 and regulate its stability with in the cell. Calpain 1 is capable of undertaking proteolytic cleavage of p53 [230]. Conversely, high levels of β-catenin promotes the accumulation of transcriptionally active p53 [231], whilst Sin3a binds to the proline-rich domain of p53 and prevents the ubiquitination dependent proteolysis of p53 in response to DNA damage [232].

### 1.5.4.2 Phosphorylation of p53

Covalent modifications such as phosphorylation can regulate conformational and/or promote specificity to p53 for protein binding and promotion of transcription. Phosphorylation of the p53 protein *in vivo* has been shown to occur at multiple serine and threonine residues. The phosphorylation sites have been identified by several approaches including phosphopeptide mapping, direct sequencing of phosphopeptides and site-directed mutagenesis. These sites of phosphorylation are

| Proteins interacting with p53 | Amino acid phosphorylated | Effect on the p53 protein |
|---|---|---|
| ATM | Ser 15 | Stabilization, transcriptional activation, growth arrest. |
| DNA-PK | Ser 15, 37 | Stabilization, transcriptional activation. |
| ATR | Ser 15 | Stabilization, transcriptional activation. |
| JNK | Thr 81 | Stabilisation (in UV stressed cells). |
| CDK7/CycH/p36 | Ser 33 | Transcriptional activation. |
| Homeodomain-interacting protein Kinase-2 | Ser 46 | Transcriptional activation of p53A1P1 and apoptosis inducing genes. |
| p53DINPI | Ser 46 | Promotion of Apoptosis |
| Wip1 | Ser 46 | Dephosphorylatory inhibition of apoptosis |
| CHK1 | Ser 20 | Stabilisation |
| CHK2 | Ser 20 | Stabilisation |
| CDK4 | | |
| CDK's | Ser 315 | Transcriptional activation. |
| COP9 | Thr 155 | Proteolysis |
| p38 | Ser 392 | Transcriptional activation. |
| CK2/hSpt16/SSRP1 | Ser392 | Transcriptional activation |
| Casein Kinase I | | |
| Casein Kinase II | Ser 392 | Transcriptional activation. |
| Polo-like kinase-3 | Ser 20 | Stabilisation |
| Protein Kinase C | Ser 371, 376, 378 | Phosphorylation led ubiquitination/proteolysis. Dephosphorylation induced transcriptional activation. |
| RAF-1 | Serine | Unknown |

**Table 4.** The protein interactions with p53, and the phosphorylation events associated with these protein-protein interactions.

summarised in Table 4 above. Phosphorylation of p53 on Serine 46, for example, is required for the induction of the apoptotic gene p53A1P1 [233] and inhibition of the kinase responsible for Serine 46 phosphorylation by the phosphatase WIP1, which is also p53-inducable, inhibiting the ability of p53 to activate apoptosis [234]. The induction of tetramerisation of p53 could be stimulated by the phosphorylation of p53 at serine-392 [235]. A number of kinases have been implicated in the phosphorylation of p53. Double-stranded DNA activated protein kinase (DNA-PK) [236], Casein Kinase I [237] and Casein Kinase II [238] have been shown to affect the DNA binding potential of p53 [239]. The cell cycle kinase CDK4, whose ablation results in the non-phosphorylation of p53 [240] and of significance to this study the MAP Kinase pathway has been shown to phosphorylate p53 [241, 242].

#### 1.5.4.3 Ubiquitination

Ubiquitination of p53 represents an essential activity of MDM2 in the regulation of the level of cellular p53 protein. The half-life of p53 protein is relatively short [243]. However, following DNA damage, such as that caused by ionising radiation, there is a rapid accumulation of the p53 protein [225]. A key component in this regulation of p53 protein level is MDM2. This MDM2 regulation of p53 is multifaceted. MDM2 acts specifically as an E3 ligase for p53 by linking E2-conjugated ubiquitin molecules to p53 via an isopeptide bond [244] and has been shown both *in vitro* and *in vivo* to cause p53 degradation [245]. Additionally, MDM2 binds p53 transactivation domain, inhibiting p53 promoted transcription and promotes p53 nuclear export to the cytosol where it is degraded by the 26S proteosome [246, 247]. The human papillomarvirus HVP E6 also utilises the same process to promote p53 degradation by the ubiquitin-proteasome [248]. Limiting p53 protein life-span may seem beneficial in promoting tumourogenesis, as elevation of MDM2 has been

observed in tumours retaining wt-p53 [249]. However, MDM2 mediated ubiquitination and destruction of p53 is essential for embryonic development and survival [250], in the adult MDM2 over-expression can subvert cellular mechanisms to give rise to cancer [251].

#### 1.5.4.4 Acetylation of p53

Acetylation has been shown to be an important modification of histone proteins and correlates with transcriptional activity [252, 253], although the precise role played in transcriptional regulation is still unclear. Recent studies revealed several proteins that can stabilise the p53 protein. The transcriptional co-activator CBP/p300, which can mediate p53 transcription and activation is a histone acetyl transferase (HAT), has been shown to be active both *in vitro* and *in vivo* [254-257]. Acetylation directly influences DNA binding, protein-protein interactions and protein stability. p53 is acetylated at multiple lysine sites at the carboxyl terminus [258], with the level of acetylation being enhanced *in vivo* and has been shown to be essential for radiation induced accumulation of c-JUN protein through activation of wt-p53 [259]. The acetylation of p53 by p300 is inhibited by MDM2 [260]. These acetylation sites of p53 are essential for ubiquitination and the subsequent degradation of p53 by MDM2 as described above [261, 262].

### 1.5.4.5 Sub-cellular localisation of p53

p53 transcriptional activity requires nuclear localisation of p53 protein [263]. Nuclear localisation of cytosolic p53 has been observed as a cellular response to various cellular assaults [264]. The active transport of p53 by dynein and the microtubule network is fundamentally important [265, 266], as are the C-terminal nuclear localisation motifs on p53 itself [267]. Following nuclear localisation relocation to the cytosol is an actively process. p53 possesses several nuclear export sequences, one in the oligomerisation domain [268] and a second in the N-terminal MDM2 binding region [244, 269]. The activity of the N-terminal nuclear export sequence is regulated by phosphorylation and is down-regulated in response to DNA damage [69].

## 1.5.5 Determination of cellular fate and p53 function

p53 may promote growth arrest and potentially survival, or conversely cell death via apoptosis. How the cell decides between these two cellular responses is unclear [270, 271]. The determinants of these alternatives appear to be diverse and include the origin of the cell, the oncogenic genotype, external cellular stimuli and the intensity and duration of the genotoxic stress incurred, as well as the level of p53 expression within the cell. These processors are not activated in a simple linear fashion because the damage recognition elicits multiple signal transduction cascades that can trigger both repair and apoptosis. Individually, and in concert, these factors may all influence the response of the cells decision-making process.

### 1.5.6 The nature of the cellular assault and p53 response

The different nature and the severity of cellular damage may contribute to the level of, and be surveyed by p53 within the cell. Exposure of fibroblasts to different doses and different forms of UV-irradiation induced different expression responcses. Low doses of UV-B (50 $J/m^2$) caused a p53 dependent induction of p21 gene expression, whilst at higher doses (>200 $J/m^2$), the pro-apoptotic protein, bax was induced [272]. Similar trends were observed following exposure to UV-C [273]. However, in contrast to UV-irradiation, high doses of γ-radiation act to further potentiate p21 gene transcription [274], whilst Matrix metalloproteinase-1 is elevated by UV radiation and may promote long term cell damage and cancer by suppressing p53 expression by recruiting p300 and c-Jun [275].

### 1.5.7 Anti-proliferative nature of p53

As previously descussed, p53 is capable of mediating powerful inhibition of cell proliferation. It is not unreasonable to surmise that the tumour suppressor function of p53 depends principally on its ability to prevent cellular proliferation in response to stress stimuli that are encountered during tumour genesis. In this context, activated p53 has been shown to lead to cell cycle delays and apoptosis. Activated p53 can also play a role in the induction of differentiation and the cellular response to ionising radiation [276-278].

The role of wild type p53 as a negative growth regulator was indicated following studies of p53 complexing to viral oncogene protein products when it was found that wt-p53, but not mutant-p53, binds to SV40 large T antigen, thereby indicating that p53 interaction with the cellular homologue of T antigen could be critical for cell cycle control [279]. This has been further demonstrated in gene transfer experiments

in which a functional wt-p53 gene was re-introduced into transformed cells that had lost endogenous p53 gene expression through a recessive mutation. The most common outcome of these studies was growth arrest of the recipient cells in a quiescent manner [280, 281]. In other studies, wt-p53 protein expression resulted in apoptosis [282, 283]. A third outcome of wt-p53 expression in p53-null tumour cells was the induction of differentiation [284]. Moreover, in many cell types terminal differentiation resulted in apoptosis. Hence, three different outcomes from restitution of wt-p53 protein reconstitution may be dependent on the lineage and maturation potential of the recipient cells.

### 1.5.8 p53 mediated response to ionising radiation

The ability of ionising radiation to induce cell cycle perturbation was demonstrated in human and rat fibroblasts, where it induced a transient and prolonged $G_1$ delay [285]. Ionising radiation induces a large variety of DNA lesions, including single-strand breaks and DSB, as well as base and sugar damage [286-288]. Though cells can adapt to low levels of irreparable DNA damage [289, 290]; one DNA DSB in a multicellular organism can be sufficient to kill a cell if it is located in an essential gene. In response to DNA damage, checkpoints induce the signal transduction cascades, which consist of sensors, transducers and effectors [291-293]. The ionising radiation induced effectors respond to DNA damage by a) perturbation of cell cycle progression, b) DNA damage repair or c) apoptosis [294].

One of the key components of cell response to ionising radiation is p53, 'the guardian of the genome' [174]. Whether a cell undergoes cell cycle arrest or apoptosis in response to p53 depends on complex array of mechanisms [295]. Several factors come into play, such as the presence of extra cellular survival factors,

the presence of other oncogenic alterations, the level of p53 and the availability of additional transcription factors or cofactors [296].

### 1.5.9 Ionising radiation mediated p53 expression level and activity

The type and magnitude of cellular stress may modulate p53 function by affecting the level or activity of the p53 protein that is induced. Modulating p53 expression level may protect cells or promote apoptosis. Interestingly, relatively low levels of p53 have been observed to possess anti-apoptotic functions [297], whilst activation of apoptosis is associated with higher levels of p53 than those required for cell cycle arrest [298]. These independent observations are further supported by the response of bone marrow cells to ionising radiation. The presence of one p53 allele is associated with induction of an intermediary response between that induced by homozygous, two allele, wt-p53 and p53-null cells which lack both p53 alleles [299]. How the level of p53 orchestrates the cellular response to ionising radiation is still unclear. However, promoters regulating expression of apoptotic genes could bind p53 with a lower affinity than those involved in cell cycle arrest, as would appear to be the case for p21 and Bax transcription. This would induce cells to undergo cell cycle arrest in preference to apoptosis. Several mutants of p53 show selective loss of the ability to activate apoptosis target genes and to induce apoptosis. Such cells potentiate cell cycle arrest [300-303]. Alternatively, the affinity of p53 to target promoters may be regulated by conformational change [304].

Beside the intrinsic level of p53 at the time of the induction of DNA damage, the level of p53 following genotoxic assault is observed to rise. In fibroblasts this elevation was associated with alterations in mediation of cell cycle distribution [305], which further increased the potential cellular response of p53 to DNA damage. This

increase of p53 level could tilt the cell balance away from cell cycle delay and survival, towards cell death and apoptosis [306].

### 1.5.10 Cell cycle delay mediated by p53

Cell exposure to genotoxic assault frequently results in abolition of cell cycle progress [307]. As previously suggested, it is assumed that the transient delays observed in $G_1$, S and $G_2$+M provide time for repair of damaged DNA prior the initiation or continuation of replicative DNA synthesis or the onset of mitotic reproduction. Such damaged DNA if not repaired could facilitate the propagation of potentially deleterious mutagenic lesions, contributing to the progressive accumulation of genetic changes that typify neoplastic transformation.

The cell cycle arrest function of p53 correlates strongly with its ability to function as a transcription factor [308, 309]. Its pivotal roles in checkpoint control result from its unique biochemical features. As stated earlier in the 'Structure of the p53 protein' (section 1.5.3) there are five conserved domains. It is within these five regions that the majority of mis-sense mutations are found in human tumours as reviewed by El-Deiry [310]. wt-p53 can both activate and repress gene transcription resulting in the mediation of the cellular response to ionising radiation and genotoxic assault. The role of p53 as a tumour suppressor protein is significantly influenced through its 'effector' proteins that are produced as a result of p53 transcriptional activities.

Of the myriad of p53 target genes identified, $p21^{waf\text{-}1,\ Cip\ 1}$ appears critical in the processess influencing cell cycle delay [126, 311]. p21 acts as a CDKI that can activate both $G_1$ and $G_2$+M arrest in a similar manner to those seen in response to p53 induction itself [312, 313]. Besides the potential modulation of cell cycle delay, it has been demonstrated that p53 can play a direct role in the repair of DNA damage,

both through nucleotide excision repair and base excision repair [314-317]. This complex and diverse nature of p53 in cell response to genotoxic events further underlines p53's importance to the cell, as of North and Hainaut put it 'Having a finger in every pie' [188].

#### 1.5.10.1 p53 in $G_1$ cell cycle checkpoint control

Checkpoints are control mechanisms that ensure the proper timing of cell cycle events by requiring the completion of earlier processes before the initiation of later cell cycle events [318]. The p53-mediated $G_1$ checkpoint can be disrupted in a number of different ways including mutation of the p53 gene [319], by expression of certain cellular or viral proteins that interact with p53 protein and interfere with its transactivation function, as well as by other mechanisms that affect upstream or downstream components of the p53 growth-control pathway. For example, over-expression of MDM2 protein results in p53-MDM2 interactions and loss of p53-mediated transactivation and $G_1$ checkpoint function in response to irradiation [320]. Cells from individuals with AT show an abnormal response to irradiation; relatively higher doses of irradiation are required for p53 induction [321]. It has been suggested that the ATM gene product is required for the induction of p53 protein. Expression of the human papilloma virus HPV-E6 and E7 sequences abrogate the p53-dependent $G_1$ checkpoint in a number of human cells treated with PALA, $\gamma$-irradiation and actinomycin D [322, 323]. In these models it has been suggested that E6 promotes the degradation of p53 while E7 protein binds and inactivates Rb protein.

### 1.5.10.2 Role of p53 in the S-phase completion checkpoint

Inhibition of DNA synthesis triggers the S-phase completion checkpoint, which blocks entry into mitosis. The signal that activates this checkpoint is generated when cells are blocked in S-phase. Signals that activate the S-phase completion checkpoint may include stalled replication machinery and DNA damage that results in prolonged inability to undertake DNA synthesis. Ionising radiation is capable of inducing progression delays in the cell cycle [324].

Treatment of cells with caffeine, okadaic acid or staurosporine can override the S-phase completion checkpoint, causing apoptotic like phenotype of premature chromatin condensation, DNA fragmentation and cell death [325-328]. In fibroblasts derived from Li-Fraumeni cells (MDAH041), treatment with hydroxyurea induces the above phenotype. But following transfected with wt-p53, prevention of cell entry into mitosis by hydroxyurea treatment is reinstated, implicating wt-p53 in S-phase checkpoint control [329]. Similarly, HPV-E6 transformation of the *in vitro* normal lung fibroblasts IMR-90, cells are more prone to caffeine-induced premature chromatin condensation than the parental cell line with functional wt-p53 [330]. The lack of functional ATM negates the S-phase checkpoint, which is also influenced by NBS1, CHK2, CDC25A, BRCA1, SMC1 and MREL1 in response to ionising radiation [331-335].

### 1.5.10.3 Regulation of the $G_2$+M transition and checkpoint control by p53

The deregulation of the $G_2$+M transition is a common feature of cell immortalisation and malignant transformations [336-339]. The $G_2$ checkpoint is triggered in cells that have completed DNA synthesis but contain damaged DNA. Intuitively, this would be essential in preventing the proliferation of genetic defects to progeny cells and both

the S-phase and $G_2$ checkpoint block entry into mitosis and could hence ensure genetic integrity. However, the $G_2$ checkpoint causes cells to arrest; determination of the significance of the role of p53 in $G_2$ arrest is problematic due to the existence of p53-independent mitotic bocks. p53-null cells still demonstrate a $G_2$ response to genotoxic events [305]. However, the nature of the response, such as the duration of cell cycle delay, may be significant in cell fate and dependent upon the function of p53, rather than solely its p53 mutational status. The role of p53 as a secondary regulator in $G_2$ delay appears convincing [338, 340].

Studies employing viral oncogenes have implicated wt-p53 in the operation and maintenance of the $G_2$ checkpoint. In IMR-E6 cell, HVP-E6 infected and transformed cells undertake an increased entry into mitosis in response to ionising radiation [341]. Thus suggesting that wt-p53 is involved in progression through the mitotic checkpoint. Alternatively, E6 could encourage genetic and epigenetic events that negate the $G_2$ checkpoint [342]. Studies utilising large T antigen of SV40 in IMR-90 cells demonstrated that though cells still delay in $G_2$, the duration of this reversible delay was reduced [330]. Although both these viral oncogenes implicate p53 in $G_2$ checkpoint progression, they both may act in a p53-independent manner. However, further studies using homologous recombination in the human colorectal carcinoma cell line HCT116 [343] reinforced the importance of wt-p53 in $G_2$ progression, by demonstrating that the duration of $G_2$ delay was shortened by the absence of functional wt-p53.

#### 1.5.10.4 Mechanisms of $G_2$ arrest

Progression of $G_2$+M is dependent upon CDK1 which is encoded by the *cdc2* gene [344]. Several of the transcriptional targets of p53 can inhibit CDK1. Briefly, p21

can inhibit CDK1 directly, via inhibition of nuclear localisation [345], as does wee1 by phosphorylating threonine14 and tyrosine15 and preventing the cdc25c mediated dephosphorylation and activation [346], 14-3-3 blocks nuclear localisation of CDK1 gain through the inhibition of cdc25c [347] and GADD45, which causes CDK1 to dissociate from cyclin B1. Repression of both the genes for cyclin B1 and CDK1 by p53 can further inhibit $G_2$+M progression. A further potential mediator of the $G_2$+M arrest is Reprimo [348]. Reprimo is a glycosylated cytoplasmic protein; its expression is induced following cellular exposure to ionising irradiation. Reprimo causes cells to arrest in $G_2$ and over-expression of this protein results in hypo-phosphorylation of CDK1, although the mechanism involved is uncertain.

Another way that p53 may regulate CDK1 is by inhibiting cyclin B1 transcription. Following over-expression of wt-p53, p53 has been shown to bind to a region of the upstream promoter of the cyclin B1 gene, inhibiting cyclin B1 expression and resulting in a reduction in cyclin B1 protein level, hence inhibiting CDK1 activity which is dependent on forming a holoenzyme complex with cyclin B1 [349, 350].

Though CDK1 may be central to wt-P53 induction of $G_2$+M cell cycle delays, it is not the only mechanism by which such delays may occur. Two such CDK1 – independent mediators of $G_2$+M transit may be B99 and MCG10 [351, 352].

### 1.5.11 Conclusion

The role of p53 in mediating progress through the mitotic cell cycle has been studied in great detail. Despite this extensive interest, the involvement of the tumour suppressor gene p53 in the transition of $G_2$+M is still unclear. A growing body of evidence is beginning to suggest that a link between the anti-proliferative effects of p53 and the mitogenic role of the MAP Kinases is significant in cell cycle

progression, not only in $G_1$, but also in $G_2$+M phases of the cell cycle [353, 354]. It may well be that p53 is involved in the checkpoint control mechanisms that ensure the proper timing of cell cycle events through enforcing the dependency of late events on the completion of earlier events [318].

Indeed there is much literature supporting p53-mediation of the $G_1$ checkpoint which can be disrupted in a number of different ways including mutation of the p53 gene [319], by expression of certain cellular or viral proteins that interact with p53 protein that interfere with p53 trans-activation, as well as by other mechanisms that affect upstream or downstream components of the p53 growth control pathway. For example, over-expression of MDM2 protein results in p53-MDM2 interactions and loss of p53-mediated transactivation and $G_1$ checkpoint function in response to irradiation [320]. Cells from individuals with AT show an abnormal response to irradiation; relatively higher doses of irradiation are required for p53 induction [321]. It has been suggested that the ATM gene product is required for the induction of p53 protein. Expression of the human papilloma virus HPV-E6 negates the p53-dependent $G_1$ checkpoint in a number of human cells treated with PALA, $\gamma$-irradiation and actinomycin D [322]. In these models it has been suggested that E6 promotes the degradation of p53. Further studies utilising viruses, in this case the large T antigen of SV40 in IMR-90 demonstrated that though cells still delay in $G_2$, the duration of this reversible delay is reduced [330]. These data highlight a role for p53 in determining cellular response to DNA damage prior to the completion of mitosis.

## 1.6 The proto-oncogene RAF-1

### 1.6.1 Introduction

The importance of the signal transduction pathway incorporating MAP Kinases in the progression and induction of human cancers was suggested when RAS protein was identified as the first human oncoprotein with its gene being a mutated version of a normal H-RAS allele [355]. Effectors of the RAS protein were then sought in an attempt to understand the molecular function and role of this oncogene. The elucidation of RAS as the initiator of a MAP Kinase pathway subsequently followed [356]. Upon stimulation of cell surface receptors by mitogenic stimuli, RAS acts as an effector molecule, conveying the signal at the plasma membrane to the nucleus via a series of complex signal transduction cascades containing many members [357]. One such cascade is the RAF-1/MEK/ERK signal transduction cascade [358].

### 1.6.2 The Raf family

The RAF family of serine/threonine-specific kinases consists, in mammals, of three members, A-RAF, B-RAF and c-RAF or RAF-1. RAF-1 has been shown to be highly conserved [359] and ubiquitously expressed in normal and tumour tissues [360, 361]. Whereas RAF-1 is ubiquitously expressed, the tissue distribution of A-RAF and B-RAF is more restricted. A-RAF is predominately expressed in urogenital tissues [362] and B-RAF in neuronal tissues [363]. In addition, the B-RAF gene encodes several isoforms of B-RAF whose expression is regulated in a tissue-specific manner by alternative splicing [364].

B-RAF has gained prominence in the literature recently because of the relevance in carcinogenesis. Moreover B-RAF has become an important target of anti-cancer

therapy. B-RAF mutations have been reported to be extensive in human astrocyte, melanomas, colon, lung and thyroid cancers [365-372]. With miss-match mutants being identified that dissociates B-RAF from the MEK/ERK signal transduction pathway [373]. Similarly, A-RAF and RAF-1 are implicated in rat cell proliferation [374]. Somewhat contradictory though, not only can over-expression of B-RAF mutants result in an increase in proliferation, but cell cycle arrest has also been observed in several cell types [375], and activated RAF-1 causes cell cycle arrest in small cell lung cancers [376]. Thus the type of RAF expressed, the isoforms, and the tissue that it is expressed in, are instrumental in determining the outcome of RAF involvement in cell cycle regulation.

The ubiquitous distribution of RAF-1 is indicative of a significant role in cellular regulation. The preservation of normal RAF-1 expression in tumours, although sometimes abrogated, suggests a significant role in cell survival as well as in tumour development.

### 1.6.3 MAP kinases and the RAF-1 signal transduction pathway

The mediation of a variety of cellular events is undertaken by protein members of the Mitogen-Activated Protein Kinase (MAP Kinase) cascade. These events are manifest in diverse actions including the induction of cell division [377, 378], differentiation [379], transcription of proto-oncogenes [380] and promotion of tumourogenesis in both *in vitro* and *in vivo* systems [381, 382], as well as, somewhat paradoxically the induction and prevention [383] of programmed cell death and the induction of senescence [384].

The MAP Kinase cascade consists of three enzymes, which undergo serial activation; an example of this is depicted in Figure 4. RAF-1, which acts as a cytosolic signal

transduction factor [385], is a MEK Kinase, a member of a diverse multi-gene family [386]. RAF-1 is the primary member of this MAP kinase cascade. RAF-1 binds to 14-3-3, a specific phosphoserine-binding protein [387], via the amino-terminal region of RAF-1 to former a dimeric complex [388]. This RAF-1-14-3-3 dimer then undergoes oligomerisation to a second RAF-1-14-3-3 dimer produce a quaternary dimeric (dimer of dimers) complex [389, 390]. RAF-1 is then sequestrated from the cytosol to the plasma membrane [391].

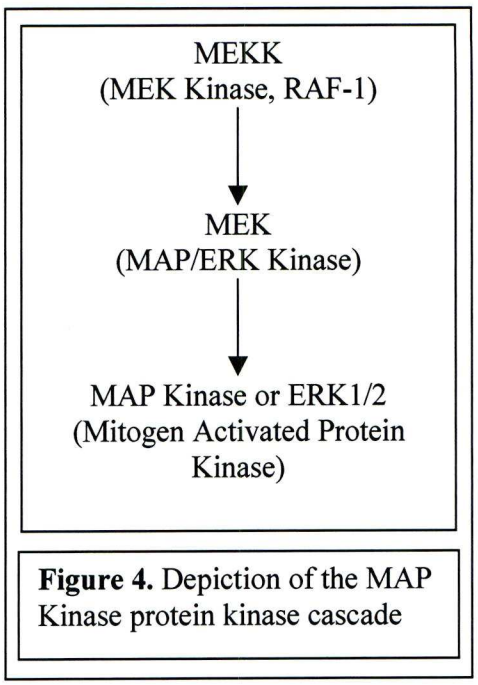


**Figure 4.** Depiction of the MAP Kinase protein kinase cascade

RAF-1 is activated following binding to and phosphorylation by the active tyrosine kinase Gs (GTP-binding, stimulator of adenylate cyclase) [392]. GTP phosphorylation of RAF-1 is carried out by the GTPase, $G_s$ protein, a membrane bound GTPase membrane bound GTPase [393-396].

The RAS binding domain in RAF-1 is located towards the amino terminal, within amino acid residues 51-131 [397], with a secondary site of interaction at residues 139-184 [398], within the conserved cysteine finger motif within the cysteine-rich domain (Figure 6, RAF-1 structure). This secondary RAS interaction site may be responsible for RAS-mediated 14-3-3-RAF-1 complex dissociation [399]. Additional, and as yet uncharacterised phosphorylation-dependent and phosphorylation-independent modifications of RAF-1 activity result in complete activity of RAF-1 kinase function [400]. Activation and indeed inactivation of RAF-1 appears to be regulated by at least seventeen sites as summarised in the Table 5 [400-412].

Activated RAF-1 species then phophorylate and activate the intermediary serine/threonine kinase MEK. This is achieved through the phosphorylation of two serine residues (Ser), Ser-218 and Ser-222 [402].

| Amino Acid | Site of phosphorylation |
|---|---|
| Serine | 29, 43, 58, 218, 222, 228, 233, 259, 289, 296, 301, 338, 339, 494, 497, 499, 619, 621, 624, 642 |
| Threonine | 268, 269, 491 |
| Tyrosin | 340, 341 |

**Table 5.** Summary of phosphorylation sites of RAF-1

RAF-1 is expressed at a relatively low abundance within cells when compared to its target kinase MEK [413]. This feature allows for rapid signal amplification from RAF-1 to MEK1/2, which can in turn be conferred to the subsequent and final member of this cascade, ERK1/2 an effector molecule with many cellular targets. Following phosphorylation of MEK, RAF-1 activity is down-regulated to pre-stimulated levels, levels that are associated with phosphorylation of RAF-1 at Ser-259 [406]and Ser-621/624 [411], re-binding of 14-3-3 to the amino terminus of RAF-1, and recycling of RAF-1 to the cytoplasm [400].

MEK demonstrates a dual specificity with regards to its ERK kinase role, as it phophorylates ERK on both a tyrosine and a threonine residue [414], thus promoting activity [415]. Tyrosine phosphorylation precedes threonine phosphorylation *in vitro* [416], and the phosphorylation of both amino acids is required for full and significant activation of RAF-1 [417].

The activated ERK1/2 are pleiotropic modulators of cell function. The activated MAP kinases exert an influence on gene expression patterns by phosphorylating cytosolic proteins, which trigger target gene transcription. ERK1/2 is also translocated to the nucleus, where ERK1/2 can then affect gene expression both directly and indirectly by phosphorylating several transcription factors [418, 419].

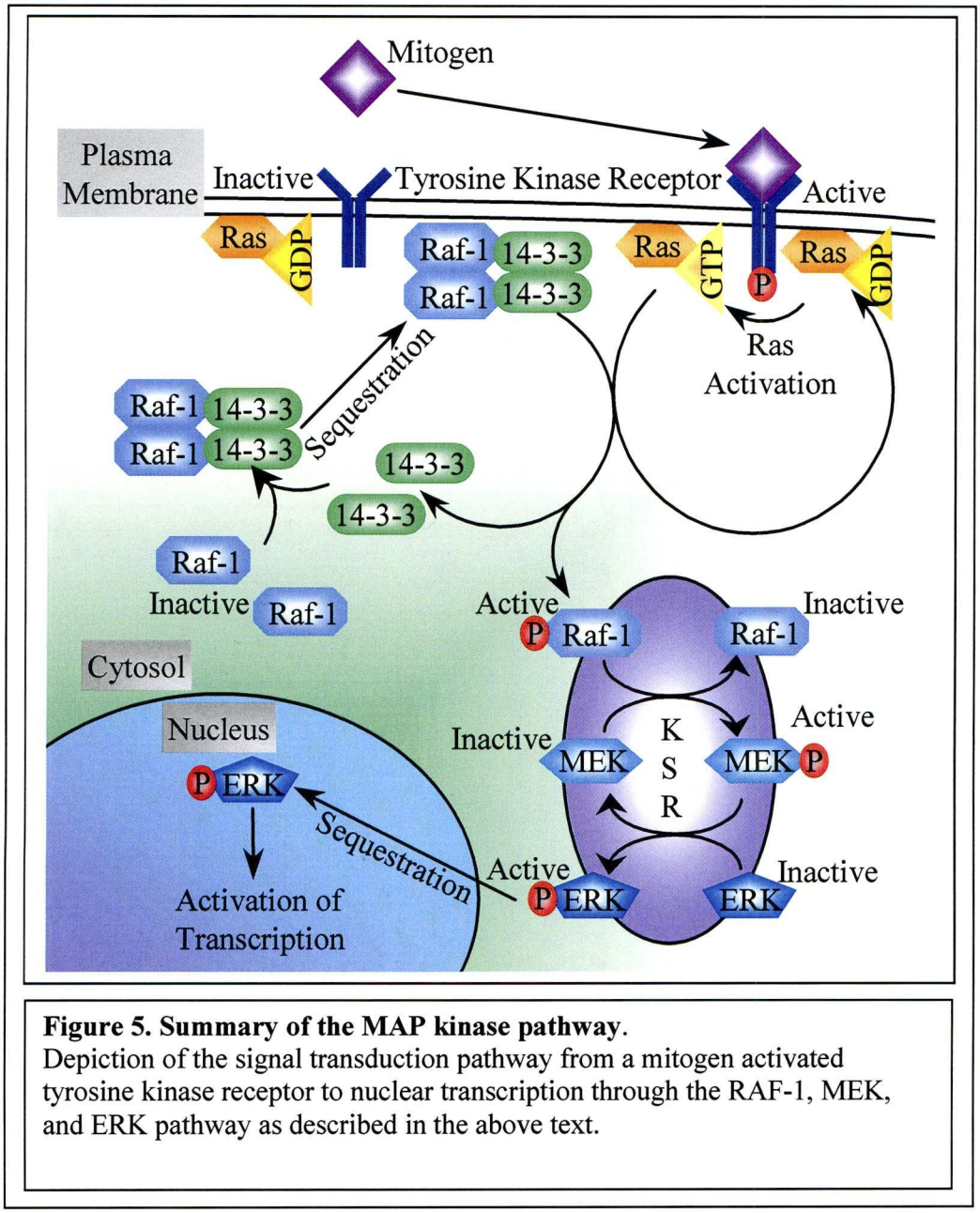


**Figure 5. Summary of the MAP kinase pathway.**
Depiction of the signal transduction pathway from a mitogen activated tyrosine kinase receptor to nuclear transcription through the RAF-1, MEK, and ERK pathway as described in the above text.

The sequential phosphorylation cascade from RAF-1 to ERK is thought to be coordinated by the Kinase Suppressor of RAS (KSR) scaffolding protein. This KSR scaffolding protein holds the three kinases of the MAP kinase pathway in close special proximity, thus facilitating the phosphate relay [420]. This mammalian homologue of the *Drosophila* and *C.Elegans* protein, associates with RAF-1 at the membrane in a RAS-dependent manner. Both RAS and RAF-1 are proto-oncogenes, so it is not surprising to find that this MAP Kinase pathway is principally involved with growth regulation, be it apoptosis, or differentiation, with the biological outcome being determined by the strength and duration of the MAP Kinase pathway activation [421]. Though considerable investigation has been undertaken into the activities of the ERK members of the MAP Kinase cascade [422], it is the primary member of this cascade, the MEK kinase RAF-1 that may prove the most significant determinant for cellular response in radio-sensitivity.

The controls that regulate the MAP kinase pathway activity appear to operate at the level of RAF-1 [423, 424]. The MAP kinase cascade that is comprised of RAF-MEK/ERK MAP kinase is described as a "singularly linear signalling pathway" [425]. RAF-1 demonstrates stronge substrate specificity for MEK both *in vivo* and *in vitro*. Additionally, ERK1/2 is the only identified substrate for MEK [426]. However, several lines of investigation have indicated that RAF-1 may have other effectors in addition to those of MEK/ERK MAP Kinase pathway (See Table 6) [427]. Similarly, several groups have indicated that MEK Kinase activity is not required for RAF-1 activity [428-443], be it in differentiation in neuronal cells [444], or adipocytes [445], or even the induction of apoptosis in cells transformed by viral oncogenes [446].

Though the exact mechanisms by which RAF-1 exerts its influence are complex and still imperfectly understand, it is obvious that RAF-1 is instrumental in determining cellular fate.

| **Substrate** | **Cellular responce** |
|---|---|
| P70 S6 Kinase | Cell proliferation |
| pRb | Cell Cycle regulation |
| p53 | Unknown |
| Tvl-1 | Transcription |
| CK2 | Cell Survival |
| BAD | Cell Survival |
| ASK-1 | Cell survival |
| Cdc25A | Cell Cycle |
| MEK | Proliferation |
| RIP2 | Stress Signalling |
| Bcl-2 | Apoptosis |
| Grb10 | Growth |
| MEKK-1 | Cell proliferation |

**Table 6.** The above table contains a summary of RAF-1 substrates and the effect upon the cell by the RAF-1-substrate interaction.

### 1.6.4 The RAF-1 protein

The RAF-1 gene codes for a 74 kDa cytosolic protein, which is positively regulated by serine/tyrosine phosphorylation [447]. The cytosolic localisation of RAF-1 may be a function of the protein complex formed between RAF-1 and the Heat Shock Protein HSP90. The interaction with the HSP90 chaperone appears essential for RAF-1 stability and function [448]. The structure of RAF-1 is depicted in Figure 6 below. RAF-1 comprises of three conserved regions [449]: CR1 is a regulatory domain containing a zinc finger-like motif homologous to that found in PKC, and is located towards the N-terminal; CR2 is a serine/threonine rich region prompting speculation that this region contains sites of regulator phosphorylation; CR3 is located in the C-terminal region and contains the protein kinase domain [450] which is negatively regulated by the CR2 domain [398, 451].

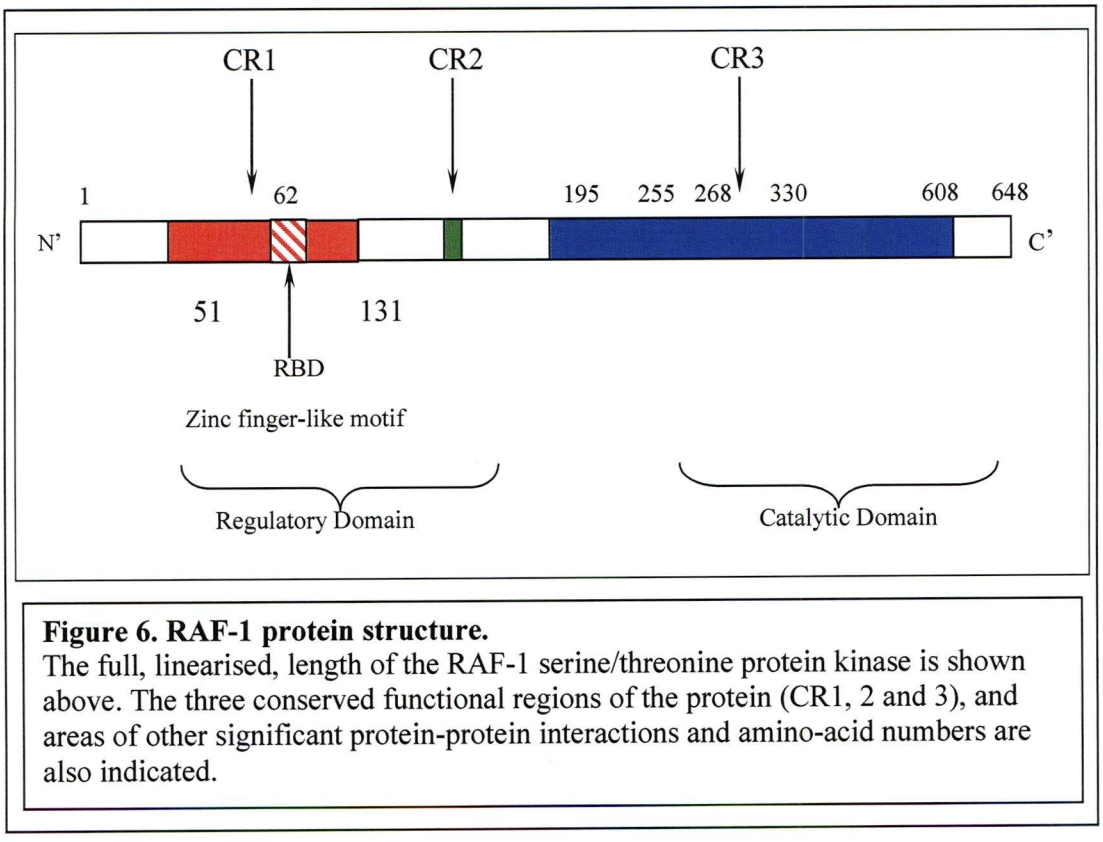


**Figure 6. RAF-1 protein structure.**
The full, linearised, length of the RAF-1 serine/threonine protein kinase is shown above. The three conserved functional regions of the protein (CR1, 2 and 3), and areas of other significant protein-protein interactions and amino-acid numbers are also indicated.

RAF-1 becomes oncogenic as a result of automatous up-regulation of the C-terminal kinase region. A common way in which this can happen is by a partial expression, which results in a truncated 48 KD protein [94]. The binding site of RAS to RAF-1 (RAS binding site-RBD) overlaps the N'-terminal region of CR1: amino acids 51-131 appear to comprise a minimal binding region for activated RAS [452, 453]. The association of the RBD with the RAS effector domain is a high-affinity interaction ($K_D$=20nM) [454], which is mediated primarily by residues Glutamine-66, Lysine 84 and Arginine 89 of RAF-1, with Lysine 84 appearing central to RAF-1 effector discrimination [455]. The secondary RAS binding site within the CRD may mediate RAF-1 interactions with 14-3-3 [399], and a putative lipid ligand [358].

### 1.6.5 Cell cycle regulation by RAF-1

Several mitogenic growth factors stimulate the entry of somatic cells into the cell cycle and subsequent cell division. Exogenous signals, which stimulate cell division via the MAP Kinase pathway, include Epidermal growth factor [456], and PDGF [457].

#### 1.6.5.1 Relationship of RAF-1 regulation in $G_1$

Over-expression of A-RAF, B-RAF, and RAF-1, results in opposing outcomes of cell cycle proliferative response, and appears mediated through the MAP kinase cascade. The RAF-1 MAP kinase signal transduction cascade plays a critical role in the regulation of growth factor-induced cellular proliferation. Cell proliferation has been observed in several model systems, both human and murine, following the over-expression of activated RAF proteins [458, 459]. RAF-1 protein, transcribed under the inducible oestrogen receptor (ΔRAF:ER), have been used to determine the

role of RAF kinases in the cell cycle control of fibroblasts through the regulation of cyclins, CDK's and CDK inhibitors including p21 and p27 [460]. When over-expressed p21 and p27 been shown to inhibit cell proliferation in human fibroblasts [125]. Prolonged strong RAF-1 signalling through the MEK/ERK proteins resulted in significant induction of p21 and cell cycle arrest [460].

### 1.6.5.2 The role of RAF-1 in mitosis

RAF-1 is hyper-phosphorylated on serine residues resulting in RAF-1 activation in a wide variety of cells reguardless of tissue origin [461-463], although ERK is a likely candidate as it demonstrates multiple potential phosphorylation sites [412]. The hyper-phosphorylation retards RAF-1 electrophoretic mobility, although the number of sites, or effect on activity, is uncertain. In Jurkat cells, Lck, a member of the Src kinase family, binds and activates RAF-1 during mitosis. This activation is absent in Lck-negative Jurkat cells [464].

Localisation to the plasma membrane or interactions with 14-3-3 does not appear to be required for RAF-1 involvement in mitosis. However the zinc-finger like motive does appear instrumental for RAF-1 mitotic activations and hyper-phosphorylation, with phosphorylation at either Ser-338 and Ser-339, or Tyrosin (Tyr)-340 and Tyr-341 facilitating activation of RAF-1 in mitosis [465].

### 1.6.6 RAF-1 and cancer

RAF-1 was originally identified as the normal cellular counterpart of *v-RAF* [466], the oncogene of murine transforming sarcoma retrovirus 3611, which encodes a fusion protein comprising the kinase domain of RAF joined to a myristylalated viral gag sequence [467]. Oncogenic RAF-1 has been reported in a variety of cancers, and RAF-1 has been shown to transform erythroid, fibroblasts and epithelial cells [468]. RAF has also been shown to promote transformation when co-expressed with the oncogenes Myc and Hras [469, 470], whilst a number of oncogenes activate the MAP Kinase pathway, which is thought to aid oncogenic transformation [471].

Besides RAS activation, RAF-1 may be activated in a RAS independent manner [399], and though the MAP kinase signal transduction pathway is often considered a singularly linear process, RAF-1 has also been reported to interact with the eukaryotic cyclin dependent kinase cdc25, in particular with cdc25B [436], directly affecting cell cycle progress. RAF-1 may also directly influence cell cycle events through the key proto-oncogene Retinoblastoma protein, and has also been shown to phosphorylate p53 *in vitro* [427].

### 1.6.7 The response of RAF-1 to ionising radiation

RAF-1 localisation and activation has been demonstrated following ionising radiation, to result in sequestration to the plasma membrane. RAF-1 subsequently undergoes tyrosine phosphorylation [472]. RAF-1 has been associated with cellular radio-resistance in several studies. Activation of the ERK pathway following radiation is influenced by both the RAS and p53 status (mutant or wild type) of a given tumour type [473]. RAF-1 has been linked with resistance to radiation in fibroblasts from patients with the Li-Fraumeni syndrome [474] and subsequent transfection of DNA from those cells into NIH3T3 mouse fibroblasts resulted in a RAF-1 linked increase in radio-resistance [475]. Similar transfections were achieved with DNA from a range of radio-resistant squamous cell carcinomas of head and neck origin with the same resultant increase in resistance of the recipient fibroblasts [476]. RAF-1 was further implicated by the use of anti-sense RAF-1 cDNA in the human laryngeal carcinoma cell line SQ20B, increasing radio-sensitivity whilst reducing tumourigenic potential [477]. Furthermore, human bronchial epithelial cells, immortalised with RAF-1 displayed an increased resistance to ionising radiation [478], and antisense oligonucleotides to RAF-1 have been shown *in vitro* and *in vivo* to enhance the radiosensitivity of tumour cells [479]. By contrast, in an extensive panel of 19 Human cancer cell lines representing a variety of malignancies, high levels of RAF-1 protein correlated with radio-sensitivity [480]. Activation of the RAF-1 Map Kinase pathway following irradiation has been found to promote radiosensitivity in some cell types by abrograting the $G_2$+M checkpoint [481, 482].

In addition to playing a role in the activity of the ERK pathway, it is important to note that radiation-stimulated RAF-1 may act upon substrates other than MEK1/2, such as the myosin-phosphatase-binding protein [483]. RAF-1 has also been

proposed to act as an inhibitor of apoptosis signalling kinase 1 (ASK1) by binding to ASK1: the inhibitory action of RAF-1 was reported to be independent of RAF-1 protein kinase activity [435].

# Chapter 2

# Materials and methods

# 2 Materials and methods

## 2.1 Routine culture of the human cancer cell lines

### 2.1.1 Introduction

Six Human cancer cell lines were chosen to reflect a variety of histological types of malignancy and also represent a range of intrinsic cellular radiosensitivities and RAF-1 protein levels as previously determined [480], and it was found that the rate of $G_2$+M exit following radiation induced $G_2$+M delay correlated with RAF-1 protein level and radiosensitivity [481]. It was subsequently established by DNA sequencing that the six cell lines initially chosen to study $G_2$+M delay transition expressed wt-p53, and an additional 13 human cancer cell lines, those used in the 1994 studies, were then screened to select a further 6 cell lines that expressed a mutant-p53 [484]. The cell lines and their histological phenotype are given in Table 7 (page 59). The intrinsic $SF_2$ and $\alpha$ values of their radiation-survival response to ionising radiation as determined by clonogenic assay are shown in Table 8 (page 63), whilst the mutational status of p53 is given in Table 9 (page 64). The culture media required for each of the twelve cell lines used here are given below, and summarised in Table 7.

### 2.1.2 Culture media of the 12 human cancer cell lines

A2780, Colo 320, NCI-H417 (H417) and RT112, were grown in RPMI 1640 (Sigma). NCI-H322 (H322), HEp2, HRT18, HT29.5, I407, MGH-U1, OAW 42 and RPMI 7951 were grown in Dulbecco's Modified Eagles Medium (DMEM) (Sigma). Medium was routinely supplemented with 10% v/v Foetal Calf Serum (FCS) (Serotec), which had been heat-inactivated by incubating at 56°C for 30 minutes (min) before aliquotting and storage at –20°C), and 2mM Glutamine (Gibco). OAW42 culture media was also supplemented with $10\mu g.ml^{-1}$ Insulin (Gibco) and Hydrocortisone (Gibco), whilst RPMI 7951 was also additionally supplemented with Sodium Pyruvate (Gibco) and Non-Essential Amino-Acids (NEAA) (Gibco). Cells were maintained in antibiotic free media as the introduction of any xenobiotic to the cultures might have unforeseen consequences. The histological origins, culture media and original references are summarised in Table 7.

### 2.1.3 Passaging of cancer cell lines

Cells were passaged approximately every 2-3 days to maintain a sub-confluent, asynchronously growing exponential culture. Adherent monolayers were passaged as follows:

The Culture media was pipetted from the flask and discarded into bleach (final concentration greater than 20% v/v) (Domestos). Any residual media was then washed off by the addition of 10ml of PBS, which was pipetted onto the cells. The PBS was then decanted into bleach. Trypsin/EDTA (0.25% w/v porcine Trypsin in PBS supplemented with 0.2 w/v EDTA) was pipetted into each flask. 1ml, 2ml and 3ml of Trypsin/EDTA was sufficient to cover the surface of a $25cm^2$, $75cm^2$ and $162cm^2$ culture flask respectively. The cell monolayer was then coated with a layer

of Trypsin/EDTA by rocking the flask from side to side and the excess Trypsin/EDTA was then decanted.

The culture flask was then transferred to a 37°C incubator for typically less than 6 min, checking approximately every min until the adherent cells had detached from the culture flask. This was confirmed by examining the flask under a microscope.

Once the cells had detached from the culture flask supplemented media was added to the Trypsin/cell suspension and this resultant cell suspension was then pipetted into a 25ml universal tube and centrifuged for 5 min at 200G at room temperature.

The supernatant was then decanted and the cell pellet was resuspended in 10ml of the appropriately supplemented media. 1ml of this cell suspension was then pipetted back into the culture flask along with 5ml, 20ml, or 40ml of supplemented media per $25cm^2$, $75cm^2$ and $162cm^2$ flasks respectively.

For H417, which grows as a cell suspension, the media containing the cells was pipetted into a 25ml universal tube and centrifuged as above. For Colo 320, which grows as a semi-suspension cell line, any attached cells were suspended by tapping the side of the flask until they all detached, as confirmed by examination under a microscope. As with the H417 cell line, the cell suspension was then transferred to a 25ml universal tube and centrifuged as for the monolayer cell lines.

Once pelleted, the supernatant was decanted and the cells were resuspended in 10ml of supplemented media. A cell count was undertaken, and then $2.5x10^6$ cells were pipetted back into a $75cm^2$ culture flask, along with 25ml of supplemented media. The suspension cells were always maintained below $10^6 cells/ml^{-1}$ to ensure exponential growth.

| Cell Line | Histology | Culture media | Reference |
|---|---|---|---|
| A2780 | Ovarian Carcinoma | RPMI+10%v/v FCS | Behrens *et al* [3]; |
| Colo 320DM | Colon Adenocarcinoma | RPMI+10%v/v FCS | Quinn *et al* [5] |
| NCI-H322 | Non Small-cell Lung carcinoma | DMEM + 10%v/v FCS | Gazdar *et al* [6] |
| NCI-H417 | Small-cell Lung carcinoma | RPMI + 10%v/v FCS | Marini *et al* [8] |
| Hep2 | Larynx Squamous carcinoma | DMEM + 10%v/v FCS | Toolan *et al* [9] |
| HRT18 | Rectal Adenocarcinoma | DMEM + 10%v/v FCS | Tompkins *et al* [10] |
| HT29.5 | Colon Adenocarcinoma | DMEM + 10%v/v FCS | Warenius *et al* [14] |
| I-407 | Embryonic Intestinal Epithelium | DMEM + 10%v/v FCS | Henle *et al* [15] |
| MGH-U1 | Bladder Transitional cell carcinoma | DMEM + 10%v/v FCS | Evens *et al* [17] |
| OAW 42 | Ovarian Carcinoma | DMEM + 10%v/v FCS + Insulin + Hydrocortisone | Marshall *et al* [19] |
| RPMI 7951 | Melanoma | DMEM + 10%v/v FCS + Na Pyruvate + NEAA | Deposited in ATCC by G Moore, derived 1971 |
| RT112 | Bladder Transitional cell carcinoma | RPMI + 10%v/v FCS | Marshall *et al* [19] |

**Table 7. The twelve human cancer cell lines utilised in this study**
The culture media, tumour of origin and the reference for the twelve cell lines used in this study are given above.

### 2.1.4 *In situ* staining for mycoplasma contamination of cell lines

Cells were routinely stained to ensure that cultures were kept mycoplasma free. Any cells found to be infected with mycoplasma were discarded and fresh cells removed from liquid nitrogen storage. The staining protocol for mycoplasma detection is given below.

Forceps and $1cm^2$ coverslips were first cleaned with 70% v/v Ethanol in reverse osmosis (RO) water before sterilising in an autoclave for 15 min at pressure of 1 atmosphere and a temperature of 125°C.

Cells from asynchronously growing exponential culture were harvested with Trypsin /EDTA as above. Following centrifugation for 5 min at 200G, $10^4$ cells in 1ml of supplemented media were pipetted onto sterilised $1cm^2$ coverslips that was placed into a 70mm diameter culture dish (Costar) using the sterile forceps. The seeded coverslips were then transferred to a humid, 5% v/v $CO_2$ in air incubator and incubated for approximately 4h at 37°C, with care taken to maintain the meniscus of the cell suspension on the coverslip. After 4h 3ml of supplemented culture media was added to the culture dishes and the cells were left to grow for 2-4 days, or until they were at approximately 50% confluence. The media was pipetted from the culture dish, and the culture plate was then washed twice with 3ml of ice-cold sterile PBS. The cells were then fixed by the addition of 2ml of Carnoy's fixative (75% v/v Methanol (Sigma); 25% v/v Glacial Acetic Acid (BDH)), for 2 min at room temperature. The Carnoy's fixative was then pipetted of the plate, and 2ml of fresh Carnoy's was pipetted onto the coverslip, and left to fix for a further 10 min. The Carnoy's fixative was then pipetted off and the plate was then washed twice with 2ml of ice-cold sterile RO water. The cells were then stained with 100µl of the DNA intercalating dye Hoechst 33254 ($500ng.ml^{-1}$ Stock, from sigma) for 30 min at room

temperature in the dark. The stained cells were then washed twice with ice-cold sterile reverse osmosis water and the coverslip was allowed to air dry for 30 min, in the dark. The coverslip was then mounted cell side down on a glass slide using Buffered Glycerol Mountant. This mountant was prepared by dissolving 2.1g of Citric Acid Monohydrate in 100ml of sterile RO water to make solution A; Dissolving 2.8g of Disodium phosphate in 100ml of sterile RO water to make solution B; and then combining 22.2ml of Solution A with 27.8ml of Solution B with 50ml Glycerol. The pH of this mountant solution was then adjusted to 5.5 using solution A or B as appropriate (A-acidic; B-Alkaline). The cells were then examined on a microscope under UV light through an x60 objective (Leitz), and a x10 eye piece (Leitz).

### 2.1.5 Establishment of a cryogenic bank of cell lines

Early passage cells were cultured as outlined above. With the number of flasks expanded until sufficient cells were in culture to allow 20 vials of cells could be prepared for freezing for each cell line used in the study.

Cells for freezing were harvested as appropriate, as indicated previously and resuspended in complete media at $2x10^6$ cells per ml. An equal volume of complete media supplemented with 20% v/v Dimethyl Sulfoxide (DMSO) was added to the cell suspension and 20 vials of 1ml of $1x10^6$ cells was aliquoted into Cryovials (Nunc). These vials of cells were then transferred immediately to vapour phase of liquid nitrogen for 1h before transferring and storing by immersion in liquid nitrogen until required.

### 2.1.6 Thawing of cryopreserved human cancer cell lines

A cyrovial of cells were thawed by removal from liquid nitrogen and standing the cryovial containing the cells in a type II laminar flow culture hood until the cell suspension had completely thawed, approximately 10 min, before gently pipetting the cell suspension into a $25cm^2$ tissue culture flask. The flask containing the cells was then transferred to a 37°C humid incubator for approximately 4h (or until the cells had attached to the culture flask for monolayer cultures), and the culture media containing DMSO was decanted and replaced with appropriate fresh culture media.

## 2.2 Determination of radiosensitivity and clonogenic survival of twelve human cancer cell lines

### 2.2.1 Introduction

The radiosensitivity of the 12 human cancer cell lines used in this study was determined by clonogenic survival following ionising radiation. This work was undertaken prior to the initiation of my doctoral studies, and formed part of the basis for the rational of the studies I have undertaken. The survival fractions for each of the cell lines that I have utilised in my study are given in the adjacent table (Table 8) and I confirmed that these values held for the cell lines I utilised in this thesis following the establishment of a cell line bank by repeating the clonogenic assay at 2Gy, as outlined below, and testing if the resulting survival fraction matched the values given in Table 8 (as determined by t-test).

| Cell Line | Radiosensitivity | | |
|---|---|---|---|
| | α | SEM | $SF_2$ |
| 2780/735 | 0.525 | 0.05 | 0.299 |
| Colo320 | 0.334 | 0.06 | 0.34 |
| H322 | 0.280 | 0.03 | 0.529 |
| H417 | 0.189 | 0.03 | 0.48 |
| Hep2 | 0.113 | 0.03 | 0.646 |
| HRT18 | 0.411 | 0.04 | 0.412 |
| HT29.5 | 0.189 | 0.04 | 0.589 |
| I407 | 0.230 | 0.04 | 0.539 |
| MGH-U1 | 0.200 | 0.06 | 0.608 |
| OAW 42 | 0.705 | 0.07 | 0.222 |
| RPMI 7951 | 0.111 | 0.03 | 0.56 |
| RT112 | 0.210 | 0.10 | 0.599 |

**Table 8. Clonogenical relevant value α, the standard error of the mean of α (SEM) and the $SF_2$ value for the twelve cell lines utilised in this study**
The α value of each cell line was determined by clonogenic survival calculated following exposure to 0-10 Gy of ionising radiation, and the Survival fraction for each cell line at 2 Gy is given above. Adapted from Warenius et al, 1998 [4].

### 2.2.2 Clonogenic determination of survival fraction for monolayer cultures

Cells were maintained in pre-confluent exponentially growing cultures. For monolayer cultures cells were harvested by trypsinisation as outlined in the section on Passaging of Culture Cells (see above). This involved pipetting of the culture media and then washing the flask with 10ml of sterile PBS. This PBS was then pipetted of, and 2ml of Trypsin in Versene (1mM EDTA in PBS) was pipetted onto the cell monolayer. The culture flask was then incubated for approximately 5 min, until the cells were seen to have detached from the culture flask when observed under a microscope. Once the cells had detached from the flask 10ml of supplemented HAMS F12 (containing 10%v/v FCS, and 10mM L-Glutamine, along with any additional supplementation recommended for the culture of that cell line, as summarised in Table 2.1) was added to the flask. The resultant cell suspensions were then pipetted into a 25ml universal tube and centrifuged at 200G for 5 min at room temperature.

Following centrifugation the supernatant was decanted. Gentle flicking of the universal was then used to disrupt the cell pellet. The

| Cell Number Per ml | Exposed Dose of γ-Irradiation |
|---|---|
| $10^2$ | 0 Gy (Control) |
| $10^2$ | 1 Gy |
| $10^2$ | 2 Gy |
| $5x10^2$ | 0 Gy (Control) |
| $5x10^2$ | 3 Gy |
| $5x10^2$ | 4 Gy |
| $10^3$ | 6 Gy |
| $10^3$ | 7 Gy |
| $5x10^3$ | 8 Gy |
| $10^4$ | 9 Gy |
| $5x10^4$ | 10 Gy |

**Table 9. Cell dilutions and dose of radiation received for clonogenic determination of survival fraction**

The above Table contains the typical cell dilutions utilised for clonogenic assays.

cells were then resuspended in a known volume of supplemented HAMS F12 media and a cell count of the number of cells per ml was obtained using a Neubauer improved haemocytometer. Cell suspensions of $10^2$ to $5x10^4$ cells per ml were then prepared by serial dilution, again in supplemented HAMS F12.

The cell suspensions were then exposed to increasing doses of radiation over a range of 0-10 Gy from GammaCell 1000 (Atomic Energy of Canada Ltd, Ottawa, Canada) utilising a $^{137}Cs$ source. The GammaCell 1000 utilises a linearised $^{137}Cs$ source to irradiate the cells on a revoling platform designed to give a uniform dose to the cells within the irradiation chamber. The irradiated cells were then plated in six well plates sufficient colonies formed in each well to be able to determine the surviving fraction at each dose. 1ml of the appropriately irradiated cell suspension along with 3ml of supplemented HAMS F12 was then pipetted into each of the six well plates, such that the final volume of media in each well was 4mls. Each cell concentration and radiation dose was plated in triplicate with triplicate wells of un-irradiated, control cells being prepared for the two cell densities of $10^2$ and $5x10^2$, to allow the determination of plating efficiency for each assay. This percentage plating efficiency was then used when calculating the true surviving fraction of cells at each dose, as indicated in Figure 7. The seeded six well plates were then incubated at 37°C in 5%v/v $CO_2$ in air for 10-14 days to allow the colonies of surviving cells to grow without merging with neighbouring colonies.

### 2.2.3 Clonogenic determination of surviving fraction of semi-adherent and suspension human cancer cell lines

The Small Cell Lung Carcinoma H417 is a suspension culture, whilst the Colon Adenocarcinoma Colo 320 grows as a semi-adherent culture. Colo 320 can be suspended by gentle tapping of the culture flask. At this stage the H417 and Colo 320 could be handled in the same manor. 10ml of the cell suspension was removed by pipetting, and transferred to a 25ml universal. The cells were centrifuged, and cell number was determined as above for the monolayer cultures (2.1.3). As these cells grow in suspension, there clonogenicity was determined using the Courtenay technique [485, 486].

### 2.2.4 Staining and counting of clonogenic assays

Following incubation for 10-14 days at 37°C, the media from six well culture plates was then decanted and the cells in each well were fixed by the addition of 2ml of 70%v/v Ethanol in RO water overnight at room temperature. The 70%v/v Ethanol in water was then decanted of and the fixed colonies were stained by the addition of 10%v/v Giemsa in Ethanol for 1h at room temperature.

The Giemsa was the pipetted of and retained for subsequent staining, and excess stain was rinsed of with water and run to waste. The Plates were then allowed to air-dry overnight.

Colonies of greater than 50 cells, which represent a single cell undergoing greater then seven exponential doublings, were then counted and the surviving fraction of cells at each dose was then determined. The choice of 50 cells is such that any colony formed is as a result of an irradiated cell possessing a long-term proliferative survival

capability, as demonstrated by Terasima and Tolmach in 1963 [25] with time lapse photography and reviewed by Okada [487].

Each cell line was assayed in triplicate, with each dose and cell concentration undertaken in triplicate in each assay. The mean of the triplicate assays was determined, and the mean of the means for each of the triplicate assays was then determined.

### 2.2.5 Calculation of clonogenic survival

Survival fraction for each dose was determined as demonstrated in Figure 7B, with the plating efficiency being calculated from the control plates as shown in Figure 7A.

The plating efficiency at $10^2$ and $5x10^2$ was used to determine the surviving fraction for the irradiated cells plated at these two plating efficiencies. The average plating efficiency for the cells at $10^2$ and $5x10^2$ was then used as the plating efficiency for cells plated at $10^3$ through $5x10^4$, in determining the survival fraction at doses of 5-10 Gy.

From the determinations of the Surviving Fractions for the doses employed, a curve of best fit was then generated using the linear quadratic equation given in part C of Figure 7, by a method of non-linear least-squares regression analysis [488]. The interpolated value of $\alpha$ represent the initial slope prior to the 'shoulder' that is typical of a dose response curve, and is indicative of a single hit mode of cell killing, whilst $\beta$ represents cell death as a result of multiple radiation induced cell lesions (See Figure 8).

A) Plating Efficiency

$$Plating\ Efficiency\,(P.E.) = \frac{Average\ No.of\ Colonies\ Counted}{No.of\ Cells\ Plated\ Per\ Well}$$

i.e. For an average number of colonies from three wells of 81 in the control un-irradiated plated at 100 cells per well;

$$P.E. = \frac{81}{100} = 0.81$$

B) Surviving Fraction

$$Surviving\ Fraction\,(SF_D) = \frac{Average\ No.of\ Colonies\ Counted}{No.of\ Cells\ Plated \times P.E.}$$

i.e. For an average number of colonies from three wells of 36 colonies/clones in the plate where the cells have been exposed to 2 Gy of γ-radiation ($\therefore D$=2), and with a Plating Efficiency of 0.81 then;

$$SF_2 = \frac{36}{100 \times 0.81} = 0.4\,44$$

C) Linear Quadratic Dose Response Curve

$$SF_D = \exp(-\alpha D - \beta D^2)$$

**Figure 7 Determination of the surviving fraction** The above equations demonstrate the hypothetical surviving fraction of cells exposed to 2 Gy of γ radiation given a plating efficiency of 81% at a platting density of 100 cells per well in a six well plate. Part A) depicts the determination of Plating Efficiency P.E., whilst part B) depicts the determination of Surviving Fraction at 2 Gy, $SF_2$. Part C demonstrates the linear-quadratic equation used to 'fit' the line of best fit to the Surviving Fraction data.

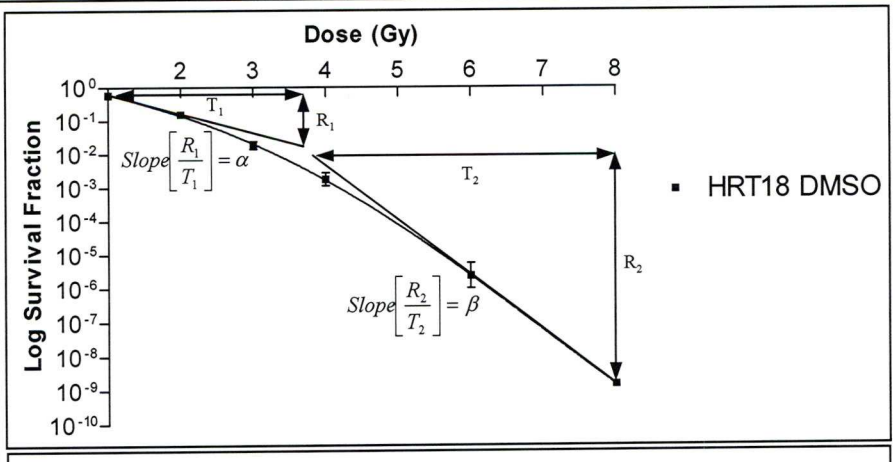


**Figure 8. Post-irradiative clonogenic survival in the human cancer cell lines HRT18 following pre-incubation with the organic solvent DMSO**
The depiction of the alpha and beta constants of the non-linear quadratic equation that is used to fit the logarithmically transformed data obtained from post-irradiative clonogenic survival curve is shown above.

## 2.3 Determination of $G_2$+M cell cycle delay following 2 Gy of γ-radiation

### 2.3.1 Plating of cells for the determination of $G_2$+M delay

All experiments were carried out on asynchronous, exponentially growing, mycoplasma-free cultures, which were maintained as outlined in section 2.1. Cells were plated out in 25cm$^2$ tissue culture flasks (Costar) at a density of 1.5-2.0 x $10^5$ per flask. The optimum density was determined for each line by culturing the cells for the period of the proposed experiment and ensuring that cells had enough room to divide unhindered, i.e. were still growing as a pre-confluent culture.

Samples were taken every 2h for a period of 24h. Thus thirteen time points were undertaken for each experiment of 0, 2, 4, ... and 24h. Each sample was done in duplicate for both irradiated and control samples, i.e. four flasks per time point, and 52 flasks per experiment. Each time course for each cell line was undertaken in triplicate.

On the day before the experiment, cells were plated out in 5ml of normal culture medium. For each time point a flask for irradiation and a control flask were seeded and incubated at 37°C in an atmosphere of 5%v/v $CO_2$ in air. Once the cells had attached to the culture surface, confirmed by visual inspection using a microscope, flasks were completely filled with normal medium containing 20mM HEPES and incubated at 37°C overnight prior to irradiation.

### 2.3.2 Irradiation of cells for determination of $G_2$+M delay

Cells were irradiated using a $^{137}Cs$ GammaCell-1000 unit (Atomic Energy of Canada Ltd., Ottawa, Canada) and given a dose of 2 Gy at a dose rate of 3 Gy per min. In order to ensure an even radiation dose, flasks were irradiated full of medium, 4 at a time due to space limitation of the source utilised, and the empty space in the canister was filled with bolus (Boots, Nottingham, U.K.). Care was taken to minimise thermal shock by transporting the flasks to the irradiation source in polystyrene boxes containing sand, which had been pre-warmed to 37°C. As well as the flasks being irradiated, the controls were also taken for 'sham-irradiation', thus ensuring that the effects of removing the culture flasks removal from the incubator were accounted for when determining cell cycle delay. All flasks were returned to the incubator immediately and cultured at 37°C following irradiation.

### 2.3.3 Harvesting of cells following γ-radiation for flow cytometric analysis

For monolayer cultures, the medium was decanted from the culture flask and the culture flask was then rinsed by the addition of 5ml PBS, which was then decanted. Cells were then harvesting using 1ml Trypsin/EDTA at 37°C for approximately 5 min. Once the cell monolayers had detached, as determined visually by microscope, 1ml of heat inactivated FCS was added to the cell suspension to prevent over-trypsinisation of the cells. 2ml of PBS was added to each flask and the resultant cell suspension was pipetted into a 4ml Falcon tube (Becton Dickinson).

For the suspension cell line H417, trypsinisation is unnecessary. The post-irradiated suspension cell culture was transferred directly from the culture flask to the 50ml Centrifugation tubes. This cell suspension was then centrifuged for 6 min at 250G at

4°C. The supernatant was then decanted and the cell pellet was resuspended in 4ml of ice cold sterile PBS. This cell suspension was then pipetted into a 4ml Falcon tube. Similarly, to harvest the semi-suspension Colo 320 culture, tapping the flask was sufficient to detach the any adhered cells from the culture flask surface to generate a cell suspension. This cell suspension was then handled as per the H417 cell lines.

Cell suspensions were then centrifuged at 200G for 5 min at 4°C. The supernatant was then aspirated and the cell pellet resuspended by gentle agitation, and the addition of 4ml of PBS. The centrifugation was repeated. The supernatant was then aspirated to leave approximately 200µl of PBS in each tube, and the cell pellet was resuspended by initial gentle agitation and then by repeatedly passing the cell suspension through a p200 Gilson pipette tip to achieve a single cell suspension. The cell suspension was then fixed by the addition of 4ml of ice cold 70% v/v ethanol in RO water and stored at 4°C. Samples could be stored for several months without affecting the quality of the results of the flow cytometric analysis.

### 2.3.4 Propidium Iodide (PI) staining of ethanol fixed cancer cells for flow cytometic analysis

Cells that had previously been fixed in 70% v/v ethanol in water at 4°C for a minimum over night period were pelleted by centrifugation at 250G for 5 min at room temperature. The supernatant was then aspirated and the pellet resuspended in 4ml sterile PBS. The samples were then centrifuged as above and the supernatant was again aspirated to leave the pellet and approximately 200µl of supernatant. The cells where then resuspended in the residual PBS initially by agitation, and then by repeated passing through a p200 pipette tip to give a single cell suspension as

confirmed by microscopy. 500µl of PI solution, containing 100µg/ml RNase A (Sigma) and 20µg/ml PI (Sigma), both in sterile PBS, was then added to each sample. Samples were incubated at 37°C in the dark for 30 min.

### 2.3.5 Flow cytometric analysis of PI post-irradiation samples

Following incubation in PI solution, samples were analysised on a FACScan Fluorescence Activated Cell Analyser (Becton Dickinson). Stained cell suspensions are passed perpendicularly through the beam of a 488nm Argon air-cooled laser utilising fluid dynamic focusing. The reflected and refracted light produced as the cells intersect the laser beam is collected and used to 'gate' the cell population from debris (see Figure 9).

The emitted light from PI fluorochrome used to stain the genomic DNA was then collected via a Photo Multiplier Tube (PMT) on the FL3-channal utilising a 590nm long-pass filter (Becton Dickinson). This red fluorescent feature was used to 'threshold' the flow cytometic data to further eliminate debris. This was achieved by adjusting the gain-settings and the PMT voltage such that the mean $G_1$ peak was displayed at channel 200 on a linear scale. It should be noted that the PMT-voltage was always used at the linear range of 300-900 volts, with the Gain-settings adjusted to utilise this range. 1 x $10^4$ events were then captured and recorded in real-time using List-mode data acquisition of the Consort 32 computer system running LYSIS II data package.

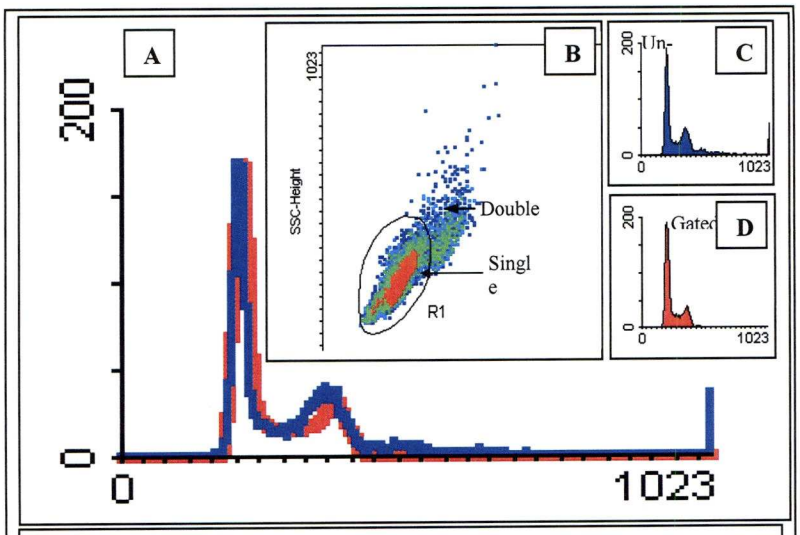


**Figure 9. The gating protocol for the analysis of PI-labelled ethanol-fixed human colonic cancer cell HT29.5** Initially the threshold value is set at 100 on the red channel (PMT3), to collect whole cells, and the Region R1 is used to eliminate any doublet cells by density plot of light scatter (Panel B). The un-gated PI distribution is shown in the frequency plot of DNA content, panel C, with the gated PI population in panel D. The comparative overlaid view of gated (red), and un-gated (blue) is shown in panel A.

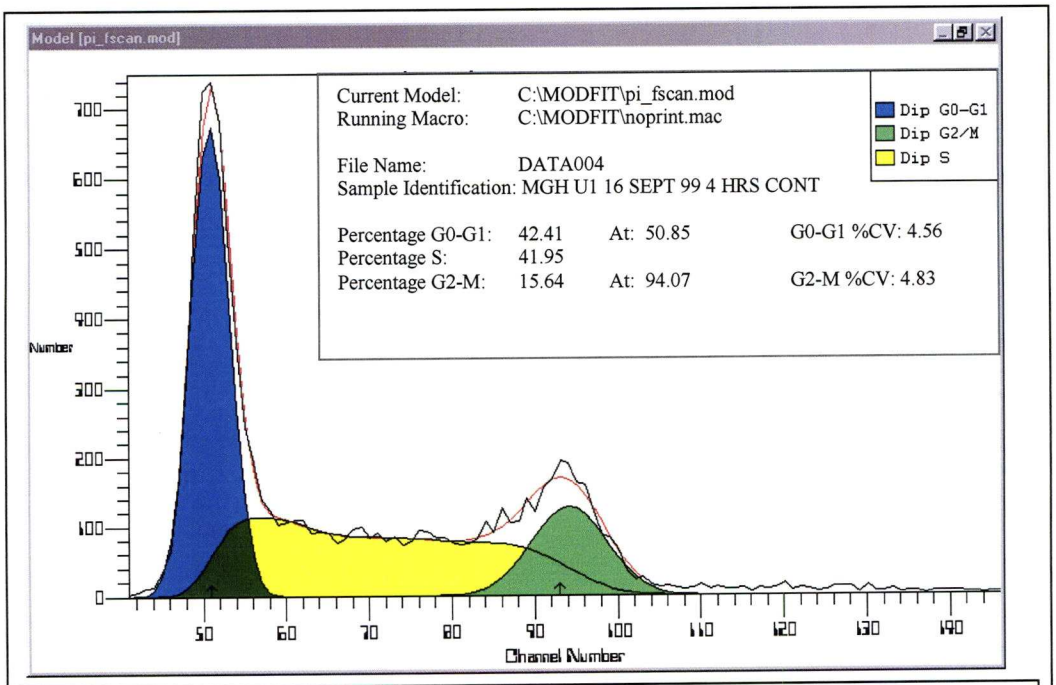


**Figure 10. Determination of cell cycle distribution for flow cytometric data** The above histogram is the frequency plot of cell fluorescence following staining of ethanol fixed MGH-U1 4h control cells with PI. The mathematical modelling program ModFit was used to 'fit' curves to the above histogram such that the cells distribution throughout the cell cycle can be determined.

### 2.3.6 Analysis of flow cytometric data

List-mode data was translated into MS-Dos using HP-Lif to Dos converter, DataMate2.0 (Dako).Determination of cell cycle distribution of the analysed samples was then undertaken using the mathematical modelling program ModFit cell cycle analysis software (Verity, Topsham, ME, U.S.A.). DNA histograms were fitted with a model, which calculated the relative distribution of cells in $G_1$, S and $G_2$+M phases of the cell cycle. The model used was primarily as indicated below in Figure 10. Both $G_1$ (blue) and $G_2$+M (green) peaks were fitted with Gaussian curves. ModFit automatically locates the $G_1$ peak (from a pre-determined estimate value) and then uses a 'multiplier' to determine the location of the $G_2$+M peak. The S-phase boundaries are then determined from the location of the $G_1$ and $G_2$+M population peaks, and are fitted with three rectangular curves (yellow curve). The areas of the curves defining these three populations are then used to calculate the percentage of cells in each cell cycle population. The red line on the graph depicts the mathematically modelled distribution of the cell population from the histograms fitted to the cell data.Only samples that gave a $G_1$ and $G_2$+M Coefficient of Variance (CV) of less than 9 were analysised. The CV of these Gaussian curves is calculated indicated in Figure 11.

A)

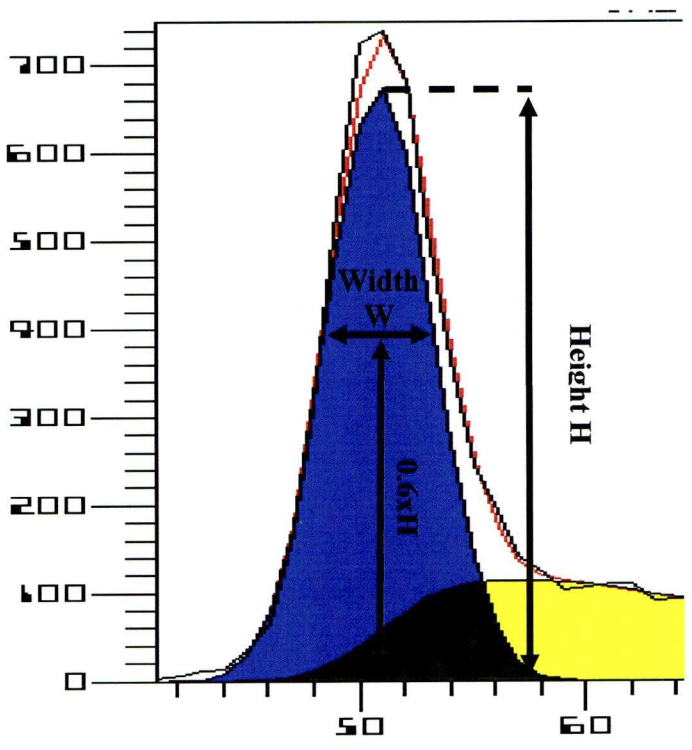


B) Determination of the coefficient of variance for a given distribution is:

$$CV = \frac{CurveHeight\ H}{Width\ W}$$

Where H is the height of the curve, and W is the width of the curve at 0.6 of the curve height (0.6xH).

**Figure 11. Determination of the CV** The CV for a given curve, as represented in panel A), is determined as calculated in panel B).

### 2.3.7 Quantification of the duration of $T_{50}$ following $G_2$+M cell cycle accumulation

Exit from $G_2$+M accumulation was specified as the time taken from maximal $G_2$+M phase accumulation (peak value from which the maximum percentage of cells in $G_2$+M phase begins to decrease) to the point at which the percentage of cells in $G_2$+M has decreased to 50% of this value [479]. This duration is referred to as the $T_{50}$ value for each cell line. This method of quantitation is similar to that described by Cheong *et al.* [168].

Figure 12 depicts examples of $T_{50}$ determinations as used in Warenius *et al.* [481]. The graphs of the percentage cells that had accumulated $G_2$+M were produced using GraphPad Prism version 3.02 (GraphPad Software Incorporated). The percentage of cells in each part of the cell cycle as determined using ModFit were entered into the Graphpad Prism, and the percentage of cells present in each phase of the cell cycle for the controls was subtracted from the matched irradiated samples and plotted as below along with the calculated ± SEM. GraphPad Prism provided coordinate positions in cm. I utilised this function to measure precisely the exact height of the $G_2$+M population by 'drawing' lines directly onto the graph, and noting the line start and end position as given by GraphPad Prism. The length of the x and y-axis was set to 5cm and 4cm respectively. Thus the mid-point of the $G_2$+M accumulation plot, and subsequently the duration of the exit time $T_{50}$ was determined by drawing in a line from the time of maximum accumulation started to decrease to where this line intercepted the downward slope of the graph (as indicated in Figure 12A). The length of this line could then be determined from the start and end position of the line, as given by GraphPad Prism, and hence the $T_{50}$ time could be calculated (as indicated in Figure 12B).

**A) Accumulation of cells in $G_2$+M following irradiation**

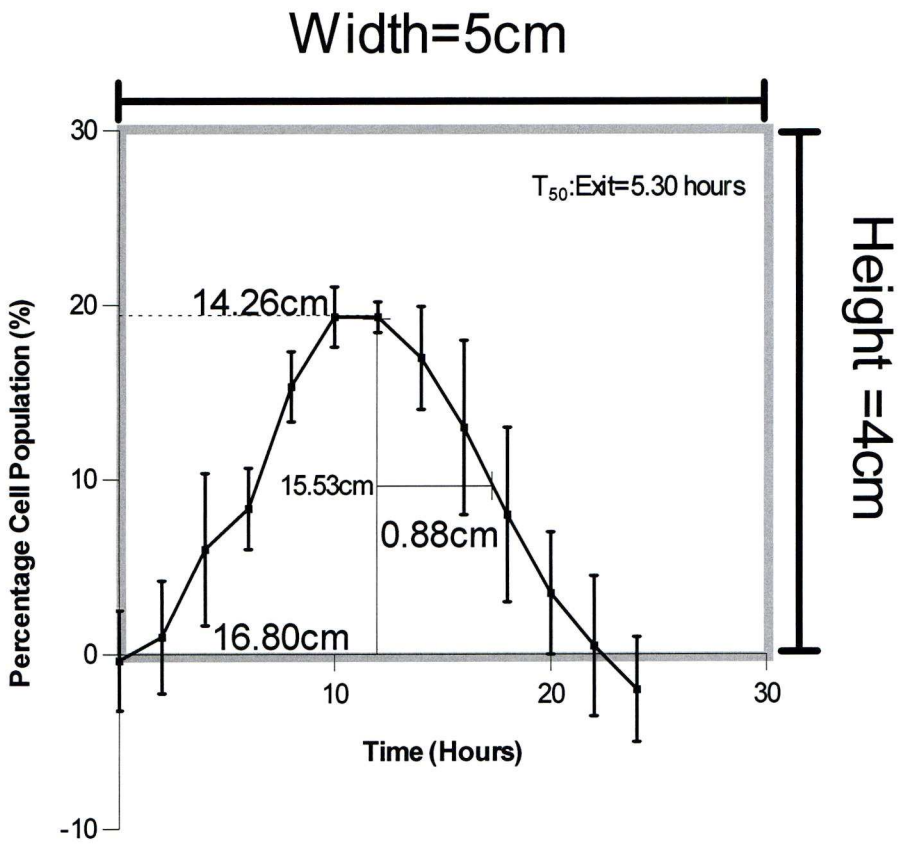


B) Calculation of $G_2$+M Exit ($T_{50}$)

X-axis duration is 30h, which has a length of 5cm, thus:

$$1\ hour = \frac{5\ cm}{30\ hours} = 0.167\ cm.hours^{-1}$$

Length of $T_{50}$ is 0.88cm, therefore:

$$Duration of T_{50} = \frac{0.88 cm}{0.167 cm.hour^{-1}} = 5.3 hours$$

Thus the duration of $T_{50}$ for I407 following 2Gy of ionising radiation is 5.30h.

**Figure 12. Determination of $G_2$+M exit in human cancer cell lines** The above figure contains an examples of the $T_{50}$ determinations of $G_2$+M exit for human embryonic cell line I407 following exposure to 2Gy of ionising radiation. Panel A shows the percentage of cells accumulation in $G_2$+M, whilst panel B demonstrates how the $T_{50}$ was calculated.

## 2.4 Determination of protein expression levels by western blotting

### 2.4.1 Preparation of cell lysates

Cancer cell lines were grown in asynchronous exponential cultures as described previously. For monolayer cell cultures, the media was decanted into bleach and the culture flask was then washed by pipetting ice cold sterile PBS into the culture flask, and gently tilting the flask from side-to-side, before the PBS was decanted into bleach. 2ml of trypsin/EDTA was then pipetted onto the cells and the culture flask was then incubated at 37°C. The flasks were checked microscopically approximately ever 2 min to determine whether the cells had detached from the culture surface. Once the cells had detached 8ml of ice cold PBS was pipetted onto the cell/trypsin suspension and the resultant cell suspension was then pipetted into a 25ml universal tube and centrifuged for 5 min at 200G at 4°C. The supernatant was then decanted and the universal tube was gentle flicked to disrupt the cell pellet. 10ml of ice cold PBS was then pipetted onto the cells. A 10µl aliquot was then taken with a Gilson pipette and the cells loaded onto an improved Neubeuer haemocytometer and a cell count undertaken. The universal containing the counted cell suspension was then centrifuged as above. The supernatant was again decanted and the universal tube left inverted for 1 min to drain off any excess PBS. The universal was then righted, capped, and the tube flicked to disrupt the cell pellet. One 'Complete-mini-protease-inhibitor-cocktail-tablet' (Roche) was dissolved in 10ml of lysis buffer (1%w/v SDS, 0.8% v/v glycerol, 50mM Tris pH 6.8 in elga water) and then 1ml of this lysis buffer with protease inhibitors was added to the cell slurry per $3x10^7$ cells. The cell lysate was then sonicated on ice for 10s. The sonicated lysates were then left to stand on ice for 5 min. The cell lysate was then transferred to a sterile 1.5ml eppendorf tube and centrifuged in a chilled rotor at 20,000G for 30 min at 4°C. The centrifuged lysates

were then aloquated into 100µl aliquots in sterile 0.5ml eppendorf tubes and stored at –70°C.

### 2.4.2 Determination of protein concentration of cell lysates

The protein concentration of cell lysates was determined using the 'MicroBCA-Protein-Kit' (Peirce). This method employs bi-chromic acid to stabilise the transition of $Cu^{2+}$ to $Cu^{1+}$ in the presence of reducing amino acids.

A standard curve was prepared from the provided 1mg.ml$^{-1}$ ampoules of bovine serum albumin (BSA), as indicated in Table 10A. A BSA stock was produced from an initial dilution of the BSA in lysis buffer stock (standard diluent, 1 in 125 lysis buffer in sterile RO water) in 1.5ml eppendorf tubes; each sample was undertaken in duplicate.

The cell lysates to be assayed was initial dilution by 1 in 125 in sterile RO water to produce a sample stock. This sample stock was then diluted further in sterile RO water to give 600µl at a final concentration of 1 in 250, 1 in 500, 1 in 750 and 1 in 1000, as indicated in Table 4.

The BCA colourimetric reagents were then prepared as indicated in the instructions, with 50 parts of A;

**A) Preparation of standard curve**

| Protein content (µg.ml$^{-1}$) | Volume of BSA stock (µl). | Volume of standard diluent (µl) | Volume of sterile RO water (µl). |
|---|---|---|---|
| 0 | 0 | 300 | 300 |
| 1.0 | 12 | 300 | 288 |
| 2.5 | 30 | 300 | 270 |
| 5.0 | 60 | 300 | 240 |
| 10.0 | 120 | 300 | 180 |
| 15.0 | 180 | 300 | 120 |
| 20.0 | 240 | 300 | 60 |
| 25.0 | 300 | 300 | 0 |

**B) Dilution of cell lysate to be assayed**

| Sample dilution | Volume of sample stock (µl). | Volume of standard diluent (µl). | Volume of sterile RO water (µl). |
|---|---|---|---|
| 1 in 250 | 300 | 0 | 300 |
| 1 in 500 | 150 | 150 | 300 |
| 1 in 750 | 100 | 200 | 300 |
| 1 in 1000 | 75 | 225 | 300 |

**Table 10. Preparation of standard curve and cell lysate dilutions for determination of protein concentration** To determination the protein concentration of cancer cell lysates, the above standard curve and cell lysate dilutions were undertaken.

49 parts B; and 1 part C, being combined before 600µl of this mixture being added to each sample. Enough colourimetric reagents were mixed to do all the samples, the standard curve, plus five additional tubes for surplus (i.e. 3ml).

The sample/BSA reagents were then incubated at 70°C for 30 min in a pre-heated water bath. Following incubation, the samples were then removed and allowed to cool to room temperature. The sample mixture was then decanted into a 1ml plastic cuvette and the optical density (O.D.) at 560nm was determined using a bench top spectrometer.

The range of dilutions of BSA used was such that a standard curve of 0-1.0 O.D. units was produced. This standard curve was then analysed by linear regression using Microsoft Windows Excel by plotting the O.D. on the ordinate, against protein concentration on the abscissa. Only the sample dilution who's O.D. fell within this linear range of the standard curve were used to calculate the protein concentration of each cell lysate assayed, by interpolation from the linear regression equation. The average of the appropriate dilutions was then taken, and the concentration of each protein determined in $mg.ml^{-1}$.

### 2.4.3 Polyacylamide Gel Electrophoresis of total cellular protein

Laemmli buffered discontinuous sodium docecyl sulphate- polyacrylamide gel electrophoresis (SDS-PAGE) was employed to separate proteins by size homogenous cell lysate solution. The buffers utilised are listed below.

#### 2.4.3.1 Buffers

0.5M Tris; pH 6.7 was prepared by blending the prepared solutions of 0.5M Tris-HCl, with 0.5M Tris-base to produce the required pH.

1.5M Tris; pH 7.4, was produced by blending the prepared solutions of 1.5M Tris-HCl with 1.5M Tris-base to produce the required pH.

10% w/v Sodium dodecyl sulphate (SDS); 10g of SDS was dissolved in 90ml of Sterile RO water. Once dissolved the final volume was made to 100ml.

Tris buffered saline (TBS) was prepared by dissolving 50mM Tris base and 150mM sodium chloride in 900ml of RO water. The pH was then adjusted to 7.6 by the addition of concentrated hydrochloric acid (HCl). The volume was then made to 1L.

Tris buffered saline with Tween-20 (TTBS); Tween-20 was added to TBS to give a final concentration of 0.1% v/v Tween-20.

Loading buffer; 10% v/v glycerol, 1% w/v SDS, 62.5mM Tris in RO water with the pH adjusted to 6.8 with HCl

40% w/v Acrylamide solution ethanol free (BDH)

4% w/v Bis-acrylamide solution ethanol free (BDH)

### 2.4.3.2 Sample preparation for polyacrylamide gel electrophoresis

Whole cell lysates prepared as indicated previously were first fully thawed at room temperature before diluting to 1.5mg.ml$^{-1}$ with loading buffer. 5µl of a 10% w/v bromophenol blue and 15µl 2-mercapoethanol were added to each 150µl of diluted lysate to be loaded. The samples were then denatured by heated to 95°C for 5 min before being allowed to cool to room temperature. 50µl of this denatured cell lysate solution was then loaded into each lane of the gel. Empty lanes were loaded with 50µl of loading buffer containing 0.3% w/v bromophenol blue and 10% 2-mercaptoethanol.

### 2.4.3.3 SDS-PAGE

Denatured linearised whole cell protein lysates were electrophoretically separated on vertical discontinuous SDS-PAGE gels. The discontinuous gel consisted of a 4% w/v polyacrylamide with 2.6% cross-linker at pH 6.8, and the resolving gel utilised was a 10% w/v polyacrylamide gel with 2.6% cross-linker at pH 8.8 were run on a 'Protein II' electrophoresis 16x16cm gel system (Bio-Rad).

### 2.4.3.4 Blocking of membranes

Following blotting, the nitrocellulose membrane was removed from the blotting cassette using ethanol cleaned forceps, and transferred to a stainless steel tray containing 40ml of TBS. The membrane was then washed for 5 min at room temperature on a rocking platform. The TBS was then decanted and 40ml of TTBS was pipetted into the tray and the membrane was washed for a further 5 min. The TTBS was then decanted and replaced by 40ml fresh TTBS and the wash repeated. The second TTBS was then decanted and the nitrocellulose membrane was then

blocked in decanting 300ml of 5% w/v marvel in TTBS into the tray for 1h at room temperature, ensuring that the membrane was covered at all times.

### 2.4.3.5 Antibody probing of electrophoretically blotted proteins

The electrophoretically acrylamide-gel separated proteins were measured using a two-stage 'sandwich' antibody staining technique. 'Blocked' nitrocellulose membranes were initially probed with commercially available primary antibody generated to the proteins of interest.

Following blocking the blocking buffer was decanted and 40ml of TTBS was pipetted into the tray containing the membrane. The membrane was then washed for 5 min at room temperature on a rocking platform. The TTBS was then decanted and 40ml of fresh TTBS was pipetted into the tray. The wash was then repeated, followed by a third repeat wash in TTBS.

The third TTBS wash was then decanted and the membrane was transferred to a plastic bag using ethanol cleaned forceps, where it was then probed with the appropriate antibody to either p53 (clone DO-1, Santa Cruz at 1 in 1000), RAF-1 (clone 1H4, Abnova at 1 in 500), or pan-actin (C-2, Santa Cruz at 1 in 1000)(loading control) in 10ml of 5% w/v Marvel in TTBS at the appropriate dilution and sealed using a bag sealer, and incubated under an up-turned tray to protect the membrane and exclude light. Air-bubbles were squeezed out of the bag immediately prior to sealing to ensure that all of the membrane could be exposed to the primary antibody solution.

The bags containing the probed membranes were then carefully cut using a scalpel, the probing solution was decanted and the membrane was removed from the bag using ethanol-cleaned forceps, and transferred to a stainless steel tray containing

40ml of TTBS. The membrane was then washed for 5 min at room temperature on a rocking platform. The TTBS was then decanted and 40ml of fresh TTBS was then pipetted into the tray and the wash repeated. The second wash was then decanted and third repeats wash undertaken as above.

The membrane was then transferred to a fresh plastic bag with ethanol-cleaned forceps, which was then sealed using a bag sealer with air-bubbles excluded after 10ml of a secondary antibody, a Horse radish peroxidase conjugated Goat anti mouse IgG (Fc) antibody (AbD Serotec) was used at 1 in 1000 dilution in 5% w/v Marvel in TTBS.

The secondary antibody was then incubated for 1h at room temperature on the rocking with an up-turned tray covering the membrane.

#### 2.4.3.6 Detection of protein following antibody incubation

Amersham ECL$^{TM}$ western blotting detection reagent (GE Healthcare) system was used to visualise the amount of p53, RAF-1 and actin protein present in each sample. The nitrocellulose membrane following incubation with the appropriate antibodies as outlined above was washed three times in PBS prior to incubation with the ECL reagents as per manufactures instructions. Hyperfilm ECL western (GE Healthcare) was then exposed to the film in the dark for typically 10 seconds. The film was then developed and fixed in Tmax 100 professional developer (Kodak) for 1 min and washed three times in tap water before fixing in Kodak Rapid Fixer (Kodak) for 5 min. The film was then washed in running water for at least 5 min prior to being drip dried at room temperature.

### 2.4.3.7 Re-Probing of nitrocellulose membranes

Nitrocellulose membranes that have been probed for the expression of RAF-1 were stripped and re-probed for p53. The membrane was stripped for 30 min in 100ml of pre-warmed stripping buffer (100mM 2-Mercaptoethanol, 2%w/v SDS, 62.5mM Tris; pH6.7) at 50°C for 30 min. The stripped membrane was then transferred to a fresh tray containing 40ml TBS for 5 min at room temperature and washed on a rocking platform. The TBS was then decanted and 40ml of TTBS was pipetted into the tray. The membrane washed for a further 5 min at room temperature. This TTBS was then decanted and 40ml of fresh TTBS was then pipetted into the tray, and the wash repeated. The TTBS was then decanted and the membrane was blocked as above.

# Chapter 3

## p53 mutational status and the level of key cell cycle proteins in relation to radiosensitivity at 2Gy in twelve human cancer cell lines

# 3 p53 mutational status and the level of key cell cycle proteins in relation to radiosensitivity at 2Gy in twelve human cancer cell lines

.

## 3.1 Introduction

### 3.1.1 Oncogene expression can be related to radiosensitivity

Oncogenes may confer both a proliferative and radioresistant phenotype [474]. Transfection of several *in vitro* cell cultures with a variety of recombinant oncogenes results in an increase in radioresistance when compared to that of the parental line [489]. In the haematopoietic progenitor cell line 32d CL3, transfection with *v-abl, c-fms*, and *v-myc* induced resistance to doses of γ-radiation similar to those employed clinically [476]. Additionally, transfection of cultured cells with oncogenic signal transduction components such as *H-Ras* and *K-Ras* results in both increased transformation and radioresistance [153, 155]. In the human colon carcinoma cell line HCT 116, *H-Ras* radioresistance was demonstrated to be heregulin dependent demonstrating that several disparate cell surface receptors can co-operate to reduce radiosensitivity as a result of extra-cellular signalling [490].

### 3.1.2 The relationship of RAF-1 protein expression to cellular radiosensitivity

The mitogen activated signal transduction protein RAF-1 [359] has been observed to promote transformation, whilst inducing radioresistance in several cultured cell lines in transfection models [475]. However, in contrast to these observations made primarily on the oncogenic product of RAF-1, studies in 19 human cancer cell lines, which possessed a full-length 74kDa RAF-1 protein, RAF-1 protein level was found to be proportional to radiosensitivity, as measured by the clonogenic cell survival radiosensitivity parameter α [480]. This relationship of RAF-1 level and

radiosensitivity was not found to be indicative of cell cycle parameters such as labelling index (Li), or potential doubling time (Tpot). Nagasawa, however had demonstrated a relationship between radiosensitivity and $G_2$+M delay in the AT derived fibroblast GM2052 [491], and SCC-61 squamous cell carcinoma derived head and neck human cell line, as well as an increased delay in radiosensitive rodent derived cell lines. In addition, asynchronous cells showed that a greater $G_2$ delay was related to a greater resistance in a comparative study in HeLa cells and the human melamona line MeWo [492]. Chemical modifications inducing reductions in $G_2$+M transit following irradiation with caffeine [157], or pentoxifylline has also been found to increase radiosensitivity [493].

### 3.1.3 RAF-1 proto-oncogene expression, radiosensitivity and post-irradiation cell cycle delay

Of the 19 cell lines previously reported upon by Warenius *et al.* [4], six were initially selected to further study this potential role of $G_2$+M delay in radiosensitivity in the context of RAF-1 protein level. The cell lines chosen reflected the full range of RAF-1 protein levels and radiosensitivity as determined by the clonogenic cell survival value-$\alpha$. The cell cycle distribution of these six cell lines was then studied following 2 Gy of $\gamma$-irradiation to determine if $G_2$ arrest correlated with survival.

It was demonstrated that the rapidity of exit from a transient delay in the $G_2$+M compartment of the cell cycle was reflected in the intrinsic radiosensitivity of the cell lines, which correlated positively to intrinsic RAF-1 protein level [481].

A subsequent study involving an enlarged 'pool' of 12 cell lines, however failed to demonstrate a relationship between post-irradiated $G_2$+M exit rates and RAF-1 protein level, but did demonstrate a correlation in post-mitotic accumulation of cells

in $G_1$, which was proportional to RAF-1 protein level and related to radiosensitivity as determined by clonogenic survival [4]. Though adding to the confusion surrounding the nature of RAF-1 involvement in cell cycle modulation, this finding further enforces the role of RAF-1 protein level in cell cycle progression and intrinsic radiosensitivity of human cancer cell lines, leading to the speculation that this sensitivity may be related to insufficient time for cells to repair DNA lesions during $G_2$, or that RAF-1 could somehow negate the $G_2$ surveillance checkpoint [494].

### 3.1.4 p53 and cellular radiosensitivity

The tumour suppressor gene p53 is a central component of the DNA surveillance checkpoint that operates in both $G_1$ and $G_2$. Mutations to the p53-gene are seen to promote radiosensitivity in the autosomal disorder of AT. Further, the level of p53 protein within the cell has been seen to become elevated immediately following irradiation, implying a role in the cell's response to radiation. Covalent modifications such as acetylation [495], ubiquitination [496], and phosphorylation [497] have also been shown to alter p53 activity, function, and level. Indeed, RAF-1 was shown to phosphorylate p53 in cell free assays [427]. Thus I determined to revisit this $G_2$+M cell cycle delay and investigate this putative role of RAF-1 protein level correlation with the rate of exit from $\gamma$-radiation induced $G_2$+M delay, and if p53-mutational status affects the exit of cells from post-irradiation induced $G_2$+M accumulation.

## 3.2 Methods

### 3.2.1 Cell cycle protein levels and their relationship to radiosensitivity

As this thesis is concerned with the intrinsic level of proteins that are pertinent to the cell cycle, and post-irradiation cell cycle progression and survival, I have investigated if there was any relationship between the protein-protein levels, and the post-irradiative survival in the twelve human cancer cell lines utilised in this study. Paul Browning, Matt Jones, Laurence Seabra, and I had worked towards the accumulation of this body of results prior to the initiation of my thesis.

### 3.2.2 Intrinsic protein level measurement by western blot analysis

The intrinsic expression of proteins for the cancer cell lines was measured as outlined in Materials and Methods section 2.4. Antibodies for the detection of CDK1 (clone C-9, Santa Cruz), CDK4 (clone DCS-35, Santa Cruz), cyclin B (clone D-1, Santa Cruz), and cyclin D1 (clone DCS-6, Santa Cruz) were used at a dilition of 1 in 1000.

### 3.2.3 Determination of p53 mutational status of human cancer cell lines

The sequencing of p53 gene was undertaken within the lab by Tracey Gorman. A brief description of the methods and findings as outlined in Warenius *et al.* [14] are given below.

#### 3.2.3.1 Preparation of RNA and DNA for p53 mutational determination

Genomic DNA and RNA were obtained following guanidinium isothiocyanate CsCl gradient centrifugation [498, 499]. Cells were harvested as outlined in Materials and Methods section 2.1.3.

Following centrifugation, the medium was decanted from the cell pellet and the cells were then resuspended in ice cold PBS. The PBS cell suspension was then centrifuged at 200G for 5 min at 4°C. Following the centrifugation the supernatant was decanted and the cells were resuspended in guanidinium isothiocyanate buffer (4M Guanidinium isothiocyanate, 50mM Tris pH 7.5, 25mM EDTA pH 8.0, 0.5%w/v sodium lauryl sarcosine and 8%v/v 2-Mercaptoethanol). The cell homogenate was then cleared by centrifugation at 7,500G for 10 min at 4°C. The pre-cleared homogenate was then centrifuged through 5.7M CsCl 0.1M EDTA at 100,000G for 20h at 20°C. The RNA pellet was then re-dissolved in 0.1%w/v SDS and precipitated with ethanol overnight at –20°C. The RNA was then re-desolved in molecular grade water prior to quantification.

#### 3.2.3.2 cDNA synthesis of exons 9-11 of p53 from total RNA

As given in Warenius *et al.* [14] cDNA synthesis was undertaken from the incubation of 5μg of total RNA with 1μg oligo(dT) primer, and 20U of human placental ribonuclease inhibitor at 70°C for 10 min. Cooling the total RNA mixture on ice then stopped further primer annealing. 1x first strand buffer (50mM Tris, pH 8.3, 75mM KCl and 3mM MgCl), 0.01M DTT, dNTPs (0.5μM for each deoxribonucleoside triphosphate), 400U of superscript reverse transcriptase (Gibco) was then added to the chilled cDNA synthesis reaction mixture, which was then incubated at 37°C for 1h. PCR of exons 9-11 was then undertaken using 5μl of this cDNA template reaction mixture as stated below.

### 3.2.3.3 PCR of exons 2-8 and 9-11 for DNA sequencing

PCR Primers were designed to flank each of the exons to be sequenced. The sequences for each of the primers are given in Table 11 below. Exons 2 and 3 were co-amplified, as were exons 9 to 11 prior to sequencing. The remaing p53 exons were amplified separately and sequenced.

Genomic DNA was digested with *Eco*RI, precipitated with ethanol and resuspended in 50µl of water (Sigma) before undergoing RT-PCR amplification. The DNA (1µg) was amplified in 20µl PCR reactions containing 20pM of each primer. A 'hot-start' PCR protocol was used with the dNTPs and Taq polymerase enzyme initially separated from the rest of the reaction components on a wax cushion. The reaction mixtures were then placed in a pre-heated PCR block at 95°C for 2 min to denature the template strands before undergoing 30 repeat cycles of RT-PCR and denaturation at 95°C. For exons 2-3, 4 and 6; RT-PCR was undertaken at 60°C, whilst exons 5, and 8; were at 65°C, with exon 7 at 68°C, and exons 9-11 underwent RT-PCR at 72°C, with extension being carried out for 1 min. The PCR products were checked on a 0.8% w/v agarose gel before being purified using a Wizard minicolumn (Promega), and used directly in sequencing reactions.

| | Primers | |
|---|---|---|
| Exons | Sense | Antisense |
| 2/3 | CCC ACT TTT CCT CTT GCA AG | AGC CCA ACC CTT GTC CTT AC |
| 4 | CTG CTC TTT TCA CCC ATC TA | GCA TTG AAG TCT CAT GGA AG |
| 5 | TGT TCA CTT GTG CCC TGA CT | CAG CCC TGT CGT CTC TCC AG |
| 6 | GCC TCT GAT TCC TCA CTG AT | TTA ACC CCT CCT CCC AGA GA |
| 7 | ACT GGC CTC ATC TTG GGC CT | TGT GCA GGG TGG CAA GTG GC |
| 8 | T ATC CTG AGT AGT GG | T GCT TGC TTA CCT CG |
| 9/10/11 | AGA AAG GGG AGC CTC ACC AC | CTG ACG CAC ACC TAT TGC AA |

**Table 11 Primers for PCR of exons 2 through 11 of p53** The above table contains the primers used to amplify exons 2 through 11 of p53 genomic DNA and cDNA for DNA sequencing. The primers read 5' to 3' as per convention.

### 3.2.3.4 Nucleotide sequencing of amplified p53 exons 2 through 11

Sequencing primers were radioactively labelled with 10pM of $\gamma^{32}$P-ATP (45 μCi) at their 5' end for 30 min at 37°C using T4 polynucleotide kinase (9.7 U, Pharmacia) and 1xT4 PNK buffer (10μM Tris-Acetate, 10μM magnesium acetate and 50μM potassium acetate). The primers are as listed in Table 11 (page 92). The Sanger method of di-deoxynucleotide enzymatic sequencing was utilised [500], using the fmol DNA Sequencing System (Promega). Sequencing was repeated and putative sequencing mutations were confirmed by additional sequencing of the exon in the antisense direction.

## 3.3 Results

### 3.3.1 Intrinsic protein level in 12 human cancer cell lines and radiosensitivity

The relative levels of intrinsic protein expression in the twelve, un-irradiated, asynchronous, exponentially growing, human cancer cell lines used in this study are shown below in Figure 13. The amount of each protein was measured using western blotting, with densitometry undertaken to assign values to the relative level of that specific protein. These densitometry values were then collated with all the other cell lines used in the lab and the mean densitometry level was calculated for each protein. This mean densitometry value was then equated to an arbitrary relative mean of 5, and these relative expression patterns were then used to determine if any relationship existed between any of the protein levels and or the cell lines post-irradiative survival. The results of protein and radiosensitivity correlations are summarised in Table 12 below giving the probability of correlation (P) and the correlation coefficient (r).

As can be seen from these correlations, the only values that showed any degree of relationship, as determined Least-Squares regression, were the intrinsic level of CDK1 and CDK4 (which is the subject of a separate thesis in the lab), and the intrinsic level of the proto-oncogene RAF-1 and radiosensitivity. These findings are a little surprising because I would have expected the levels of CDK1 and CDK4 to be related to the levels of their cyclin partners (cyclin B and cyclin D1 respectively), due to the 1:1 stoichiometric binding that occurs during cell cycle progression.

I thus determined to investigate this negative relationship, i.e. high levels of RAF-1 relating to radiosensitivity (low values of $SF_2$), and compare this observation with

cell cycle progression and p53 mutational status, as p53 protein level *per se* did not appear to influence post-irradiation survival.

**Figure 13. The relative intrinsic protein expression patterns in twelve human cancer cell lines**

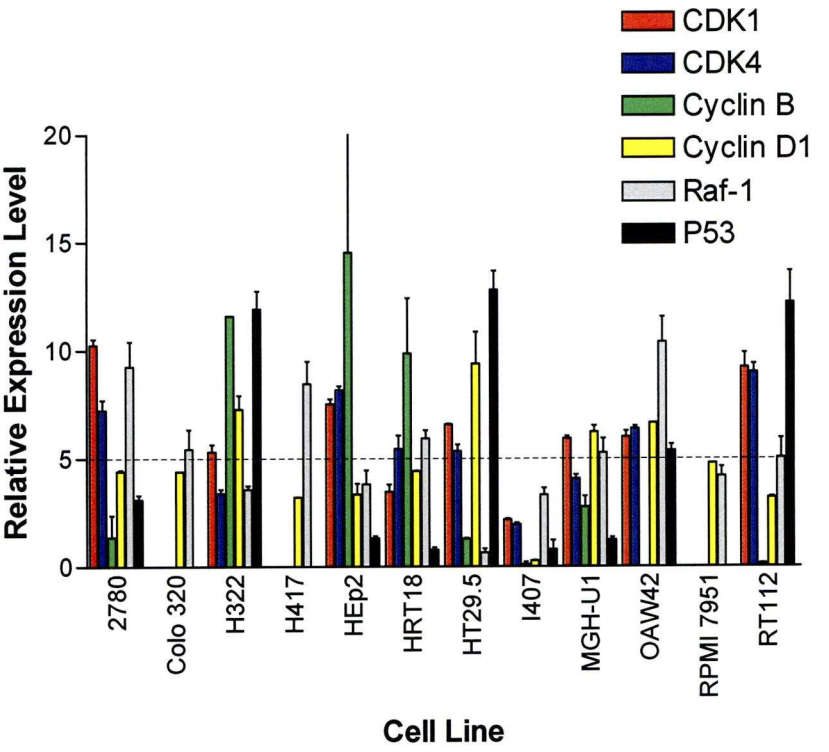


**Table 12. The relationship between cell cycle proteins and radiosensitivity at 2Gy**

| | $SF_2$ | CDK4 | Cyc B | Cyc D1 | RAF-1 | Tp53 |
|---|---|---|---|---|---|---|
| CDK1 | P=0.866 | P=0.009 | P=0.712 | P=0.655 | P=0.438 | P=0.394 |
| | r=0.066 | r=0.802 | r=0.156 | r=0.174 | r=0.297 | r=0.325 |
| CDK4 | P=0.841 | | P=0.834 | P=0.966 | P=0.394 | P=0.663 |
| | r=0.079 | | r=0.089 | r=0.017 | r=0.325 | r=0.169 |
| Cyclin B | P=0.768 | P=0.834 | | P=0.805 | P=0.865 | P=0.687 |
| | r=0.125 | r=0.089 | | r=0.105 | 耀 0.072 | r=0.170 |
| Cyclin D1 | P=0.846 | P=0.966 | P=0.805 | | P=0.614 | P=0.128 |
| | r=0.063 | r=0.017 | r=0.105 | | r=0.163 | r=0.546 |
| RAF-1 | P=0.004 | P=0.394 | P=0.865 | P=0.614 | | P=0.363 |
| | r=-0.766 | r=0.325 | r=0.072 | r=0.162 | | r=0.346 |
| Tp53 | P=0.633 | P=0.663 | P=0.687 | P=0.128 | P=0.363 | |
| | r=0.185 | r=0.169 | r=0.170 | r=0.546 | r=0.346 | |

**Figure 13.** The relative cell cycle protein levels of the key $G_1$ and $G_2$+M progression proteins and those of the cell cycle related proteins of p53 and RAF-1 are shown above.

**Table 12.** The correlation of the various protein levels and the relationship of these intrinsic protein levels to radiosensitivity is shown above. The red boxes indicate there the P (probability of correclation) and r (Pearsons product-moment correlation coefficient) values are significant.

### 3.3.2 p53 Mutational status of the cancer cell lines

Exons 5-8 of p53 messenger RNA were sequenced since these regions have previously been shown to contain the majority of mutations found to be expressed by p53 [176]. Screening of these mRNA exons revealed that seven of the twelve cancer cell lines studied utilised in this study carry mutations in their base sequence as summarised in Table 13 below. The mis-sense mutation observed in the ovarian carcinoma cell line OAW42 was silent. The CGA to CGG alteration of codon 213 still resulted in a wt- p53 protein as both codons code for Arginine. Thus, six of the cell lines studied here, 2780, HEp2, HRT18, I407, MGH-U1, and OAW 42 express wt-p53 protein.

The melanoma, RPMI 7951, and the small cell lung carcinoma, H417 have truncated p53, with stop codons at 166 and 298 respectively. The second small cell lung carcinoma line H322 and the Colonic Adenocarcinoma Colo 320 both posses a mis-sense mutation of CGG to TGG at codon 245 resulting in a basic Arginine to hydrophobic Tryptophan substitution.

| Cell line | Location of alteration | cDNA sequence | Amino-acid change | p53 protein |
|---|---|---|---|---|
| 2780 | - | Normal | None | WT |
| Colo 320 | Codon 245 | CGG-TGG | Arg to Trp | Mut |
| H322 | Codon 245 | CGG-TGG | Arg to Trp | Mut |
| H417 | Codon 298 | GAG-TAG | Glu to Stop | Mut/Truncated |
| HEp2 | - | Normal | None | WT |
| HRT18 | - | Normal | None | WT |
| HT29.5 | Codon 273 | CGT-CAT | Arg to His | Mut |
| I407 | - | Normal | None | WT |
| MGH-U1 | - | Normal | None | WT |
| OAW42 | Codon 213 | CGA-CGG | None | WT |
| RPMI 7951 | Codon 166 | TCA-TTA | Ser to Stop | Mut/Truncated |
| RT112 | Codon 248 | CCG-CAG | Arg to Gly | Mut |

**Table 13 p53 Mutational statuses of the twelve human cancer cell lines**
The above table contains a summary of the mutational status of the cell lines utilised in this study.

The transitional bladder carcinoma cell line, RT112, and the Colonic Adenocarcinoma derived HT29.5 also had a basic Arginine mutation to an uncharged Glycine and a basic Histidine. Colo320, H322, and RT112 were homozygous for p53 gene mutations, whilst HT29.5, RPMI 7951, and H417 were heterozygous, though only H417 expressed relatively high levels of wt-p53 mRNA [484].

# Chapter 4

## Expression of RAF-1 and p53 protein following 2, 4 and 8Gy of γ-radiation in twelve human cancer cell lines determined by western blotting

# 4 Expression of RAF-1 and p53 protein following 2, 4 and 8Gy of γ-radiation in twelve human cancer cell lines determined by western blotting

## 4.1 Introduction

Following exposure of cells to ionising radiation elevations in the level of p53 have been observed both *in vitro* [305] and *in vivo* [501]. It is thought that these increases may mediate the response to the damage induced following irradiation. For instance, it has been hypothesised that low levels of p53 may actually have an anti-apoptotic propensity [297], whilst high levels of p53 could have the opposite effect of inducing apoptosis [298]. The influence on cell fate following exposure to radiation is thought to be mediated through the down-stream transcriptional targets of p53 [502]. Although no evidence of direct induction of RAF-1 transcription by p53 is known, RAF-1 level does directly influence post-irradiation survival in the wt-p53 cell lines and RAF-1 is known to mediate apoptosis through MEK and AKT-dependent pathways [503, 504]. Further, it has been reported that RAF-1 is subject to constitutive regulation by many factors [505].

Here I investigated by western blot analysis the effects that 2, 4 and 8Gy of γ-radiation havd on the level of p53 and RAF-1 in twelve asynchronously growing cultures of human cancer cell lines, six cell lines with a wt-p53 protein and six cell lines with a range of mutations both at the genomic and protein level [484].

## 4.2 Methods

Post-irradiated total-cell-lysates were prepared from asynchronously growing pre-confluent cultures of human cancer cell lines. The cells were seeded, irradiated and harvested as indicated in Materials and Methods section 2.4.1. The protein content of

the cell lysates was then determined as indicated in section 2.4.2 and the level of p53 and RAF-1 determined by SDS-PAGE and western blot analysis as described in section 2.4.3 using ECL to report the level of protein in each sample.

The relative level of protein for the control and irradiated cells was then determined by densitometric analysis. The western blot radiographic image was first digitalised by scanning with a flat bed scanner and this image was then analysised using Phoretix 1D software (Phoretix, South Africa). The numerical value assigned to each sample was then plotted as percentages of irradiated divided by control for 2, 4 and 8Gy for the paired control at each time. The level of p53 and RAF-1 at any given time in the controls was assumed to be 100% of cell normal level, and fluctuations as a result of irradiation at 2, 4 and 8Gy would be seen as less than 100% for decrease in protein level, and increase in protein level of the irradiated samples compared to the paired control would be observed as a percentage greater than 100%.

## 4.3 Results

### 4.3.1 Protein level of p53 and RAF-1 in post-irradiated human cancer cell lines

Alterations in the level of p53 and RAF-1 protein were determined as indicated above. Figure 14 (page 101), shows the protein level of the proto-oncogene RAF-1 and the tumour suppressor gene p53 at control, 2, 4 and 8Gy for the wt-p53 transitional bladder cell carcinoma MGH-U1 and the mutant-p53 small cell lung carcinoma H322. These results are representative of the twelve cancer cell lines, 2780, Colo320, H322, H417, Hep2, HRT18, HT29.5, I407, MGH-U1, OAW42, RPMI7951 and RT112 used in this study and are representative of the triplicate results obtained for MGH-U1 and H322.

As can be seen for both H322 and MGH-U1 the level of p53 remains constant throughout the time course. However, fluctuations are seen in the level of RAF-1 for both H322 and MGH-U1, not only in the irradiated samples but also in the paired sham-irradiated controls during the duration of the experiment. These changes in the level of RAF-1 protein were seen at all doses of radiation.

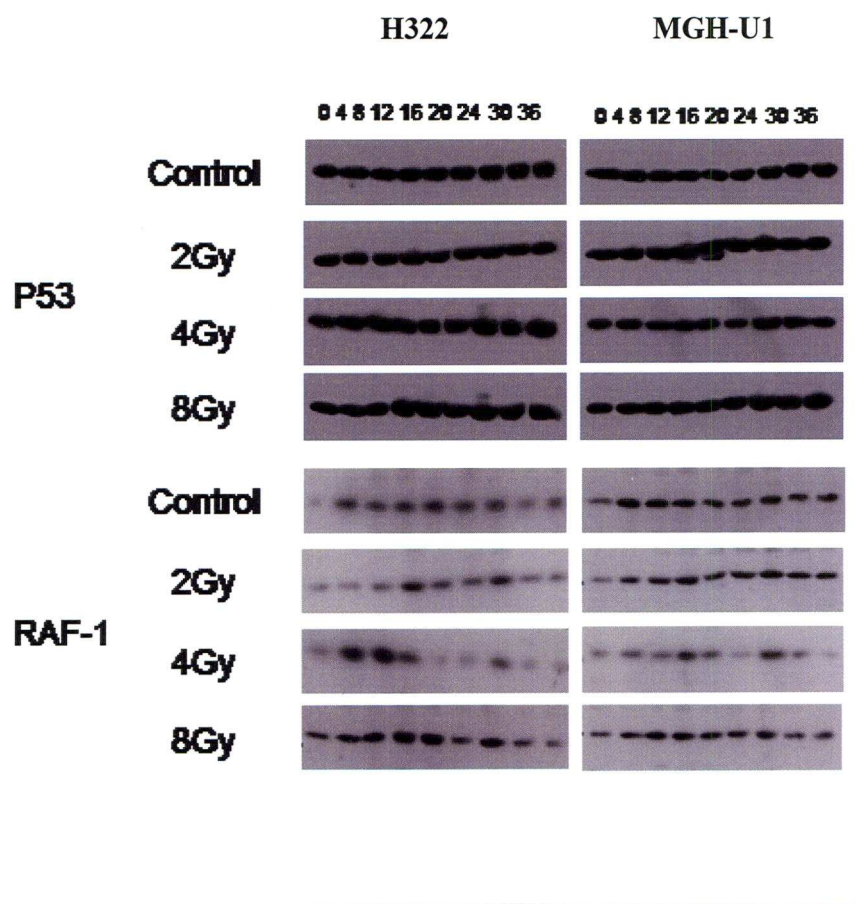


**Figure 14. Expression of p53 and RAF-1 in the human cancer cell lines H322 and MGH-U1 following 2, 4 and 8Gy of γ-radiation over 36h** The figure above depicts the protein levels of RAF-1 and p53 as determined by SDS-PAGE and western blotting. p53 and RAF-1 protein was then probed for with antibodies and ECL was used to visualise the relative level of protein expressed.

### 4.3.2 Changes in level of p53 and RAF-1 protein in human cancer cell lines following exposure to ionising radiation

Following exposure to ionising radiation the level of p53 and RAF-1 expression was determined by SDS-PAGE and western blot analysis as outlined above (section 4.2). Protein level in the control sample was designated as 100%. In post-irradiated cell lines, levels of p53 and RAF-1 proteins were expressed as relative percentage of control. The results of the analysis of p53 protein level are given in Figure 15 and 16 (page 103 and 104 respectively) whilst the analysis of RAF-1 level are given in Figures 17 and 18 (pages 105 and 106 respectively) for the wt-p53 cell lines and the mutant-p53 cell lines respectively.

In the 12 human cancer cell lines analysised, the mutant-p53 cell line HT29.5 showed the lowest changes in p53 level for the irradiated samples compared to the controls throughout the duration of the experiment, less than 20% difference to the control. Conversely, the mutant-p53 small cell lung cancer cell line H417 had the largest decrease in p53 level following 2, 4 and 8Gy, of up to 25%, whilst several cell lines had an increase in p53 level of 25%. However, no apparent significant changes were observed in the level of p53 protein from the control samples in any of the 12 cell lines examined over 36h following exposure to γ-radiation at 2, 4 or 8Gy.

The level of RAF-1 protein showed large fluctuations in all the cell lines in the control, 2, 4 and 8Gy samples throughout the 36h time course (see representative data in Figure 14). The wt-p53 cell lines 2780/735 and Hep2 had the highest degree of RAF-1 protein level changes (see Figure 17). For Hep2, increases of 70% and decreases of 60% were measured for individual time points. In the mutant-p53 cell lines (see Figure 18) RAF-1 protein levels gave consistent increases, up to 30% above the control samples throughout the duration of the experiment for all doses

used. However, changes in the level of RAF-1 protein were not significant (as tested by t-test for individual time points).

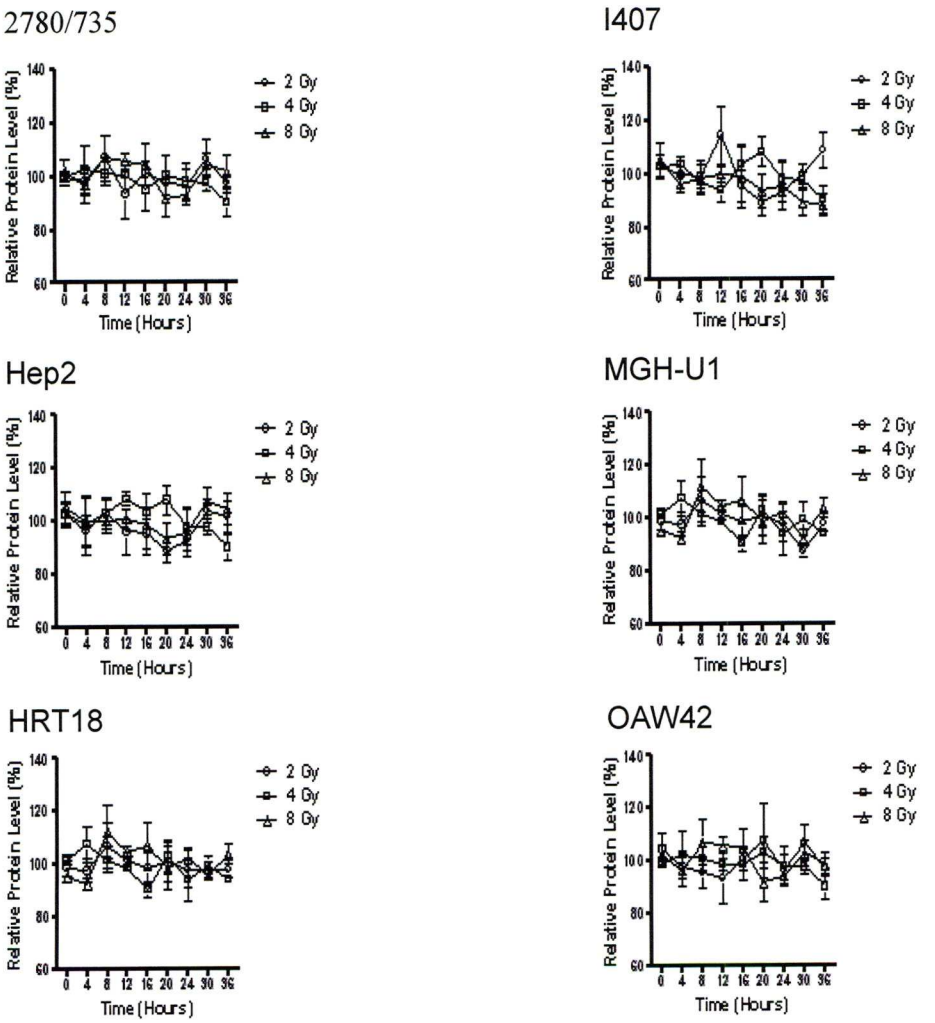


**Figure 15. Relative p53 protein level following exposure to 2, 4 and 8Gy of γ-radiation in six wt-p53 cell lines** The effect of increasing doses of ionising radiation on p53 protein expression in 6 wt-p53 cell lines is shown as percentage of relative protein level compared to the paired controls.

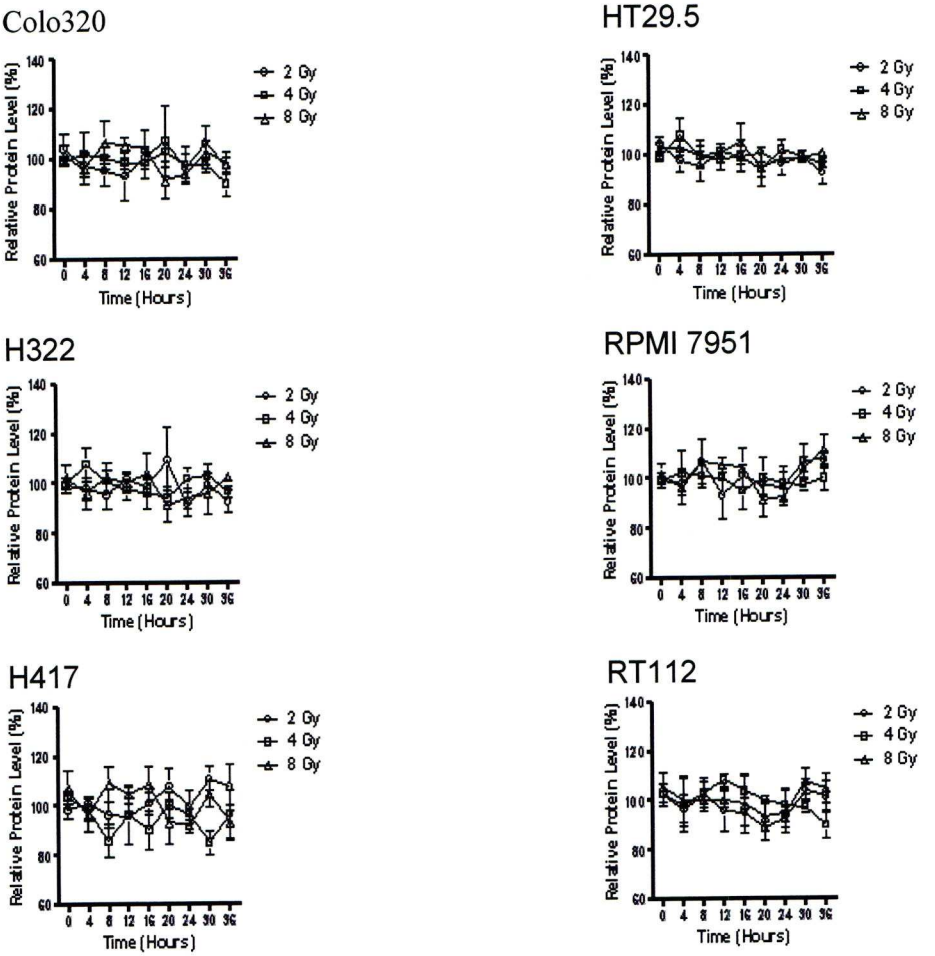


**Figure 16. Relative p53 protein level following exposure to 2, 4 and 8Gy of γ-radiation in six mutant-p53 cell lines** The effect of increasing doses of ionising radiation on p53 protein expression in 6 p53-mutant cell lines is shown as percentage of relative protein level compared to the paired controls.

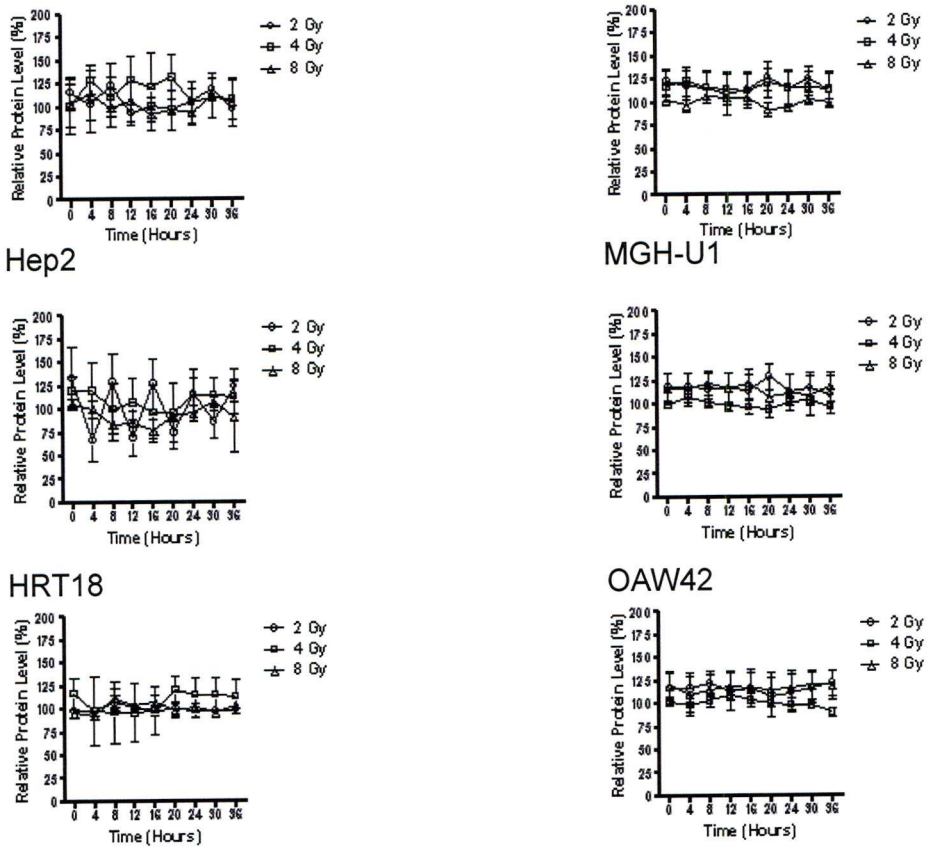


**Figure 17. Relative RAF-1 protein level following exposure to 2, 4 and 8Gy of γ-radiation in six wt-p53 cell lines** The effect of increasing doses of ionising radiation on RAF-1 protein expression in 6 wt-p53 cell lines is shown as percentage of relative protein level compared to the paired controls.

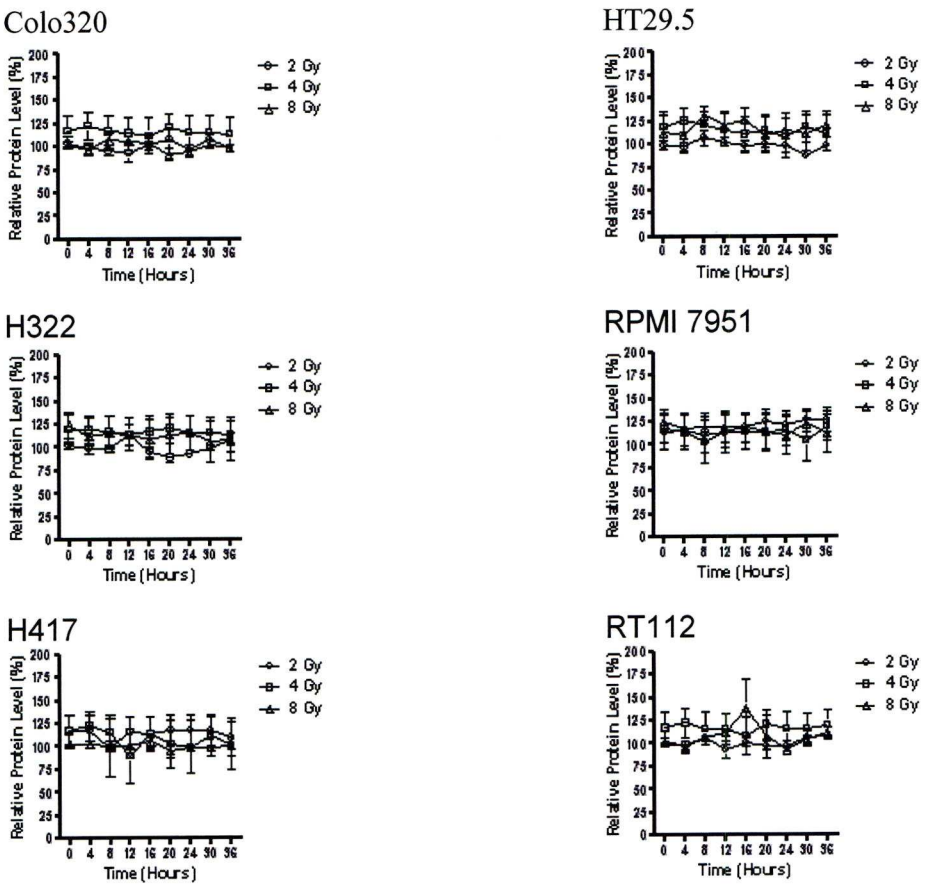


**Figure 18. Relative RAF-1 protein level following exposure to 2, 4 and 8Gy of γ-radiation in six p53-mutant cell lines** The effect of increasing doses of ionising radiation on p53 protein expression in 6 mutant-p53 cell lines is shown as percentage of relative protein level compared to the paired controls.

# Chapter 5

# The relationship between RAF-1 protein expression, $G_2$+M accumulation and radiosensitivity in wt-p53 and mutant-p53 cell lines following radiation at increasing dose levels

# 5 The relationship between RAF-1 protein expression, $G_2$+M accumulation and radiosensitivity in wt-p53 and mutant-p53 cell lines following radiation at increasing dose levels

## 5.1 Introduction

### 5.1.1 Radiation studies in cancer cell lines

To investigate the putative role played by RAF-1 in determining the cellular response to ionising radiation, I elected to examine the relationship of RAF-1 protein level and clonogenic cell survival following doses of 2, 4 and 8Gy of γ-radiation. Such doses are commonly used in many studies of irradiation-induced alterations in cell cycle progression. Thus to validate the work already done within the lab at 2Gy and to potentially give an insight into cell cycle delay and post-irradiation survival in a clinically relevant context I undertook to measure clonogenic survival and exit from a $G_2$+M accumulation, in the context of p53 mutational status following a single fraction of γ-radiation of 2, 4 and 8Gy.

## 5.2 Methods

### 5.2.1 Rate of $G_2$+M exit ($T_{50}$) following 2, 4 and 8Gy of γ-radiation

All experiments were undertaken on asynchronous, exponentially growing cell cultures, and the cells were irradiated at 2, 4 or 8Gy, such that the modulation of cell cycle delay and the rate of exit at these incremental doses of ionising radiation could be investigated.

Cells were plated in the appropriate culture media, allowed to recover overnight and irradiated using a $^{137}$Cs source. Samples irradiated with 2Gy where harvested at 2h intervals until 24h post-irradiation. For cells given 4 and 8Gy, samples were taken at 4h intervals initially for 24h, and then at 30, 36, 48 and finally 60h, a time period found to be sufficient for over half the cells accumulated in $G_2$+M to exit that compartment of the cell cycle. The actual times used vary from cell line to cell line, and the appropriate times were chosen for each line and dose as needed.

Preparation of cells for irradiation, irradiation of the cells and the subsequent sampling is given in sections 2.3.1-3. The cells were fixed and stained with the DNA intercalating dye PI for flow cytometric analysis asindicated in section 2.3.4-5. The method for determination of the percentage of the total cell population in each part of the cell cycle so that the subsequent rate of $G_2$+M exit ($T_{50}$) could be calculated is described in greater detail in the General Methods, section 2.3.6.

## 5.3 Results

### 5.3.1 Survival following higher doses of radiation

Following increasing exposure to ionising radiation, at 2, 4 and 8Gy, radiosensitivity in twelve human cancer cell lines, determined by clonogenic assay and expressed as $SF_2$, $SF_4$ and $SF_8$ (the survival fraction at 2, 4 and 8Gy of radiation respectively). The survival fraction data points for the twelve cancer cell lines are shown in Figure 19A. As anticipated, the fraction of surviving clonogenic cells diminished as the radiation

**A) Reduced survival in human cancer cells following progressively higher doses of γ-radiation**

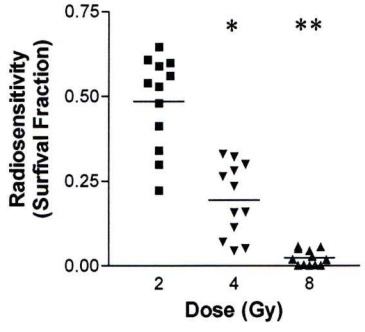


**B) p53 mutational status does not influence survival following increasing doses of γ-radiation**

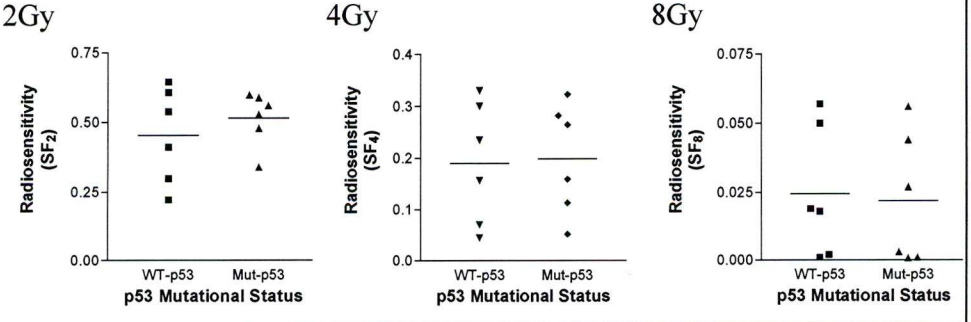


**Figure 19. Radiosensitivity as determined by survival fraction in 12 human cancer cell lines at 2, 4 and 8Gy and in the context of p53-mutational status**
The progressive decrease in cells surviving in each of the twelve human cancer sell lines following 2, 4 and 8Gy of ionising γ-radiation is shown in panel A, whilst the effect of p53 mutational status is shown in panel B. In panel A, the single star (*) indicated that the survival fraction at 4Gy is significantly lower than at 2Gy, whilst the double (**) indicates that at 8Gy the survival fraction is significantly lower than both that at 2Gy and that at 4Gy. This was determined by t-test.

dose increased from 2 to 8Gy. These decreases in clonogenic cell survival were found to be significant at each stepwise increase in the dose of radiation received. The increase in dose from 2Gy to 4Gy resulted in a decrease in survival fraction from 0.485 (±0.05) to 0.195 (±0.046), respectively. This decrease in survival was very highly significant as measured by the one-tailed t-test ($P<0.0001$, $r=0.981$).

At 8Gy, the survival fraction ($SF_8$) was found to be 0.023 (±0.010). This 2% of total potential of reproductive survival was found to be very highly significant as compared to both 2Gy ($P<0.0001$, $r=0.967$) and also 4Gy ($P<0.0001$, $r=0.890$).

### 5.3.2 p53 mutational status and survival at increasing doses of radiation

A highly significant decrease in clonogenic survival fraction was observed with stepwise increases in the dose of γ-radiation to which the cell lines were exposed. However, these changes in survival fraction at each single dose did not result in an alteration in the relative sensitivity of the human cancer cell lines in terms of p53 mutational status (Figure 19A, 2, 4 and 8Gy). The degree to which cells were resistant to 2Gy of ionising radiation, as given by the clonogenic determinant survival fraction ($SF_2$), and the influence of p53-mutational status on survival is shown in Figure 19B.

The six wt-p53 cell lines demonstrated a lower mean survival, along with a broader range of survival (0.455±0.071 (SEM)), as compared to that of the mutant-p53 cell lines (0.517±0.040). The means of the populations, however, demonstrated no significant difference (two tailed t-test; $p=0.4648$).

Likewise, at 4Gy, the 6 mutant-p53 cell lines demonstrated an almost identical mean survival fraction of 0.1993±0.044, as compared to 0.1903±0.048 for the wt-p53 cells. The t-test of these means resulted in a very weak value of $P=0.8929$, $r=0.0044$.

At 8Gy, the statistically insignificant relative increase of the mutant-p53 cell lines was reversed, with the wt-p53 cell lines demonstrating a mean survival fraction of 0.0245±0.0097 as compared to a mean of 0.0220±0.0099 for the mutant-p53 cell lines. This difference was however found to not be significant by an unpaired t-test, P=0.8576, r=0.058.

### 5.3.3 Accumulation of cells in $G_2$+M cell cycle phase following progressively higher steps in γ-radiation dose

The percentage of cells accumulating in $G_2$+M following 2, 4 and 8Gy of ionising irradiation for the twelve cancer cell lines used in this study is shown in Figures 20-25.

Post-irradiation $G_2$+M accumulation may be expressed as the area under the $G_2$+M accumulation curve. Where exit is not complete however, this value may be unreliable, and may not 'necessarily' reflect changes in the rate of progress through the latter phase of the cell cycle.

Also indicated on the Figures 20 to 25 are the times taken for the cells to reach 50% following peak accumulation ($T_{50}$) in the pre-division stage, and the method employed to determine the duration of $T_{50}$ in $G_2$+M exit, as described in the methods (section 2.3), is also indicated.

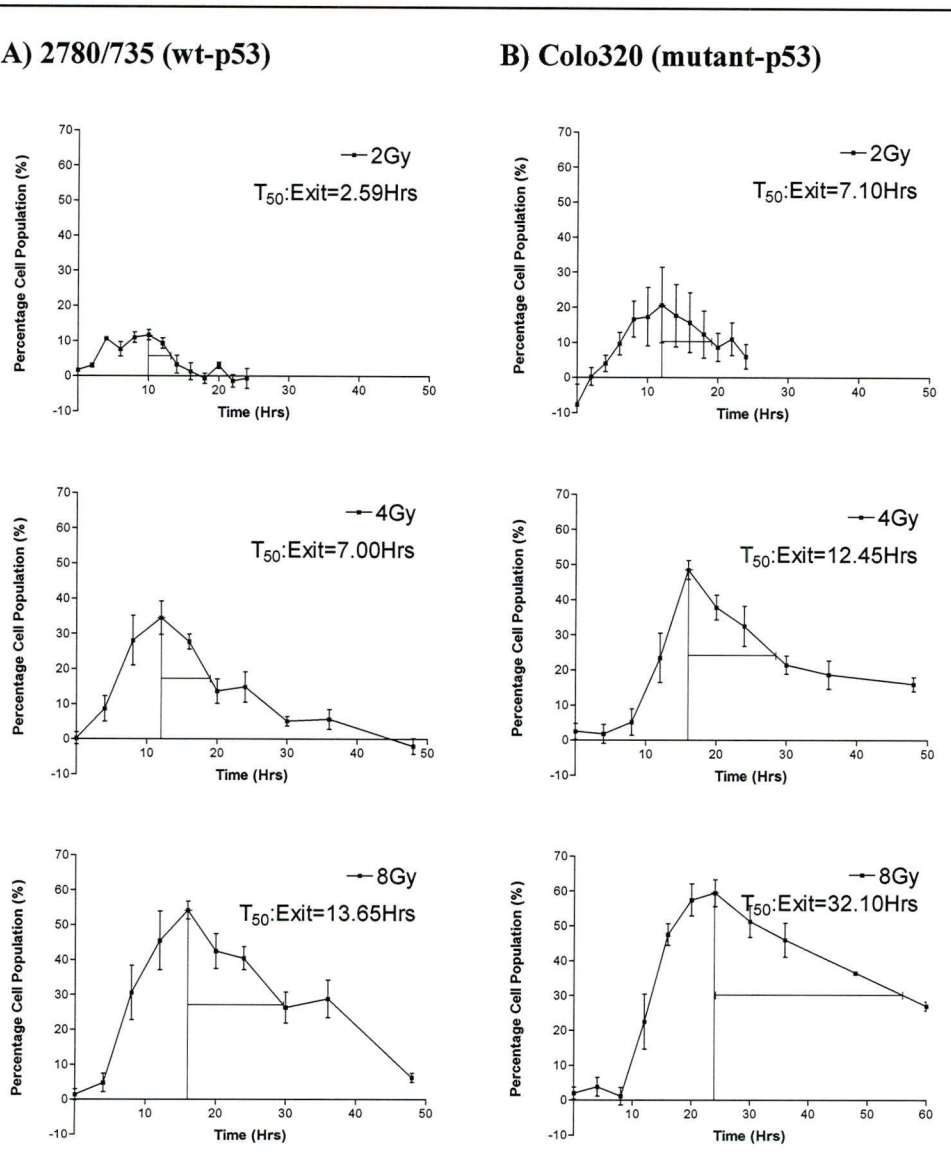


**Figure 20. Percentage of cells in $G_2$+M cell cycle phase following 2, 4 and 8Gy of ionising radiation and determination of $T_{50}$.**

The amount of post-irradiated $G_2$+M accumulation as measured by PI DNA staining and flow cytometry on 2780/735 and Colo 320 cell lines is shown above. Enumeration of the percentage of total cells in $G_2$+M was interpolated using ModFit (Verity Software), the mathematical modelling package. These graphs were then used to determine the $T_{50}$ value, the rate of exit from the $G_2$+M accumulation, for each cell line.

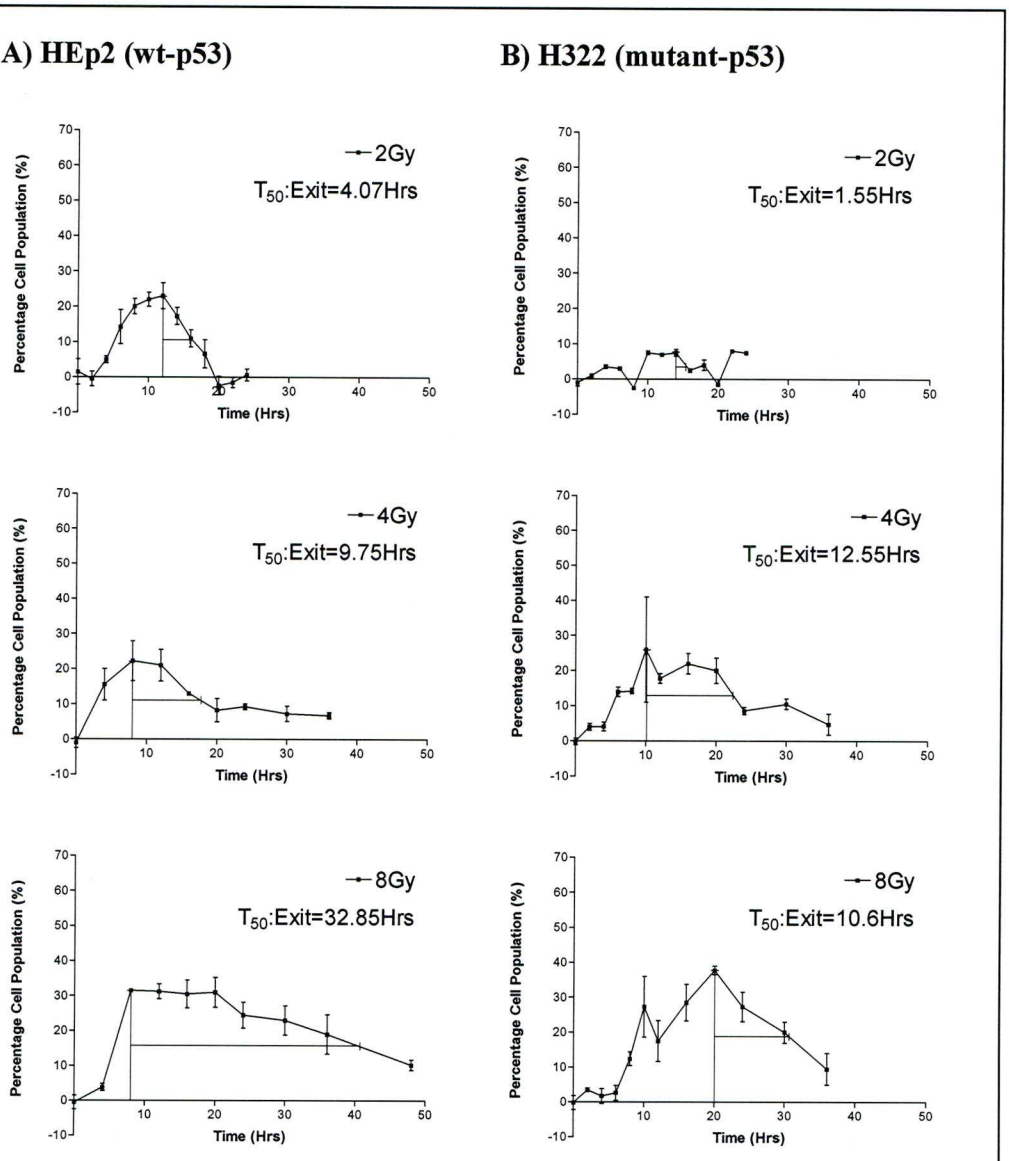


**Figure 21. Percentage of cells in the $G_2$+M cell cycle phase following 2, 4 and 8Gy of ionising radiation and determination of $T_{50}$**

The amount of post-irradiated $G_2$+M accumulation as measured by PI DNA staining and flow cytometry on HEp 2 and H322 cell lines is shown above. Enumeration of the percentage of total cells in $G_2$+M was interpolated using ModFit (Verity Software), the mathematical modelling package. These graphs were then used to determine the $T_{50}$ value, the rate of exit from the $G_2$+M accumulation, for each cell line.

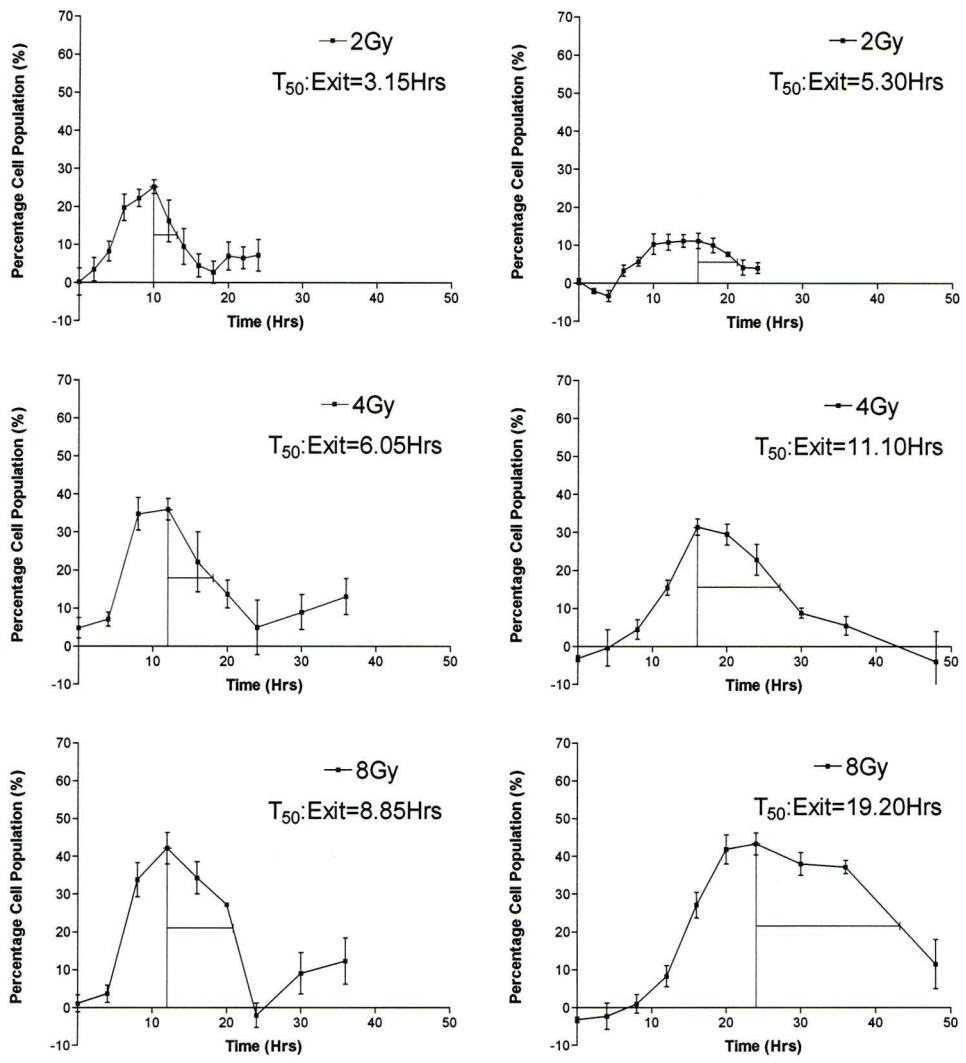


**Figure 22. Percentage of cells in the $G_2$+M cell cycle phase following 2, 4 and 8Gy of ionising radiation and determination of $T_{50}$**

The amount of post-irradiated $G_2$+M accumulation as measured by PI DNA staining and flow cytometry on HRT18 and H417 cell lines is shown above. Enumeration of the percentage of total cells in $G_2$+M was interpolated using ModFit (Verity Software), the mathematical modelling package. These graphs were then used to determine the $T_{50}$ value, the rate of exit from the $G_2$+M accumulation, for each cell line.

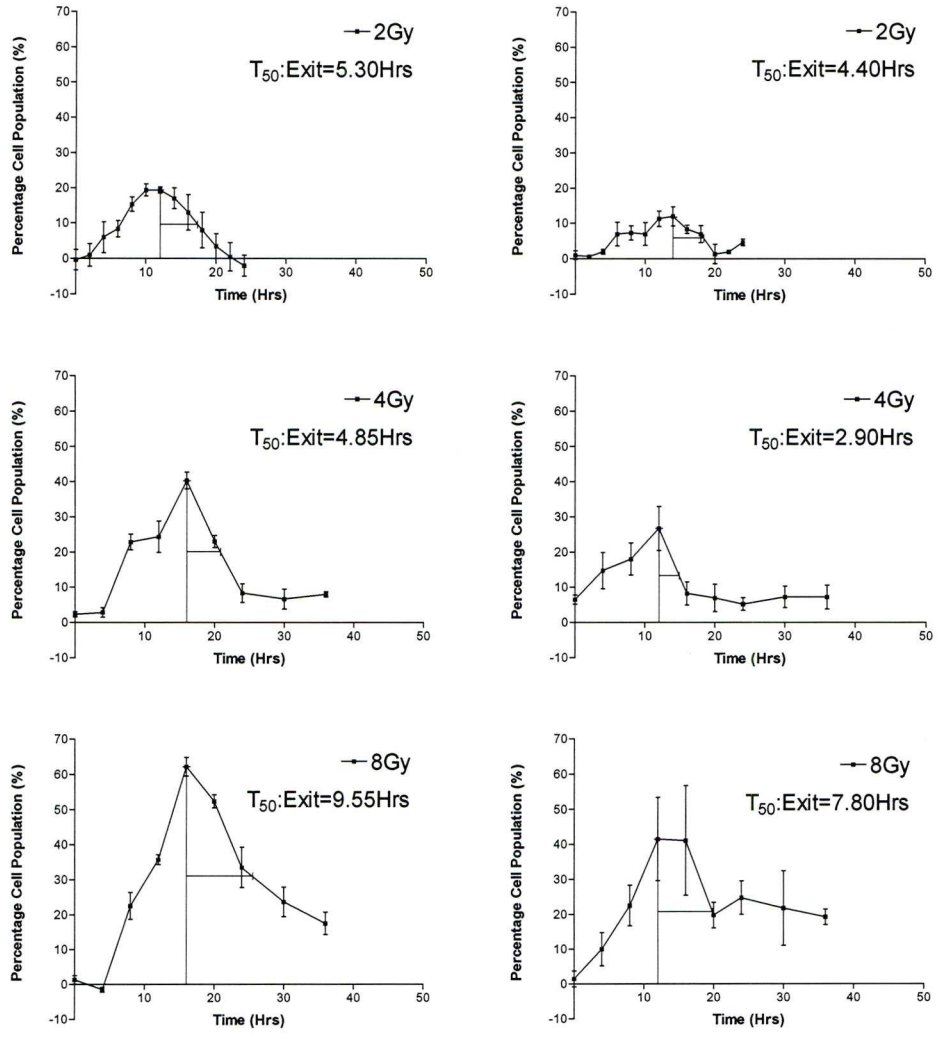


**Figure 23. Percentage of cells in the $G_2$+M cell cycle phase following 2, 4 and 8Gy of ionising radiation and determination of $T_{50}$**

The amount of post-irradiated $G_2$+M accumulation as measured by PI DNA staining and flow cytometry on I407 and HT29.5 cell lines is shown above. Enumeration of the percentage of total cells in $G_2$+M was interpolated using ModFit (Verity Software), the mathematical modelling package. These graphs were then used to determine the $T_{50}$ value, the rate of exit from the $G_2$+M accumulation, for each cell line.

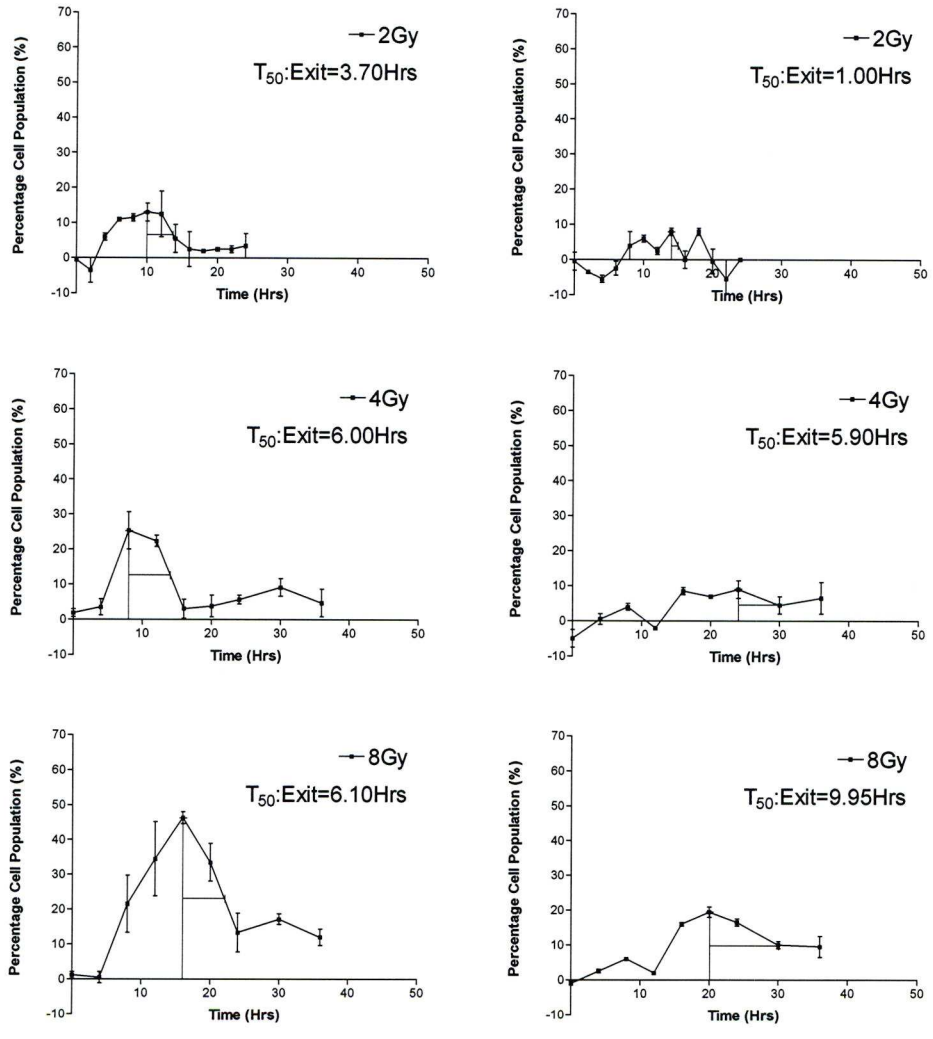


**Figure 24. Percentage of cells in the $G_2$+M cell cycle phase following 2, 4 and 8Gy of ionising radiation and determination of $T_{50}$**

The amount of post-irradiated $G_2$+M accumulation as measured by PI DNA staining and flow cytometry on MGH-U1 and RPMI 7951 cell lines is shown above. Enumeration of the percentage of total cells in $G_2$+M was interpolated using ModFit (Verity Software), the mathematical modelling package. These graphs were then used to determine the $T_{50}$ value, the rate of exit from the $G_2$+M accumulation, for each cell line.

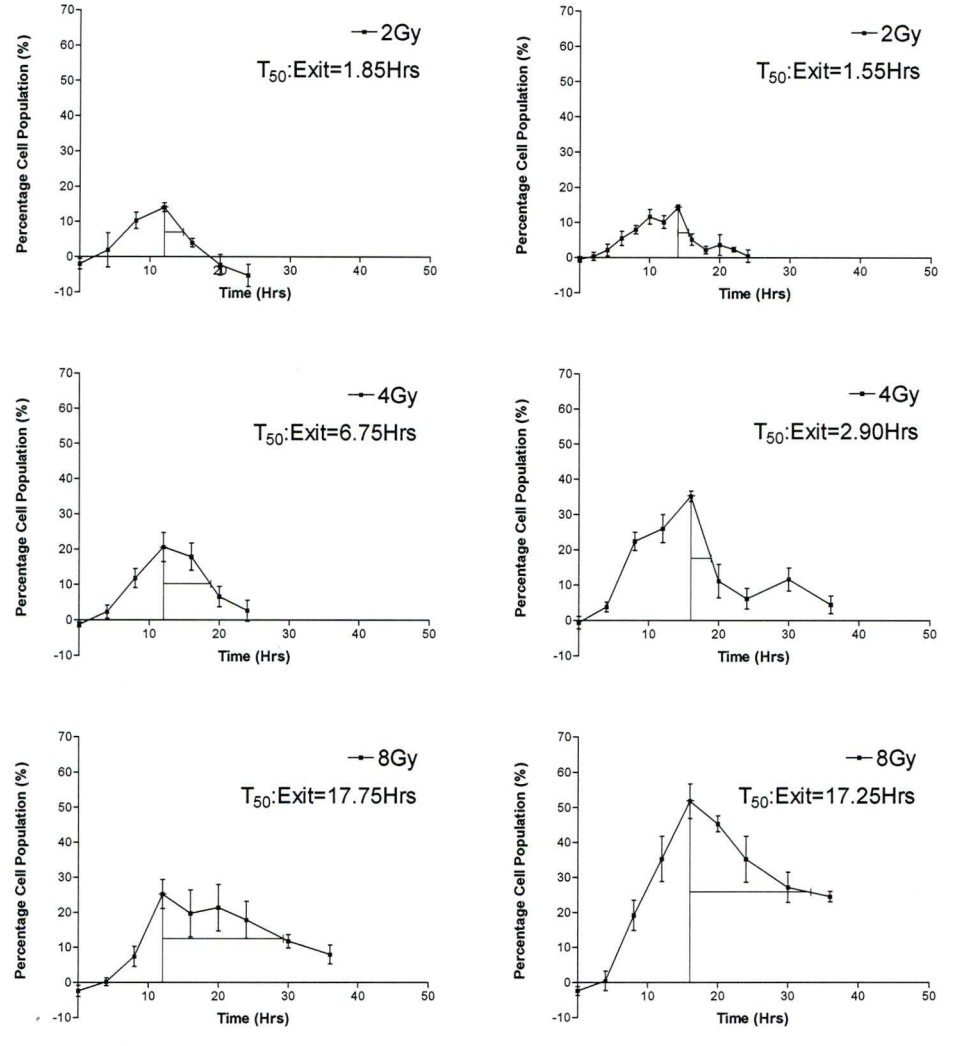


**Figure 25. Percentage of cells in the $G_2$+M cell cycle phase following 2, 4 and 8Gy of ionising radiation and determination of $T_{50}$**

The amount of post-irradiated $G_2$+M accumulation as measured by PI DNA staining and flow cytometry on OAW42 and RT112 cell lines is shown above. Enumeration of the percentage of total cells in $G_2$+M was interpolated using ModFit (Verity Software), the mathematical modelling package. These graphs were then used to determine the $T_{50}$ value, the rate of exit from the $G_2$+M accumulation, for each cell line.

### 5.3.4 Cells accumulate in $G_2$+M in progressively greater numbers following increasing levels of ionising radiation

As dose increases, the cell lines studied showed a progressively great accumulation of cell $G_2$+M, as indicated by area under the curve of the percentage of cells in $G_2$+M over the course of the experiment. I consided the magnitude of the $G_2$+M accumulation at 2Gy only, as at 4 and 8Gy the majority of the irradiated cells used did not returned to the level of the controls within the duration of the time course undertaken. At 2Gy, the mean of the two populations (mutant- and wt-p53), was greater in the wt-p53 cell lines than in the corresponding mutant-p53 cell lines. However, there was no significantly difference between the set of six wt-p53 and mutant-p53 cell lines (two tailed t-test; p=0.2483). As can be seen in Figure 26, in general, the mutant-p53 cell line demonstrated a lower degree of $G_2$+M accumulation

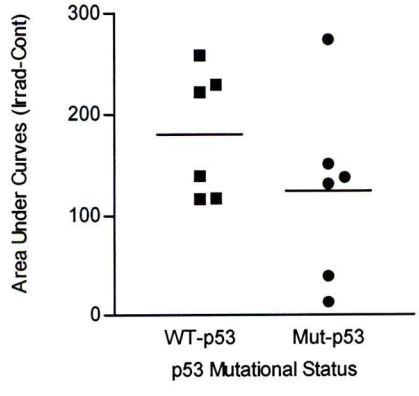


**Figure 26. Effect of p53 mutational status on size $G_2$+M accumulation following 2Gy of γ-radiation in human cancer cell lines**
The above column scatter plots depict the post-irradiation accumulation of the six wt-p53 and the six mutant-p53 cell lines in $G_2$+M cell cycle phase following 2Gy of γ-radiation.

following irradiation. However, in the the mutant-p53 cell line; the colorectal carcinoma Colo 320, the percentage of cells in $G_2$+M for the irradiated sample did not return to the level of the controls by 24h, resulting in the largest $G_2$+M accumulation of any of the cell lines examined. This single result skewed the statistical analysis. However, though a formal analysis at 4 and 8Gy for the reason mentioned above, the mutant-p53 cell lines appeared to demonstrate a progressively higher accumulation in $G_2$+M following irradiation as compared to wt-p53 cell lines.

### 5.3.5 Higher γ-radiation doses result in the later onset of $G_2$+M cell cycle maximum accumulation

The time at which the maximum accumulation of cells in $G_2$+M cell cycle phase was seen to occur in twelve human cancer cell lines increased as doses of ionising radiation increased (Figure 27A). The average time at which the maximum percentage of cells accumulated at 2Gy was 11.00h after irradiation. This increased to 13.33h following irradiation at 4Gy in the twelve cancer cell lines. This increase of 2.33h, an increase of 21% following 4Gy as compared to 2Gy was, however, not found to be significant by t-test (P=0.0839, r=0.408).

As denoted '**' in Figure 27 A, the increase in time taken for the maximum cell accumulation to occur at 8Gy, 16.33h post-irradiation, was significantly greater than that at 2Gy (P=0.0042, r=0.695), as was that observed at 8Gy as compared to 4Gy (P=0.027, r=0.545). Thus, the relatively high dose of 8Gy was shown to significantly increase the time at which twelve human cancer cell lines maximally accumulate in $G_2$+M.

**A) Time to maximum accumulation in $G_2$+M increases with γ-radiation dose**

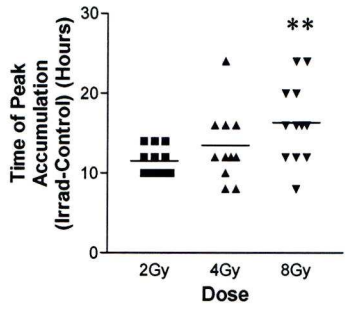


**B) p53 mutational status and time of peak accumulation in $G_2$+M following increasing doses of γ-radiation**

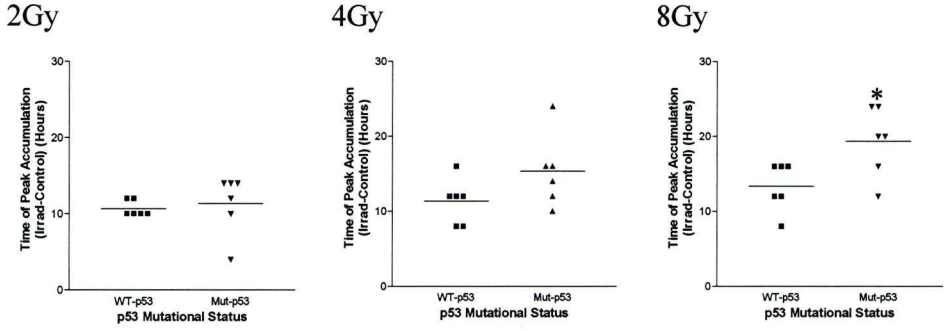


**Figure 27. The time of peak accumulation in $G_2$+M cell cycle phase in 12 human cancer cell lines and p53-mutational status at 2, 4 and 8Gy**

The influence of increasing doses of radiation and p53-mutational status on the timing of maximum percentage cell accumulation in the $G_2$+M phase of the cell cycle as shown Figures 20-25 (page 113-118), is given above. The timing of maximal cell accumulation for the twelve human cancer sell lines following 2, 4 and 8Gy of ionising γ-radiation is shown in panel A, whilst the effect of p53 mutational status at these increasing doses of radiation is in the 6 wt-p53, and 6 mutant-p53 cell lines is shown in panel B, 2Gy, 4Gy and 8Gy. The double star (**) in panel A denotes that the peak accumulation at 8Gy was significantly later than that at 2 and 4Gy. The star (*) in panel B-8Gy, donotes that the onset of peak accumulation in the mutant-p53 cell lines is significantly later than that in the wt-p53 cell lines.

### 5.3.6 p53 mutational status and the onset of peak accumulation at increasing doses of γ-radiation

In general the wt-p53 cell lines appeared to reach maximum accumulation earlier than the mutant-p53 cell lines (See Figure 27B for results at 2, 4 and 8Gy). The timing at which the mean maximum number of cell accumulated in $G_2$+M at 2Gy was found to be 10.67±0.42h and 11.33±1.61h for the six wt-p53 and six mutant-p53 cell lines respectively. However, the rapidity with which the cancer cell lines reached this maximum delay in $G_2$+M following exposure to γ-radiation, showed no significant difference between the 6 wt-p53 or the 6 mutant-p53 cancer cell lines as determined by the Welch's correction to the t-test (p=0.7046). After a dose of 4Gy there was a similarly longer interval between irradiation and the time to peak accumulation in the $G_2$+M cell cycle phase, with the mutant-p53 cell lines taking longer to accumulate maximally than the wt-p53 cell lines. As at 2Gy, this difference in time to peak accumulation failed to reach significance. The six wt-p53 cell lines on average had a maximal accumulation at 11.33±1.23h as compared to that of the mutant-p53 cell lines; that of 15.33±1.98h, with the differences in mean accumulation giving a P value of 0.0583 r=0.477 (Unpaired t-test).

At 8Gy, the same relative increase in the time to peak accumulation following irradiation was again seen. However, when considering the cell lines in terms of their p53 mutational status, the difference in mean time to peak accumulation was significant. The time taken for the onset of peak accumulation in $G_2$+M cell cycle phase for the wt-p53 cell lines was 13.33±1.33h following irradiation. This compares to 19.33±1.91h for the mutant-p53 cell lines. This shorter period, that the wt-p53 cell lines required to reach peak accumulation, was significantly different to that of the mutant-p53 cell lines (P=0.0411, Unpaired t-test). Thus, the high level of 8Gy of

ionising radiation was not only sufficient to induce a significant increase in the time taken for human cancer cell lines to reach maximal accumulation, as compared to 2 and 4Gy, but also that this high level of γ-radiation was sufficient to manifest a difference in the response of wt-p53 human cancer cell lines when compared to human cancer cell lines possessing mutant-p53. This result was unexpected, as it could be predicted that the wt-p53 cell lines could have been delayed in the $G_1$-S cell cycle phase transit, thus resulting in a longer time to maximum $G_2$+M accumulation. These data may indicate that the human cancer cell lines respond differently at 8Gy than they do at 2 and 4Gy.

### 5.3.7 Increasing doses of ionising radiation cause a greater level of the percentage of total cells to accumulate in $G_2$+M

Following increasing doses of γ-radiation, the percentage of total cells accumulating in the $G_2$+M phase of the cell cycle; the magnitude of the peak accumulation in the the post-irradiation period, was seen to increase with dose (see Figure 28A). The average peak percentage of total cells accumulating in $G_2$+M was 14.85±1.734%; 29.66±2.980%; and 42.92±3.780% following 2, 4 and 8Gy respectively. The increases in the peak accumulation were both significant at 4Gy as compared to 2Gy (P=0.0005, One tailed Wilcox-Paired t-test), and at 8Gy as compared to 2Gy (P=0.0002, One tailed Wilcox-Paired t-test), and also at 8Gy as compared to 4Gy (P=0.0002, One-tailed, Wilcox-Paired t-test). Thus, at each and every increase in the level of γ- radiation that the cells were exposed to, the response of the human cancer cell lines was shown to be an increase in peak accumulation in the $G_2$+M cell cycle phase.

**A) Peak accumulation of cells in $G_2$+M following progressively higher doses of γ-radiation**

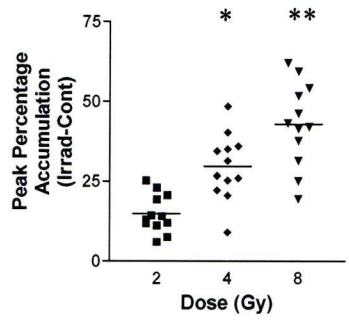


**B) p53 mutational status and peak cell accumulation in $G_2$+M following increasing doses of γ-radiation**

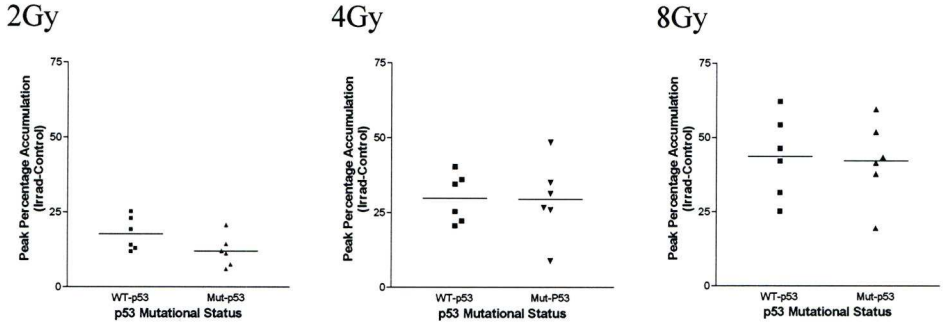


**Figure 28. The peak percentage of total cells accumulating in $G_2$+M cell cycle phase in 12 human cancer cell lines the effect of p53-mutational status at 2, 4 and 8Gy**

The influence of increasing doses of radiation and p53-mutational status on the level of maximum percentage cells accumulation in the $G_2$+M phase of the cell cycle as shown Figures 20-25 (pages 113-118), is given above. The peak percentage population of cells accumulation for the twelve human cancer sell lines following 2, 4 and 8Gy of ionising γ-radiation is shown in panel A, whilst the effect of p53 mutational status at these increasing doses of radiation is in the 6 wt-p53, and 6 mutant-p53 cell lines is shown in panel B, 2Gy, 4Gy and 8Gy. In panel A, the star (*) at 4Gy indicates that the average magnitude of peak accumulation in $G_2$+M is significantly greater than that at 2Gy, whilst the double star (**) at 8Gy indicates that the magnitude of delay in $G_2$+M is significantly greater than that at 2gy and 4Gy. This was determined by two-tailed t-test as indicated in section 5.3.7.

### 5.3.8 Peak percentage accumulation and p53 mutational status following incrementally higher ionising radiation doses

The relationship between the peak percentage accumulation of cells in the $G_2$+M phase of the cell cycle and p53 mutational status was not found to be significantly different at 2Gy (p=0.085; two tailed t-test), nor was it seen to influence the peak level of cell accumulation at 4Gy with mean accumulation of 29.84±3.33% and 29.48±5.29% for wt-p53 and mutant-p53 respectively. A t-test of these means gave a P value of 0.937, showing no significant difference. Similarly, at 8Gy of γ-radiation, the mean values for the 6 wt-p53 cell lines, and six mutant-p53 cell lines for the peak percentage accumulation was 43.61±5.63% and 42.23±5.56% respectively. These means were not found to be significantly different (P=0.818, by Mann-Whitney U-test). Though increasing doses of ionising radiation resulted in increases in the peak level of the percentage of cells accumulation in the $G_2$+M phase of the cell cycle, this dose dependent cellular response did not appear to be p53 dependent as the increase was seen in both the wt-p53 and mutant-p53 cell lines.

### 5.3.9 $G_2$+M Exit in human cancer cell lines following increasing doses of γ-radiation

The determination of the rate of exit of cells accumulated in $G_2$+M phase of the cell cycle was performed as described in Chapter 2, of the methods. As can be seen from the values in Table 14, generally, as the dose of radiation received increased, so did the time taken for the cells to exit the accumulation in $G_2$+M phase of the cell cycle. For all twelve cell lines an increased average $T_{50}$ times of 3.46±0.54h, 7.35±0.97h, and 15.47±2.59h was observed at 2, 4 and 8Gy respectively.

| P53 Status | | Dose | $G_2$+M Accumulation ($T_{50}$) 2 Gy | 4Gy | 8 Gy |
|---|---|---|---|---|---|
| Wild-Type | | 2780 | 2.59 | 7.00 | 13.65 |
| | | HEp 2 | 4.07 | 9.75 | 32.85 |
| | | HRT18 | 3.15 | 6.05 | 8.85 |
| | | I407 | 5.30 | 4.85 | 9.55 |
| | | MGH-U1 | 3.70 | 6.00 | 6.10 |
| | | OAW42 | 1.85 | 6.75 | 17.75 |
| | | ***Average*** | ***3.44*** | ***6.73*** | ***14.79*** |
| Mutant | | Colo 320 | 7.10 | 12.45 | 32.10 |
| | | H322 | 1.55 | 12.55 | 10.60 |
| | | H417 | 5.30 | 11.10 | 19.20 |
| | | HT29.5 | 4.40 | 2.90 | 7.80 |
| | | RPMI 7951 | 1.00 | 5.90 | 9.95 |
| | | RT112 | 1.55 | 2.90 | 17.25 |
| | | ***Average*** | ***3.48*** | ***7.97*** | ***16.15*** |
| Pan-P53 | | ***Average*** | ***3.46*** | ***7.35*** | ***15.47*** |

**Table 14. $G_2$+M exit ($T_{50}$) in twelve human cancer cell lines following increasing doses of ionising radiation**
The above table contains the $T_{50}$ values for the twelve human cancer cell lines used in this study at 2, 4 and 8Gy of γ-radiation from a GammaCell 1000 with a $^{137}Cs$ source. The cell lines are ranked alphabetically and by p53 Mutational Status, with the average time of exit from $G_2$+M cell cycle accumulation calculated for both wt-p53 and mutant-p53, and for pan-p53, i.e. all cells regardless of mutational status.

Although an increase in the $T_{50}$ was the general trend, it was not always present in the cell lines when considered individually as can be seen in the wt-p53 embryonic intestinal epithelial cell line I407, and the mutant-p53 colonic adenocarcinoma clonal variant HT29.5, where the $T_{50}$ times for 4Gy were greater than at 2Gy, and as is the 4Gy $T_{50}$ time as compared to the 8Gy time in the mutant-p53 small cell carcinoma cell line H322.

The obvious increases in the duration of the rate of $G_2$+M exit as measured by $T_{50}$ following increases in exposure of human cancer cells to ionising radiation as represented by the increases in the mean exit times for the twelve cell lines was

supported by the fact that these increases were significant by a Paired t-test. The increase in $T_{50}$ following 2Gy and 4Gy irradiation gave a P-value of 0.002; r=0.776. This difference was greater when comparing the $T_{50}$ at 2Gy to that of 8Gy, which generated a P-value of 0.0004, r=0.832. The increase in the mean $T_{50}$ at 8Gy compared to 4Gy gave a P-value of 0.004, r=0.744. Thus each and every increase in the dose of $\gamma$-radiation that the cells were exposed to resulted in a significant increase in the time taken for the cells to exit the $G_2$+M cell cycle phase accumulation.

**A) $T_{50}$ exit of cells in $G_2$+M following progressively higher doses of γ-radiation**

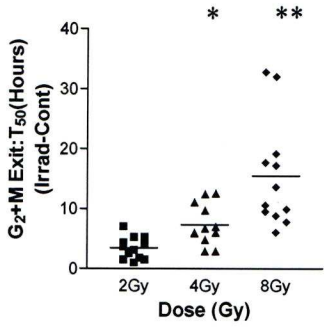


**B) p53 mutational status and $T_{50}$ exit from the $G_2$+M cell cycle phase following increasing doses of γ-radiation**

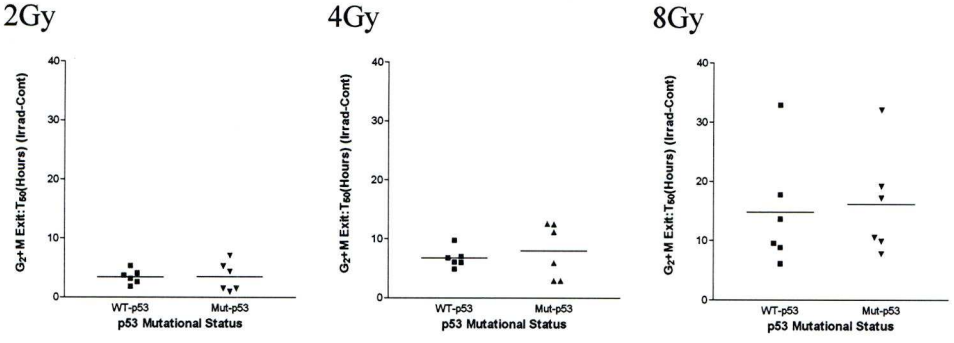


**Figure 29. The peak percentage of total cells accumulating in $G_2$+M cell cycle phase in 12 human cancer cell lines the effect of p53-mutational status at 2, 4 and 8Gy**

The influence of increasing doses of radiation and p53-mutational status on the level of maximum percentage cells accumulation in the $G_2$+M phase of the cell cycle as shown figures 20-25, is given above. The peak percentage population of cells accumulation for the twelve human cancer sell lines following 2, 4 and 8Gy of ionising γ-radiation is shown in panel A, whilst the effect of p53 mutational status at these increasing doses of radiation is in the 6 wt-p53, and 6 mutant-p53 cell lines is shown in panel B, 2Gy, 4Gy and 8Gy.

### 5.3.10 Increasing doses of γ-radiation, p53-mutational status, and the rate of exit from $G_2$+M accumulation ($T_{50}$) in human cancer cell lines

Following ionising radiation, the six mutant-p53 cell lines, on average, delayed longer than the six wt-p53 cell lines in $G_2$+M cell cycle phase. In the wt-p53 cell lines the mean (±S.E.M) $T_{50}$ exit times from a $G_2$+M accumulation following exposure to γ-radiation were 3.44±0.49h, 6.73±0.68h and 14.79±3.98h, at 2, 4 and 8Gy respectively. The mutant-p53 cell lines had a $T_{50}$ exit times of 3.48±1.01h, 7.97±1.88h and 16.15±3.67h at 2, 4 and 8Gy respectively.

Though the mutant-p53 cell lines appeared to take longer to exit the $G_2$+M phase of the cell cycle following maximum accumulation at all doses, the increases did not translate to a significant difference as determined by the unpaired t-test at either 2Gy (P=0.972, r=0.011), 4Gy (P=0.5517, r=0.191), or 8Gy (P=0.8069, r=0.079). Thus, though the mutant-p53 cells appear to take progressively longer to exit $G_2$+M following maximum accumulation, this increase in $T_{50}$ appears to be independent of p53 mutational status, though not necessarily independent of p53 protein.

### 5.3.11 Survival fraction following increasing doses of γ-radiation and the intrinsic level of RAF-1 protein in 12 human cancer cell lines

The intrinsic level of RAF-1 protein showed a negative relationship to post-irradiation survival of cells following 2, 4 and 8Gy of ionising radiation, in the twelve cancer cell lines studied. Following 2Gy of ionising radiation, the percentage of clonogenic cells as measured by $SF_2$ in the twelve cancer cell lines studied and the level of RAF-1 protein showed a significant negative relationship (r=-0.766, p=0.004) (see Figure 30A). This trend in decreased survival with higher levels of RAF-1 protein was similarly found at 4Gy ($SF_4$) (P=0.01, r=0.708) (see Figure 30B) and although such a negative trend could be seen in RAF-1 protein level and surviving fraction at 8Gy ($SF_8$) (see Figure 30C), it was not found to be significant (P=0.202, r=0.397). However it should be noted that at 8Gy very few cells demonstrated the ability to proliferate, typically less than 1 in 18 of the cells plated

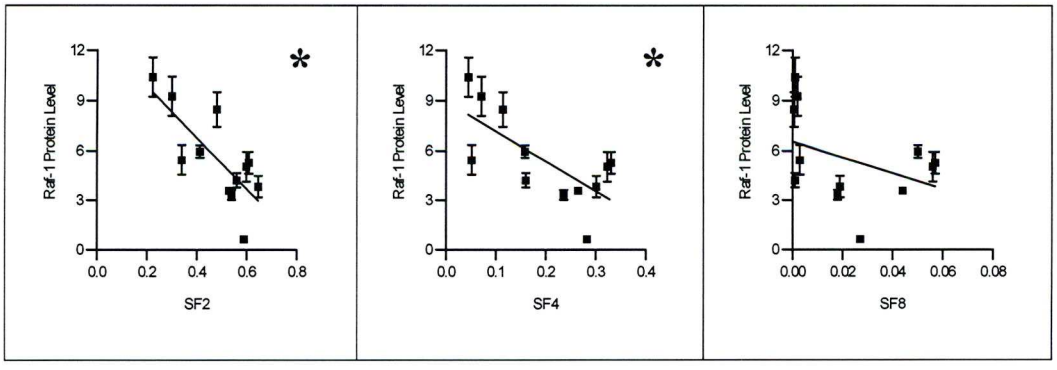


**Figure 30. Survival fraction following 2, 4 and 8Gy, and intrinsic RAF-1 protein level in 12 human cancer cell lines**
The relationship between intrinsic RAF-1 protein level on post-irradiated survival fraction (SF) at 2, 4, and 8Gy, in twelve human cancer cell lines is shown in graphs A, B, and C respectively. Statistical significant correlation (i.e. p≤0.05) is indicated by a star (*).

for clonogenic assay.

### 5.3.12 Survival fraction, RAF-1 protein level and p53-mutational status in human cancer cell lines following increasing doses of γ-radiation

When the p53 mutational status was taken into account when considering the intrinsic level of RAF-1 protein and $SF_2$, the wt-p53 cancer cell lines showed a very strong negative relationship, (r=-0.918, p=0.004). This relationship demonstrates that the cells with a shorter exit show a greater survival ($SF_2$). A similar trend relating $SF_2$ to RAF-1 protein expression was seen to be present within the mutant-p53 cell lines, whilst this relationship was negative, this relationship did not reach statistical significance in the six mutant-p53 cancer cell lines (r=-0.464, p=0.354).

As at 2Gy, the increased dose of 4Gy resulted in a decrease in survival fraction with an increase in the level of RAF-1 protein (See figure 31B and 31E). The resultant correlation between RAF-1 protein level and radiosensitivity, as determined by the survival fraction at 4Gy ($SF_4$), was only found to be statistically significant in those cells with a wt-p53. The correlation coefficients of the wt-p53 cell lines was P=0.0243, r=0.870, whilst the values generated for the mutant-p53 cell lines was P=0.2378, r=0.570.

A similar trend relating $SF_8$ to RAF-1 protein expression was seen to be present within both the wt-p53 and mutant-p53 cell lines (Figure 31C and F respectively). Whilst this relationship was negative, the correlation did not reach statistical significance in either the six wt-p53 or the six mutant-p53 cancer cell lines (P=0.311; r=0.501 and P=0.4584; r=0.379 respectively).

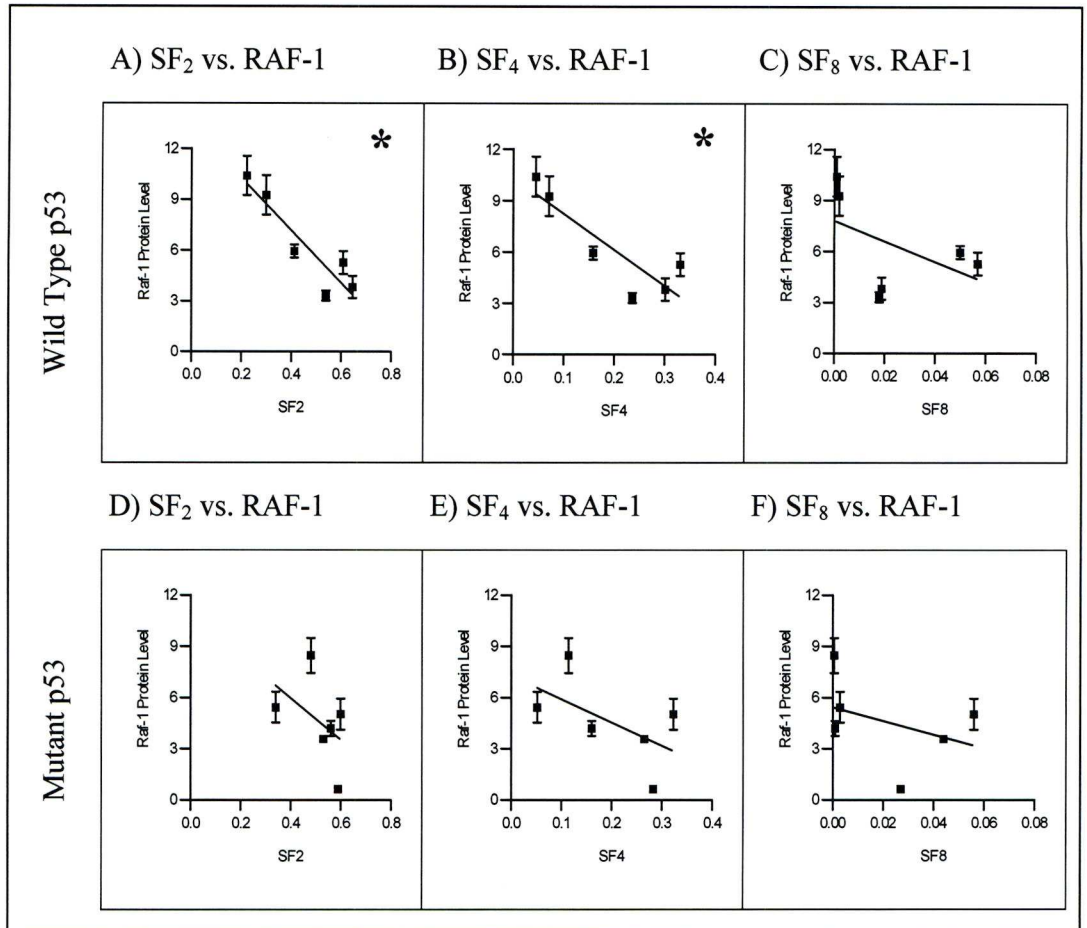


**Figure 31. The relationship between RAF-1, survival ($SF_2$), the exit from a post-irradiated $G_2$+M accumulation, and p53 mutational status**

The effect of RAF-1 protein level on post-irradiated survival fraction, in the context of p53 mutational status in twelve human cancer cell lines is shown above. The intrinsic RAF-1 protein level is plotted against survival fraction at for the six wt-p53 cell lines in A, B, and C, with the six mutant-p53 cell lines in D, E, and F at the increasing doses of 2Gy, 4Gy and 8Gy respectively. Plots that demonstrate a statistically significant relationship (i.e. $p \leq 0.05$) are indicated by a star (*).

### 5.3.13 Rate of $G_2$+M exit following increasing doses of γ-radiation and the intrinsic level of RAF-1 protein in 12 human cancer cell lines

At 2Gy of γ-radiation, the intrinsic level of RAF-1 was not found to correlate with the rate of $G_2$+M exit ($T_{50}$) when all twelve human cancer cell lines were considered together (P=0.897, r=-0.042).As at 2Gy, the intrinsic level of RAF-1 protein did not correlate to the rate of exit from radiation induced accumulation at 4Gy (P=0.976, r=0.098), see figure 32B, or at 8Gy (P=0.347, r=0.298), see figure 32C.

A) $T_{50}$ at 2Gy and RAF-1 B) $T_{50}$ at 4Gy and RAF-1 C) $T_{50}$ at 8Gy and RAF-1

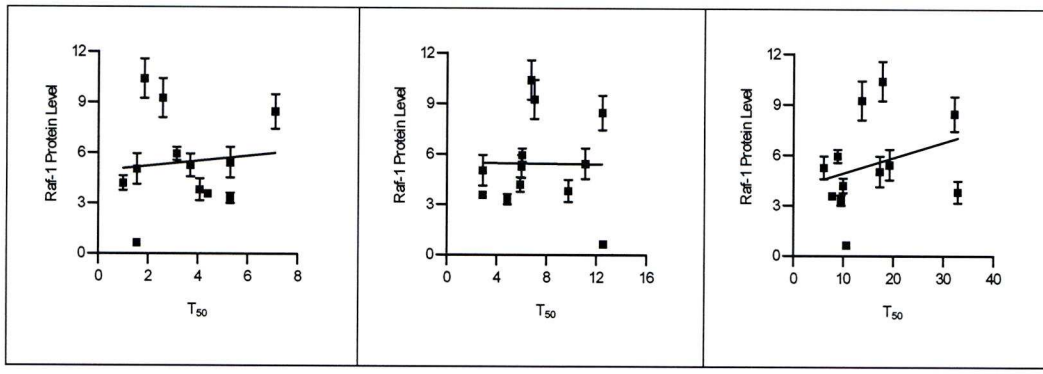


**Figure 32. Exit from $G_2$+M accumulation following 2, 4 and 8Gy, and intrinsic RAF-1 protein level in 12 human cancer cell lines**
The relationship between intrinsic RAF-1 protein level on the rate of exit from $G_2$+M following γ-radiated doses of 2, 4 and 8Gy, in twelve human cancer cell lines is shown in graphs A, B, and C respectively.

### 5.3.14 $G_2$+M exit, RAF-1 protein level and p53 mutational status in human cancer cell lines following increasing doses of γ-radiation

The mutational status of p53 was shown to contribute to the correlation between RAF-1 protein level and the rate at which cells exit the $G_2$+M post-irradiation accumulation, as determined by $T_{50}$ at 2Gy. For the wt-p53 cell lines a relationship of high RAF-1 protein level and rapid exit from $G_2$+M accumulation was observed (P=0.002, r=0.965). This positive relationship observed in the wt-p53 cell lines between the high levels of RAF-1 protein and the rapidity of exit from a $G_2$+M accumulation, as indicated by a low $T_{50}$, was reversed in the mutant-p53 cell lines and was not statistically significant (P=0.070, r=-0.775).

As can be seen from Figure 33B and E, at 4Gy there was no apparent relationship in the rate of $G_2$+M exit and intrinsic RAF-1 protein level in either the wt-p53 or mutant-p53 cell lines (P=0.998;r=0.001, or P=0.858; r=0.095, respectively). A similar absence of a correlation between the $T_{50}$ of $G_2$+M exit following 8Gy to the intrinsic level of RAF-1 protein expression was seen to be present within the wt-p53, P=0.900; r=0.097 (Figure33C), However, in the mutant-p53 cell lines a strong positive relationship between the rate of exit from γ-radiation induced $G_2$+M accumulation and the level of intrinsic RAF-1 protein expression was demonstrated (P=0.032; r=0.850).

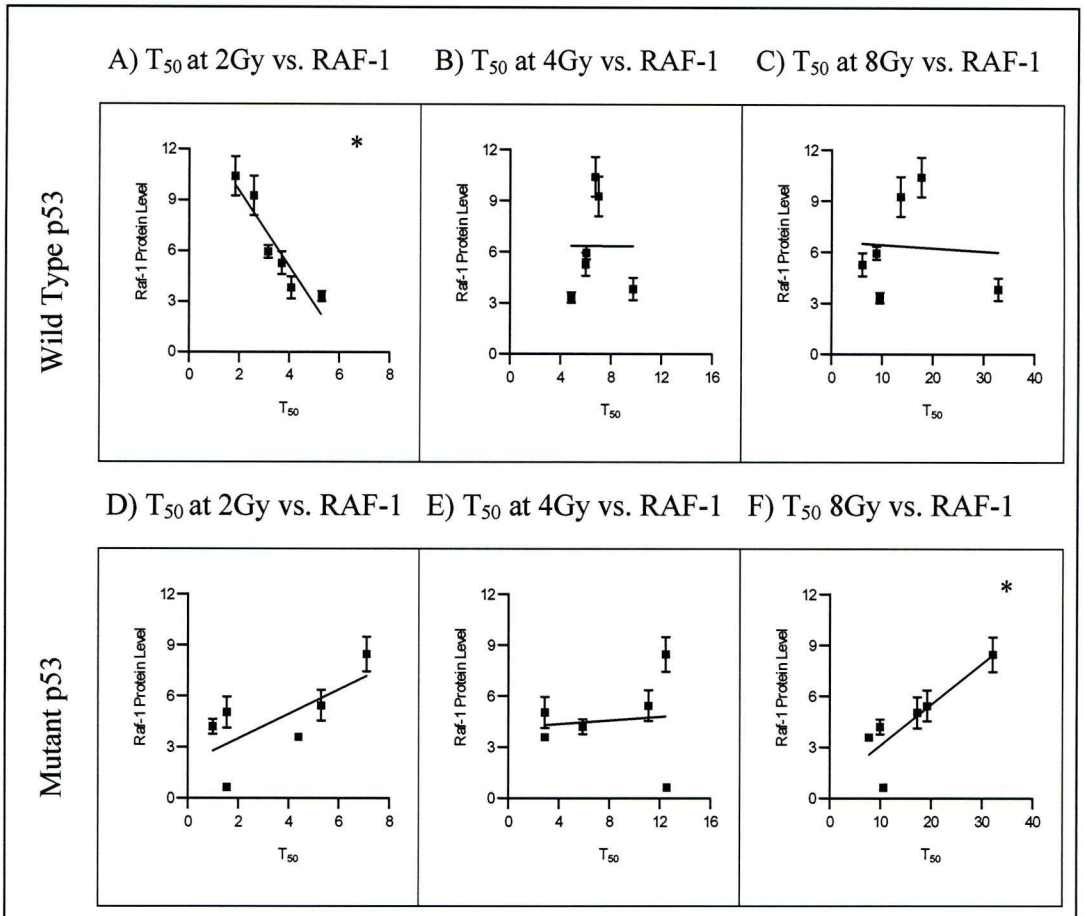


**Figure 33. Exit from post-irradiated $G_2$+M accumulation, RAF-1 protein level, and p53 mutational status**

The effect of RAF-1 protein level on post-irradiated exit from $G_2$+M accumulation ($T_{50}$), in the context of p53 mutational status in twelve human cancer cell lines is shown above. The intrinsic RAF-1 protein level is plotted against $T_{50}$ for the six wt-p53 cell lines in A, B, and C, and for the six mutant-p53 cell lines in D, E, and F at the increasing doses of 2Gy, 4Gy and 8Gy respectively. Plots that demonstrate a statistically significant relationship (i.e. $p \leq 0.05$) are indicated by a star (*).

### 5.3.15 Increasing doses of radiation, rate of exit from $G_2$+M accumulation and post-irradiation clonogenisity in human cancer cell lines

Following a single fraction of γ-radiation at 2Gy from a $^{137}Cs$ source, no apparent relationship was found at this clinically relevant dose in the twelve human cancer cell lines between the rate of exit from $G_2$+M accumulation, $T_{50}$, and proliferative fraction as measured by clonogenic assay (correlation coefficient P=0.897, r=-0.04). At 4 and 8Gy, a tentative negative relationship between the time taken for cells to exit a pre-mitotic cell cycle accumulation and survival fraction appeared to develop. With increasing doses of radiation, 4 and 8Gy, a trend of decreased radiosensitivity with decreased $T_{50}$ transit time (Figure 34B and 34C respectively). When this putative relationship was tested, no significant link between survival fraction and $T_{50}$ was found (P=0.352; r=0.294 and P=0.152, r=0.440 respectively), although the correlation at 8Gy was closer to significance than at 4Gy.

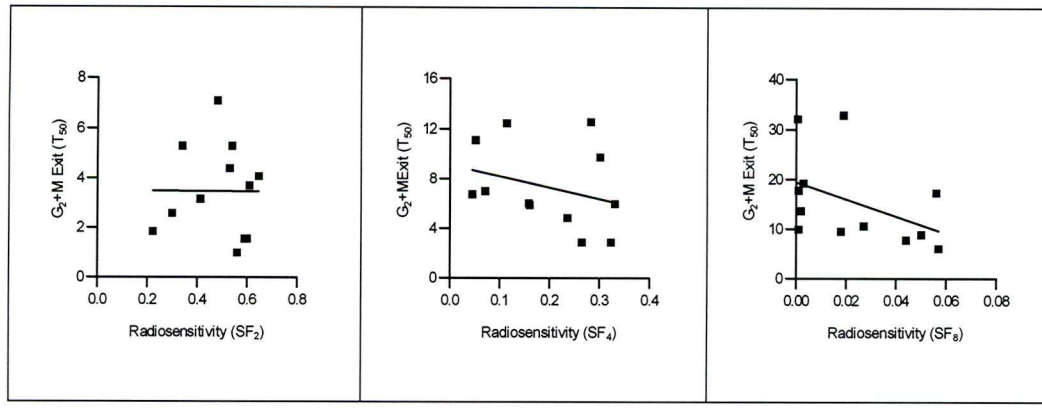


**Figure 34. Intrinsic radiosensitivity and the rate of exit from $G_2$+M cell cycle accumulation following 2, 4 and 8Gy single fraction of γ-radiation in 12 human cancer cell lines**

The relationship between survival fraction on the rate of exit from $G_2$+M following γ-radiated doses of 2, 4 and 8Gy, in twelve human cancer cell lines is shown in graphs A, B, and C respectively. All points are shown with error bars (S.E.M.). However, the error bars lie within the data point symbol.

### 5.3.16 Progressively higher doses of radiation and its effect on the rate of $G_2$+M exit ($T_{50}$) on radiosensitivity (survival fraction) in wt-p53 as compared to mutant-p53 cancer cell lines

As depicted in Figure 35A wt-p53 did appear to contribute to the rate of post-irradiation $G_2$+M exit, $T_{50}$, with relation to post-irradiation clonogenic survival following 2Gy of γ-radiation, $SF_2$. In the cells lines expressing wt-p53 the rate at which cells exit the post-irradiation $G_2$+M cell cycle accumulation appears to have a strong positive influence on radiosensitivity, i.e. the longer cells take to exit the post-irratiation induced $G_2$+M accumulation the more cells survive. This relationship was not present in the mutant-p53 cell lines, see Figure 35D. In the wt-p53 cell lines the relationship between the rate of $G_2$+M exit and $SF_2$ was found to give a linear regression of r=0.965 with a significance of P=0.002. In the mutant-p53 cell lines the relationship between $T_{50}$ and $SF_2$ failed to reach significance at 5%. Thus the strong positive relationship observed in the wt-p53 cell lines switched to a non-significant negative relationship, that is cells exiting the $G_2$+M accumulation more rapidly demonstrated a greater clonogenic survival (P=0.070, r=-0.775).

At 4Gy (Figure 35B), the trend of radiosensitivity and rapid exit from $G_2$+M cell cycle phase delay still appeared in wt-p53 cell lines, however this relationship was not found to be significant in either the 6 wt-p53 cell lines or the 6 mutant-p53 cell lines (Figure 35E)(P=0.799; r=0.135 and P=0.263; r=0.545 respectively). As at 4Gy, following 8Gy of γ-radiation (Figure 35C and F), both the 6 wt-p53 cell lines and the mutant-p53 cell lines resulted in a decreased survival fraction following a more rapid exit from $G_2$+M exit. Similarly, as at 4Gy this apparent trend was not found to be significant with P-values of 0.349 and 0.424 and r-values of 0.468 and 0.407 for the wt-p53 and mutant-p53 cell lines respectively.

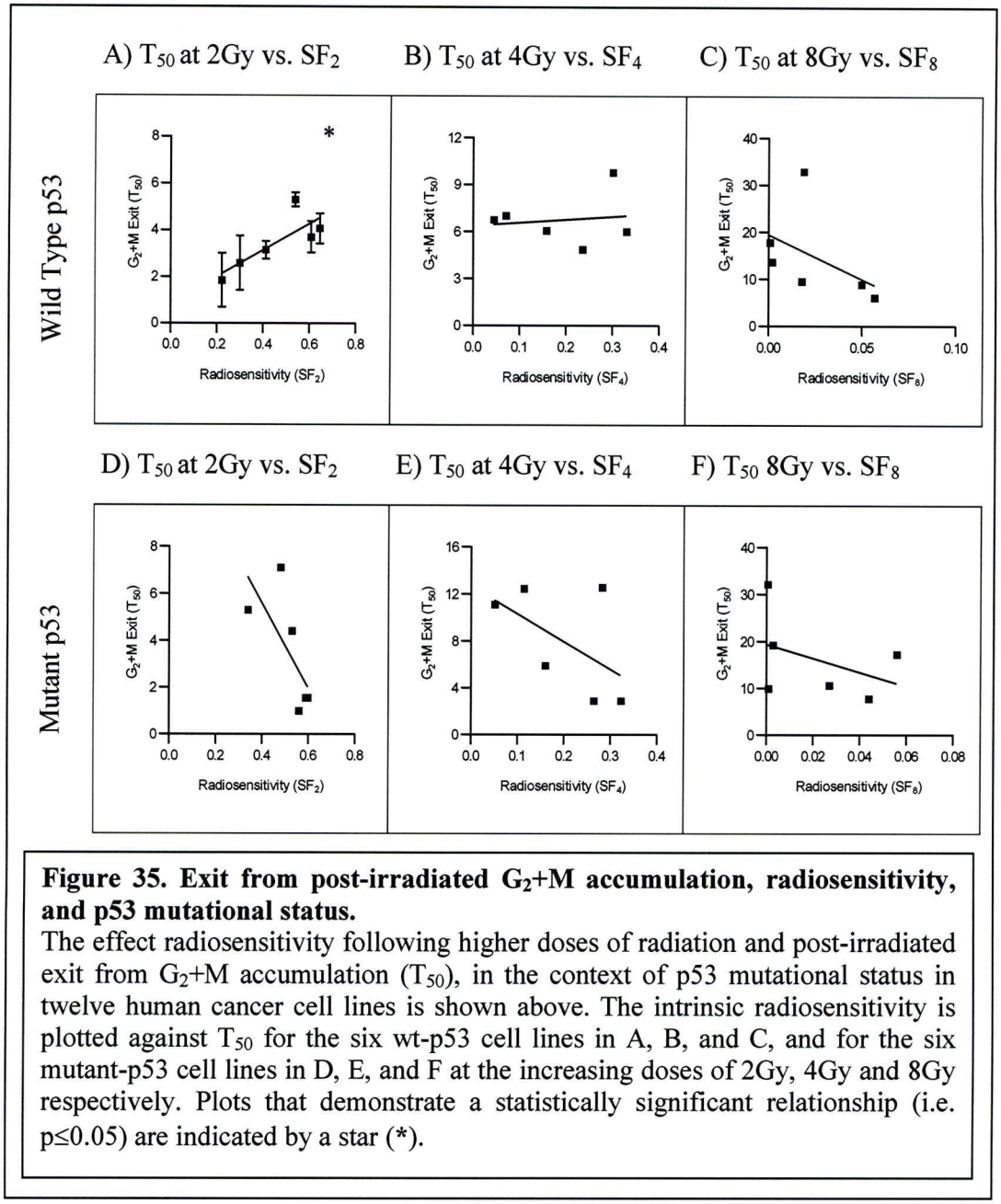


**Figure 35. Exit from post-irradiated $G_2$+M accumulation, radiosensitivity, and p53 mutational status.**

The effect radiosensitivity following higher doses of radiation and post-irradiated exit from $G_2$+M accumulation ($T_{50}$), in the context of p53 mutational status in twelve human cancer cell lines is shown above. The intrinsic radiosensitivity is plotted against $T_{50}$ for the six wt-p53 cell lines in A, B, and C, and for the six mutant-p53 cell lines in D, E, and F at the increasing doses of 2Gy, 4Gy and 8Gy respectively. Plots that demonstrate a statistically significant relationship (i.e. $p \leq 0.05$) are indicated by a star (*).

# Chapter 6

## Post-irradiative relationship between RAF-1 protein expression, $G_2$+M accumulation and radiosensitivity in human cancer cell lines following inhibition of p53 by the small molecule inhibitor Pifithrin-α

# 6 Post-irradiative relationship between RAF-1 protein expression, $G_2$+M accumulation and radiosensitivity in human cancer cell lines following inhibition of p53 by the small molecule inhibitor Pifithrin-α

## 6.1 Introduction

Previous studies to explore the putative relationship between RAF-1 protein level, radiosensitivity and $G_2$+M cell cycle phase accumulation following 2, 4 and 8Gy of γ-radiation have yielded some conflicting results [480, 506]. The key observation throughout this thesis is the relationship between the proto-oncogene RAF-1 protein level, exit from post-irradiated $G_2$+M cell cycle accumulation and radiosensitivity at 2Gy which is present in wt-p53 but not mutant-p53.

In 1999 Andrea Gudkov and co-workers published data on a small molecule, Pifithrin α (derived from P-fifty-three inhibitor) (PFTα), which was capable of protecting normal mouse tissue from the effects of high levels of radiation. It was postulated that this increased radioresistance was by inhibition of p53-mediated apoptosis [507]. Therefore PFTα was used to further explore the influence of p53 mutational status on RAF-1 radiosensitivity and the rate of exit of cells from $G_2$+M.

## 6.2 Methods

### 6.2.1 Toxicity determination of the small molecule inhibitor of p53-PFTα in 10 human cancer cell lines

In the following experiments, the effect of post-irradiation clonogenic cell survival of modulating p53 function by PFTα is studied. It was initially necessary to identify a dose of PFTα that was not itself toxic to the cells in a clonogenic cell survival assays.

The effect of exposure to PFTα in ten adherent human cancer cell lines with a range of PFTα doses was therefore studied.

Cells were seeded into 6 well tissue culture plates at 100, 200 and 500 cells per well in triplicate, along with control plates to determine plating efficiency and were incubated at 37°C in a humid incubator with 5% v/v $CO_2$ in air, for 6h such, that the cells attached. This was visually confirmed microscopically. Cells were then treated with 2, 5, 10, 15, 20 and 25μM PFTα in DMSO. The final concentration of DMSO was at 0.1%v/v for all samples. Following drug application the cells were then returned to the incubator and examined frequently over a two-week period.

The clonogenic assay was terminated once large colonies had formed, but before the colonies started to merge. This was usually around 10 to 14 days after the initiation of the assay. The media were aspirated; the plates were carefully washed twice with PBS and then fixed overnight in 70% v/v ethanol in RO water at room temperature.

The six-well plates were then stained in a 10% w/v giemsa in ethanol for 30 min at room temperature. Excess giemsa was washed off the plates by one wash in 70% v/v ethanol followed by one wash in cold tap water. The plates were then allowed to dry overnight at room temperature before counting. Only colonies containing over 50 cells were counted (as outlined in Materials and methods, section 2.2).

### 6.2.2 Determination of clonogenisity in 10 human cancer cell lines following ionising radiation in the presence of the p53-inhibitor PFTα

Radiosensitivity, the measurement of how sensitive cells are to radiation, is determined clonogenically and expressed in terms of survival fraction $SF_n$, at a given dose, n. The $SF_n$ was determined for the ten adherent human cancer cell lines used in this study by exposure to a range of radiation doses following an overnight pre-

treatment with 10μM PFTα, a maximal non-toxic dose predetermined to cause less than 5% death in the majority of the cell lines. PFTα was initially dissolved in DMSO and then diluted to the required concentration by the addition of complete HAMS F12 supplemented with 10% v/v FCS. The final DMSO concentration in complete tissue culture media was 0.1% v/v.

Each of the ten human cancer cell lines was exposed to progressively stepped doses of γ-radiation at 0, 1, 2, 3, 4, 6 and 8Gy. The clonogenic assays were otherwise carried out as highlighted in section 2.2, with the same principles being used in the calculation of the survival curves and determination of the alpha and beta values.

The survival curves were calculated using GraphPad Prism 3.0 (GraphPad Software, Inc). The data was first transformed using Y=log (Y) and then a second order polynomial non-linear regression was undertaken, with constants A set to 0, i.e. no death at 0Gy and the second and third constants variable (second and third constants being the initial and late gradients of the curve and called α and β respectively) giving the equation of $SF_D=\exp(-\alpha D - \beta D^2)$, where D is dose and SF is survival fraction. These survival curves are shown in Figures 36 and 37 and analysed to determine whether the PFTα had affected radiation induced clonogenic cell survival using two-way ANOVA of the survival fraction data.

### 6.2.3 Rate of $G_2$+M exit ($T_{50}$) following 2, 4 and 8Gy of γ-radiation in the presence of PFTα.

All experiments were undertaken on asynchronous, exponentially growing cell cultures as outlined in section 2.3 of the materials and methods. Prior to irradiation the cells were pre-incubated with 10μM PFTα for 24h under normal culture conditions. Following pre-incubation with PFTα the cells were irradiated at 2, 4 or 8Gy such that the modulation of cell cycle delay and the rate of exit at these incremental doses of ionising radiation could be investigated. The cells were seeded, irradiated, harvested and analysed as indicated in section 2.3 in the Materials and Methods.

## 6.3 Results

### 6.3.1 PFTα toxicity assays.

The toxicity of PFTα on the 10 human cancer cell lines was determined by clonogenic assay following incubation with PFTα at 2, 5, 10, 15, 20 and 25μM. This experiment was undertaken to determine the maximum dose that could be used on the human cancer cell lines before significant levels of cell death were induced. It was determined that this should be no greater than 95% in the majority of the cell lines, i.e. 6 of the 10. As can be seen in Figure 36, all the cancer cell lines survived 10μM PFTα, however at 15μM only the wt-p53 cell lines 2780 and Hep2 survived. Thus the highest dose of PFTα that 95% clonogenic survival cut-off criteria achieved was 10μM.

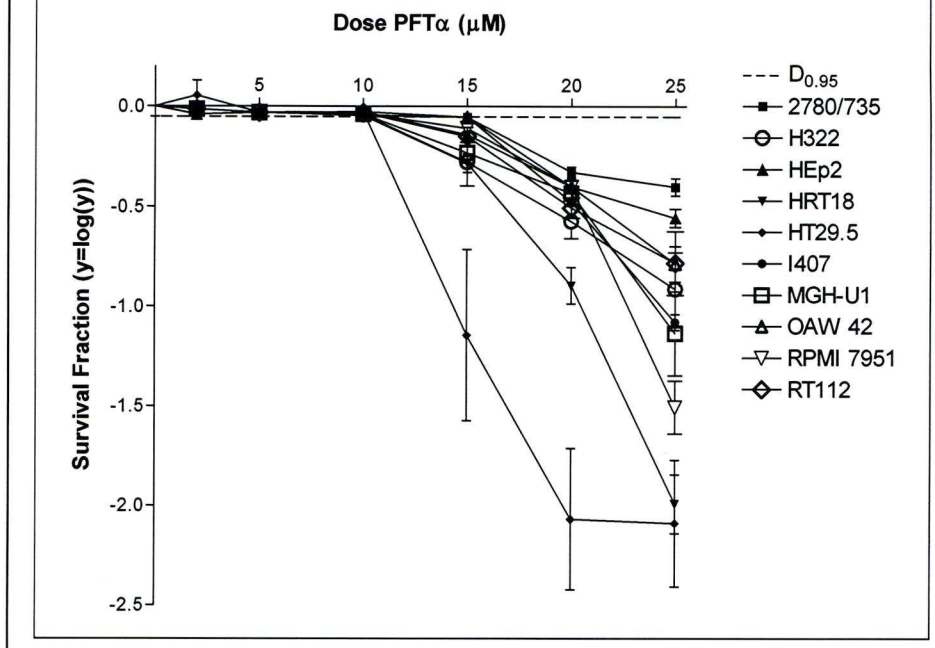


**Figure 36. Clonogenic determination of PFTα toxicity.**
Clonogenic assays were undertaken on the ten adherent human cancer cell lines used in this study. All ten adherent cancer cell lines are shown above (see legend), along with the $D_{0.95}$ cut of point, i.e. the level of 95% cloning efficiency, which was used to determine the optimal incremental doses of PFTα to be utilised in the post-irradiation studies.

### 6.3.2 Effect of the solvent DMSO on cellular radiosensitivity

The organic solvent DMSO can act as an anti-oxidant and as such is capable of scavenging short lived free radicals of $H^+$ and $OH^-$ generated by ionising radiation and thus protect against radiation induced damage and clonogenic cell death [508, 509].

Thus, as DMSO was the solvent for the p53 inhibitor PFTα, clonogenic assays were undertaken for the ten adherent human cancer cell lines in 0.1% v/v DMSO in complete culture media and compared these findings to historical clonogenic data, which has been used previously.

The 0.1% DMSO pre-treatment had little or no effect on the post-irradiation survival of the wt-p53 cell lines 2780, HEp2, MGH-U1 and OAW 42, with ANOVA analysis resulting in P values of 0.0991, 0.6380, 0.9950 and 0.105 respectively when compared to the untreated post-radiation clonogenic cell assays (see Figure 37A, 37B, 37E and 37F).

In two of the cell lines HRT18 and I407 increases in radiosensitivity resulted from pre-treatment with 0.1% v/v DMSO in the clonogenic media HAMS 12 supplemented with 10% foetal calf serum (See Figure 37C and 37D respectively). For I407 a highly significant P value of 0.0012 was generated from a two way ANOVA, whilst the HRT18 cell lines gave a very highly significant P value of $<0.0001$ for cells treated with DMSO as opposed to untreated cells.

In the four p53 mutant cell lines, H322, HT29.5, RPMI7951 and RT112 pre-treatment did not result in any significant alterations on the post-irradiative clonogenic survival (see Figure 38).

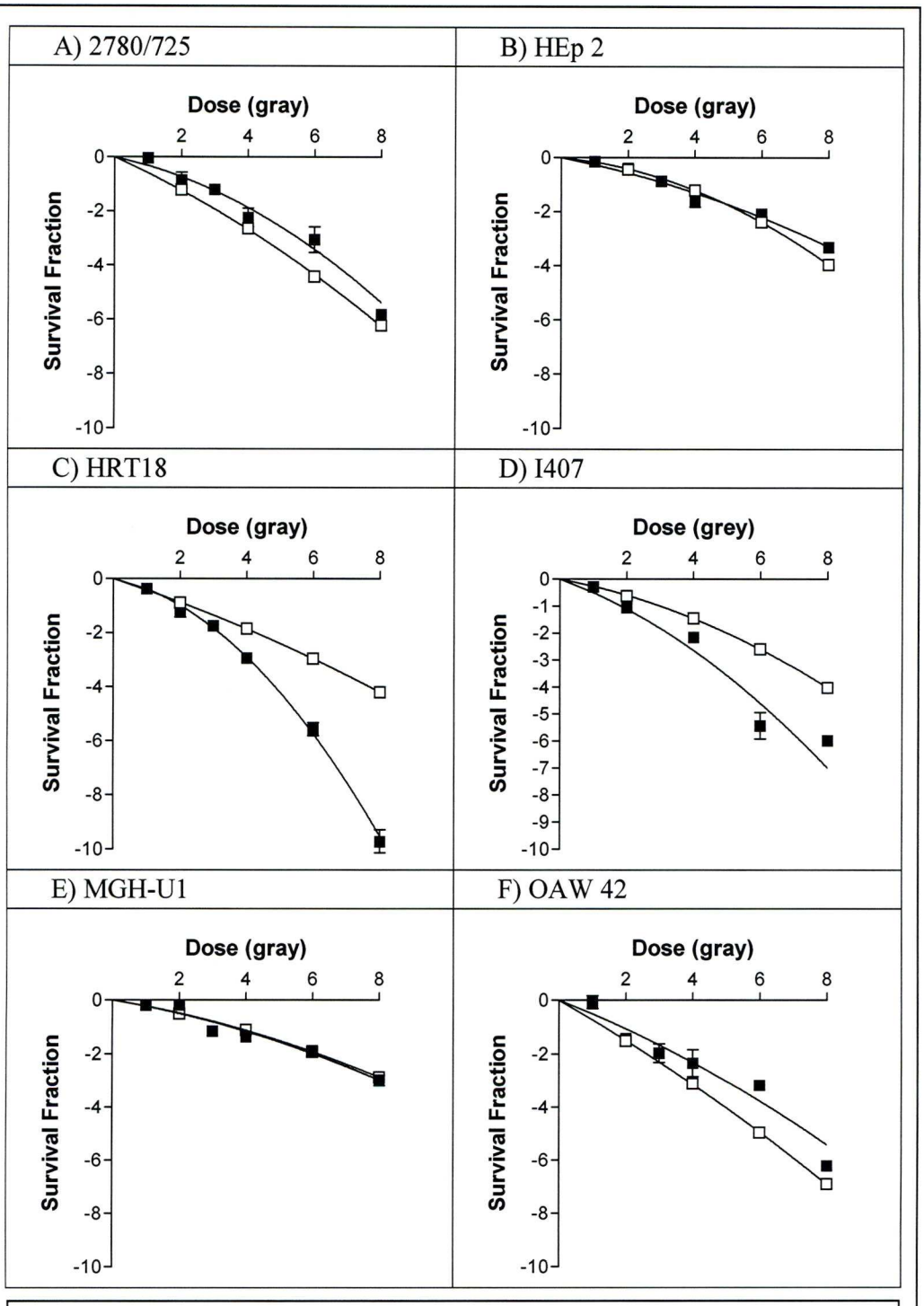


**Figure 37. The effect of the anti-oxidant DMSO and clonogenic survival following γ-irradiation in six wt-p53 cell lines**

The clonogenic survival curves for six-wt-p53 cell lines following a range of doses (0-8Gy) of γ-radiation are shown above. The open squares represent the historical data whilst the filled squares represent the 0.1% v/v DMSO pre-treated cells. All data points are plotted with error bars (S.E.M.).

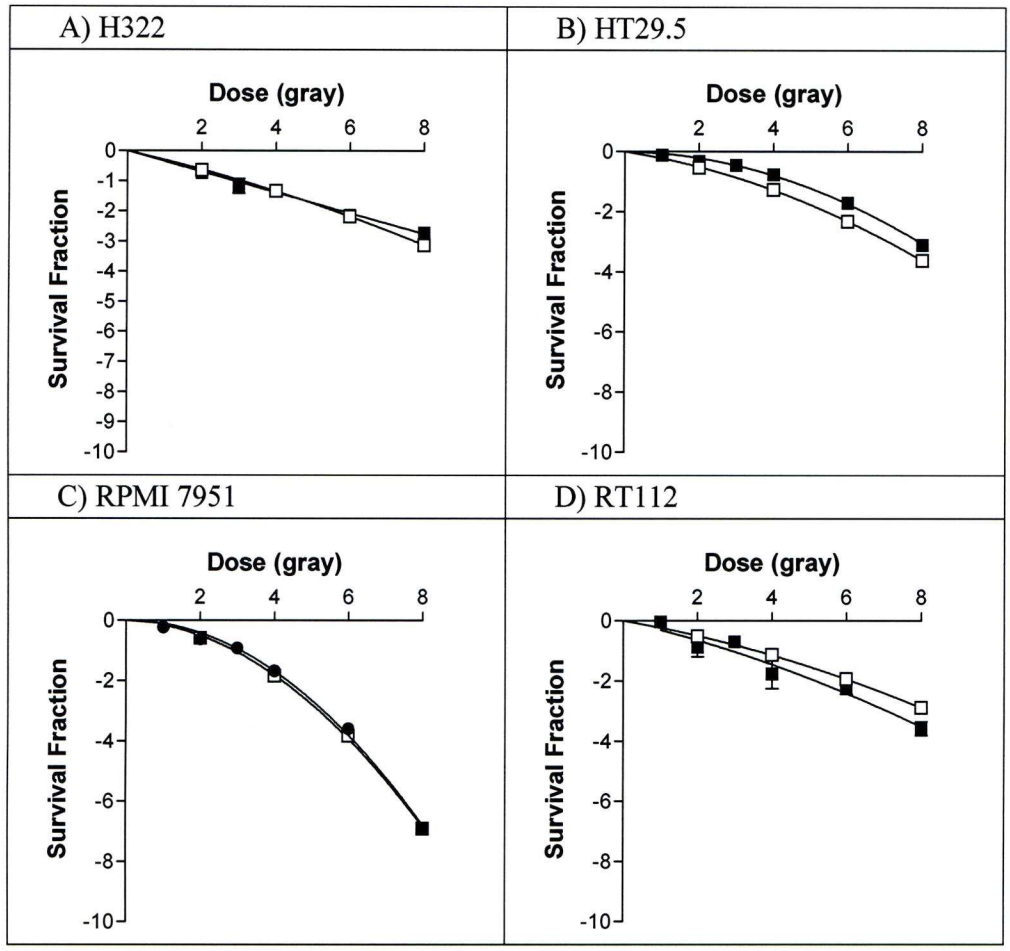


**Figure 38. The effect of the anti-oxidant DMSO and clonogenic survival following γ-irradiation in four mutant-p53 cell lines.**
The clonogenic survival curves for four mutant-p53 cell lines following a range of doses (0-8Gy) of γ-radiation are shown above. The open squares represent the historical data whilst the filled squares represent the 0.1% v/v DMSO pre-treated cells. All data points are plotted with error bars (S.E.M.).

### 6.3.3 Effect of 10μM PFTα on cellular radiosensitivity

Comparison of the radiosensitivity of human cancer lines with and without 10μM PFTα pre-treatment had little or no effect on the post-irradiation survival at 0, 2, 4, 6 and 8Gy of γ-radiation in three of the six wt-p53 cell lines (see Figure 39). ANOVA analysis of the ovarian carcinoma 2780, squamous carcinoma of the Larynx HEp2 and the Transitional bladder carcinoma MGH-U1 resulted in P values of 0.8165, 0.9318 and 0.7729 respectively.

One cell line demonstrated a decrease in radiosensitivity with PFTα treatment. The ovarian cancer cell line OAW 42 gave a significant increase in post-irradiative clonogenic survival (P=0.0189 as determined by two-way ANOVA).

As in the 0.1% v/v DMSO treated cells, the rectal adenocarcinoma HRT18 and the intestinal epithelium I407, demonstrated an increases in radiosensitivity following pre-treatment with 10μM PFTα in the clonogenic media HAMS 12 supplemented with 10%v/v foetal calf serum. The responses of both these cell lines, HRT18 and I407, mirrored that seen in the DMSO pre-treated cell lines (see Figures 37 and 39). In I407, the toxic effect of 10μM PFTα in DMSO increased as compared to that of the cells without PFTα, (see Figures 37D and 39D). This increase was found to be significant (P=0.001).

As in the DMSO pre-treatment post-irradiation clonogenic assay, the four mutant-p53 cell lines, H322, HT29.5, RPMI7951 and RT112 pre-treatment with 10μM PFTα did not result in any significant alterations on the post-irradiative clonogenic survival (see Figure 40) (ANOVA $P \geq 0.8253$ for the four cell lines) .

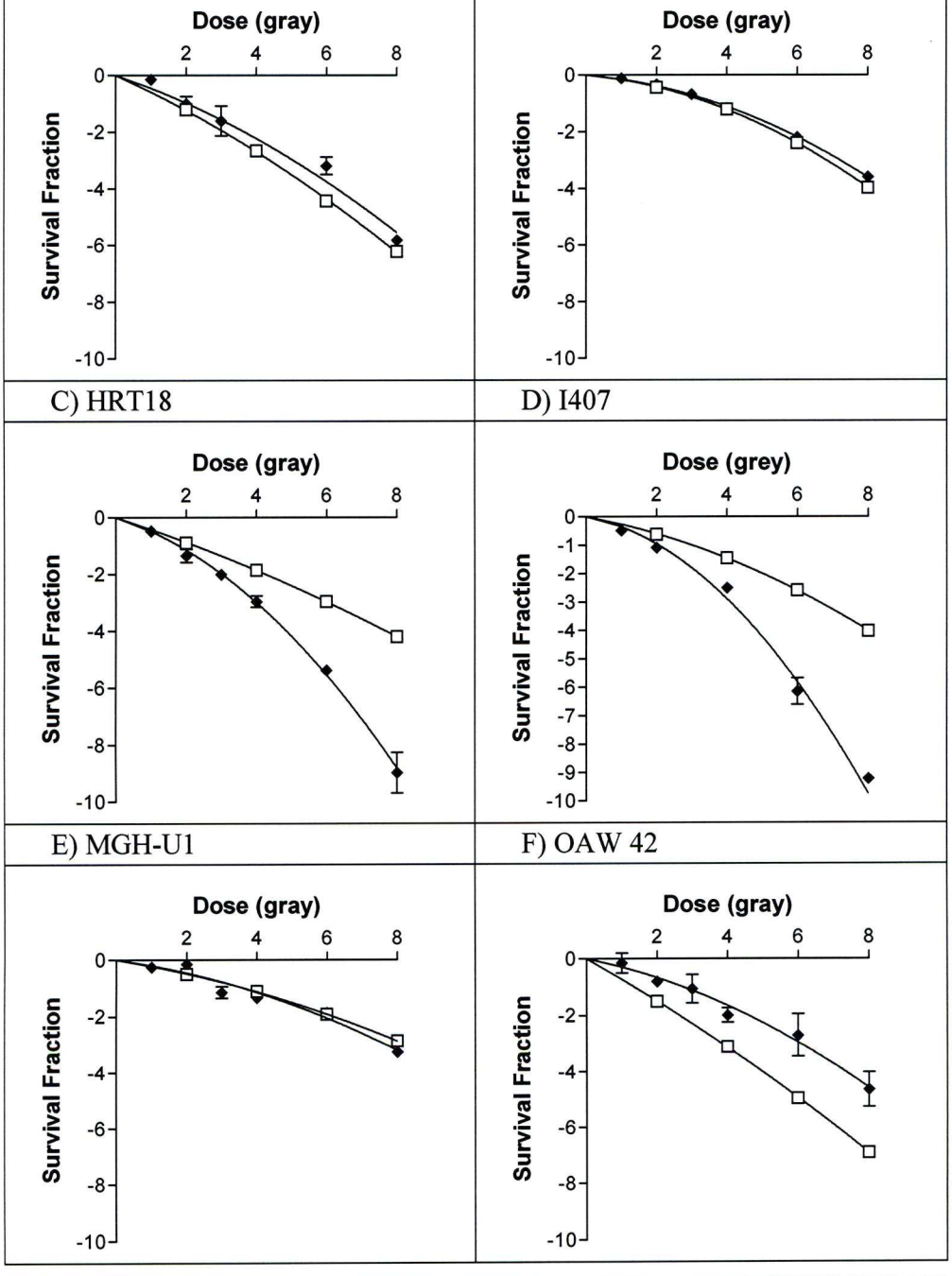


**Figure 39. p53 inhibition with 10μM PFTα and clonogenic survival following irradiation in six wt-p53 cell lines**

The clonogenic survival curves for six wt-p53 cell lines following a range of doses (0-8Gy) of γ-radiation are shown above. The open squares represent the historical data whilst the filled diamonds represent the 10μM PFTα pre-treated cells. All data points were plotted with error bars (S.E.M.).

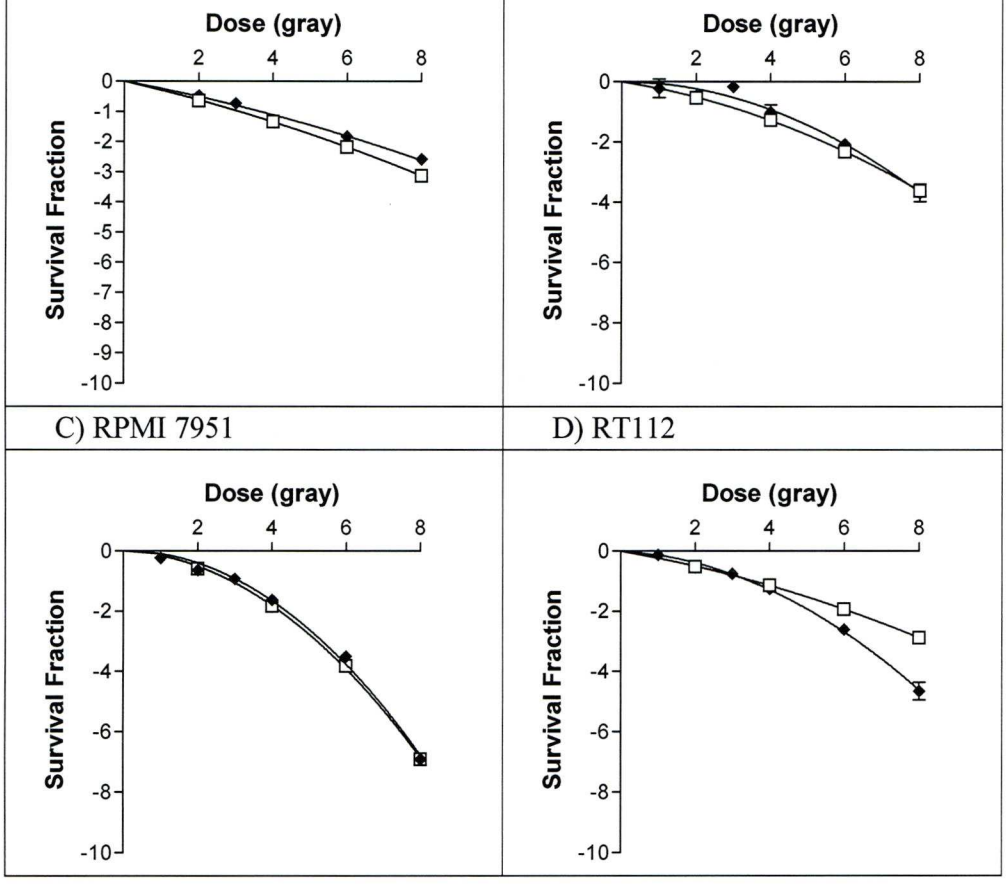


**Figure 40. p53 inhibition with 10μM PFTα and clonogenic survival following irradiation in four mutant-p53 cell lines**
The clonogenic survival curves for four mutant-p53 cell lines following a range of doses (0-8Gy) of γ-radiation are shown above. The open squares represent the historical data whilst the filled diamonds represent the 10μM PFTα pre-treated cells. All data points are plotted with error bars (S.E.M.).

### 6.3.4 Comparison of the p53 inhibitor PFTα and DMSO in post-irradiation radiosensitivity in human cancer cell lines

The next aim was to compare the effect of the small molecule p53 inhibitor PFTα to the organic solvent DMSO on radiosensitivity in six wt-p53 and four mutant-p53 human cancer cell lines. Four of the six wt-p53 cell lines, 2780, HEp2, HRT18 and MGH-U1 demonstrated no significant difference in their radiosensitivity for cells treated with 0.1% v/v DMSO or 10μM PFTα (determined by two-way ANOVA analysis with P values of 0.109, 0.395, 0.616 and 0.557 respectively) (Figures 40A, 40B, 40C and 40E respectively).

In the I407 cells, the 10μM PFTα had an additional radiosensitising effect, in addition to that seen in cells with 0.1% v/v DMSO alone ($P<0.0001$) (figure 41D), whilst in OAW42, the PFTα showed the predicted radio-protective response, although the difference in radiosensitivity is only slightly more than that of the DMSO alone pre-treated cells, this decrease in post-irradiation sensitivity was found to be significant by two-way ANOVA ($P=0.033$) (figure 40F). In the mutant-p53 cell lines, no effect for the pre-incubation in 10μM PFTα as compared to 0.1% v/v DMSO was observed (H322; $P=0.062$, HT29.5; $P=0.067$, RPMI 7951; $P=0.986$, RT112; $P=0.367$) (see Figure 41).

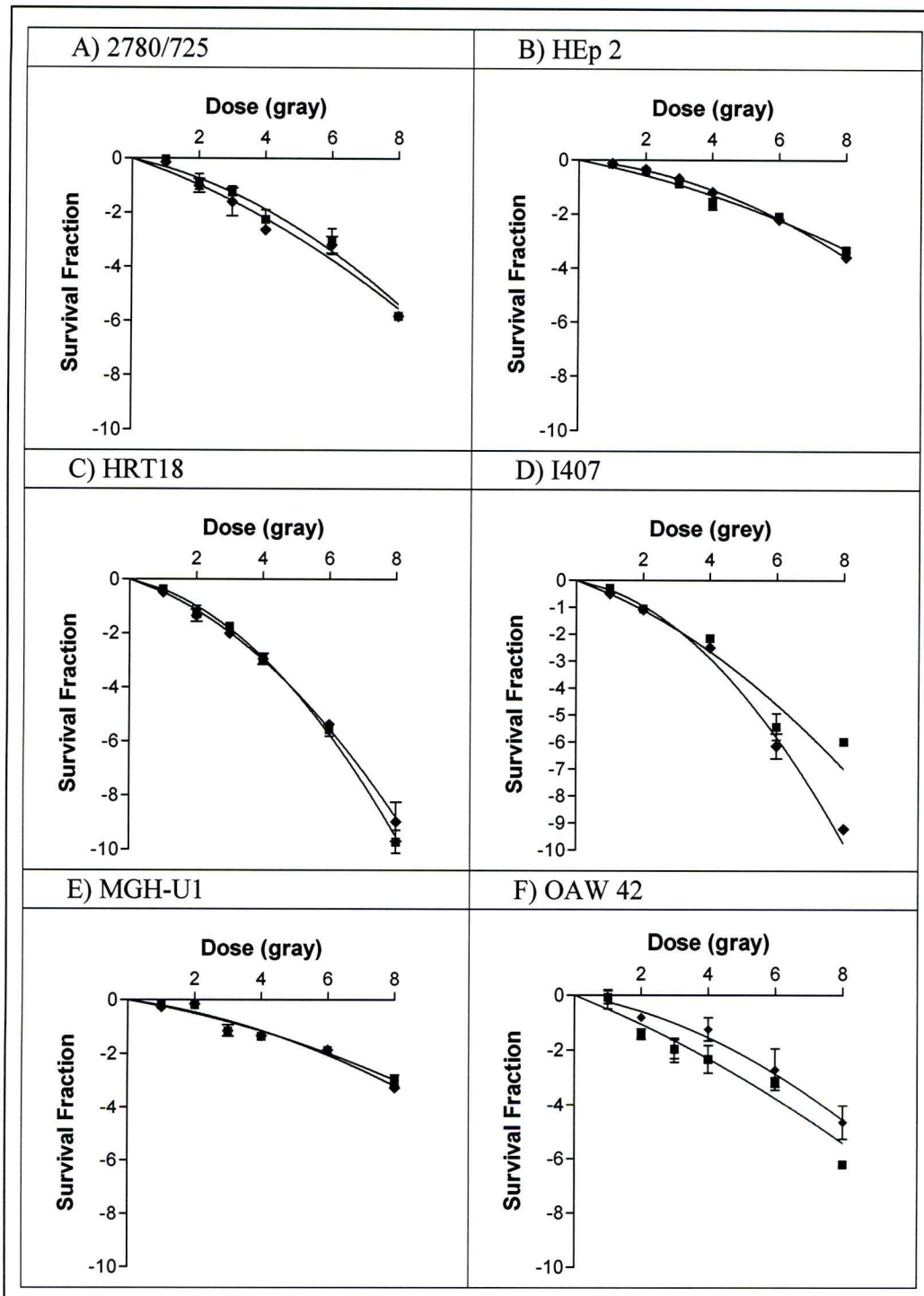


**Figure 41. p53 inhibition with 10μM PFTα and clonogenic survival following irradiation in six wt-p53 cell lines**

The clonogenic survival curves for six wt-p53 cell lines following a range of doses (0-8Gy) of γ-radiation are shown above. The filled squares represent the 0.1% v/v DMSO data whilst the filled diamonds represent the 10μM PFTα pre-treated cells. All data points are plotted with error bars (S.E.M.).

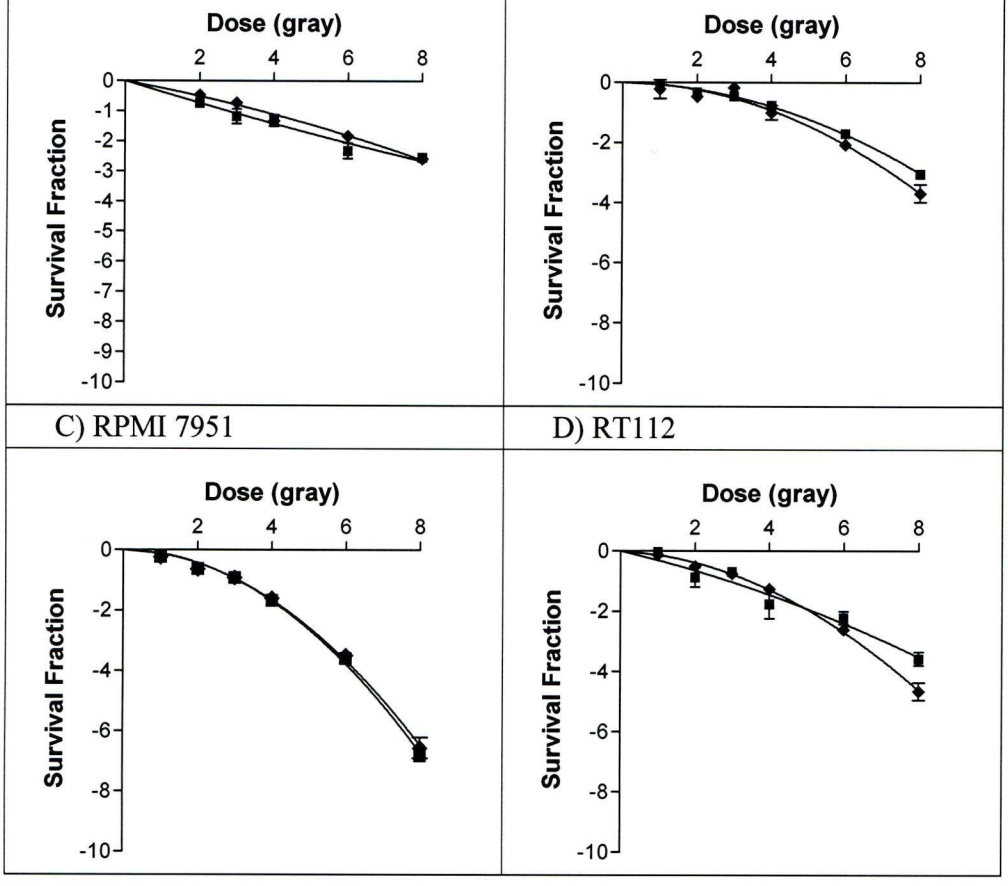


**Figure 42. p53 inhibition with 10μM PFTα and clonogenic survival following irradiation in four mutant-p53 cell lines**
The clonogenic survival curves for four mutant-p53 cell lines following a range of doses (0-8Gy) of γ-radiation are shown above. The filled squares represent the 0.1% v/v DMSO data whilst the filled diamonds represent the 10μM PFTα pre-treated cells. All data points are plotted with error bars (S.E.M.).

### 6.3.5 Accumulation of cells in $G_2$+M cell cycle phase following progressively higher steps in γ-radiation dose following pre-treatment with PFTα

I have previously examined the percentage of cells accumulating in $G_2$+M following 2, 4 and 8Gy of ionising irradiation in a range of cancer cell lines (shown in Figures 20-25, section 5.3.3). Investigated here was whether the small molecule inhibitor of p53, PFTα, affected the time taken for irradiated cells to exit the $G_2$+M cell cycle accumulation. The time taken for the cells to reach 50% following peak accumulation ($T_{50}$) in the pre-division stage and the method employed to determine the duration of $T_{50}$ in $G_2$+M exit following 2, 4 and 8Gy were as outlined in section 2.3.7.

As can be seen in Figures 43 to 48, in the cells pre-treated with 10μM PFTα, following a single fraction of γ-radiation of 2, 4 or 8Gy, generally, resulted in an increased time taken to exit the resulting $G_2$+M accumulation at 4Gy when compared to cells irradiaded at 2Gy and 8Gy as compared to 4Gy. The mutant-p53 cell line HT29.5 demonstrated the smallest variation in $T_{50}$ at 2, 4 and 8Gy, increasing from 5.30h, 6.20h and 6.50h respectively, whilst the mutant-p53 colonic carcinoma cell line Colo320 gave the greatest increase in the duration of $T_{50}$, increasing from 4.70h at 2Gy, to 7.45h at 4Gy and then 22.45h at 8Gy.

Though the duration of $T_{50}$ generally increased along with increases in exposure to ionising radiation, in 4 of the 10 cell lines a decrease in the duration of time taken to exit from $G_2$+M accumulation was seen. Specifically, in OAW42 the $T_{50}$ of exit from $G_2$+M accumulation was 4.95 and 3.20h at 2 and 4Gy respectively. A decrease in the duration of $T_{50}$ was also observed H322 (2.75h, 2.60h), RT112 (8.65h, 5.30h) and RPMI 7951 (6.85h, 4.50h) following 2 and 4Gy respectively. Similarly, following exposure to 4 and 8Gy of γ-radiation generally resulted in an increase in $T_{50}$ duration.

However, in the wt-p53 cell line HRT18 and the mutant-p53 cell lines, $T_{50}$ exit from $G_2$+M accumulation decreased (8.05h, 10.10h and 6.20h, 6.95h at 8 and 4Gy for the two cell lines respectively). A statistical analysis of these data follows in section 6.3.8.

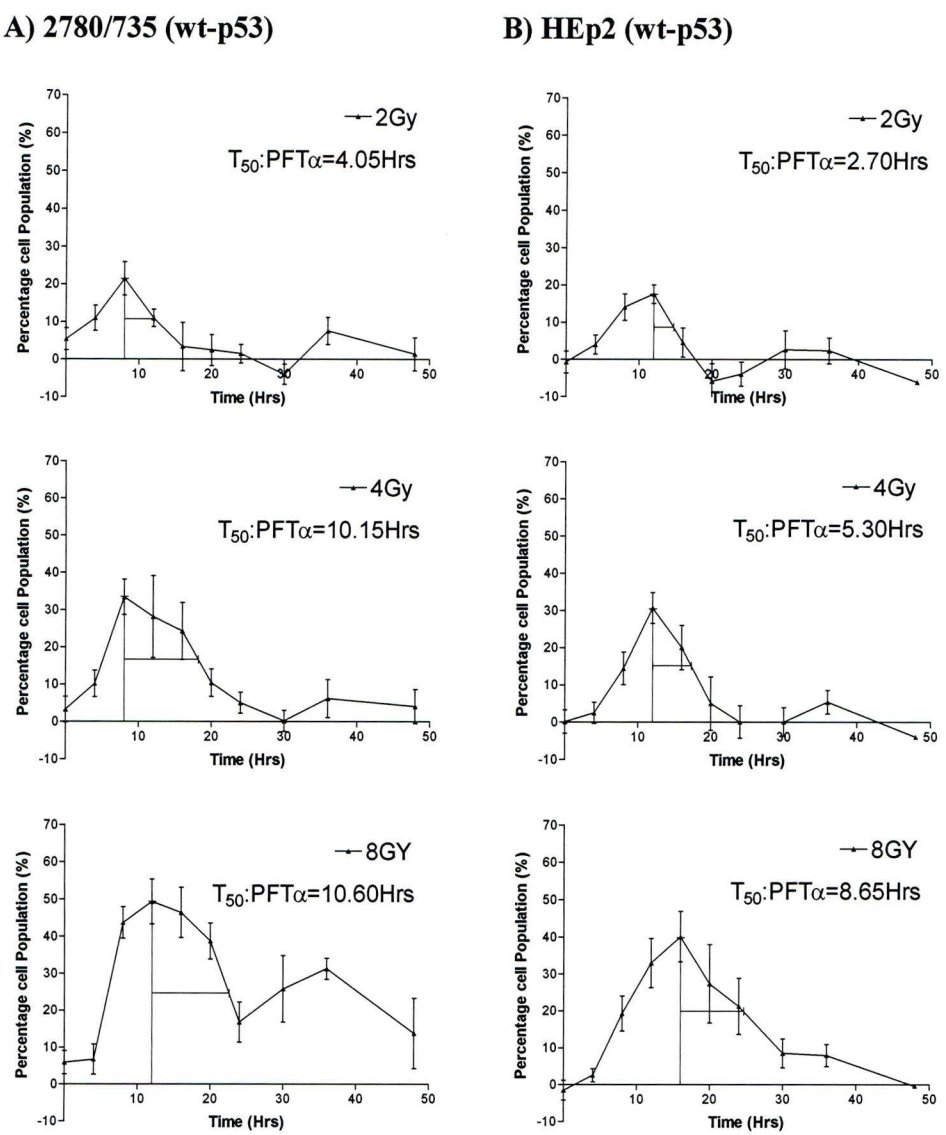


**Figure 43. $T_{50}$ determination of $G_2$+M exit following pre-incubation with PFTα and 2, 4 and 8Gy of γ-radiation**

The amount of post-irradiated $G_2$+M accumulation, as measured by PI DNA staining and flow cytometry, in 2780/735 and H322 cells pre-incubated with 10μM PFTα is shown above. Enumeration of the percentage of total cells in $G_2$+M was interpolated using ModFit (Verity Software), the mathematical modelling package. These graphs were then used to determine the $T_{50}$ value, the rate of exit from the $G_2$+M accumulation, for each cell line.

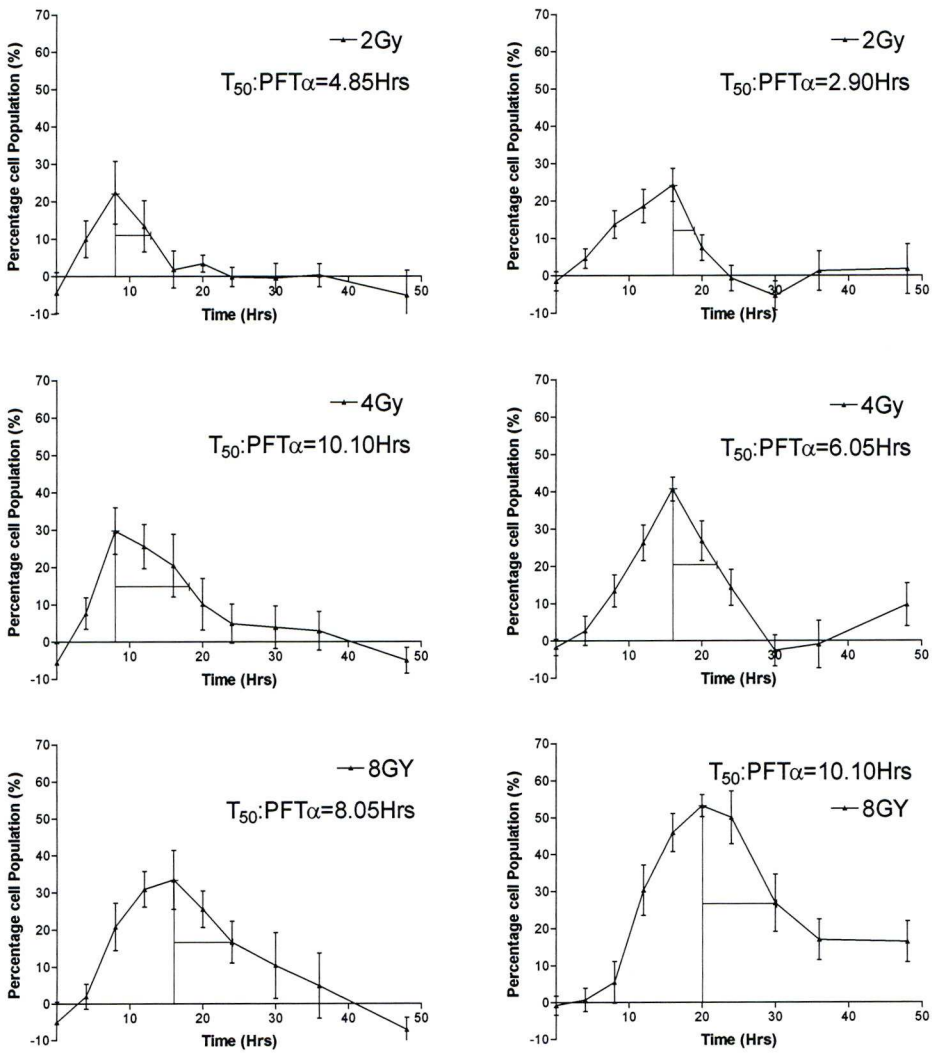


**Figure 44. $T_{50}$ determination of $G_2$+M exit following pre-incubation with PFTα and 2,4 and 8Gy of γ-radiation.**

The amount of post-irradiated $G_2$+M accumulation, as measured by PI DNA staining and flow cytometry, in HRT18 and I407 cells pre-incubated with 10μM PFTα is shown above. Enumeration of the percentage of total cells in $G_2$+M was interpolated using ModFit (Verity Software), the mathematical modelling package. These graphs were then used to determine the $T_{50}$ value, the rate of exit from the $G_2$+M accumulation, for each cell line.

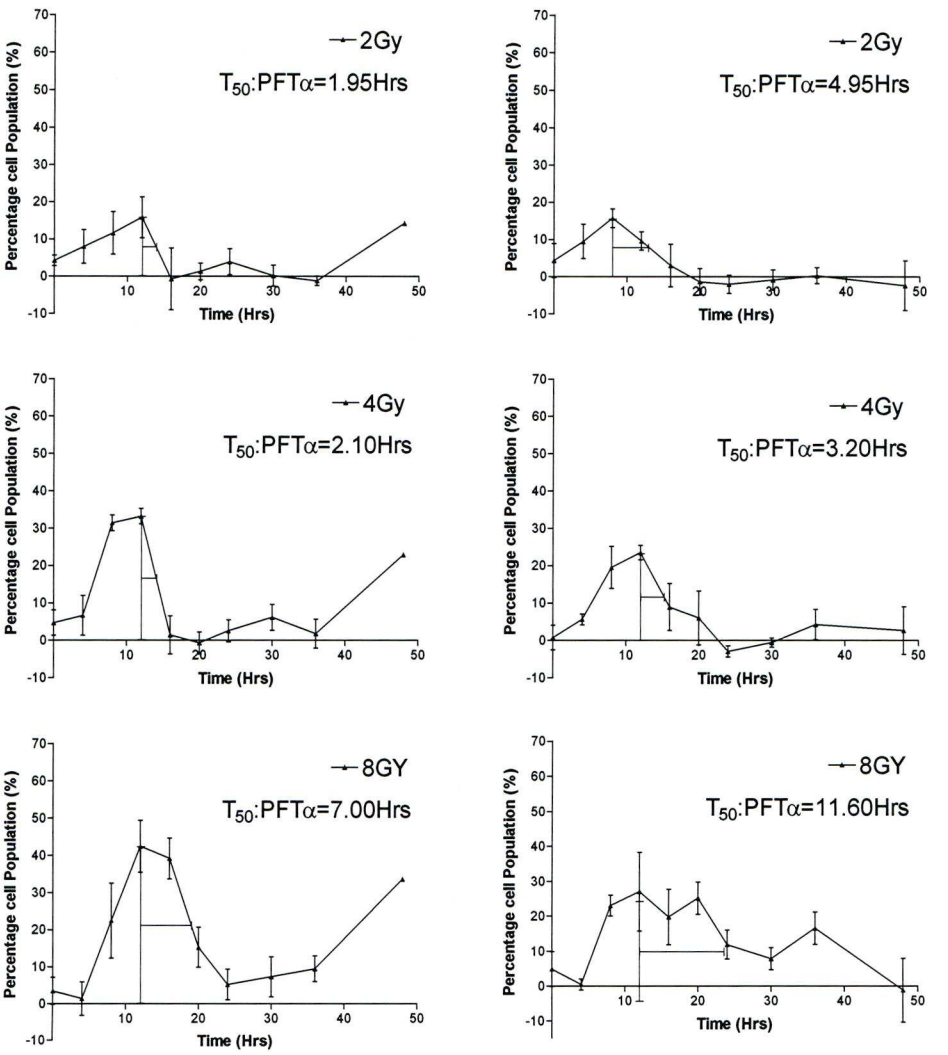


**Figure 45. $T_{50}$ determination of $G_2$+M exit following pre-incubation with PFTα and 2, 4 and 8Gy of γ-radiation**

The amount of post-irradiated $G_2$+M accumulation, as measured by PI DNA staining and flow cytometry, in MGH-U1 and OAW42 cells pre-incubated with 10μM PFTα is shown above. Enumeration of the percentage of total cells in $G_2$+M was interpolated using ModFit (Verity Software), the mathematical modelling package. These graphs were then used to determine the $T_{50}$ value, the rate of exit from the $G_2$+M accumulation, for each cell line.

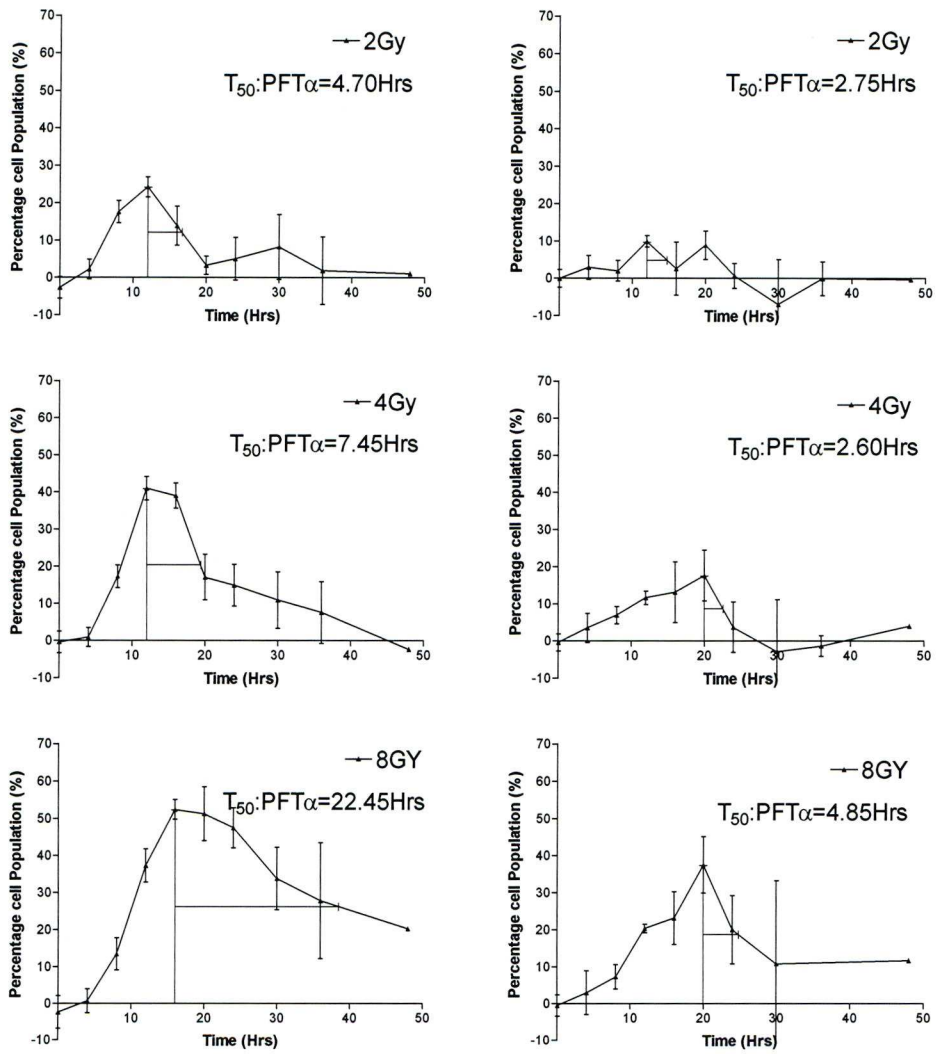


**Figure 46. $T_{50}$ determination of $G_2$+M exit following pre-incubation with PFTα and 2, 4 and 8Gy of γ-radiation**

The amount of post-irradiated $G_2$+M accumulation, as measured by PI DNA staining and flow cytometry, in Colo 320 and H322 cells pre-incubated with 10μM PFTα is shown above. Enumeration of the percentage of total cells in $G_2$+M was interpolated using ModFit (Verity Software), the mathematical modelling package. These graphs were then used to determine the $T_{50}$ value, the rate of exit from the $G_2$+M accumulation, for each cell line.

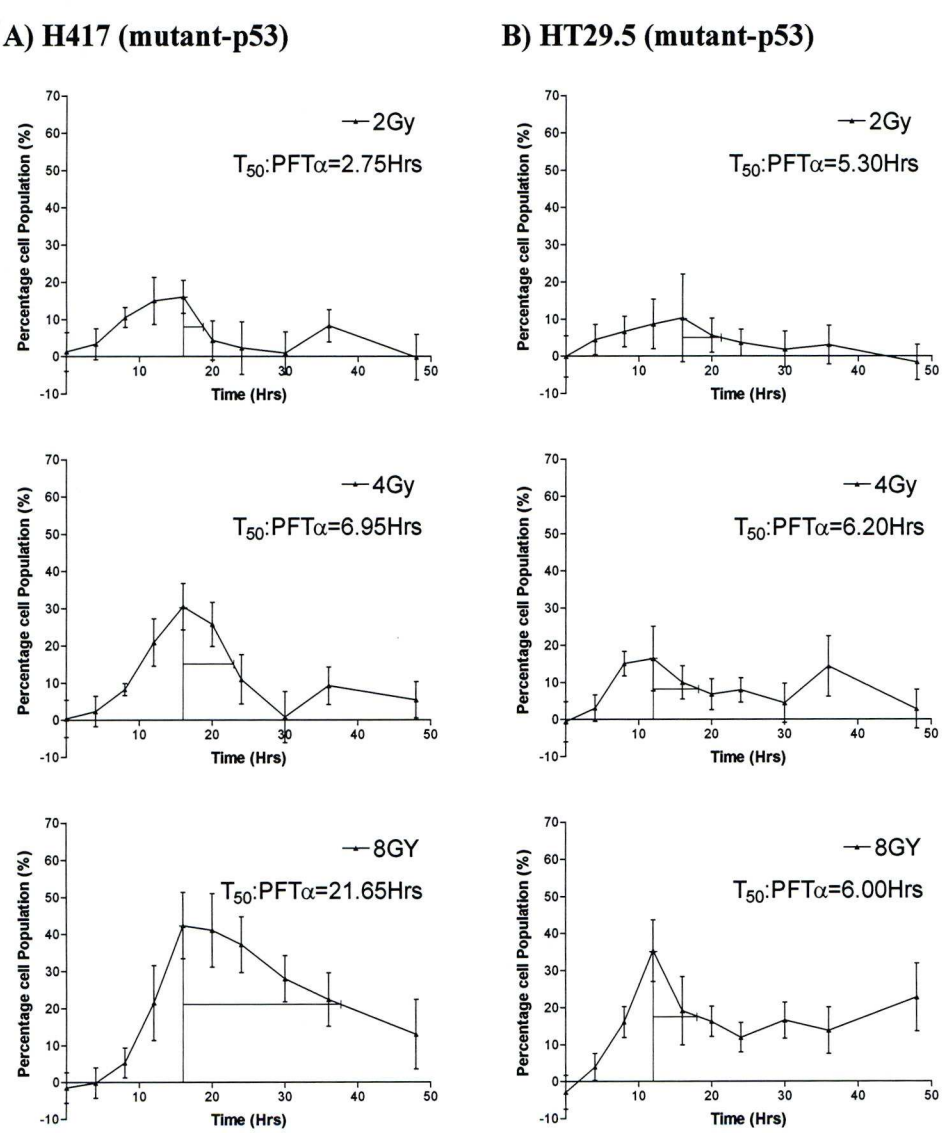


**Figure 47. $T_{50}$ determination of $G_2$+M exit following pre-incubation with PFTα and 2, 4 and 8Gy of γ-radiation**

The amount of post-irradiated $G_2$+M accumulation, as measured by PI DNA staining and flow cytometry, in H417 and HT29.5 cells pre-incubated with 10μM PFTα is shown above. Enumeration of the percentage of total cells in $G_2$+M was interpolated using ModFit (Verity Software), the mathematical modelling package. These graphs were then used to determine the $T_{50}$ value, the rate of exit from the $G_2$+M accumulation, for each cell line.

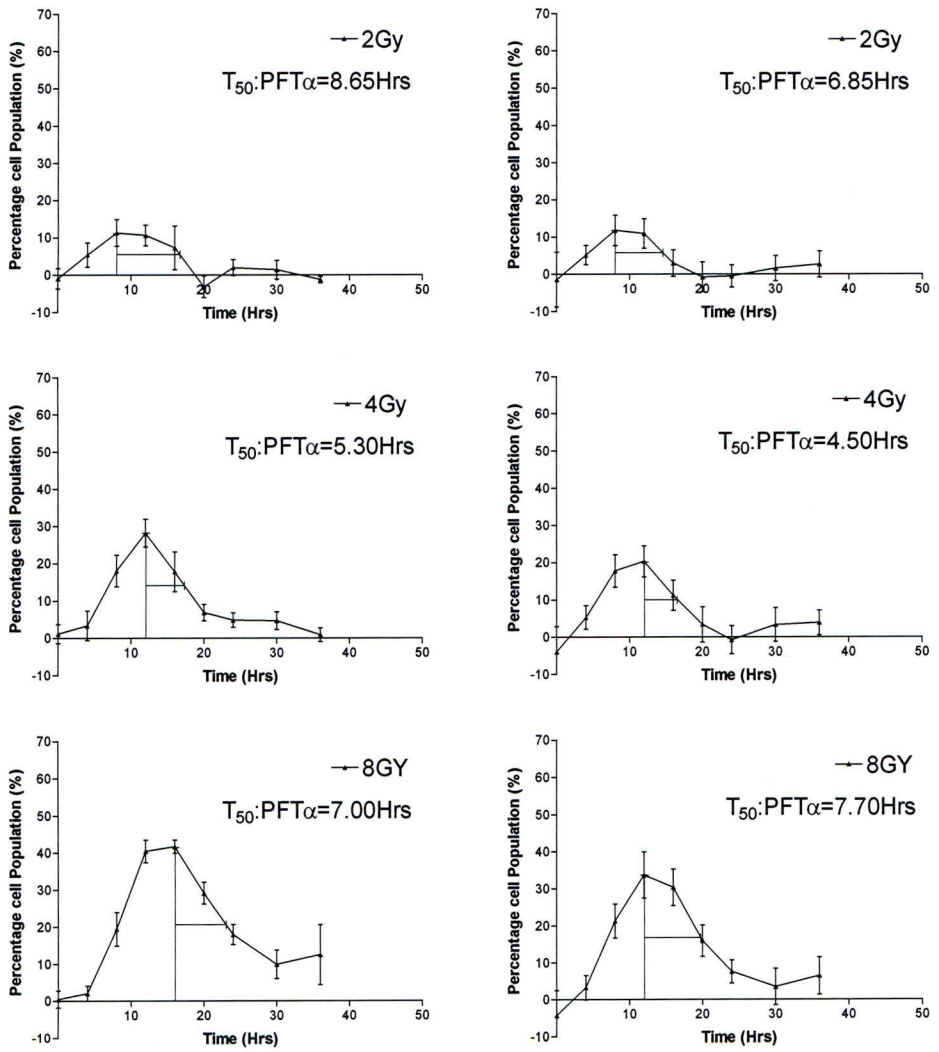


**Figure 48. $T_{50}$ determination of $G_2$+M exit following pre-incubation with PFTα and 2, 4 and 8Gy of γ-radiation**

The amount of post-irradiated $G_2$+M accumulation, as measured by PI DNA staining and flow cytometry, in RT112 and RPMI 7951 cells pre-incubated with 10μM PFTα is shown above. Enumeration of the percentage of total cells in $G_2$+M was interpolated using ModFit (Verity Software), the mathematical modelling package. These graphs were then used to determine the $T_{50}$ value, the rate of exit from the $G_2$+M accumulation, for each cell line.

### 6.3.6 Higher γ-radiation doses still result in the later onset of $G_2$+M cell cycle maximum accumulation in cells pre-incubation with PFTα and DMSO

As described previously (section 5.3.5), the time at which the maximum accumulation of cells in $G_2$+M cell cycle phase increased with higher doses of ionising radiation (Figure 27A, page 122). The average time at which the maximum percentage of cells accumulated at 2Gy was 11.00h after irradiation. This increased to 13.33h following irradiation at 4Gy in the twelve cancer cell lines. This increase was, however, not significant at 4Gy as compared to 2Gy. At 8Gy when compared to 2 and 4Gy, with the mean time to maximum accumulation of 16.33h post-irradiation. Following pre-treatment of the cells with 10μM PFTα in the presence of 0.1% v/v DMSO, the time of maximal accumulation across the ten cell lines (2780, H322, HEp2, HRT18, HT29.5, I407, MGH-U1, RT112, RPMI 7951) remained 11.00h following 2Gy of ionising radiation (see Figure 49A below). At the doses of 4 and 8Gy, the cells pre-treated with the p53 inhibitor and DMSO reached the Peak accumulation earlier than the 'untreated' irradiated cells. This would be expected if the PFTα had negated p53 function, thus reducing the ability of cells to accumulate in $G_1$, although why this observation was not seen at 2Gy is unclear. It may be that 2Gy of γ-radiation is insufficient to trigger a $G_1$ arrest in the human cancer cell lines used in this study.

Following 4Gy, the time of maximum accumulation across ten of the twelve cell lines was 12.67±0.964h, was not significantly altered from the untreated cells (13.50h) ($P=0.5913$, $r= 0.913$). Similarly, at 8Gy, though the cells reached the maximum level of accumulation earlier than the untreated cells (15.00h as compared to 16.33h respectively), this decrease in the time to peak accumulation following irradiation, was however not significant (two-tailed paired t-test, $P=0.3944$, $r=0.258$).

**A) Time to maximum accumulation in $G_2$+M increases with γ-radiation dose**

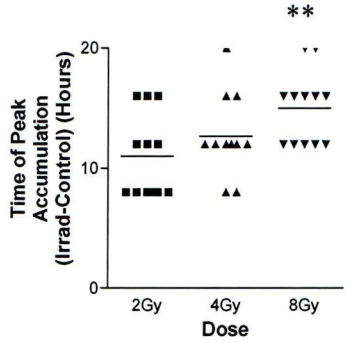


**B) p53 mutational status and time of peak accumulation in $G_2$+M following increasing doses of γ-radiation**

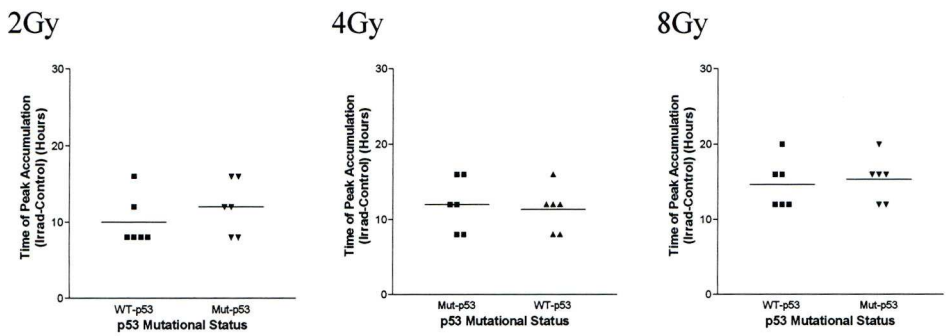


**Figure 49. The time of peak accumulation in $G_2$+M cell cycle phase in 12 human cancer cell lines and p53-mutational status at 2, 4 and 8Gy**

The influence of increasing doses of radiation and p53-mutational status on the timing of maximum percentage cell accumulation in the $G_2$+M phase of the cell cycle as shown Figures 43-48, is given above. The timing of maximal cell accumulation for the twelve human cancer cell lines following 2, 4 and 8Gy of ionising γ-radiation is shown in panel A, whilst the effect of p53 mutational status at these increasing doses of radiation is in the six wt-p53, and six mutant-p53 cell lines is shown in panel B, 2Gy, 4Gy and 8Gy.

### 6.3.7 p53 mutational status and the onset of peak accumulation following pre-treatment with PFTα and DMSO at increasing doses of γ-radiation

Pre-treatment of the wt-p53 and the mutant-p53 cell lines with PFTα in the presence of DMSO did not yield obvious differences in the time taken for the cells to attain maximum $G_2$+M accumulation following irradiation. At 2, 4 or 8Gy the time to maximum accumulation in $G_2$+M for wt-p53 compared to the mutant-p53 cell lines was not found to be change (student t-test P = 0.534; r= 0.643, P=0.876; r=0.913 and P=0.835; r=0.895 respectively) (see Figure 49B). Whereas, cells that were not pre-treated with PFTα, the wt-p53 cell lines accumulated in the $G_2$+M cell cycle phase earlier than their mutant-p53 counterparts (section 5.3.6). Pre-treatment of the twelve cancer cell lines studied with PFTα and 0.1% v/v DMSO negated this relationship. This may suggest the earlier accumulation of cells in $G_2$+M could be p53 mediated, however no significant change in the time taken for wt-p53 cell lines pre-treated with PFTα as compared to those without PFTα was observed at 2, 4 or 8Gy.

### 6.3.8 $G_2$+M exit in human cancer cell lines following increasing doses of γ-radiation

The determination of the rate of exit of cells accumulated in $G_2$+M phase of the cell cycle was performed as described in chapter 2. The results of these calculations are given in Table 15 and their determination is demonstrated in Figures 43-48 (above), by the graphs of $G_2$+M accumulation following 2, 4 and 8Gy of γ-radiation along with the depiction of $T_{50}$ calculation.

As can be seen from the values in Table 15, as the dose of radiation received increased, so did the time taken for the cells to exit the accumulation in $G_2$+M phase

of the cell cycle. This is reflected in the increased average $T_{50}$ times of 5.17, 5.50 and 11.61h for 2, 4 and 8Gy respectively.

Although, increased $T_{50}$ exit time resulted following increased dose of γ-radiation, this general trend was is not always observed in the cell lines when considered individually. In the wt-p53 rectal adenocarcinoma, HRT18 and the mutant-p53 colonic adenocarcinoma clonal variant HT29.5, the $T_{50}$ times at 4Gy were greater than at 8Gy and as was the 2Gy $T_{50}$ time as compared to the 4Gy time in the mutant-p53 small cell carcinoma cell line H322, the melanoma cancer cell lines RPMI 7951 and the transitional bladder carcinoma RT112.

| | | | $G_2$+M accumulation ($T_{50}$) | | |
|---|---|---|---|---|---|
| | | Dose | 2 Gy | 4Gy | 8 Gy |
| p53 Status | Wild-Type | 2780 | 4.05 | 10.15 | 10.60 |
| | | HEp 2 | 2.70 | 5.30 | 8.65 |
| | | HRT18 | 4.85 | 10.10 | 8.05 |
| | | I407 | 2.90 | 6.05 | 10.10 |
| | | MGH-U1 | 1.95 | 2.10 | 7.00 |
| | | OAW42 | 4.95 | 3.20 | 11.60 |
| | | ***Average*** | ***3.57*** | ***6.15*** | ***9.33*** |
| | Mutant | Colo 320 | 4.70 | 7.45 | 22.45 |
| | | H322 | 2.75 | 2.60 | 4.85 |
| | | H417 | 2.75 | 6.95 | 21.65 |
| | | HT29.5 | 5.30 | 6.20 | 6.00 |
| | | RPMI 7951 | 6.85 | 4.50 | 7.70 |
| | | RT112 | 8.65 | 5.30 | 7.00 |
| | | ***Average*** | ***5.17*** | ***5.5*** | ***11.61*** |
| Pan-p53 | | ***Average*** | ***4.37*** | ***5.83*** | ***10.47*** |

**Table 15. $G_2$+M exit ($T_{50}$) in twelve human cancer cell lines following incubation with 10μM PFTα and increasing doses of ionising radiation**

The above table contains the $T_{50}$ values for the twelve human cancer cell lines used in this study at 2, 4 and 8Gy of γ-radiation from a GammaCell 1000 with a $^{137}Cs$ source. The cell lines are ranked alphabetically and by p53 mutational status, with the average time of exit from $G_2$+M cell cycle accumulation calculated for both wt-p53 and mutant-p53, and for pan-p53, i.e. all cells regardless of mutational status.

**A) $T_{50}$ exit of human cancer cells in $G_2$+M following p53 inhibition and progressively higher doses of γ-radiation**

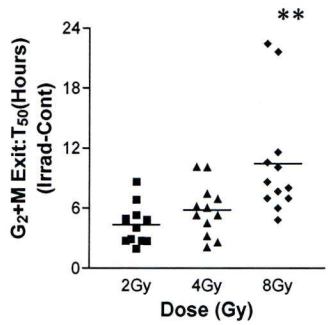


**B) p53 mutational status and $T_{50}$ exit from the $G_2$+M cell cycle phase following increasing doses of γ-radiation**

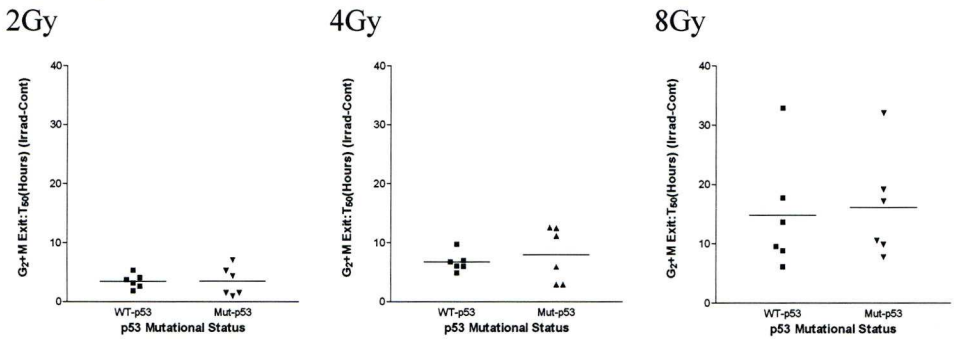


**Figure 50. The peak percentage of total cells accumulating in $G_2$+M cell cycle phase in 12 human cancer cell lines the effect of p53-mutational status at 2, 4 and 8Gy**

The influence of increasing doses of radiation and p53-mutational status on the rate of exit from $G_2$+M accumulation shown Figures 43-48, is given above. The $T_{50}$ for cells accumulating in $G_2$+M for the twelve human cancer cell lines following 2, 4 and 8Gy of ionising γ-radiation is shown in panel A, whilst the effect of p53 mutational status at these increasing doses of radiation is in the six wt-p53 and the six mutant-p53 cell lines is shown in panel B, 2, 4 and 8Gy. The double stars (**) in panel A indicate that the $T_{50}$ following 8Gy is significantly higher than that at either 2 or 4Gy.

### 6.3.9 8Gy results in a significant increase in time taken to exit a $G_2$+M delay in human cancer cell lines following p53 inhibition.

The apparent increases in the duration of the rate of $G_2$+M exit as measured by $T_{50}$ following increases in exposure of human cancer cells to ionising radiation as represented by the increases in the mean exit times for the twelve cancer cell lines is indicated in Figure 50A. However, a significant change was only present, as tested by a Paired t-test, at 8Gy. The increase in $T_{50}$ following 2Gy and 4Gy gave a P-value of 0.1250; r=0.448. Treatment of the cell with PFTα prior to irradiation resulted in an increase in the duration of $G_2$+M accumulation following 2Gy, 3.46 to 4.37h (see Table 14, section 5.8.9), along with a decrease in the average time spent in $G_2$+M following 4Gy of γ-radiation (7.35h without PFTα decreasing to 5.83h following 10μM PFTα). The difference between 2Gy to that of 8Gy $T_{50}$ was highly significant, which generated a P-value of 0.0067, r=0.709. Likewise, the increase in the mean $T_{50}$ at 8Gy as compared to 4Gy gave a significant P-value of 0.0132, r=0.665.

### 6.3.10 Increasing doses of γ-radiation, p53-mutational status and the rate of exit from $G_2$+M accumulation ($T_{50}$) in human cancer cell lines

Following ionising radiation the six mutant-p53 cell lines, on average, delayed longer than the six wt-p53 cell lines. The mean (±S.E.M) $T_{50}$ exit times were 3.57±0.50h, 6.15±1.38h and 9.33±0.70h, for the wt-p53 cell lines and the mutant-p53 cell lines having $T_{50}$ values of 5.17±0.95h, 5.50±0.73h and 11.61±3.33h at 2, 4 and 8Gy respectively. Though the mutant-p53 cell lines did take longer to exit the $G_2$+M phase of the cell cycle following maximum accumulation at 2 and 8Gy, the changes in $T_{50}$ duration did not translate to a significant response as determined by the unpaired t-test at either 2Gy (P=0.8983, r=0.060), 4Gy (P=0.5577, r=0.270), or 8Gy

(P=0.5331, r=0.082). Thus, though the cells did take longer to exit $G_2$+M following maximum accumulation, inhibition of p53 by the small molecule PFTα did not alter $T_{50}$ in the wt-p53, or mutant-p53 cell lines. Similarly, when checked against the mean $T_{50}$ values for cell lines not treated with PFTα, no significant change in the mean $T_{50}$ was observed.

### 6.3.11 Survival fraction following increasing doses of γ-radiation and the intrinsic level of RAF-1 protein in human cancer cell lines pre-treated with PFTα and DMSO

In contrast to p53 mutational status, the intrinsic level of RAF-1 protein was related to both the duration of $G_2$+M exit as measured by $T_{50}$ and cellular radiosensitivity (Chapter 3), although the former was shown to be wt-p53 dependent, whilst the radiosensitivity as measured by $SF_2$ was found to be present in all twelve cell lines as a whole, although being strongest in the wt-p53 cell lines. The intrinsic level of RAF-1 protein showed a negative relationship to post-irradiation survival of cells following 2, 4 and 8Gy. This trend in decreased post-irradiative survival with higher levels of RAF-1 protein is seen across the doses, although failing to be significant at 8Gy. In the cells which underwent pre-treatment with the p53 inhibitor PFTα in the presence of the organic solvent DMSO, this trend in decreased post-irradiative survival in cells with high intrinsic RAF-1 levels is maintained (see Figure 51).

A) $SF_{2PFT\alpha}$ and RAF-1 B) $SF_{4PFT\alpha}$ and RAF-1 C) $SF_{8PFT\alpha}$ and RAF-1

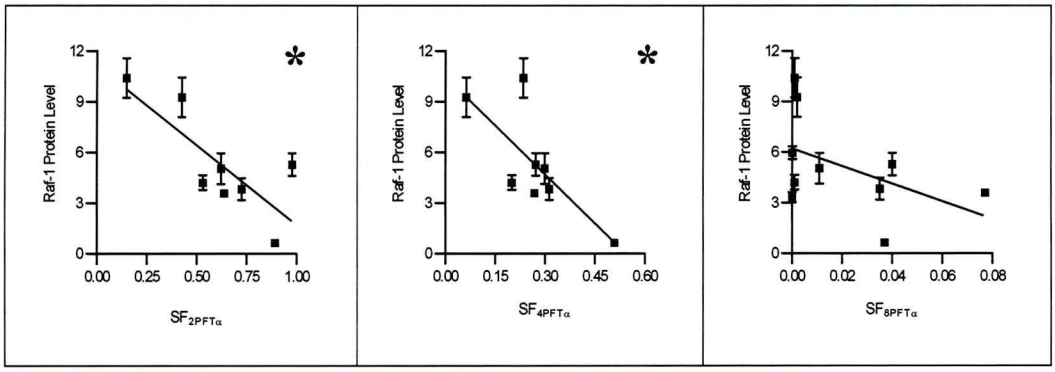


**Figure 51. Survival fraction following 2, 4 and 8Gy and intrinsic RAF-1 protein level in 12 human cancer cell lines**

The relationship between intrinsic RAF-1 protein level on post-irradiated survival fraction (SF) at 2, 4 and 8Gy, in twelve human cancer cell lines is shown in graphs A, B, and C respectively. Statistical significant correlation (i.e. $p \leq 0.05$) is indicated by a star (*).

### 6.3.12 Disruption of p53 by PFTα, survival fraction, RAF-1 protein level and p53-mutational status in human cancer cell lines following increasing doses of γ-radiation

The mutational status of p53 was shown to contribute to the correlation between RAF-1 protein level and radiosensitivity at 2Gy (chapter 3) and at 4Gy (chapter 4) following ionising radiation, with the wt-p53, but not the mutant-p53, cell lines presenting this correlation. As can be seen from Figure 52 (below), the relationship that held at both 2Gy and 4Gy in the absence of PFTα is abolished by the incubation of the cells in 10μM PFTα and 1% v/v DMSO. This is still the case when the two wt-p53 cell lines, HRT18 and I407, are removed from the analysis. This does suggest that 10μM PFTα is capable of affecting p53 function in human cancer cell lines and tentatively supports the observation that RAF-1 level is inversely related to post-irradiation survival in cells processing wt-p53.

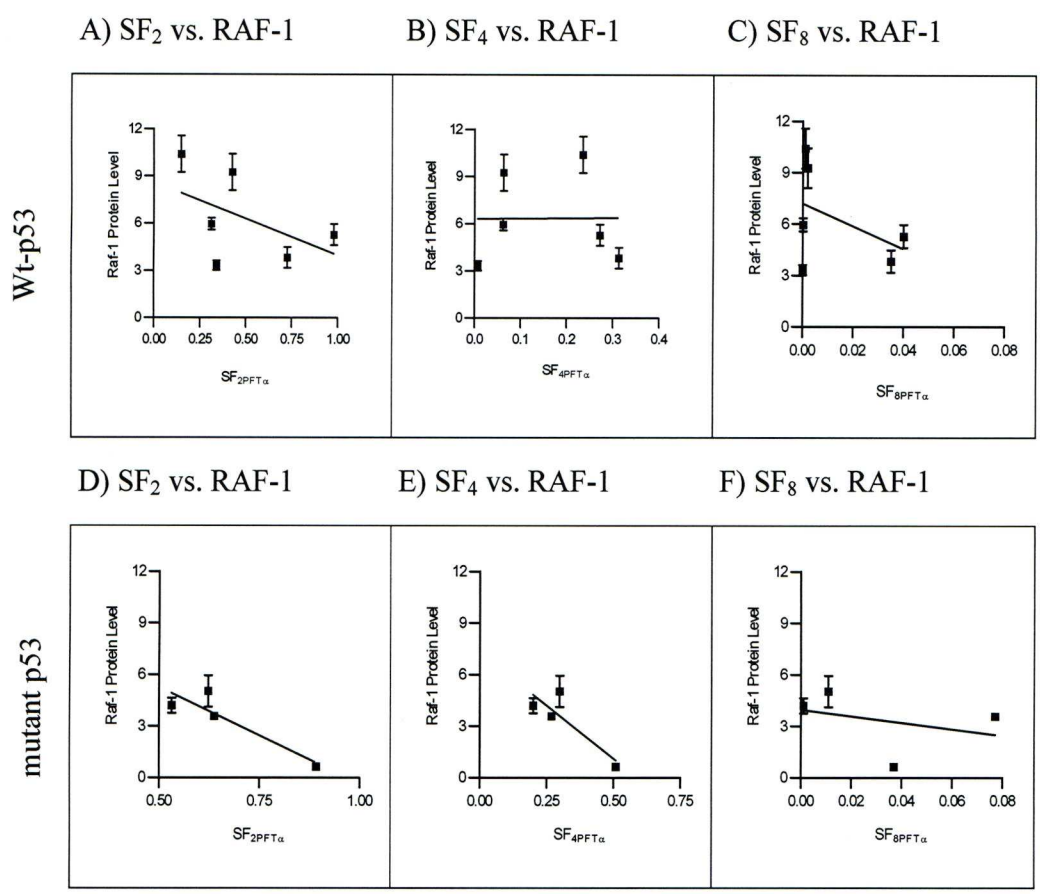


**Figure 52. The relationship between RAF-1 protein level and survival at 2, 4 and 8Gy and p53 mutational status**

The effect of RAF-1 protein level on post-irradiated survival fraction, in the context of p53 mutational status in twelve human cancer cell lines is shown above. The intrinsic RAF-1 protein level is plotted against survival fraction for the six wt-p53 cell lines in A, B, and C, with the six mutant-p53 cell lines in D, E, and F at the increasing doses of 2Gy, 4Gy and 8Gy respectively.

### 6.3.13 Survival fraction following increasing doses of γ-radiation and the rate of exit from radiation induced $G_2$+M accumulation in human cancer cell lines pre-treated with PFTα and DMSO

In contrast to p53 mutational status, the intrinsic level of RAF-1 protein was related to both the duration of $G_2$+M exit as measured by $T_{50}$ and cellular radiosensitivity (chapter 3), although the former was shown to be wt-p53 dependent, whilst the radiosensitivity as measured by $SF_2$ was found to be present in all twelve cell lines as a whole, although being strongest in the wt-p53 cell lines. The rate of exit from the post-irradiative induced $G_2$+M accumulation decreases with increases in post-irradiation survival of cells following 2, 4 and 8Gy. This trend in decreased post-irradiative survival with longer $T_{50}$ times is seen across the doses, although it was only significant at 2Gy. Depicted in Figure 53 are the data from ten adherent cell lines which underwent pre-treatment with the p53 inhibitor PFTα in the presence of the organic solvent DMSO. Earlier exit from the $G_2$+M accumulation resulted in

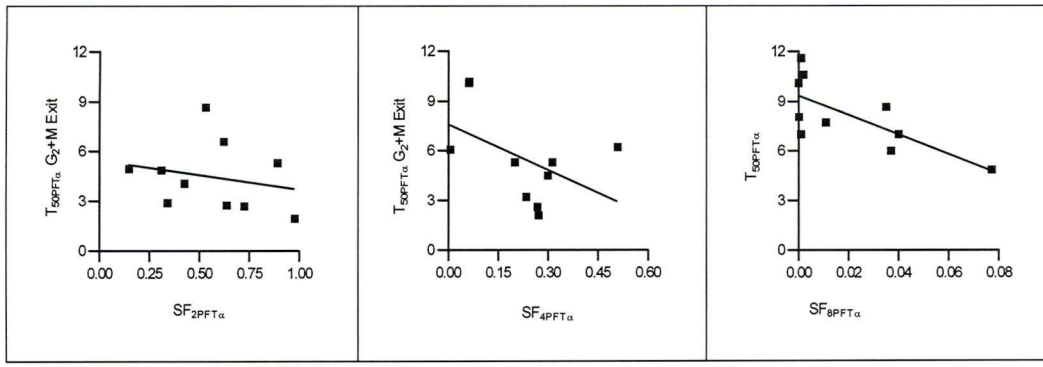


**Figure 53. Survival fraction following 2, 4 and 8Gy, and $T_{50PFT\alpha}$ in 10 human cancer cell lines**
The relationship between $T_{50PFT\alpha}$ and post-irradiated survival fraction (SF) at 2, 4 and 8Gy, in twelve human cancer cell lines is shown in graphs A, B and C respectively.

decreased survival at 2, 4 and 8Gy. However, these relationships at 2, 4 and 8Gy failed to reach significance irrespective of dose.

### 6.3.14 Disruption of p53 by PFTα, survival fraction, the rate of $G_2$+M exit and p53-mutational status in human cancer cell lines following increasing doses of γ-radiation

The mutational status of p53 was shown to contribute to the correlation between exit from a post-irradiative $G_2$+M accumulation and radiosensitivity at 2Gy (Chapter 3), with the wt-p53, but not the mutant-p53, cell lines presenting this correlation. The chief reason behind using the small molecule p53 inhibitor, PFTα, was to try to destabilise this putative relationship between radiosensitivity and $T_{50}$ and wt-p53 protein function. As can be seen from Figure 54 (below), the relationship that held at 2Gy is still maintained by the incubation of the cells in 10μM PFTα and 0.1% v/v DMSO.

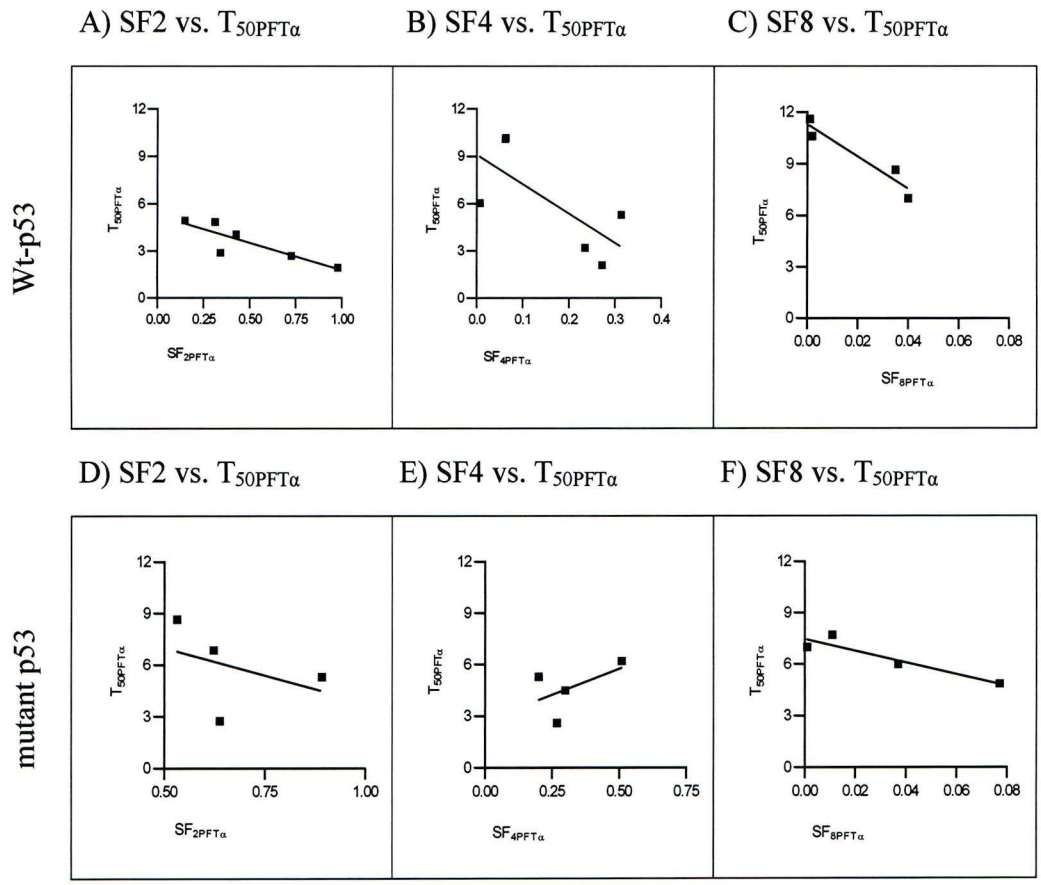


**Figure 54. The relationship between $T_{50PFT\alpha}$, the exit from a post-irradiated $G_2$+M accumulation, survival at 2, 4 and 8Gy and p53-mutational status**
$T_{50PFT\alpha}$ and post-irradiated survival fraction, in the context of p53-mutational status in twelve human cancer cell lines is shown above. The $T_{50PFT\alpha}$ is plotted against survival fraction for the six wt-p53 cell lines in A, B and C, with the six mutant-p53 cell lines in D, E and F at the increasing doses of 2, 4 and 8Gy respectively.

# Chapter 7

# Discussion and future work

## 7 Discussion and future work

There were 154,161 deaths from cancer in 2006 in the UK alone. This is in excess of 27 percent of all recorded deaths for 2006 (figures from Cancer Research UK). For the treatment of cancer, radiotherapy is still the primary non-surgical method used for most malignancies and although the use of radiation has long been known to an effective form of treatment, for certain local early stage tumours such as breast [510], colon [511] and lung [512], many tumours still prove resistant to radiotherapy [513]. Furthermore, there are still no clear markers to aid in the identification of patients that harbour tumours that are not radioresponsive. For this reason I chose to study 12 cell lines with a varied histological background to reflect many of the common cancers.

The ability of radiation to cause a multitude of both reversible and irreversible delays in cell cycle progression in $G_1$, S and $G_2$+M have been demonstrated for over 50 years [514], thus it is reasonable to suggest that the proteins controling cell cycle progression could influence radiosensitivity [515]. At the time the work for this thesis commenced great steps had been taken in identify the molecular mechanisms controlling cell cycle progression. The tumour suppressor gene p53 and positive signal transduction factors such as RAS [516], RAF-1 [4] and MYC [517] have been shown to play important roles in cell cycle progression and may also be used as predictive indicators for malignancy and radiotherapeutic outcome . It is against this background that I undertook a study into the possible relationship of proteins involved in the cell cycle in an attempt to see if levels of these cell cycle related proteins correlated with radiosensitivity at the therapeutically significant dose of 2Gy. In the current study, at 2Gy, no relationship was found for the intrinsic protein

expression for CDK4, CDK1 or their regulatory partners Cyclin B and Cyclin D1 respectively with regard to radiosensitivity, however, a positive relationship between the level of RAF-1 and radiosensitivity was found in all cell lines tested. Furthermore, the relationship was strongest in cells with a wt-p53 protein. Additionally, the level of RAF-1 and the surviving fraction of cells at 2Gy correlated to the rate at which cells exited a radiation induced $G_2$+M cell cycle accumulation.

To test whether the relationship between RAF-1 level, radiosensitivity and the rate at which cells exit from a post-irradiative cell cycle accumulation at 2Gy would hold true at higher doses of radiation. I elected to undertake further studies on cell cycle disruption at the widely used doses of 4 and 8Gy.

The relationship between intrinsic RAF-1 protein level and radiosensitivity, as measured by the clonogenically determined post-irradiation survival fraction, still held at 4Gy in the wt-p53 but not the mutant-p53 cell lines. However, this relationship was not found in cancer cells at 8Gy regardless of p53 mutational status. Similarly, the relationship between radiosensitivity and the rate at which the cell exited the radiation induced $G_2$+M accumulation was not manifest at 4 or 8Gy independent of p53 mutational status. As the majority of cells die following the comparatively high doses of 4 and 8Gy, (approximately 75% and 95% respectively), whilst only approximately 50% the cells die following 2Gy, it may be conceivably that the relationship between the intrinsic level of RAF-1 and post-irradiative cell cycle $G_2$+M accumulation is associated with ionising radiation damage repair mechanisms rather than cell death.

In 1999, Andrea Gudkov and Co-workers presented data on the use of a p53 inhibitor, PFTα. They postulated that by the transient inhibition of p53 systemically could allow for more aggressive use of radiotherapy by negating some of the adverse side-

effects such as the formation of secondary tumours [507]. Gudkov reported that "pifithrin-alpha, protected mice from the lethal genotoxic stress associated with anticancer treatment without promoting the formation of tumours". With the exception of the wt-p53 ovarian carcinoma cell line OAW42, PFTα did not increase radioresistance in the human cancer cells studied in this thesis. Therefore my data show that the initial concept of using PFTα as a protective agent for non-malignant wt-p53 cells in subjects undergoing radiotherapy is supported. However, I did not include any normal cells in my investigation, i.e. foreskin derived human fibroblasts, thus I cannot comment directly on the protective nature of PFTα in normal human cells to ionising radiation. I therefore hypothesise that PFTα does not increase radiosensitivity in human tumours *in vivo* or *in vitro*.

In the human colon carcinoma cell line HCT116, PFTα failed to stop p53 accumulation following genotoxic stress, as observed in Gudkov's original work [507]. However expression of p21 following etoposide treatment was observed along with a reduction in the level of apoptosis, leading to speculation that PFTα modulates p53 transcriptional activities [518]. PFTα modulation of p53 transcriptional activity was supported by the observation that p53 mediated up-regulation of CD95 following Doxorubicin exposure was ablated by PFTα [519]. It is in the context as a transcriptional regulator of p53 that I utilised PFTα since the mutant-p53 cells demonstrate a $G_1$ and $G_2$+M cell cycle arrest following γ-irradiation [4, 484], I initially hypothesised that not all the p53-mutations present within the cell line panel may be functionally active. The six mutant-p53 cell lines used in this study demonstrate a variety of mutations. Both Colo320 and H322 share a common mutation of arginine to tryptophan substitution in domain IV at codon 245 and RT112 has a arginine to glycine substitution at codon 248, whilst HT29.5 also within

domain IV of p53 protein, has a point mutation at codon 273, a substitution of arginine to histidine. Both H417 and RPMI7951 are truncated at codons 298 and 166 respectively. The p53 truncation in RPMI 7951 lies within the SV40 large T antigen binding region and the truncation of H417 lies between DNA-binding domain and the tetramerization domain (see the structure of p53 section 1.5.3).

Since impairment of p53 tetramerization reduced p53 DNA binding [520, 521] I expected that PFTα would not alter cell cycle arrest or radiosensitivity in H417 or RPMI7951, although I thought that Colo320, H322, RT112 and HT29.5 may undergo modification to cell cycle delay and radiosensitivity. RT112 and H322 have a mutation in the region of p53 associated to Li Fraumeni syndrome, a disorder associated with the early onset of cancer and radioresistance [522]. RT112 demonstrated an increase in radiosensitivity, although not significant. Radiosensitivity was increased in HT29.5 following treatment with PFTα, although again this small change was not found to be significant. Thus I could not ascribe any mutational functionality to transcriptional inactivation of p53 by PFTα in the p53 mutants used in this thesis. To determine the role played by PFTα in modulating p53 transcription, a more informative approach, other than relying on the 'random' mutations found in various cancer cell lines, may be to systematically mutate p53 by site-directed mutagenesis. A specific RNA array aimed at known p53 transcriptional targets following irradiation could then be undertaken. This approach would reduce any artefacts that may result from the complex variations that exist between un-related cancer cell lines.

I also employed PFTα to investigate the relationship between RAF-1 level, radiosensitivity and exit from $G_2$+M accumulation following ionising radiation in the context of p53-mutational status. My data supports the hypothesis that RAF-1

requires wt-p53 in determining the duration of $G_2$+M accumulation and radiosensitivity following 2Gy of γ-radiation, a relationship that is not found at the higher doses of 4 and 8Gy. Thus I elected to disrupt wt-p53 function using the small molecule inhibitor PFTα and studied the cell cycle delay and clonogenic survival at doses of 2, 4 and 8Gy.

Surprisingly, post-irradiation survival of the cancer cells was not significantly altered by incubation with PFTα prior to irradiation in the wt-p53 or the mutant-p53 cell lines (as determined clonogenically), when considered irrespective of p53 mutational status or when grouped by p53-muational status. Since PFTα had been postulated to inhibit p53 function and promote post-irradiation survival in wt-p53 cells, I would have anticipated significant increases in radioresistance in the wt-p53 cancer cell lines utilised in my study.

Despite the lack of any apparent mediation of radiosensitivity by PFTα in the cancer cell lines used in this study, pre-incubation with PFTα disrupted the relationship between the intrinsic level of RAF-1 in the wt-p53 cells and the post-irradiation rate of exit from $G_2$+M accumulation. This outcome supports the notion of a co-operative relationship, be it direct or otherwise, between the intrinsic level of RAF-1 and p53 in determining radiosensitivity.

Following irradiation, the mutant-p53 cell lines reached a peak accumulation in $G_2$+M cell cycle phase earlier than the wt-p53 cell lines. I therefore hypothesise that this is because the mutant-p53 cells do not undergo an early delay in $G_1$ following irradiation. However, following incubation of cells with PFTα, the earlier onset of maximal $G_2$+M accumulation following exposure to ionising radiation was not observed in any of the cell lines tested independent of their p53 status. Thus it is

likely that addition of PFTα disrupts a p53 dependent early $G_1$ delay following ionising radiation.

Due to the use of PI to visualise cell cycle accumulation only a snap-shot of cell distribution at any given time is obtained. Therefore, it is not practicle to determine the precise cell cycle kinetics for any given cell using PI. A conventional method used to examine cell progression through the cell cycle is to pulse-label cells with bromodeoxyuridine [523]. However, the inclusion of halogenated pyrimidines into a cell to undergo radiation studies is complicated by induction of the Auger cascade which increases the effective dose recieved by cells following ionising radiation [524]. Thus it may be preferential to use cyclin D3 and cyclin B fluorescent fusion proteins [525] and time lapse imagining to measure precisely the rate at which cells progress through each part of the cell cycle following radiation. This method could also be used to determine if PFTα negates a putative early post-irradiation $G_1$ delay.

The precise mechanism by which PFTα acts in humans is unclear and the majority of data published to date is from rodent models. PFTα may promote binding of p53 to the transcription factor p300, thus competitively inhibiting NF-Kappa B [526]. In 2003 Gudkov showed that PFTα inhibitory capacity could act through a mechanism other than p53. Indeed, PFTα reduced signalling through Heat Shock Transcription Factor 1 and reduce glucocorticoid receptor activity in mouse thymocytes [527]. In a recent paper Sohn *et al.* demonstrated that although PFTα did reduce apoptosis following genotoxic assault, this was independent of p53 [528], whilst Kaji *et al.* found that PFTα enhanced apoptosis in JB6 mouse epithelial cells following exposure to UVB and doxorubicin [529].

In 2005 Walton and co-workers [530] published data that support my observations; PFTα did not alter post-irradiation clonogenisity in two human cancer cell lines,

HCT116 and 2780. This manuscript reported that PFTα was unstable in *in vitro* cell culture media. In agreement with my observations Walter *et al.* found that above 20μM PFTα was toxic to 2780 cells ($IC_{50}$ of 21.3±8.1μM). There was no effect on the expression of p53, p21 or MDM-2 protein following ionising radiation. No evidence of abrogation of p53-dependent ionising radiation induced cell cycle arrest by PFTα was observed. In this study Walton employed UV radiation and only looked at cell cycle distribution at 16h post-irradiation. In the 2780 cells utilised in my study I observed differences in the distribution of cells in the cell cycle following irradiation in both PFTα treated and non-PFTα-treated cells. However at 16h post-irradiation the number of cells in $G_2$+M converged for irradiated cells with or without 20μM PFTα. Thus differences observed between my current study and that carried out by Walton *et al.* may be explained by the more comprehensive examination of cell cycle distribution at a greater range of time points investigated in this thesis.

In the mouse fibroblast cell line LMCAT, Murphy *et al.* reported that PFTα was capable of inhibiting p53 signalling, but only following hsp90 mediated nuclear translocation [531]. Taking this observation along with the instability of PFTα in cell culture media [530], it may be necessary to add PFTα at the time of cell irradiation. If more time was available to investigate whether p53 mediates the rate of exit of cells from accumulation in $G_2$+M following γ-radiation I would add PFTα to the cell culture media immediately prior to irradiation in an attempt to verify that PFTα is functional in the assays utilised in this thesis. Additionally, the advent of a new PFTα salt, PFTβ, which demonstrates lower levels of toxicity than PFTα would allow re-evaluation of the effects of PFTα on the HRT18 and I407 cell lines that showed a toxic response by clonogenic assay.

In addition to the cell lines already used in the current study I would also include a normal cell line, i.e. foreskin fibroblasts, to investigate whether PFTα also promotes radioresistance in p53 normal cell lines. It might also be informative to explore the role of PFTα on human fibroblasts immortalised with the viral proteins SV40 large T antigen [532], as well as or instead by E2F [533]. I would predict that if PFTα interact directly through p53 to make normal cells radioresistant then these viral proteins would negate PFTα induced radioresistance. Further, it may be possible to utilise FRET [534] to investigate whether PFTα interacts directly with p53 protein. The tetrahydrobenzothiazol ring of PFTα contains a primary amine making PFTα easily amenable to conjugation with many fluorochromes. FRET could be employed on fluorescently conjugated PFTα in a cell line expressing a p53 fluorecent fusion protein [535]. This approach could demonstrate PFTα direct interaction with p53 and also could highlight the temperal and cell compartmental nature of any possible interactions.

In conclusion I have shown here that the level of the protoncogene RAF-1 correlates strongly with radiosensitivity at the clinically relavant dose of 2Gy. Further, in cells expressing wt-p53 the intrinsic level of RAF-1 is predictive of the rate at which cells exit from a γ-radiation induced accumulation in $G_2$+M cell cycle phase and that this rate is correlative to post-irradiation cell survival. These findings point to a role for both p53 and RAF-1 in $G_2$+M cell cyle progression following genotoxic assault.

# Chapter 8

# References

## 8 References


1. Pelc, S.R. and A. Howard, *Effect of various doses of x-rays on the number of cells synthesizing deoxyribonucleic acid.* Radiat Res, 1955. **3**(2): p. 135-42.
2. Johnson, D.G. and C.L. Walker, *Cyclins and cell cycle checkpoints.* Annu Rev Pharmacol Toxicol, 1999. **39**: p. 295-312.
3. Behrens, B.C., et al., *Characterization of a cis-diamminedichloroplatinum(II)-resistant human ovarian cancer cell line and its use in evaluation of platinum analogues.* Cancer Res, 1987. **47**(2): p. 414-8.
4. Warenius, H.M., et al., *Late G1 accumulation after 2 Gy of gamma-irradiation is related to endogenous Raf-1 protein expression and intrinsic radiosensitivity in human cells.* Br J Cancer, 1998. **77**(8): p. 1220-8.
5. Quinn, L.A., et al., *Cell lines from human colon carcinoma with unusual cell products, double minutes, and homogeneously staining regions.* Cancer Res, 1979. **39**(12): p. 4914-24.
6. Gazdar, A.F., et al., *Peripheral airway cell differentiation in human lung cancer cell lines.* Cancer Res, 1990. **50**(17): p. 5481-7.
7. Mitchison, T.J. and E.D. Salmon, *Mitosis: a history of division.* Nat Cell Biol, 2001. **3**(1): p. E17-21.
8. Marini, A.M., et al., *The neurotoxin 1-methyl-4-phenylpyridinium: a selective cytostatic agent in small-cell lung cancer cell lines with neuroendocrine properties.* J Natl Cancer Inst, 1992. **84**(20): p. 1582-7.
9. Toolan, H.W., *Transplantable human neoplasms maintained in cortisone-treated laboratory animals: H.S. No. 1; H.Ep. No. 1; H.Ep. No. 2; H.Ep. No. 3; and H.Emb.Rh. No. 1.* Cancer Res, 1954. **14**(9): p. 660-6.
10. Tompkins, W.A., et al., *Cultural and antigenic properties of newly established cell strains derived from adenocarcinomas of the human colon and rectum.* J Natl Cancer Inst, 1974. **52**(4): p. 1101-10.
11. Pardee, A.B., et al., *Animal cell cycle.* Annu Rev Biochem, 1978. **47**: p. 715-50.
12. Liu, Y., et al., *p53 regulates hematopoietic stem cell quiescence.* Cell Stem Cell, 2009. **4**(1): p. 37-48.
13. Coller, H.A., L. Sang, and J.M. Roberts, *A new description of cellular quiescence.* PLoS Biol, 2006. **4**(3): p. e83.
14. Warenius, H.M., et al., *The influence of hypoxia on the relative sensitivity of human tumor cells to 62.5 MeV (p-->Be) fast neutrons and 4 MeV photons.* Radiat Res, 2000. **154**(1): p. 54-63.
15. Henle, G. and F. Deinhardt, *The establishment of strains of human cells in tissue culture.* J Immunol, 1957. **79**(1): p. 54-9.
16. Kerr, J.F., A.H. Wyllie, and A.R. Currie, *Apoptosis: a basic biological phenomenon with wide-ranging implications in tissue kinetics.* Br J Cancer, 1972. **26**(4): p. 239-57.
17. Evans, D.R., et al., *The activity of the pyrimidine biosynthetic pathway in MGH-U1 transitional carcinoma cells grown in tissue culture.* J Urol, 1977. **117**(6): p. 712-9.
18. Lajtha, L.G., *Radiation effects on steady-state cell populations.* Radiat Res, 1968. **33**(3): p. 659-69.

19. Marshall, C.J., L.M. Franks, and A.W. Carbonell, *Markers of neoplastic transformation in epithelial cell lines derived from human carcinomas.* J Natl Cancer Inst, 1977. **58**(6): p. 1743-51.
20. Zimmermann, A., *Regulation of liver regeneration.* Nephrol Dial Transplant, 2004. **19 Suppl 4**: p. iv6-10.
21. Potten, C.S., et al., *The recruitability and cell-cycle state of intestinal stem cells.* Int J Cell Cloning, 1984. **2**(2): p. 126-40.
22. Bucker, N.L.M., R.A., *Regeneration of Liver and Kidney.* 1971, Boston: Little, Brown and Co.
23. Shields, R., *Transition probability and the origin of variation in the cell cycle.* Nature, 1977. **267**(5613): p. 704-7.
24. Temin, H.M., *Stimulation by serum of multiplication of stationary chicken cells.* J Cell Physiol, 1971. **78**(2): p. 161-70.
25. Terasima, T. and L.J. Tolmach, *Growth and nucleic acid synthesis in synchronously dividing populations of HeLa cells.* Exp Cell Res, 1963. **30**: p. 344-62.
26. Prescott, D.M. and M.A. Bender, *Synthesis of RNA and protein during mitosis in mammalian tissue culture cells.* Exp Cell Res, 1962. **26**: p. 260-8.
27. Blondel, B. and L.J. Tolmach, *Studies on Nuclear Fine Structure. Three Phases of the Hela Cell Cycle.* Exp Cell Res, 1965. **37**: p. 497-501.
28. Radford, I.R., R.F. Martin, and L.R. Finch, *Effects of hydroxyurea on DNA synthesis in mouse L-cells.* Biochim Biophys Acta, 1982. **696**(2): p. 145-53.
29. Radford, I.R., et al., *Inhibition of DNA synthesis and cell death.* Biochim Biophys Acta, 1982. **696**(2): p. 154-62.
30. Robbins, E., G. Jentzsch, and A. Micali, *The centriole cycle in synchronized HeLa cells.* J Cell Biol, 1968. **36**(2): p. 329-39.
31. Dewey, W.C., R.M. Humphrey, and B.A. Sedita, *Cell cycle kinetics and radiation-induced chromosomal aberrations studied with C14 and H3 labels.* Biophys J, 1966. **6**(3): p. 247-60.
32. Kasten, F.H. and F.F. Strasser, *Amino acid incorporation patterns during the cell cycle of synchronized human tumor cells.* Natl Cancer Inst Monogr, 1966. **23**: p. 353-68.
33. Koch, J. and E.L. Storstad, *Incorporation of[3H]thymidine into nuclear and mitochondrial DNA in synchronized mammalian cells.* Eur J Biochem, 1967. **3**(1): p. 1-6.
34. Tobey, R.A., E.C. Anderson, and D.F. Petersen, *RNA stability and protein synthesis in relation to the division of mammalian cells.* Proc Natl Acad Sci U S A, 1966. **56**(5): p. 1520-7.
35. Robbins, E. and N.K. Gonatas, *Histochemical and Ultrastructural Studies on Hela Cell Cultures Exposed to Spindle Inhibitors with Special Reference to the Interphase Cell.* J Histochem Cytochem, 1964. **12**: p. 704-11.
36. Murray, A.W., M.J. Solomon, and M.W. Kirschner, *The role of cyclin synthesis and degradation in the control of maturation promoting factor activity.* Nature, 1989. **339**(6222): p. 280-6.
37. Murray, A.W. and M.W. Kirschner, *Dominoes and clocks: the union of two views of the cell cycle.* Science, 1989. **246**(4930): p. 614-21.
38. Minshull, J., et al., *The role of cyclin synthesis, modification and destruction in the control of cell division.* J Cell Sci Suppl, 1989. **12**: p. 77-97.
39. Morgan, D.O., *The dynamics of cyclin dependent kinase structure.* Curr Opin Cell Biol, 1996. **8**(6): p. 767-72.

40. Hunt, T., *Cyclins and their partners: from a simple idea to complicated reality.* Semin Cell Biol, 1991. **2**(4): p. 213-22.
41. Sherr, C.J. and J.M. Roberts, *Inhibitors of mammalian G1 cyclin-dependent kinases.* Genes Dev, 1995. **9**(10): p. 1149-63.
42. Norbury, C. and P. Nurse, *Animal cell cycles and their control.* Annu Rev Biochem, 1992. **61**: p. 441-70.
43. Morgan, D.O., *Principles of CDK regulation.* Nature, 1995. **374**(6518): p. 131-4.
44. Lee, H.H., et al., *Regulation of cyclin D1, DNA topoisomerase I, and proliferating cell nuclear antigen promoters during the cell cycle.* Gene Expr, 1995. **4**(3): p. 95-109.
45. Nigg, E.A., *Cyclin-dependent protein kinases: key regulators of the eukaryotic cell cycle.* Bioessays, 1995. **17**(6): p. 471-80.
46. Nurse, P., P. Thuriaux, and K. Nasmyth, *Genetic control of the cell division cycle in the fission yeast Schizosaccharomyces pombe.* Mol Gen Genet, 1976. **146**(2): p. 167-78.
47. Meyerson, M., et al., *A family of human cdc2-related protein kinases.* EMBO J, 1992. **11**(8): p. 2909-17.
48. Jeffrey, P.D., et al., *Mechanism of CDK activation revealed by the structure of a cyclinA-CDK2 complex.* Nature, 1995. **376**(6538): p. 313-20.
49. Nigg, E.A., *Cyclin-dependent kinase 7: at the cross-roads of transcription, DNA repair and cell cycle control?* Curr Opin Cell Biol, 1996. **8**(3): p. 312-7.
50. Pines, J. and T. Hunter, *Human cyclin A is adenovirus E1A-associated protein p60 and behaves differently from cyclin B.* Nature, 1990. **346**(6286): p. 760-3.
51. Tsai, L.H., E. Harlow, and M. Meyerson, *Isolation of the human cdk2 gene that encodes the cyclin A- and adenovirus E1A-associated p33 kinase.* Nature, 1991. **353**(6340): p. 174-7.
52. Grana, X. and E.P. Reddy, *Cell cycle control in mammalian cells: role of cyclins, cyclin dependent kinases (CDKs), growth suppressor genes and cyclin-dependent kinase inhibitors (CKIs).* Oncogene, 1995. **11**(2): p. 211-9.
53. Chan, P.K., et al., *Indirect immunofluorescence studies of proliferating cell nuclear antigen in nucleoli of human tumor and normal tissues.* Cancer Res, 1983. **43**(8): p. 3770-7.
54. Tyers, M. and P. Jorgensen, *Proteolysis and the cell cycle: with this RING I do thee destroy.* Curr Opin Genet Dev, 2000. **10**(1): p. 54-64.
55. Germain, D., et al., *Ubiquitination of free cyclin D1 is independent of phosphorylation on threonine 286.* J Biol Chem, 2000. **275**(16): p. 12074-9.
56. Sherr, C.J., et al., *D-type cyclins and their cyclin-dependent kinases: G1 phase integrators of the mitogenic response.* Cold Spring Harb Symp Quant Biol, 1994. **59**: p. 11-9.
57. Sherr, C.J., *Mammalian G1 cyclins.* Cell, 1993. **73**(6): p. 1059-65.
58. Kato, J.Y. and C.J. Sherr, *Inhibition of granulocyte differentiation by G1 cyclins D2 and D3 but not D1.* Proc Natl Acad Sci U S A, 1993. **90**(24): p. 11513-7.
59. Matsushime, H., et al., *Colony-stimulating factor 1 regulates novel cyclins during the G1 phase of the cell cycle.* Cell, 1991. **65**(4): p. 701-13.
60. Baldin, V., et al., *Cyclin D1 is a nuclear protein required for cell cycle progression in G1.* Genes Dev, 1993. **7**(5): p. 812-21.

61. Knight, G.B., J.M. Gudas, and A.B. Pardee, *Coordinate control of S phase onset and thymidine kinase expression.* Jpn J Cancer Res, 1989. **80**(6): p. 493-8.
62. Quelle, D.E., et al., *Overexpression of mouse D-type cyclins accelerates G1 phase in rodent fibroblasts.* Genes Dev, 1993. **7**(8): p. 1559-71.
63. Matsushime, H., et al., *D-type cyclin-dependent kinase activity in mammalian cells.* Mol Cell Biol, 1994. **14**(3): p. 2066-76.
64. Meyerson, M. and E. Harlow, *Identification of G1 kinase activity for cdk6, a novel cyclin D partner.* Mol Cell Biol, 1994. **14**(3): p. 2077-86.
65. Kato, J.Y., et al., *Regulation of cyclin D-dependent kinase 4 (cdk4) by cdk4-activating kinase.* Mol Cell Biol, 1994. **14**(4): p. 2713-21.
66. Fisher, R.P. and D.O. Morgan, *A novel cyclin associates with MO15/CDK7 to form the CDK-activating kinase.* Cell, 1994. **78**(4): p. 713-24.
67. Makela, T.P., et al., *A cyclin associated with the CDK-activating kinase MO15.* Nature, 1994. **371**(6494): p. 254-7.
68. Matsuoka, S., M. Yamaguchi, and A. Matsukage, *D-type cyclin-binding regions of proliferating cell nuclear antigen.* J Biol Chem, 1994. **269**(15): p. 11030-6.
69. Xiong, Y., H. Zhang, and D. Beach, *D type cyclins associate with multiple protein kinases and the DNA replication and repair factor PCNA.* Cell, 1992. **71**(3): p. 505-14.
70. Ludlow, J.W., et al., *The retinoblastoma susceptibility gene product undergoes cell cycle-dependent dephosphorylation and binding to and release from SV40 large T.* Cell, 1990. **60**(3): p. 387-96.
71. Cobrinik, D., et al., *The retinoblastoma protein and the regulation of cell cycling.* Trends Biochem Sci, 1992. **17**(8): p. 312-5.
72. Dowdy, S.F., et al., *Physical interaction of the retinoblastoma protein with human D cyclins.* Cell, 1993. **73**(3): p. 499-511.
73. Ewen, M.E., et al., *Functional interactions of the retinoblastoma protein with mammalian D-type cyclins.* Cell, 1993. **73**(3): p. 487-97.
74. Kato, J., et al., *Direct binding of cyclin D to the retinoblastoma gene product (pRb) and pRb phosphorylation by the cyclin D-dependent kinase CDK4.* Genes Dev, 1993. **7**(3): p. 331-42.
75. Nevins, J.R., *E2F: a link between the Rb tumor suppressor protein and viral oncoproteins.* Science, 1992. **258**(5081): p. 424-9.
76. Dynlacht, B.D., et al., *Differential regulation of E2F transactivation by cyclin/cdk2 complexes.* Genes Dev, 1994. **8**(15): p. 1772-86.
77. Krek, W., et al., *Negative regulation of the growth-promoting transcription factor E2F-1 by a stably bound cyclin A-dependent protein kinase.* Cell, 1994. **78**(1): p. 161-72.
78. Mastrangelo, D., et al., *The retinoblastoma paradigm revisited.* Med Sci Monit, 2008. **14**(12): p. RA231-40.
79. Kaelin, W.G., Jr., et al., *Identification of cellular proteins that can interact specifically with the T/E1A-binding region of the retinoblastoma gene product.* Cell, 1991. **64**(3): p. 521-32.
80. Kato, Y., et al., *Genomic DNA analysis of rat retinal tumor induced by adenovirus type 12.* Acta Pathol Jpn, 1991. **41**(11): p. 811-7.
81. Serrano, M., G.J. Hannon, and D. Beach, *A new regulatory motif in cell-cycle control causing specific inhibition of cyclin D/CDK4.* Nature, 1993. **366**(6456): p. 704-7.

82. Ohtani, K., J. DeGregori, and J.R. Nevins, *Regulation of the cyclin E gene by transcription factor E2F1.* Proc Natl Acad Sci U S A, 1995. **92**(26): p. 12146-50.
83. Ohtsubo, M., et al., *Human cyclin E, a nuclear protein essential for the G1-to-S phase transition.* Mol Cell Biol, 1995. **15**(5): p. 2612-24.
84. Dulic, V., E. Lees, and S.I. Reed, *Association of human cyclin E with a periodic G1-S phase protein kinase.* Science, 1992. **257**(5078): p. 1958-61.
85. Koff, A., et al., *Formation and activation of a cyclin E-cdk2 complex during the G1 phase of the human cell cycle.* Science, 1992. **257**(5077): p. 1689-94.
86. O'Connor, P.M., et al., *G2 delay induced by nitrogen mustard in human cells affects cyclin A/cdk2 and cyclin B1/cdc2-kinase complexes differently.* J Biol Chem, 1993. **268**(11): p. 8298-308.
87. Tsai, L.H., et al., *The cdk2 kinase is required for the G1-to-S transition in mammalian cells.* Oncogene, 1993. **8**(6): p. 1593-602.
88. Hinds, P.W., et al., *Regulation of retinoblastoma protein functions by ectopic expression of human cyclins.* Cell, 1992. **70**(6): p. 993-1006.
89. Won, K.A., et al., *Maturation of human cyclin E requires the function of eukaryotic chaperonin CCT.* Mol Cell Biol, 1998. **18**(12): p. 7584-9.
90. Schulze, A., et al., *Cell cycle regulation of the cyclin A gene promoter is mediated by a variant E2F site.* Proc Natl Acad Sci U S A, 1995. **92**(24): p. 11264-8.
91. Girard, F., et al., *Cyclin A is required for the onset of DNA replication in mammalian fibroblasts.* Cell, 1991. **67**(6): p. 1169-79.
92. Lehner, C.F. and P.H. O'Farrell, *Expression and function of Drosophila cyclin A during embryonic cell cycle progression.* Cell, 1989. **56**(6): p. 957-68.
93. Walker, D.H. and J.L. Maller, *Role for cyclin A in the dependence of mitosis on completion of DNA replication.* Nature, 1991. **354**(6351): p. 314-7.
94. Devoto, S.H., et al., *A cyclin A-protein kinase complex possesses sequence-specific DNA binding activity: p33cdk2 is a component of the E2F-cyclin A complex.* Cell, 1992. **68**(1): p. 167-76.
95. Beach, D., B. Durkacz, and P. Nurse, *Functionally homologous cell cycle control genes in budding and fission yeast.* Nature, 1982. **300**(5894): p. 706-9.
96. Hartwell, L.H., et al., *Genetic control of the cell division cycle in yeast.* Science, 1974. **183**(120): p. 46-51.
97. Simanis, V. and P. Nurse, *The cell cycle control gene cdc2+ of fission yeast encodes a protein kinase potentially regulated by phosphorylation.* Cell, 1986. **45**(2): p. 261-8.
98. Lee, M.G. and P. Nurse, *Complementation used to clone a human homologue of the fission yeast cell cycle control gene cdc2.* Nature, 1987. **327**(6117): p. 31-5.
99. Gautier, J., et al., *Purified maturation-promoting factor contains the product of a Xenopus homolog of the fission yeast cell cycle control gene cdc2+.* Cell, 1988. **54**(3): p. 433-9.
100. Draetta, G., et al., *Cdc2 protein kinase is complexed with both cyclin A and B: evidence for proteolytic inactivation of MPF.* Cell, 1989. **56**(5): p. 829-38.
101. Riabowol, K., et al., *The cdc2 kinase is a nuclear protein that is essential for mitosis in mammalian cells.* Cell, 1989. **57**(3): p. 393-401.
102. Evans, T., et al., *Cyclin: a protein specified by maternal mRNA in sea urchin eggs that is destroyed at each cleavage division.* Cell, 1983. **33**(2): p. 389-96.

103. Booher, R. and D. Beach, *Involvement of cdc13+ in mitotic control in Schizosaccharomyces pombe: possible interaction of the gene product with microtubules.* EMBO J, 1988. **7**(8): p. 2321-7.
104. Goebl, M.G., et al., *The yeast cell cycle gene CDC34 encodes a ubiquitin-conjugating enzyme.* Science, 1988. **241**(4871): p. 1331-5.
105. Hagan, I., J. Hayles, and P. Nurse, *Cloning and sequencing of the cyclin-related cdc13+ gene and a cytological study of its role in fission yeast mitosis.* J Cell Sci, 1988. **91 ( Pt 4)**: p. 587-95.
106. Minshull, J., J.J. Blow, and T. Hunt, *Translation of cyclin mRNA is necessary for extracts of activated xenopus eggs to enter mitosis.* Cell, 1989. **56**(6): p. 947-56.
107. Pines, J. and T. Hunter, *p34cdc2: the S and M kinase?* New Biol, 1990. **2**(5): p. 389-401.
108. Pines, J. and T. Hunter, *Isolation of a human cyclin cDNA: evidence for cyclin mRNA and protein regulation in the cell cycle and for interaction with p34cdc2.* Cell, 1989. **58**(5): p. 833-46.
109. Gallant, P. and E.A. Nigg, *Identification of a novel vertebrate cyclin: cyclin B3 shares properties with both A- and B-type cyclins.* EMBO J, 1994. **13**(3): p. 595-605.
110. Kreutzer, M.A., et al., *Caenorhabditis elegans cyclin A- and B-type genes: a cyclin A multigene family, an ancestral cyclin B3 and differential germline expression.* J Cell Sci, 1995. **108 ( Pt 6)**: p. 2415-24.
111. Nguyen, T.B., et al., *Characterization and expression of mammalian cyclin b3, a prepachytene meiotic cyclin.* J Biol Chem, 2002. **277**(44): p. 41960-9.
112. Richardson, H., et al., *Cyclin-B homologs in Saccharomyces cerevisiae function in S phase and in G2.* Genes Dev, 1992. **6**(11): p. 2021-34.
113. Kuhne, C. and P. Linder, *A new pair of B-type cyclins from Saccharomyces cerevisiae that function early in the cell cycle.* EMBO J, 1993. **12**(9): p. 3437-47.
114. Schwob, E. and K. Nasmyth, *CLB5 and CLB6, a new pair of B cyclins involved in DNA replication in Saccharomyces cerevisiae.* Genes Dev, 1993. **7**(7A): p. 1160-75.
115. Bueno, A., et al., *A fission yeast B-type cyclin functioning early in the cell cycle.* Cell, 1991. **66**(1): p. 149-59.
116. Bueno, A. and P. Russell, *Two fission yeast B-type cyclins, cig2 and Cdc13, have different functions in mitosis.* Mol Cell Biol, 1993. **13**(4): p. 2286-97.
117. Martin-Castellanos, C., K. Labib, and S. Moreno, *B-type cyclins regulate G1 progression in fission yeast in opposition to the p25rum1 cdk inhibitor.* EMBO J, 1996. **15**(4): p. 839-49.
118. Sherr, C.J. and J.M. Roberts, *CDK inhibitors: positive and negative regulators of G1-phase progression.* Genes Dev, 1999. **13**(12): p. 1501-12.
119. Sherr, C.J., *Cell cycle control and cancer.* Harvey Lect, 2000. **96**: p. 73-92.
120. Guan, K.L., et al., *Growth suppression by p18, a p16INK4/MTS1- and p14INK4B/MTS2-related CDK6 inhibitor, correlates with wild-type pRb function.* Genes Dev, 1994. **8**(24): p. 2939-52.
121. Hirai, H., et al., *Novel INK4 proteins, p19 and p18, are specific inhibitors of the cyclin D-dependent kinases CDK4 and CDK6.* Mol Cell Biol, 1995. **15**(5): p. 2672-81.

122. Quelle, D.E., et al., *Alternative reading frames of the INK4a tumor suppressor gene encode two unrelated proteins capable of inducing cell cycle arrest.* Cell, 1995. **83**(6): p. 993-1000.
123. Serrano, M., et al., *Inhibition of ras-induced proliferation and cellular transformation by p16INK4.* Science, 1995. **267**(5195): p. 249-52.
124. LaBaer, J., et al., *New functional activities for the p21 family of CDK inhibitors.* Genes Dev, 1997. **11**(7): p. 847-62.
125. Xiong, Y., et al., *p21 is a universal inhibitor of cyclin kinases.* Nature, 1993. **366**(6456): p. 701-4.
126. el-Deiry, W.S., et al., *WAF1, a potential mediator of p53 tumor suppression.* Cell, 1993. **75**(4): p. 817-25.
127. Waga, S., et al., *The p21 inhibitor of cyclin-dependent kinases controls DNA replication by interaction with PCNA.* Nature, 1994. **369**(6481): p. 574-8.
128. Ball, K.L. and D.P. Lane, *Human and plant proliferating-cell nuclear antigen have a highly conserved binding site for the p53-inducible gene product p21WAF1.* Eur J Biochem, 1996. **237**(3): p. 854-61.
129. Nourse, J., et al., *Interleukin-2-mediated elimination of the p27Kip1 cyclin-dependent kinase inhibitor prevented by rapamycin.* Nature, 1994. **372**(6506): p. 570-3.
130. Toyoshima, H. and T. Hunter, *p27, a novel inhibitor of G1 cyclin-Cdk protein kinase activity, is related to p21.* Cell, 1994. **78**(1): p. 67-74.
131. Fero, M.L., et al., *A syndrome of multiorgan hyperplasia with features of gigantism, tumorigenesis, and female sterility in p27(Kip1)-deficient mice.* Cell, 1996. **85**(5): p. 733-44.
132. Rivard, N., et al., *Abrogation of p27Kip1 by cDNA antisense suppresses quiescence (G0 state) in fibroblasts.* J Biol Chem, 1996. **271**(31): p. 18337-41.
133. *Nobel Lectures, Physics 1901-1921.* 1967, Amsterdam: Elsevier Publishing Company.
134. Kogelnik, H.D., *Inauguration of radiotherapy as a new scientific speciality by Leopold Freund 100 years ago.* Radiother Oncol, 1997. **42**(3): p. 203-11.
135. Lengauer, C. and J.P. Issa, *The role of epigenetics in cancer. DNA Methylation, Imprinting and the Epigenetics of Cancer--an American Association for Cancer Research Special Conference. Las Croabas, Puerto Rico, 12-16 1997 December.* Mol Med Today, 1998. **4**(3): p. 102-3.
136. Lengauer, C., K.W. Kinzler, and B. Vogelstein, *Genetic instabilities in human cancers.* Nature, 1998. **396**(6712): p. 643-9.
137. Suit, H., et al., *Clinical implications of heterogeneity of tumor response to radiation therapy.* Radiother Oncol, 1992. **25**(4): p. 251-60.
138. Barranco, S.C., et al., *Intratumor variability in prognostic indicators may be the cause of conflicting estimates of patient survival and response to therapy.* Cancer Res, 1994. **54**(20): p. 5351-6.
139. Deacon, J., M.J. Peckham, and G.G. Steel, *The radioresponsiveness of human tumours and the initial slope of the cell survival curve.* Radiother Oncol, 1984. **2**(4): p. 317-23.
140. Fertil, B. and E.P. Malaise, *Intrinsic radiosensitivity of human cell lines is correlated with radioresponsiveness of human tumors: analysis of 101 published survival curves.* Int J Radiat Oncol Biol Phys, 1985. **11**(9): p. 1699-707.
141. West, C.M., *Invited review: intrinsic radiosensitivity as a predictor of patient response to radiotherapy.* Br J Radiol, 1995. **68**(812): p. 827-37.

142. West, C.M., et al., *The intrinsic radiosensitivity of cervical carcinoma: correlations with clinical data.* Int J Radiat Oncol Biol Phys, 1995. **31**(4): p. 841-6.
143. West, C.M., et al., *Intrinsic radiosensitivity and prediction of patient response to radiotherapy for carcinoma of the cervix.* Br J Cancer, 1993. **68**(4): p. 819-23.
144. Deschavanne, P.J. and B. Fertil, *A review of human cell radiosensitivity in vitro.* Int J Radiat Oncol Biol Phys, 1996. **34**(1): p. 251-66.
145. Stausbol-Gron, B. and J. Overgaard, *Relationship between tumour cell in vitro radiosensitivity and clinical outcome after curative radiotherapy for squamous cell carcinoma of the head and neck.* Radiother Oncol, 1999. **50**(1): p. 47-55.
146. Bjork-Eriksson, T., et al., *Tumor radiosensitivity (SF2) is a prognostic factor for local control in head and neck cancers.* Int J Radiat Oncol Biol Phys, 2000. **46**(1): p. 13-9.
147. Nagasawa, H. and J.B. Little, *Comparison of kinetics of X-ray-induced cell killing in normal, ataxia telangiectasia and hereditary retinoblastoma fibroblasts.* Mutat Res, 1983. **109**(2): p. 297-308.
148. Painter, R.B. and B.R. Young, *Radiosensitivity in ataxia-telangiectasia: a new explanation.* Proc Natl Acad Sci U S A, 1980. **77**(12): p. 7315-7.
149. Slichenmyer, W.J., et al., *Loss of a p53-associated G1 checkpoint does not decrease cell survival following DNA damage.* Cancer Res, 1993. **53**(18): p. 4164-8.
150. Lee, J.M. and A. Bernstein, *p53 mutations increase resistance to ionizing radiation.* Proc Natl Acad Sci U S A, 1993. **90**(12): p. 5742-6.
151. McIlwrath, A.J., et al., *Cell cycle arrests and radiosensitivity of human tumor cell lines: dependence on wild-type p53 for radiosensitivity.* Cancer Res, 1994. **54**(14): p. 3718-22.
152. Toby, A.L. and C.L. Kemp, *Mutant enrichment in the colonial alga, Eudorina elegans.* Genetics, 1975. **81**(2): p. 243-51.
153. McKenna, W.G., et al., *Increased G2 delay in radiation-resistant cells obtained by transformation of primary rat embryo cells with the oncogenes H-ras and v-myc.* Radiat Res, 1991. **125**(3): p. 283-7.
154. Cheong, N., Y. Wang, and G. Iliakis, *Radioresistance induced in rat embryo cells by transfection with the oncogenes H-ras plus v-myc is cell cycle dependent and maximal during S and G2.* Int J Radiat Biol, 1993. **63**(5): p. 623-9.
155. Su, L.N. and J.B. Little, *Prolonged cell cycle delay in radioresistant human cell lines transfected with activated ras oncogene and/or simian virus 40 T-antigen.* Radiat Res, 1993. **133**(1): p. 73-9.
156. Jung, M. and A. Dritschilo, *Modification of the radiosensitivity of human testicular cancer cells by simian virus 40 sequences.* Radiat Res, 1994. **140**(2): p. 186-90.
157. Busse, P.M., et al., *The action of caffeine on X-irradiated HeLa cells. III. Enhancement of X-ray-induced killing during G2 arrest.* Radiat Res, 1978. **76**(2): p. 292-307.
158. Scott, D. and F. Zampetti-Bosseler, *Cell cycle dependence of mitotic delay in X-irradiated normal and ataxia-telangiectasia fibroblasts.* Int J Radiat Biol Relat Stud Phys Chem Med, 1982. **42**(6): p. 679-83.

159. Zampetti-Bosseler, F. and D. Scott, *Cell death, chromosome damage and mitotic delay in normal human, ataxia telangiectasia and retinoblastoma fibroblasts after x-irradiation.* Int J Radiat Biol Relat Stud Phys Chem Med, 1981. **39**(5): p. 547-58.
160. Beamish, H., K.K. Khanna, and M.F. Lavin, *Ionizing radiation and cell cycle progression in ataxia telangiectasia.* Radiat Res, 1994. **138**(1 Suppl): p. S130-3.
161. Beamish, H. and M.F. Lavin, *Radiosensitivity in ataxia-telangiectasia: anomalies in radiation-induced cell cycle delay.* Int J Radiat Biol, 1994. **65**(2): p. 175-84.
162. Lavin, M.F., et al., *Defect in radiation signal transduction in ataxia-telangiectasia.* Int J Radiat Biol, 1994. **66**(6 Suppl): p. S151-6.
163. Weinert, T.A. and L.H. Hartwell, *The RAD9 gene controls the cell cycle response to DNA damage in Saccharomyces cerevisiae.* Science, 1988. **241**(4863): p. 317-22.
164. Rowley, R., *Radiation-induced mitotic delay: a genetic characterization in the fission yeast.* Radiat Res, 1992. **132**(2): p. 144-52.
165. al-Khodairy, F. and A.M. Carr, *DNA repair mutants defining G2 checkpoint pathways in Schizosaccharomyces pombe.* EMBO J, 1992. **11**(4): p. 1343-50.
166. Enoch, T., A.M. Carr, and P. Nurse, *Fission yeast genes involved in coupling mitosis to completion of DNA replication.* Genes Dev, 1992. **6**(11): p. 2035-46.
167. van Oostrum, I.E., et al., *The relationship between radiosensitivity and cell kinetic effects after low- and high-dose-rate irradiation in five human tumors in nude mice.* Radiat Res, 1990. **122**(3): p. 252-61.
168. Cheong, N., et al., *Radiation-sensitive irs mutants rejoin DNA double-strand breaks with efficiency similar to that of parental V79 cells but show altered response to radiation-induced G2 delay.* Mutat Res, 1992. **274**(2): p. 111-22.
169. Terasima, T. and L.J. Tolmach, *Variations in several responses of HeLa cells to x-irradiation during the division cycle.* Biophys J, 1963. **3**: p. 11-33.
170. Whitmore, G.F., et al., *Nucleic acid synthesis and the division cycle in x-irradiated L-strain mouse cells.* Biochim Biophys Acta, 1961. **47**: p. 66-77.
171. Walters, R.A. and D.F. Petersen, *Radiosensivity of mammalian cells. I. Timing and dose-dependence of radiation-induced division delay.* Biophys J, 1968. **8**(12): p. 1475-86.
172. Leeper, D.B., M.H. Schneiderman, and W.C. Dewey, *Radiation-induced cycle delay in synchronized Chinese hamster cells: comparison between DNA synthesis and division.* Radiat Res, 1973. **53**(2): p. 326-37.
173. Smeets, M.F., et al., *Differential repair of radiation-induced DNA damage in cells of human squamous cell carcinoma and the effect of caffeine and cysteamine on induction and repair of DNA double-strand breaks.* Radiat Res, 1994. **140**(2): p. 153-60.
174. Lane, D.P., *Cancer. p53, guardian of the genome.* Nature, 1992. **358**(6381): p. 15-6.
175. Levine, A.J., *p53, the cellular gatekeeper for growth and division.* Cell, 1997. **88**(3): p. 323-31.
176. Hollstein, M., et al., *p53 mutations in human cancers.* Science, 1991. **253**(5015): p. 49-53.

177. Zuffa, E., et al., *P53 oncosuppressor influences selection of genomic imbalances in response to ionizing radiations in human osteosarcoma cell line SAOS-2.* Int J Radiat Biol, 2008. **84**(7): p. 591-601.
178. Griesmann, H., et al., *p53 and p73 in suppression of Myc-driven lymphomagenesis.* Int J Cancer, 2009. **124**(2): p. 502-6.
179. Troester, M.A., et al., *Gene expression patterns associated with p53 status in breast cancer.* BMC Cancer, 2006. **6**: p. 276.
180. Malkin, M.G. and W.R. Shapiro, *Brain tumors.* Cancer Chemother Biol Response Modif, 1990. **11**: p. 555-74.
181. Donehower, L.A., *The p53-deficient mouse: a model for basic and applied cancer studies.* Semin Cancer Biol, 1996. **7**(5): p. 269-78.
182. Bargonetti, J., et al., *Wild-type but not mutant p53 immunopurified proteins bind to sequences adjacent to the SV40 origin of replication.* Cell, 1991. **65**(6): p. 1083-91.
183. Kern, S.E., et al., *Oncogenic forms of p53 inhibit p53-regulated gene expression.* Science, 1992. **256**(5058): p. 827-30.
184. el-Deiry, W.S., et al., *Definition of a consensus binding site for p53.* Nat Genet, 1992. **1**(1): p. 45-9.
185. Fields, S. and S.K. Jang, *Presence of a potent transcription activating sequence in the p53 protein.* Science, 1990. **249**(4972): p. 1046-9.
186. Chin, K.V., et al., *Modulation of activity of the promoter of the human MDR1 gene by Ras and p53.* Science, 1992. **255**(5043): p. 459-62.
187. el-Deiry, W.S., *p21/p53, cellular growth control and genomic integrity.* Curr Top Microbiol Immunol, 1998. **227**: p. 121-37.
188. Vogelstein, B., D. Lane, and A.J. Levine, *Surfing the p53 network.* Nature, 2000. **408**(6810): p. 307-10.
189. Lane, D.P. and L.V. Crawford, *T antigen is bound to a host protein in SV40-transformed cells.* Nature, 1979. **278**(5701): p. 261-3.
190. Crawford, L., et al., *Cellular proteins reactive with monoclonal antibodies directed against simian virus 40 T-antigen.* J Virol, 1982. **42**(2): p. 612-20.
191. Jenkins, J.R., K. Rudge, and G.A. Currie, *Cellular immortalization by a cDNA clone encoding the transformation-associated phosphoprotein p53.* Nature, 1984. **312**(5995): p. 651-4.
192. Eliyahu, D., et al., *Participation of p53 cellular tumour antigen in transformation of normal embryonic cells.* Nature, 1984. **312**(5995): p. 646-9.
193. Parada, L.F., et al., *Cooperation between gene encoding p53 tumour antigen and ras in cellular transformation.* Nature, 1984. **312**(5995): p. 649-51.
194. Eliyahu, D., et al., *Meth A fibrosarcoma cells express two transforming mutant p53 species.* Oncogene, 1988. **3**(3): p. 313-21.
195. Hinds, P., C. Finlay, and A.J. Levine, *Mutation is required to activate the p53 gene for cooperation with the ras oncogene and transformation.* J Virol, 1989. **63**(2): p. 739-46.
196. Finlay, C.A., P.W. Hinds, and A.J. Levine, *The p53 proto-oncogene can act as a suppressor of transformation.* Cell, 1989. **57**(7): p. 1083-93.
197. Chen, P.L., et al., *Genetic mechanisms of tumor suppression by the human p53 gene.* Science, 1990. **250**(4987): p. 1576-80.
198. Benchimol, S., et al., *Transformation associated p53 protein is encoded by a gene on human chromosome 17.* Somat Cell Mol Genet, 1985. **11**(5): p. 505-10.

199. Matlashewski, G., et al., *Isolation and characterization of a human p53 cDNA clone: expression of the human p53 gene.* EMBO J, 1984. **3**(13): p. 3257-62.
200. Rigaudy, P. and W. Eckhart, *Nucleotide sequence of a cDNA encoding the monkey cellular phosphoprotein p53.* Nucleic Acids Res, 1989. **17**(20): p. 8375.
201. Jenkins, J.R., et al., *Cloning and expression analysis of full length mouse cDNA sequences encoding the transformation associated protein p53.* Nucleic Acids Res, 1984. **12**(14): p. 5609-26.
202. Soussi, T., et al., *Cloning and characterization of a cDNA from Xenopus laevis coding for a protein homologous to human and murine p53.* Oncogene, 1987. **1**(1): p. 71-8.
203. Soussi, T., et al., *Nucleotide sequence of a cDNA encoding the chicken p53 nuclear oncoprotein.* Nucleic Acids Res, 1988. **16**(23): p. 11383.
204. Soussi, T., et al., *Nucleotide sequence of a cDNA encoding the rat p53 nuclear oncoprotein.* Nucleic Acids Res, 1988. **16**(23): p. 11384.
205. Kraiss, S., et al., *Oligomerization of oncoprotein p53.* J Virol, 1988. **62**(12): p. 4737-44.
206. McCormick, F., et al., *SV40 T antigen binds specifically to a cellular 53 K protein in vitro.* Nature, 1981. **292**(5818): p. 63-5.
207. Sturzbecher, H.W., et al., *A C-terminal alpha-helix plus basic region motif is the major structural determinant of p53 tetramerization.* Oncogene, 1992. **7**(8): p. 1513-23.
208. Slingerland, J.M., J.R. Jenkins, and S. Benchimol, *The transforming and suppressor functions of p53 alleles: effects of mutations that disrupt phosphorylation, oligomerization and nuclear translocation.* EMBO J, 1993. **12**(3): p. 1029-37.
209. Friedman, P.N., et al., *The p53 protein is an unusually shaped tetramer that binds directly to DNA.* Proc Natl Acad Sci U S A, 1993. **90**(8): p. 3319-23.
210. Chene, P., *The role of tetramerization in p53 function.* Oncogene, 2001. **20**(21): p. 2611-7.
211. Scoumanne, A., K.L. Harms, and X. Chen, *Structural basis for gene activation by p53 family members.* Cancer Biol Ther, 2005. **4**(11): p. 1178-85.
212. Soussi, T., C. Caron de Fromentel, and P. May, *Structural aspects of the p53 protein in relation to gene evolution.* Oncogene, 1990. **5**(7): p. 945-52.
213. Lee, W., et al., *Solution structure of the tetrameric minimum transforming domain of p53.* Nat Struct Biol, 1994. **1**(12): p. 877-90.
214. Mateu, M.G. and A.R. Fersht, *Mutually compensatory mutations during evolution of the tetramerization domain of tumor suppressor p53 lead to impaired hetero-oligomerization.* Proc Natl Acad Sci U S A, 1999. **96**(7): p. 3595-9.
215. Mateu, M.G., M.M. Sanchez Del Pino, and A.R. Fersht, *Mechanism of folding and assembly of a small tetrameric protein domain from tumor suppressor p53.* Nat Struct Biol, 1999. **6**(2): p. 191-8.
216. Clore, G.M., et al., *High-resolution structure of the oligomerization domain of p53 by multidimensional NMR.* Science, 1994. **265**(5170): p. 386-91.
217. Shaulsky, G., et al., *Nuclear accumulation of p53 protein is mediated by several nuclear localization signals and plays a role in tumorigenesis.* Mol Cell Biol, 1990. **10**(12): p. 6565-77.

218. Fiscella, M., et al., *The carboxy-terminal serine 392 phosphorylation site of human p53 is not required for wild-type activities.* Oncogene, 1994. **9**(11): p. 3249-57.
219. Balagurumoorthy, P., et al., *Four p53 DNA-binding domain peptides bind natural p53-response elements and bend the DNA.* Proc Natl Acad Sci U S A, 1995. **92**(19): p. 8591-5.
220. Okorokov, A.L., et al., *The structure of p53 tumour suppressor protein reveals the basis for its functional plasticity.* EMBO J, 2006. **25**(21): p. 5191-200.
221. Ashcroft, M., M.H. Kubbutat, and K.H. Vousden, *Regulation of p53 function and stability by phosphorylation.* Mol Cell Biol, 1999. **19**(3): p. 1751-8.
222. Ashcroft, M. and K.H. Vousden, *Regulation of p53 stability.* Oncogene, 1999. **18**(53): p. 7637-43.
223. Amundson, S.A., T.G. Myers, and A.J. Fornace, Jr., *Roles for p53 in growth arrest and apoptosis: putting on the brakes after genotoxic stress.* Oncogene, 1998. **17**(25): p. 3287-99.
224. el-Deiry, W.S., *Regulation of p53 downstream genes.* Semin Cancer Biol, 1998. **8**(5): p. 345-57.
225. Giaccia, A.J. and M.B. Kastan, *The complexity of p53 modulation: emerging patterns from divergent signals.* Genes Dev, 1998. **12**(19): p. 2973-83.
226. Bates, S. and K.H. Vousden, *Mechanisms of p53-mediated apoptosis.* Cell Mol Life Sci, 1999. **55**(1): p. 28-37.
227. Janus, F., et al., *The dual role model for p53 in maintaining genomic integrity.* Cell Mol Life Sci, 1999. **55**(1): p. 12-27.
228. Jayaraman, L. and C. Prives, *Covalent and noncovalent modifiers of the p53 protein.* Cell Mol Life Sci, 1999. **55**(1): p. 76-87.
229. Gaiddon, C., et al., *A subset of tumor-derived mutant forms of p53 down-regulate p63 and p73 through a direct interaction with the p53 core domain.* Mol Cell Biol, 2001. **21**(5): p. 1874-87.
230. Kubbutat, M.H. and K.H. Vousden, *Proteolytic cleavage of human p53 by calpain: a potential regulator of protein stability.* Mol Cell Biol, 1997. **17**(1): p. 460-8.
231. Damalas, A., et al., *Excess beta-catenin promotes accumulation of transcriptionally active p53.* EMBO J, 1999. **18**(11): p. 3054-63.
232. Zilfou, J.T., et al., *The corepressor mSin3a interacts with the proline-rich domain of p53 and protects p53 from proteasome-mediated degradation.* Mol Cell Biol, 2001. **21**(12): p. 3974-85.
233. Oda, K., et al., *p53AIP1, a potential mediator of p53-dependent apoptosis, and its regulation by Ser-46-phosphorylated p53.* Cell, 2000. **102**(6): p. 849-62.
234. Takekawa, M., et al., *p53-inducible wip1 phosphatase mediates a negative feedback regulation of p38 MAPK-p53 signaling in response to UV radiation.* EMBO J, 2000. **19**(23): p. 6517-26.
235. Sakaguchi, K., et al., *Phosphorylation of serine 392 stabilizes the tetramer formation of tumor suppressor protein p53.* Biochemistry, 1997. **36**(33): p. 10117-24.
236. Lees-Miller, S.P., et al., *Human DNA-activated protein kinase phosphorylates serines 15 and 37 in the amino-terminal transactivation domain of human p53.* Mol Cell Biol, 1992. **12**(11): p. 5041-9.

237. Milne, D.M., R.H. Palmer, and D.W. Meek, *Mutation of the casein kinase II phosphorylation site abolishes the anti-proliferative activity of p53.* Nucleic Acids Res, 1992. **20**(21): p. 5565-70.
238. Meek, D.W., et al., *The p53 tumour suppressor protein is phosphorylated at serine 389 by casein kinase II.* EMBO J, 1990. **9**(10): p. 3253-60.
239. Hupp, T.R., et al., *Regulation of the specific DNA binding function of p53.* Cell, 1992. **71**(5): p. 875-86.
240. Bischoff, J.R., et al., *Human p53 is phosphorylated by p60-cdc2 and cyclin B-cdc2.* Proc Natl Acad Sci U S A, 1990. **87**(12): p. 4766-70.
241. Milne, D.M., et al., *Phosphorylation of the tumor suppressor protein p53 by mitogen-activated protein kinases.* J Biol Chem, 1994. **269**(12): p. 9253-60.
242. Fuchs, S.Y., et al., *MEKK1/JNK signaling stabilizes and activates p53.* Proc Natl Acad Sci U S A, 1998. **95**(18): p. 10541-6.
243. Blagosklonny, M.V., *Loss of function and p53 protein stabilization.* Oncogene, 1997. **15**(16): p. 1889-93.
244. Zhang, Y. and Y. Xiong, *Control of p53 ubiquitination and nuclear export by MDM2 and ARF.* Cell Growth Differ, 2001. **12**(4): p. 175-86.
245. Fuchs, S.Y., et al., *Mdm2 association with p53 targets its ubiquitination.* Oncogene, 1998. **17**(19): p. 2543-7.
246. Gottifredi, V. and C. Prives, *Molecular biology. Getting p53 out of the nucleus.* Science, 2001. **292**(5523): p. 1851-2.
247. Michael, D. and M. Oren, *The p53 and Mdm2 families in cancer.* Curr Opin Genet Dev, 2002. **12**(1): p. 53-9.
248. Freedman, D.A. and A.J. Levine, *Nuclear export is required for degradation of endogenous p53 by MDM2 and human papillomavirus E6.* Mol Cell Biol, 1998. **18**(12): p. 7288-93.
249. Ramos, Y.F., et al., *Aberrant expression of HDMX proteins in tumor cells correlates with wild-type p53.* Cancer Res, 2001. **61**(5): p. 1839-42.
250. Jones, S.N., et al., *Rescue of embryonic lethality in Mdm2-deficient mice by absence of p53.* Nature, 1995. **378**(6553): p. 206-8.
251. Liang, Y.Y., et al., *p53 mutations in esophageal tumors from high-incidence areas of China.* Int J Cancer, 1995. **61**(5): p. 611-4.
252. Kouzarides, T., *Acetylation: a regulatory modification to rival phosphorylation?* EMBO J, 2000. **19**(6): p. 1176-9.
253. Jain, N., A. Rossi, and G. Garcia-Manero, *Epigenetic therapy of leukemia: An update.* Int J Biochem Cell Biol, 2009. **41**(1): p. 72-80.
254. Gu, W. and R.G. Roeder, *Activation of p53 sequence-specific DNA binding by acetylation of the p53 C-terminal domain.* Cell, 1997. **90**(4): p. 595-606.
255. Avantaggiati, M.L., et al., *Recruitment of p300/CBP in p53-dependent signal pathways.* Cell, 1997. **89**(7): p. 1175-84.
256. Sang, N., M.L. Avantaggiati, and A. Giordano, *Roles of p300, pocket proteins, and hTBP in E1A-mediated transcriptional regulation and inhibition of p53 transactivation activity.* J Cell Biochem, 1997. **66**(3): p. 277-85.
257. Gamper, A.M., J. Kim, and R.G. Roeder, *The STAGA subunit ADA2b is an important regulator of human GCN5 catalysis.* Mol Cell Biol, 2009. **29**(1): p. 266-80.
258. Appella, E. and C.W. Anderson, *Post-translational modifications and activation of p53 by genotoxic stresses.* Eur J Biochem, 2001. **268**(10): p. 2764-72.

259. Shklyaev, S.S., et al., *Involvement of wild-type p53 in radiation-induced c-Jun N-terminal kinase activation in human thyroid cells.* Anticancer Res, 2001. **21**(4A): p. 2569-75.
260. Kobet, E., et al., *MDM2 inhibits p300-mediated p53 acetylation and activation by forming a ternary complex with the two proteins.* Proc Natl Acad Sci U S A, 2000. **97**(23): p. 12547-52.
261. Grossman, S.R., et al., *p300/MDM2 complexes participate in MDM2-mediated p53 degradation.* Mol Cell, 1998. **2**(4): p. 405-15.
262. Tan, F., et al., *Proteomic analysis of ubiquitinated proteins in normal hepatocyte cell line Chang liver cells.* Proteomics, 2008. **8**(14): p. 2885-96.
263. Gostissa, M., et al., *Regulation of p53 functions: let's meet at the nuclear bodies.* Curr Opin Cell Biol, 2003. **15**(3): p. 351-7.
264. Shaulsky, G., et al., *Nuclear localization is essential for the activity of p53 protein.* Oncogene, 1991. **6**(11): p. 2055-65.
265. Giannakakou, P., et al., *Paclitaxel selects for mutant or pseudo-null p53 in drug resistance associated with tubulin mutations in human cancer.* Oncogene, 2000. **19**(27): p. 3078-85.
266. Giannakakou, P., et al., *p53 is associated with cellular microtubules and is transported to the nucleus by dynein.* Nat Cell Biol, 2000. **2**(10): p. 709-17.
267. Cardoso, F.M., et al., *An early function of the adenoviral E1B 55 kDa protein is required for the nuclear relocalization of the cellular p53 protein in adenovirus-infected normal human cells.* Virology, 2008. **378**(2): p. 339-46.
268. Stommel, J.M., et al., *A leucine-rich nuclear export signal in the p53 tetramerization domain: regulation of subcellular localization and p53 activity by NES masking.* EMBO J, 1999. **18**(6): p. 1660-72.
269. Zhang, Y. and Y. Xiong, *A p53 amino-terminal nuclear export signal inhibited by DNA damage-induced phosphorylation.* Science, 2001. **292**(5523): p. 1910-5.
270. Elledge, R.M., *Assessing p53 status in breast cancer prognosis: where should you put the thermometer if you think your p53 is sick?* J Natl Cancer Inst, 1996. **88**(3-4): p. 141-3.
271. Hirao, A., et al., *DNA damage-induced activation of p53 by the checkpoint kinase Chk2.* Science, 2000. **287**(5459): p. 1824-7.
272. Li, W.W., et al., *Overexpression of p21waf1 leads to increased inhibition of E2F-1 phosphorylation and sensitivity to anticancer drugs in retinoblastoma-negative human sarcoma cells.* Cancer Res, 1997. **57**(11): p. 2193-9.
273. Reinke, V. and G. Lozano, *Differential activation of p53 targets in cells treated with ultraviolet radiation that undergo both apoptosis and growth arrest.* Radiat Res, 1997. **148**(2): p. 115-22.
274. Bissonnette, N., B. Wasylyk, and D.J. Hunting, *The apoptotic and transcriptional transactivation activities of p53 can be dissociated.* Biochem Cell Biol, 1997. **75**(4): p. 351-8.
275. Kim, M.K., et al., *The role of p300 histone acetyltransferase in UV-induced histone modifications and MMP-1 gene transcription.* PLoS ONE, 2009. **4**(3): p. e4864.
276. Carlessi, L., et al., *DNA-damage response, survival and differentiation in vitro of a human neural stem cell line in relation to ATM expression.* Cell Death Differ, 2009.
277. Almog, N. and V. Rotter, *Involvement of p53 in cell differentiation and development.* Biochim Biophys Acta, 1997. **1333**(1): p. F1-27.

278. Lundberg, A.S., et al., *Genes involved in senescence and immortalization.* Curr Opin Cell Biol, 2000. **12**(6): p. 705-9.
279. Levine, A.J., J. Momand, and C.A. Finlay, *The p53 tumour suppressor gene.* Nature, 1991. **351**(6326): p. 453-6.
280. Mercer, W.E., et al., *Growth suppression induced by wild-type p53 protein is accompanied by selective down-regulation of proliferating-cell nuclear antigen expression.* Proc Natl Acad Sci U S A, 1991. **88**(5): p. 1958-62.
281. Rao, V.A. and W. Plunkett, *Activation of a p53-mediated apoptotic pathway in quiescent lymphocytes after the inhibition of DNA repair by fludarabine.* Clin Cancer Res, 2003. **9**(8): p. 3204-12.
282. Shaw, P., et al., *Induction of apoptosis by wild-type p53 in a human colon tumor-derived cell line.* Proc Natl Acad Sci U S A, 1992. **89**(10): p. 4495-9.
283. Lu, C. and W.S. El-Deiry, *Targeting p53 for enhanced radio- and chemo-sensitivity.* Apoptosis, 2009. **14**(4): p. 597-606.
284. Johnson, P., S. Chung, and S. Benchimol, *Growth suppression of Friend virus-transformed erythroleukemia cells by p53 protein is accompanied by hemoglobin production and is sensitive to erythropoietin.* Mol Cell Biol, 1993. **13**(3): p. 1456-63.
285. Vierling, A.F., E.P. Radford, Jr., and J.B. Little, *Circulating antidiuretic hormone in the X-irradiated rat.* Radiat Res, 1968. **36**(3): p. 441-53.
286. Frankenberg-Schwager, M., et al., *Single-strand annealing, conservative homologous recombination, nonhomologous DNA end joining, and the cell cycle-dependent repair of DNA double-strand breaks induced by sparsely or densely ionizing radiation.* Radiat Res, 2009. **171**(3): p. 265-73.
287. Hutchinson, F., *Chemical changes induced in DNA by ionizing radiation.* Prog Nucleic Acid Res Mol Biol, 1985. **32**: p. 115-54.
288. Komori, K., et al., *A novel protein, MAPO1, that functions in apoptosis triggered by O6-methylguanine mispair in DNA.* Oncogene, 2009. **28**(8): p. 1142-50.
289. Partridge, M., *A radiation damage repair model for normal tissues.* Phys Med Biol, 2008. **53**(13): p. 3595-608.
290. Wahl, G.M., et al., *Maintaining genetic stability through TP53 mediated checkpoint control.* Cancer Surv, 1997. **29**: p. 183-219.
291. Cuddihy, A.R. and R.G. Bristow, *The p53 protein family and radiation sensitivity: Yes or no?* Cancer Metastasis Rev, 2004. **23**(3-4): p. 237-57.
292. Bartek, J. and J. Lukas, *Pathways governing G1/S transition and their response to DNA damage.* FEBS Lett, 2001. **490**(3): p. 117-22.
293. Boddy, M.N. and P. Russell, *DNA replication checkpoint control.* Front Biosci, 1999. **4**: p. D841-8.
294. Khanna, K.K. and S.P. Jackson, *DNA double-strand breaks: signaling, repair and the cancer connection.* Nat Genet, 2001. **27**(3): p. 247-54.
295. Wahl, G.M. and A.M. Carr, *The evolution of diverse biological responses to DNA damage: insights from yeast and p53.* Nat Cell Biol, 2001. **3**(12): p. E277-86.
296. Vousden, K.H. and G.F. Woude, *The ins and outs of p53.* Nat Cell Biol, 2000. **2**(10): p. E178-80.
297. Lassus, P., et al., *Anti-apoptotic activity of low levels of wild-type p53.* EMBO J, 1996. **15**(17): p. 4566-73.

298. Chen, X., et al., *p53 levels, functional domains, and DNA damage determine the extent of the apoptotic response of tumor cells.* Genes Dev, 1996. **10**(19): p. 2438-51.
299. Lotem, J. and L. Sachs, *Hematopoietic cells from mice deficient in wild-type p53 are more resistant to induction of apoptosis by some agents.* Blood, 1993. **82**(4): p. 1092-6.
300. Ryan, K.M. and K.H. Vousden, *Characterization of structural p53 mutants which show selective defects in apoptosis but not cell cycle arrest.* Mol Cell Biol, 1998. **18**(7): p. 3692-8.
301. Flaman, J.M., et al., *The human tumour suppressor gene p53 is alternatively spliced in normal cells.* Oncogene, 1996. **12**(4): p. 813-8.
302. Friedlander, P., et al., *A mutant p53 that discriminates between p53-responsive genes cannot induce apoptosis.* Mol Cell Biol, 1996. **16**(9): p. 4961-71.
303. Ludwig, R.L., S. Bates, and K.H. Vousden, *Differential activation of target cellular promoters by p53 mutants with impaired apoptotic function.* Mol Cell Biol, 1996. **16**(9): p. 4952-60.
304. Thornborrow, E.C. and J.J. Manfredi, *One mechanism for cell type-specific regulation of the bax promoter by the tumor suppressor p53 is dictated by the p53 response element.* J Biol Chem, 1999. **274**(47): p. 33747-56.
305. Kastan, M.B., et al., *Participation of p53 protein in the cellular response to DNA damage.* Cancer Res, 1991. **51**(23 Pt 1): p. 6304-11.
306. Offer, H., et al., *The onset of p53-dependent DNA repair or apoptosis is determined by the level of accumulated damaged DNA.* Carcinogenesis, 2002. **23**(6): p. 1025-32.
307. Lin, Y. and S. Benchimol, *Cytokines inhibit p53-mediated apoptosis but not p53-mediated G1 arrest.* Mol Cell Biol, 1995. **15**(11): p. 6045-54.
308. Crook, T., et al., *Transcriptional activation by p53 correlates with suppression of growth but not transformation.* Cell, 1994. **79**(5): p. 817-27.
309. Pietenpol, J.A., et al., *Sequence-specific transcriptional activation is essential for growth suppression by p53.* Proc Natl Acad Sci U S A, 1994. **91**(6): p. 1998-2002.
310. El-Deiry, W.S., *The role of p53 in chemosensitivity and radiosensitivity.* Oncogene, 2003. **22**(47): p. 7486-95.
311. Brugarolas, J., et al., *Radiation-induced cell cycle arrest compromised by p21 deficiency.* Nature, 1995. **377**(6549): p. 552-7.
312. Harper, J.W., et al., *The p21 Cdk-interacting protein Cip1 is a potent inhibitor of G1 cyclin-dependent kinases.* Cell, 1993. **75**(4): p. 805-16.
313. Bates, S., et al., *Cell cycle arrest and DNA endoreduplication following p21Waf1/Cip1 expression.* Oncogene, 1998. **17**(13): p. 1691-703.
314. Ford, J.M. and P.C. Hanawalt, *Li-Fraumeni syndrome fibroblasts homozygous for p53 mutations are deficient in global DNA repair but exhibit normal transcription-coupled repair and enhanced UV resistance.* Proc Natl Acad Sci U S A, 1995. **92**(19): p. 8876-80.
315. Wani, M.A., et al., *Influence of p53 tumor suppressor protein on bias of DNA repair and apoptotic response in human cells.* Carcinogenesis, 1999. **20**(5): p. 765-72.
316. Offer, H., et al., *Structural and functional involvement of p53 in BER in vitro and in vivo.* Oncogene, 2001. **20**(5): p. 581-9.

317. Zhou, J., et al., *A role for p53 in base excision repair.* EMBO J, 2001. **20**(4): p. 914-23.
318. Hartwell, L.H. and T.A. Weinert, *Checkpoints: controls that ensure the order of cell cycle events.* Science, 1989. **246**(4930): p. 629-34.
319. Kastan, M.B., et al., *A mammalian cell cycle checkpoint pathway utilizing p53 and GADD45 is defective in ataxia-telangiectasia.* Cell, 1992. **71**(4): p. 587-97.
320. Chen, C.Y., et al., *Interactions between p53 and MDM2 in a mammalian cell cycle checkpoint pathway.* Proc Natl Acad Sci U S A, 1994. **91**(7): p. 2684-8.
321. Canman, C.E., et al., *The p53-dependent G1 cell cycle checkpoint pathway and ataxia-telangiectasia.* Cancer Res, 1994. **54**(19): p. 5054-8.
322. Slebos, R.J., et al., *p53-dependent G1 arrest involves pRB-related proteins and is disrupted by the human papillomavirus 16 E7 oncoprotein.* Proc Natl Acad Sci U S A, 1994. **91**(12): p. 5320-4.
323. Hickman, E.S., S.M. Picksley, and K.H. Vousden, *Cells expressing HPV16 E7 continue cell cycle progression following DNA damage induced p53 activation.* Oncogene, 1994. **9**(8): p. 2177-81.
324. Painter, R.B., *Altered DNA synthesis in irradiated and unirradiated ataxia-telangiectasia cells.* Kroc Found Ser, 1985. **19**: p. 89-100.
325. Ghosh, S., D. Schroeter, and N. Paweletz, *Okadaic acid overrides the S-phase check point and accelerates progression of G2-phase to induce premature mitosis in HeLa cells.* Exp Cell Res, 1996. **227**(1): p. 165-9.
326. Schlegel, R. and A.B. Pardee, *Caffeine-induced uncoupling of mitosis from the completion of DNA replication in mammalian cells.* Science, 1986. **232**(4755): p. 1264-6.
327. Steinmann, K.E., et al., *Chemically induced premature mitosis: differential response in rodent and human cells and the relationship to cyclin B synthesis and p34cdc2/cyclin B complex formation.* Proc Natl Acad Sci U S A, 1991. **88**(15): p. 6843-7.
328. Yoshida, M., et al., *Biochemical differences between staurosporine-induced apoptosis and premature mitosis.* Exp Cell Res, 1997. **232**(2): p. 225-39.
329. Taylor, J.K., et al., *Inhibition of Bcl-xL expression sensitizes normal human keratinocytes and epithelial cells to apoptotic stimuli.* Oncogene, 1999. **18**(31): p. 4495-504.
330. Chang, T.H., et al., *Disregulation of mitotic checkpoints and regulatory proteins following acute expression of SV40 large T antigen in diploid human cells.* Oncogene, 1997. **14**(20): p. 2383-93.
331. Lim, D.S., et al., *ATM phosphorylates p95/nbs1 in an S-phase checkpoint pathway.* Nature, 2000. **404**(6778): p. 613-7.
332. Falck, J., et al., *Functional impact of concomitant versus alternative defects in the Chk2-p53 tumour suppressor pathway.* Oncogene, 2001. **20**(39): p. 5503-10.
333. Koumenis, C., et al., *Regulation of p53 by hypoxia: dissociation of transcriptional repression and apoptosis from p53-dependent transactivation.* Mol Cell Biol, 2001. **21**(4): p. 1297-310.
334. Kim, M.Y., et al., *Mutations of the p53 and PTCH gene in basal cell carcinomas: UV mutation signature and strand bias.* J Dermatol Sci, 2002. **29**(1): p. 1-9.

335. Baggio, L., et al., *Relative biological effectiveness of light ions in human tumoural cell lines: role of protein p53.* Radiat Prot Dosimetry, 2002. **99**(1-4): p. 211-4.
336. Hartwell, L., *Defects in a cell cycle checkpoint may be responsible for the genomic instability of cancer cells.* Cell, 1992. **71**(4): p. 543-6.
337. Levedakou, E.N., et al., *p21CIP1 is not required for the early G2 checkpoint response to ionizing radiation.* Cancer Res, 1995. **55**(12): p. 2500-2.
338. Paules, R.S., et al., *Defective G2 checkpoint function in cells from individuals with familial cancer syndromes.* Cancer Res, 1995. **55**(8): p. 1763-73.
339. Kaufmann, W.K., *Cell cycle checkpoints and DNA repair preserve the stability of the human genome.* Cancer Metastasis Rev, 1995. **14**(1): p. 31-41.
340. Stewart, B.W., *Mechanisms of apoptosis: integration of genetic, biochemical, and cellular indicators.* J Natl Cancer Inst, 1994. **86**(17): p. 1286-96.
341. Thompson, D.A., et al., *The human papillomavirus-16 E6 oncoprotein decreases the vigilance of mitotic checkpoints.* Oncogene, 1997. **15**(25): p. 3025-35.
342. Filatov, L., et al., *Chromosomal instability is correlated with telomere erosion and inactivation of G2 checkpoint function in human fibroblasts expressing human papillomavirus type 16 E6 oncoprotein.* Oncogene, 1998. **16**(14): p. 1825-38.
343. Bunz, F., et al., *Requirement for p53 and p21 to sustain G2 arrest after DNA damage.* Science, 1998. **282**(5393): p. 1497-501.
344. Nurse, P., *Universal control mechanism regulating onset of M-phase.* Nature, 1990. **344**(6266): p. 503-8.
345. Kaldis, P., et al., *Localization and regulation of the cdk-activating kinase (Cak1p) from budding yeast.* J Cell Sci, 1998. **111 ( Pt 24)**: p. 3585-96.
346. Berry, L.D. and K.L. Gould, *Regulation of Cdc2 activity by phosphorylation at T14/Y15.* Prog Cell Cycle Res, 1996. **2**: p. 99-105.
347. Conklin, D.S., K. Galaktionov, and D. Beach, *14-3-3 proteins associate with cdc25 phosphatases.* Proc Natl Acad Sci U S A, 1995. **92**(17): p. 7892-6.
348. Ohki, R., et al., *Reprimo, a new candidate mediator of the p53-mediated cell cycle arrest at the G2 phase.* J Biol Chem, 2000. **275**(30): p. 22627-30.
349. Innocente, S.A., et al., *p53 regulates a G2 checkpoint through cyclin B1.* Proc Natl Acad Sci U S A, 1999. **96**(5): p. 2147-52.
350. Taylor, W.R., et al., *Mechanisms of G2 arrest in response to overexpression of p53.* Mol Biol Cell, 1999. **10**(11): p. 3607-22.
351. Utrera, R., et al., *A novel p53-inducible gene coding for a microtubule-localized protein with G2-phase-specific expression.* EMBO J, 1998. **17**(17): p. 5015-25.
352. Zhu, J., et al., *The potential tumor suppressor p73 differentially regulates cellular p53 target genes.* Cancer Res, 1998. **58**(22): p. 5061-5.
353. Agapova, L.S., et al., *P53-dependent effects of RAS oncogene on chromosome stability and cell cycle checkpoints.* Oncogene, 1999. **18**(20): p. 3135-42.
354. Agarwala, S., T.A. Sanders, and C.W. Ragsdale, *Sonic hedgehog control of size and shape in midbrain pattern formation.* Science, 2001. **291**(5511): p. 2147-50.
355. Barbacid, M., *ras genes.* Annu Rev Biochem, 1987. **56**: p. 779-827.
356. Leevers, S.J. and C.J. Marshall, *Activation of extracellular signal-regulated kinase, ERK2, by p21ras oncoprotein.* EMBO J, 1992. **11**(2): p. 569-74.

357. Avruch, J., X.F. Zhang, and J.M. Kyriakis, *Raf meets Ras: completing the framework of a signal transduction pathway.* Trends Biochem Sci, 1994. **19**(7): p. 279-83.
358. Daum, G., et al., *The ins and outs of Raf kinases.* Trends Biochem Sci, 1994. **19**(11): p. 474-80.
359. Bonner, T.I., et al., *The complete coding sequence of the human raf oncogene and the corresponding structure of the c-raf-1 gene.* Nucleic Acids Res, 1986. **14**(2): p. 1009-15.
360. Storm, S.M., et al., *raf oncogenes in carcinogenesis.* Crit Rev Oncog, 1990. **2**(1): p. 1-8.
361. Storm, S.M., J.L. Cleveland, and U.R. Rapp, *Expression of raf family proto-oncogenes in normal mouse tissues.* Oncogene, 1990. **5**(3): p. 345-51.
362. Lee, J.E., et al., *Regulation of A-raf expression.* Oncogene, 1996. **12**(8): p. 1669-77.
363. Dugan, L.L., et al., *Differential effects of cAMP in neurons and astrocytes. Role of B-raf.* J Biol Chem, 1999. **274**(36): p. 25842-8.
364. Barnier, J.V., et al., *The mouse B-raf gene encodes multiple protein isoforms with tissue-specific expression.* J Biol Chem, 1995. **270**(40): p. 23381-9.
365. Yang, J., et al., *Molecular determinants of melanoma malignancy: selecting targets for improved efficacy of chemotherapy.* Mol Cancer Ther, 2009. **8**(3): p. 636-47.
366. Zheng, B., et al., *Oncogenic B-RAF negatively regulates the tumor suppressor LKB1 to promote melanoma cell proliferation.* Mol Cell, 2009. **33**(2): p. 237-47.
367. Smalley, K.S. and K.T. Flaherty, *Integrating BRAF/MEK inhibitors into combination therapy for melanoma.* Br J Cancer, 2009. **100**(3): p. 431-5.
368. Wong, K.K., *Recent developments in anti-cancer agents targeting the Ras/Raf/ MEK/ERK pathway.* Recent Pat Anticancer Drug Discov, 2009. **4**(1): p. 28-35.
369. Hagemann, C., et al., *RAF expression in human astrocytic tumors.* Int J Mol Med, 2009. **23**(1): p. 17-31.
370. Ogino, S., et al., *CpG island methylator phenotype, microsatellite instability, BRAF mutation and clinical outcome in colon cancer.* Gut, 2009. **58**(1): p. 90-6.
371. Zou, M., et al., *Oncogenic activation of MAP kinase by BRAF pseudogene in thyroid tumors.* Neoplasia, 2009. **11**(1): p. 57-65.
372. Pratilas, C.A., et al., *Genetic predictors of MEK dependence in non-small cell lung cancer.* Cancer Res, 2008. **68**(22): p. 9375-83.
373. Davies, H., et al., *Mutations of the BRAF gene in human cancer.* Nature, 2002. **417**(6892): p. 949-54.
374. Cioffi, C.L., et al., *Selective inhibition of A-Raf and C-Raf mRNA expression by antisense oligodeoxynucleotides in rat vascular smooth muscle cells: role of A-Raf and C-Raf in serum-induced proliferation.* Mol Pharmacol, 1997. **51**(3): p. 383-9.
375. Lloyd, A.C., et al., *Cooperating oncogenes converge to regulate cyclin/cdk complexes.* Genes Dev, 1997. **11**(5): p. 663-77.
376. Ravi, R.K., et al., *Activated Raf-1 causes growth arrest in human small cell lung cancer cells.* J Clin Invest, 1998. **101**(1): p. 153-9.

377. Petersen, J., *TOR signalling regulates mitotic commitment through stress-activated MAPK and Polo kinase in response to nutrient stress.* Biochem Soc Trans, 2009. **37**(Pt 1): p. 273-7.
378. Estrada, Y., J. Dong, and L. Ossowski, *Positive crosstalk between ERK and p38 in melanoma stimulates migration and in vivo proliferation.* Pigment Cell Melanoma Res, 2009. **22**(1): p. 66-76.
379. Wang, J., et al., *Akt regulates vitamin D3-induced leukemia cell functional differentiation via Raf/MEK/ERK MAPK signaling.* Eur J Cell Biol, 2009. **88**(2): p. 103-15.
380. Gille, H., A.D. Sharrocks, and P.E. Shaw, *Phosphorylation of transcription factor p62TCF by MAP kinase stimulates ternary complex formation at c-fos promoter.* Nature, 1992. **358**(6385): p. 414-7.
381. Mansour, S.J., et al., *Transformation of mammalian cells by constitutively active MAP kinase kinase.* Science, 1994. **265**(5174): p. 966-70.
382. Robinson, D., et al., *Tyrosine kinase expression profiles of chicken erythro-progenitor cells and oncogene-transformed erythroblasts.* J Biomed Sci, 1998. **5**(2): p. 93-100.
383. Lau, Q.C., S. Brusselbach, and R. Muller, *Abrogation of c-Raf expression induces apoptosis in tumor cells.* Oncogene, 1998. **16**(14): p. 1899-902.
384. Houben, R., et al., *Proliferation arrest in B-Raf mutant melanoma cell lines upon MAPK pathway activation.* J Invest Dermatol, 2009. **129**(2): p. 406-14.
385. Hesketh, J., et al., *Targeting of c-myc and beta-globin coding sequences to cytoskeletal-bound polysomes by c-myc 3' untranslated region.* Biochem J, 1994. **298 ( Pt 1)**: p. 143-8.
386. Hanks, S.K., A.M. Quinn, and T. Hunter, *The protein kinase family: conserved features and deduced phylogeny of the catalytic domains.* Science, 1988. **241**(4861): p. 42-52.
387. Muslin, A.J., et al., *Interaction of 14-3-3 with signaling proteins is mediated by the recognition of phosphoserine.* Cell, 1996. **84**(6): p. 889-97.
388. Rommel, C., et al., *Activated Ras displaces 14-3-3 protein from the amino terminus of c-Raf-1.* Oncogene, 1996. **12**(3): p. 609-19.
389. Freed, E., F. McCormick, and R. Ruggieri, *Proteins of the 14-3-3 family associate with Raf and contribute to its activation.* Cold Spring Harb Symp Quant Biol, 1994. **59**: p. 187-93.
390. Freed, E., et al., *Binding of 14-3-3 proteins to the protein kinase Raf and effects on its activation.* Science, 1994. **265**(5179): p. 1713-6.
391. Stokoe, D., et al., *Activation of Raf as a result of recruitment to the plasma membrane.* Science, 1994. **264**(5164): p. 1463-7.
392. Zhang, X.F., et al., *Normal and oncogenic p21ras proteins bind to the amino-terminal regulatory domain of c-Raf-1.* Nature, 1993. **364**(6435): p. 308-13.
393. Farrar, M.A., I. Alberol, and R.M. Perlmutter, *Activation of the Raf-1 kinase cascade by coumermycin-induced dimerization.* Nature, 1996. **383**(6596): p. 178-81.
394. Luo, Z., et al., *Oligomerization activates c-Raf-1 through a Ras-dependent mechanism.* Nature, 1996. **383**(6596): p. 181-5.
395. Vojtek, A.B., S.M. Hollenberg, and J.A. Cooper, *Mammalian Ras interacts directly with the serine/threonine kinase Raf.* Cell, 1993. **74**(1): p. 205-14.
396. Kharbanda, S., et al., *Activation of Raf-1 and mitogen-activated protein kinases during monocytic differentiation of human myeloid leukemia cells.* J Biol Chem, 1994. **269**(2): p. 872-8.

397. Nassar, N., et al., *The 2.2 A crystal structure of the Ras-binding domain of the serine/threonine kinase c-Raf1 in complex with Rap1A and a GTP analogue.* Nature, 1995. **375**(6532): p. 554-60.
398. Brtva, T.R., et al., *Two distinct Raf domains mediate interaction with Ras.* J Biol Chem, 1995. **270**(17): p. 9809-12.
399. Michaud, N.R., et al., *14-3-3 is not essential for Raf-1 function: identification of Raf-1 proteins that are biologically activated in a 14-3-3- and Ras-independent manner.* Mol Cell Biol, 1995. **15**(6): p. 3390-7.
400. Morrison, D.K. and R.E. Cutler, *The complexity of Raf-1 regulation.* Curr Opin Cell Biol, 1997. **9**(2): p. 174-9.
401. Wu, J., et al., *Inhibition of the EGF-activated MAP kinase signaling pathway by adenosine 3',5'-monophosphate.* Science, 1993. **262**(5136): p. 1065-9.
402. Alessi, D.R., et al., *Identification of the sites in MAP kinase kinase-1 phosphorylated by p74raf-1.* EMBO J, 1994. **13**(7): p. 1610-9.
403. Chaudhary, A., et al., *Phosphatidylinositol 3-kinase regulates Raf1 through Pak phosphorylation of serine 338.* Curr Biol, 2000. **10**(9): p. 551-4.
404. King, T.R., et al., *Using a phage display library to identify basic residues in A-Raf required to mediate binding to the Src homology 2 domains of the p85 subunit of phosphatidylinositol 3'-kinase.* J Biol Chem, 2000. **275**(46): p. 36450-6.
405. Avruch, J., et al., *Ras activation of the Raf kinase: tyrosine kinase recruitment of the MAP kinase cascade.* Recent Prog Horm Res, 2001. **56**: p. 127-55.
406. Dhillon, A.S., et al., *Cyclic AMP-dependent kinase regulates Raf-1 kinase mainly by phosphorylation of serine 259.* Mol Cell Biol, 2002. **22**(10): p. 3237-46.
407. Zhang, S.H., et al., *Serine phosphorylation-dependent association of the band 4.1-related protein-tyrosine phosphatase PTPH1 with 14-3-3beta protein.* J Biol Chem, 1997. **272**(43): p. 27281-7.
408. Fabian, J.R., I.O. Daar, and D.K. Morrison, *Critical tyrosine residues regulate the enzymatic and biological activity of Raf-1 kinase.* Mol Cell Biol, 1993. **13**(11): p. 7170-9.
409. Marais, R., et al., *Ras recruits Raf-1 to the plasma membrane for activation by tyrosine phosphorylation.* EMBO J, 1995. **14**(13): p. 3136-45.
410. Chong, H., J. Lee, and K.L. Guan, *Positive and negative regulation of Raf kinase activity and function by phosphorylation.* EMBO J, 2001. **20**(14): p. 3716-27.
411. Mischak, H., et al., *Negative regulation of Raf-1 by phosphorylation of serine 621.* Mol Cell Biol, 1996. **16**(10): p. 5409-18.
412. Dougherty, M.K., et al., *Regulation of Raf-1 by direct feedback phosphorylation.* Mol Cell, 2005. **17**(2): p. 215-24.
413. Huang, C.Y. and J.E. Ferrell, Jr., *Ultrasensitivity in the mitogen-activated protein kinase cascade.* Proc Natl Acad Sci U S A, 1996. **93**(19): p. 10078-83.
414. Seger, R., et al., *Microtubule-associated protein 2 kinases, ERK1 and ERK2, undergo autophosphorylation on both tyrosine and threonine residues: implications for their mechanism of activation.* Proc Natl Acad Sci U S A, 1991. **88**(14): p. 6142-6.
415. Crews, C.M. and R.L. Erikson, *Purification of a murine protein-tyrosine/threonine kinase that phosphorylates and activates the Erk-1 gene*

*product: relationship to the fission yeast byr1 gene product.* Proc Natl Acad Sci U S A, 1992. **89**(17): p. 8205-9.
416. Robbins, D.J. and M.H. Cobb, *Extracellular signal-regulated kinases 2 autophosphorylates on a subset of peptides phosphorylated in intact cells in response to insulin and nerve growth factor: analysis by peptide mapping.* Mol Biol Cell, 1992. **3**(3): p. 299-308.
417. Khokhlatchev, A., et al., *Reconstitution of mitogen-activated protein kinase phosphorylation cascades in bacteria. Efficient synthesis of active protein kinases.* J Biol Chem, 1997. **272**(17): p. 11057-62.
418. Price, M.A., C. Hill, and R. Treisman, *Integration of growth factor signals at the c-fos serum response element.* Philos Trans R Soc Lond B Biol Sci, 1996. **351**(1339): p. 551-9.
419. Treisman, R., *Regulation of transcription by MAP kinase cascades.* Curr Opin Cell Biol, 1996. **8**(2): p. 205-15.
420. Therrien, M., et al., *KSR modulates signal propagation within the MAPK cascade.* Genes Dev, 1996. **10**(21): p. 2684-95.
421. Marshall, M.S., *Ras target proteins in eukaryotic cells.* FASEB J, 1995. **9**(13): p. 1311-8.
422. Cobb, M.H., *MAP kinase pathways.* Prog Biophys Mol Biol, 1999. **71**(3-4): p. 479-500.
423. Houslay, M.D. and W. Kolch, *Cell-type specific integration of cross-talk between extracellular signal-regulated kinase and cAMP signaling.* Mol Pharmacol, 2000. **58**(4): p. 659-68.
424. Kolch, W., *Meaningful relationships: the regulation of the Ras/Raf/MEK/ERK pathway by protein interactions.* Biochem J, 2000. **351 Pt 2**: p. 289-305.
425. Dhillon, A.S., et al., *A Raf-1 mutant that dissociates MEK/extracellular signal-regulated kinase activation from malignant transformation and differentiation but not proliferation.* Mol Cell Biol, 2003. **23**(6): p. 1983-93.
426. Schaeffer, H.J. and M.J. Weber, *Mitogen-activated protein kinases: specific messages from ubiquitous messengers.* Mol Cell Biol, 1999. **19**(4): p. 2435-44.
427. Jamal, S. and E.B. Ziff, *Raf phosphorylates p53 in vitro and potentiates p53-dependent transcriptional transactivation in vivo.* Oncogene, 1995. **10**(11): p. 2095-101.
428. Huser, M., et al., *MEK kinase activity is not necessary for Raf-1 function.* EMBO J, 2001. **20**(8): p. 1940-51.
429. Lenormand, P., M. McMahon, and J. Pouyssegur, *Oncogenic Raf-1 activates p70 S6 kinase via a mitogen-activated protein kinase-independent pathway.* J Biol Chem, 1996. **271**(26): p. 15762-8.
430. Wang, S., R.N. Ghosh, and S.P. Chellappan, *Raf-1 physically interacts with Rb and regulates its function: a link between mitogenic signaling and cell cycle regulation.* Mol Cell Biol, 1998. **18**(12): p. 7487-98.
431. Lin, J.H., et al., *The ankyrin repeat-containing adaptor protein Tvl-1 is a novel substrate and regulator of Raf-1.* J Biol Chem, 1999. **274**(21): p. 14706-15.
432. Janosch, P., et al., *The Raf-1 kinase associates with vimentin kinases and regulates the structure of vimentin filaments.* FASEB J, 2000. **14**(13): p. 2008-21.

433. Duncan, J.S. and D.W. Litchfield, *Too much of a good thing: the role of protein kinase CK2 in tumorigenesis and prospects for therapeutic inhibition of CK2.* Biochim Biophys Acta, 2008. **1784**(1): p. 33-47.
434. Wang, H.G., U.R. Rapp, and J.C. Reed, *Bcl-2 targets the protein kinase Raf-1 to mitochondria.* Cell, 1996. **87**(4): p. 629-38.
435. Chen, J., et al., *Raf-1 promotes cell survival by antagonizing apoptosis signal-regulating kinase 1 through a MEK-ERK independent mechanism.* Proc Natl Acad Sci U S A, 2001. **98**(14): p. 7783-8.
436. Galaktionov, K., C. Jessus, and D. Beach, *Raf1 interaction with Cdc25 phosphatase ties mitogenic signal transduction to cell cycle activation.* Genes Dev, 1995. **9**(9): p. 1046-58.
437. Smalley, K.S., et al., *CRAF inhibition induces apoptosis in melanoma cells with non-V600E BRAF mutations.* Oncogene, 2009. **28**(1): p. 85-94.
438. Navas, T.A., D.T. Baldwin, and T.A. Stewart, *RIP2 is a Raf1-activated mitogen-activated protein kinase kinase.* J Biol Chem, 1999. **274**(47): p. 33684-90.
439. Krieg, A., G. Le Negrate, and J.C. Reed, *RIP2-beta: A novel alternative mRNA splice variant of the receptor interacting protein kinase RIP2.* Mol Immunol, 2009. **46**(6): p. 1163-70.
440. Wang, H.G., et al., *Apoptosis regulation by interaction of Bcl-2 protein and Raf-1 kinase.* Oncogene, 1994. **9**(9): p. 2751-6.
441. Nantel, A., M. Huber, and D.Y. Thomas, *Localization of endogenous Grb10 to the mitochondria and its interaction with the mitochondrial-associated Raf-1 pool.* J Biol Chem, 1999. **274**(50): p. 35719-24.
442. Dufresne, A.M. and R.J. Smith, *The adapter protein GRB10 is an endogenous negative regulator of insulin-like growth factor signaling.* Endocrinology, 2005. **146**(10): p. 4399-409.
443. Ehrhardt, G.R., et al., *A novel potential effector of M-Ras and p21 Ras negatively regulates p21 Ras-mediated gene induction and cell growth.* Oncogene, 2001. **20**(2): p. 188-97.
444. Kuo, W.L., et al., *Raf, but not MEK or ERK, is sufficient for differentiation of hippocampal neuronal cells.* Mol Cell Biol, 1996. **16**(4): p. 1458-70.
445. Porras, A., et al., *Dissociation between activation of Raf-1 kinase and the 42-kDa mitogen-activated protein kinase/90-kDa S6 kinase (MAPK/RSK) cascade in the insulin/Ras pathway of adipocytic differentiation of 3T3 L1 cells.* J Biol Chem, 1994. **269**(17): p. 12741-8.
446. Weissinger, E.M., et al., *Inhibition of the Raf-1 kinase by cyclic AMP agonists causes apoptosis of v-abl-transformed cells.* Mol Cell Biol, 1997. **17**(6): p. 3229-41.
447. Heidecker, G., et al., *The role of Raf-1 phosphorylation in signal transduction.* Adv Cancer Res, 1992. **58**: p. 53-73.
448. Schulte, T.W., et al., *Disruption of the Raf-1-Hsp90 molecular complex results in destabilization of Raf-1 and loss of Raf-1-Ras association.* J Biol Chem, 1995. **270**(41): p. 24585-8.
449. Morrison, D.K., *The Raf-1 kinase as a transducer of mitogenic signals.* Cancer Cells, 1990. **2**(12): p. 377-82.
450. Rapp, U.R., et al., *raf family serine/threonine protein kinases in mitogen signal transduction.* Cold Spring Harb Symp Quant Biol, 1988. **53 Pt 1**: p. 173-84.

451. Marshall, M., *Interactions between Ras and Raf: key regulatory proteins in cellular transformation.* Mol Reprod Dev, 1995. **42**(4): p. 493-9.
452. Scheffler, J.E., et al., *Characterization of a 78-residue fragment of c-Raf-1 that comprises a minimal binding domain for the interaction with Ras-GTP.* J Biol Chem, 1994. **269**(35): p. 22340-6.
453. Pumiglia, K., et al., *Raf-1 N-terminal sequences necessary for Ras-Raf interaction and signal transduction.* Mol Cell Biol, 1995. **15**(1): p. 398-406.
454. Herrmann, C., G.A. Martin, and A. Wittinghofer, *Quantitative analysis of the complex between p21ras and the Ras-binding domain of the human Raf-1 protein kinase.* J Biol Chem, 1995. **270**(7): p. 2901-5.
455. Block, C., et al., *Quantitative structure-activity analysis correlating Ras/Raf interaction in vitro to Raf activation in vivo.* Nat Struct Biol, 1996. **3**(3): p. 244-51.
456. Kiefer, P.E., et al., *Different pattern of expression of cellular oncogenes in human non-small-cell lung cancer cell lines.* J Cancer Res Clin Oncol, 1990. **116**(1): p. 29-37.
457. Rossomando, A.J., et al., *Evidence that pp42, a major tyrosine kinase target protein, is a mitogen-activated serine/threonine protein kinase.* Proc Natl Acad Sci U S A, 1989. **86**(18): p. 6940-3.
458. McCubrey, J.A., et al., *Differential abilities of activated Raf oncoproteins to abrogate cytokine dependency, prevent apoptosis and induce autocrine growth factor synthesis in human hematopoietic cells.* Leukemia, 1998. **12**(12): p. 1903-29.
459. Hoyle, P.E., et al., *Differential abilities of the Raf family of protein kinases to abrogate cytokine dependency and prevent apoptosis in murine hematopoietic cells by a MEK1-dependent mechanism.* Leukemia, 2000. **14**(4): p. 642-56.
460. Woods, D., et al., *Raf-induced proliferation or cell cycle arrest is determined by the level of Raf activity with arrest mediated by p21Cip1.* Mol Cell Biol, 1997. **17**(9): p. 5598-611.
461. Mamon, H., et al., *New perspectives on Raf-1: the involvement of p21ras in the activation of Raf-1 and a potential role for Raf-1 in events occurring later in the cell cycle.* Cold Spring Harb Symp Quant Biol, 1991. **56**: p. 251-63.
462. Laird, A.D., et al., *Raf-1 is activated during mitosis.* J Biol Chem, 1995. **270**(45): p. 26742-5.
463. Lovric, J. and K. Moelling, *Activation of Mil/Raf protein kinases in mitotic cells.* Oncogene, 1996. **12**(5): p. 1109-16.
464. Pathan, N.I., et al., *Activation of T cell Raf-1 at mitosis requires the protein-tyrosine kinase Lck.* J Biol Chem, 1996. **271**(48): p. 30315-7.
465. Laird, A.D., D.K. Morrison, and D. Shalloway, *Characterization of Raf-1 activation in mitosis.* J Biol Chem, 1999. **274**(7): p. 4430-9.
466. Rapp, U.R., et al., *Structure and biological activity of v-raf, a unique oncogene transduced by a retrovirus.* Proc Natl Acad Sci U S A, 1983. **80**(14): p. 4218-22.
467. Moelling, K., et al., *Serine- and threonine-specific protein kinase activities of purified gag-mil and gag-raf proteins.* Nature, 1984. **312**(5994): p. 558-61.
468. Jansen, H.W., et al., *Homologous cell-derived oncogenes in avian carcinoma virus MH2 and murine sarcoma virus 3611.* Nature, 1984. **307**(5948): p. 281-4.

469. Klinken, S.P., U.R. Rapp, and H.C. Morse, 3rd, *raf/myc-infected erythroid cells are restricted in their ability to terminally differentiate.* J Virol, 1989. **63**(3): p. 1489-92.
470. Zhang, Y., et al., *Synergism between two growth regulatory pathways: cooperative transformation of NIH3T3 cells by G alpha 12 and c-raf-1.* Oncogene, 1996. **12**(11): p. 2377-83.
471. Waskiewicz, A.J. and J.A. Cooper, *Mitogen and stress response pathways: MAP kinase cascades and phosphatase regulation in mammals and yeast.* Curr Opin Cell Biol, 1995. 7(6): p. 798-805.
472. Kasid, U., et al., *Activation of Raf by ionizing radiation.* Nature, 1996. **382**(6594): p. 813-6.
473. Baba, I., et al., *Involvement of deregulated epiregulin expression in tumorigenesis in vivo through activated Ki-Ras signaling pathway in human colon cancer cells.* Cancer Res, 2000. **60**(24): p. 6886-9.
474. Chang, E.H., et al., *Oncogenes in radioresistant, noncancerous skin fibroblasts from a cancer-prone family.* Science, 1987. **237**(4818): p. 1036-9.
475. Pirollo, K.F., et al., *raf involvement in the simultaneous genetic transfer of the radioresistant and transforming phenotypes.* Int J Radiat Biol, 1989. **55**(5): p. 783-96.
476. Kasid, U., et al., *The raf oncogene is associated with a radiation-resistant human laryngeal cancer.* Science, 1987. **237**(4818): p. 1039-41.
477. Kasid, U.N., et al., *Sensitivities of NIH/3T3-derived clonal cell lines to ionizing radiation: significance for gene transfer studies.* Cancer Res, 1989. **49**(12): p. 3396-400.
478. Kasid, U., et al., *Effect of antisense c-raf-1 on tumorigenicity and radiation sensitivity of a human squamous carcinoma.* Science, 1989. **243**(4896): p. 1354-6.
479. Gokhale, P.C., et al., *Antisense raf oligodeoxyribonucleotide is a radiosensitizer in vivo.* Antisense Nucleic Acid Drug Dev, 1999. **9**(2): p. 191-201.
480. Warenius, H.M., et al., *C-raf-1 proto-oncogene expression relates to radiosensitivity rather than radioresistance.* Eur J Cancer, 1994. **30A**(3): p. 369-75.
481. Warenius, H.M., M.D. Jones, and C.C. Thompson, *Exit from G2 phase after 2 Gy gamma irradiation is faster in radiosensitive human cells with high expression of the RAF1 proto-oncogene.* Radiat Res, 1996. **146**(5): p. 485-93.
482. Lee, Y.J., et al., *Protein kinase Cdelta overexpression enhances radiation sensitivity via extracellular regulated protein kinase 1/2 activation, abolishing the radiation-induced G(2)-M arrest.* Cell Growth Differ, 2002. **13**(5): p. 237-46.
483. Broustas, C.G., et al., *Phosphorylation of the myosin-binding subunit of myosin phosphatase by Raf-1 and inhibition of phosphatase activity.* J Biol Chem, 2002. **277**(4): p. 3053-9.
484. Warenius, H.M., et al., *Combined RAF1 protein expression and p53 mutational status provides a strong predictor of cellular radiosensitivity.* Br J Cancer, 2000. **83**(8): p. 1084-95.
485. Courtenay, V.D., *A soft agar colony assay for Lewis lung tumour and B16 melanoma taken directly from the mouse.* Br J Cancer, 1976. **34**(1): p. 39-45.
486. Warenius, H.M. and R.A. Britten, *In vitro studies of intrinsic cellular radiosensitivity following 4 MeV photons or 62.5 MeV (p-->Be+) neutrons.*

*Potential implications for high LET therapy.* Acta Oncol, 1994. **33**(3): p. 241-9.
487. Okada, T. and M. Yoneyama, *The interaction of malignant cells with yeast. II. A new yeast extract inhibiting the growth of malignant cell.* Hiroshima J Med Sci, 1970. **19**(2): p. 99-117.
488. Lindsey, J.K., *A review of some extensions to generalized linear models.* Stat Med, 1999. **18**(17-18): p. 2223-36.
489. FitzGerald, T.J., et al., *Expression of transfected recombinant oncogenes increases radiation resistance of clonal hematopoietic and fibroblast cell lines selectively at clinical low dose rate.* Radiat Res, 1990. **122**(1): p. 44-52.
490. Caron, R.W., et al., *H-RAS V12-induced radioresistance in HCT116 colon carcinoma cells is heregulin dependent.* Mol Cancer Ther, 2005. **4**(2): p. 243-55.
491. Nagasawa, H., et al., *Relationship between gamma-ray-induced G2/M delay and cellular radiosensitivity.* Int J Radiat Biol, 1994. **66**(4): p. 373-9.
492. Tamamoto, T., et al., *Correlation between gamma-ray-induced G2 arrest and radioresistance in two human cancer cells.* Int J Radiat Oncol Biol Phys, 1999. **44**(4): p. 905-9.
493. Kim, S.H., et al., *Enhancement of radiation response on human carcinoma cells in culture by pentoxifylline.* Int J Radiat Oncol Biol Phys, 1993. **25**(1): p. 61-5.
494. Tobey, R.A., M.S. Oka, and H.A. Crissman, *Differential effects of two chemotherapeutic agents, streptozotocin and chlorozotocin, on the mammalian cell cycle.* Eur J Cancer, 1975. **11**(6): p. 433-41.
495. Liu, L., et al., *p53 sites acetylated in vitro by PCAF and p300 are acetylated in vivo in response to DNA damage.* Mol Cell Biol, 1999. **19**(2): p. 1202-9.
496. Chang, L., et al., *ATM-mediated serine 72 phosphorylation stabilizes ribonucleotide reductase small subunit p53R2 protein against MDM2 to DNA damage.* Proc Natl Acad Sci U S A, 2008. **105**(47): p. 18519-24.
497. Wittlinger, M., et al., *Time and dose-dependent activation of p53 serine 15 phosphorylation among cell lines with different radiation sensitivity.* Int J Radiat Biol, 2007. **83**(4): p. 245-57.
498. Chirgwin, J.M., et al., *Isolation of biologically active ribonucleic acid from sources enriched in ribonuclease.* Biochemistry, 1979. **18**(24): p. 5294-9.
499. Barraclough, R., et al., *Molecular cloning and sequence of the gene for p9Ka. A cultured myoepithelial cell protein with strong homology to S-100, a calcium-binding protein.* J Mol Biol, 1987. **198**(1): p. 13-20.
500. Sanger, F., S. Nicklen, and A.R. Coulson, *DNA sequencing with chain-terminating inhibitors.* Proc Natl Acad Sci U S A, 1977. **74**(12): p. 5463-7.
501. Ponten, F., et al., *Induction of p53 expression in skin by radiotherapy and UV radiation: a randomized study.* J Natl Cancer Inst, 2001. **93**(2): p. 128-33.
502. Lakin, N.D. and S.P. Jackson, *Regulation of p53 in response to DNA damage.* Oncogene, 1999. **18**(53): p. 7644-55.
503. von Gise, A., et al., *Apoptosis suppression by Raf-1 and MEK1 requires MEK- and phosphatidylinositol 3-kinase-dependent signals.* Mol Cell Biol, 2001. **21**(7): p. 2324-36.
504. Majewski, M., et al., *Activation of mitochondrial Raf-1 is involved in the antiapoptotic effects of Akt.* Cancer Res, 1999. **59**(12): p. 2815-9.

505. Patel, S., et al., *Constitutive modulation of Raf-1 protein kinase is associated with differential gene expression of several known and unknown genes.* Mol Med, 1997. **3**(10): p. 674-85.
506. Pfeifer, A., et al., *Effects of c-raf-1 and c-myc expression on radiation response in an in vitro model of human small-cell-lung carcinoma.* Biochem Biophys Res Commun, 1998. **252**(2): p. 481-6.
507. Komarov, P.G., et al., *A chemical inhibitor of p53 that protects mice from the side effects of cancer therapy.* Science, 1999. **285**(5434): p. 1733-7.
508. Koyama, S., et al., *Radiation-induced long-lived radicals which cause mutation and transformation.* Mutat Res, 1998. **421**(1): p. 45-54.
509. Stobbe, C.C., S.J. Park, and J.D. Chapman, *The radiation hypersensitivity of cells at mitosis.* Int J Radiat Biol, 2002. **78**(12): p. 1149-57.
510. Skandarajah, A.R., et al., *The role of intraoperative radiotherapy in solid tumors.* Ann Surg Oncol, 2009. **16**(3): p. 735-44.
511. Kosmider, S. and L. Lipton, *Adjuvant therapies for colorectal cancer.* World J Gastroenterol, 2007. **13**(28): p. 3799-805.
512. Hann, C.L. and C.M. Rudin, *Management of small-cell lung cancer: incremental changes but hope for the future.* Oncology (Williston Park), 2008. **22**(13): p. 1486-92.
513. Nishimura, Y., *Rationale for chemoradiotherapy.* Int J Clin Oncol, 2004. **9**(6): p. 414-20.
514. Bernhard, E.J., et al., *Effects of ionizing radiation on cell cycle progression. A review.* Radiat Environ Biophys, 1995. **34**(2): p. 79-83.
515. Lieberman, H.B., *DNA damage repair and response proteins as targets for cancer therapy.* Curr Med Chem, 2008. **15**(4): p. 360-7.
516. Peacock, J.W., et al., *The p53-mediated G1 checkpoint is retained in tumorigenic rat embryo fibroblast clones transformed by the human papillomavirus type 16 E7 gene and EJ-ras.* Mol Cell Biol, 1995. **15**(3): p. 1446-54.
517. Supino, R., et al., *A role for c-myc in DNA damage-induced apoptosis in a human TP53-mutant small-cell lung cancer cell line.* Eur J Cancer, 2001. **37**(17): p. 2247-56.
518. Mahyar-Roemer, M. and K. Roemer, *p21 Waf1/Cip1 can protect human colon carcinoma cells against p53-dependent and p53-independent apoptosis induced by natural chemopreventive and therapeutic agents.* Oncogene, 2001. **20**(26): p. 3387-98.
519. Lorenzo, E., et al., *Doxorubicin induces apoptosis and CD95 gene expression in human primary endothelial cells through a p53-dependent mechanism.* J Biol Chem, 2002. **277**(13): p. 10883-92.
520. Stenger, J.E., et al., *p53 oligomerization and DNA looping are linked with transcriptional activation.* EMBO J, 1994. **13**(24): p. 6011-20.
521. Wang, P., et al., *p53 domains: structure, oligomerization, and transformation.* Mol Cell Biol, 1994. **14**(8): p. 5182-91.
522. Sproston, A.R., et al., *Fibroblasts from Li-Fraumeni patients are resistant to low dose-rate irradiation.* Int J Radiat Biol, 1996. **70**(2): p. 145-50.
523. Stacey, D.W. and M. Hitomi, *Cell cycle studies based upon quantitative image analysis.* Cytometry A, 2008. **73**(4): p. 270-8.
524. Pignol, J.P., et al., *Clinical significance of atomic inner shell ionization (ISI) and Auger cascade for radiosensitization using IUdR, BUdR, platinum salts,*

*or gadolinium porphyrin compounds.* Int J Radiat Oncol Biol Phys, 2003. **55**(4): p. 1082-91.
525. Marangos, P. and J. Carroll, *The dynamics of cyclin B1 distribution during meiosis I in mouse oocytes.* Reproduction, 2004. **128**(2): p. 153-62.
526. Culmsee, C., et al., *Reciprocal inhibition of p53 and nuclear factor-kappaB transcriptional activities determines cell survival or death in neurons.* J Neurosci, 2003. **23**(24): p. 8586-95.
527. Komarova, E.A., et al., *p53 inhibitor pifithrin alpha can suppress heat shock and glucocorticoid signaling pathways.* J Biol Chem, 2003. **278**(18): p. 15465-8.
528. Sohn, D., et al., *Pifithrin-alpha protects against DNA damage-induced apoptosis downstream of mitochondria independent of p53.* Cell Death Differ, 2009.
529. Kaji, A., et al., *Pifithrin-alpha promotes p53-mediated apoptosis in JB6 cells.* Mol Carcinog, 2003. **37**(3): p. 138-48.
530. Walton, M.I., et al., *An evaluation of the ability of pifithrin-alpha and -beta to inhibit p53 function in two wild-type p53 human tumor cell lines.* Mol Cancer Ther, 2005. **4**(9): p. 1369-77.
531. Murphy, P.J., et al., *Pifithrin-alpha inhibits p53 signaling after interaction of the tumor suppressor protein with hsp90 and its nuclear translocation.* J Biol Chem, 2004. **279**(29): p. 30195-201.
532. Carnero, A., et al., *Loss-of-function genetics in mammalian cells: the p53 tumor suppressor model.* Nucleic Acids Res, 2000. **28**(11): p. 2234-41.
533. Bruno, T., et al., *Che-1 phosphorylation by ATM/ATR and Chk2 kinases activates p53 transcription and the G2/M checkpoint.* Cancer Cell, 2006. **10**(6): p. 473-86.
534. Zhong, W., *Nanomaterials in fluorescence-based biosensing.* Anal Bioanal Chem, 2009. **394**(1): p. 47-59.
535. Norris, P.S. and M. Haas, *A fluorescent p53GFP fusion protein facilitates its detection in mammalian cells while retaining the properties of wild-type p53.* Oncogene, 1997. **15**(18): p. 2241-7.